

Copyright is owned by the Author of the thesis. Permission is given for a copy to be downloaded by an individual for the purpose of research and private study only. The thesis may not be reproduced elsewhere without the permission of the Author.

**Impact of Quorum Sensing on Cell Aggregation in  
Enteropathogenic and Enterohaemorrhagic  
*Escherichia coli***

A thesis presented in partial fulfilment of the requirements for the  
degree of

Doctor of Philosophy  
In  
Microbiology and Genetics

At Massey University, Turitea Campus  
New Zealand

Barbara Siobhan Govan

2013

## **Abstract**

Quorum sensing has been shown to regulate phenotypic traits such as motility and biofilm production in pathogenic bacteria. *Escherichia coli* utilise both AI-2 and *N*-acylhomoserine lactones (AHL) quorum sensing systems to initiate phenotypic switches, such as changes in dissemination, in response to overall microbial population density. In addition HosA, a transcriptional regulator present in pathogenic strains of *E. coli*, was shown to be important in bacterial dissemination during this study. Deletion of *hosA* from enteropathogenic *E. coli* strain E2348/69 resulted in a non-motile population at lower temperatures, an effect that was reversed in the presence of exogenous AHL. Furthermore, addition of the same AHLs to wild-type E2348/69 decreased population motility. Bacterial aggregation has been linked to the motility of the population. Deletion of *hosA* was shown to increase aggregation, corresponding to an observed decrease in motility. Furthermore, addition of AHL was shown to decrease the propensity of the HosA mutant population to aggregate. Opposing effects were observed in the non-aggregating wildtype population. A hypothetical hierarchical association between HosA and quorum sensing was modelled to explain the relationship between motility and aggregation in E2348/69. It was observed the EAF plasmid is not essential for the formation of A/E lesions on human cell-line HT-29 by E2348/69. Infection of *Galleria mellonella* revealed increased virulence in highly aggregative populations and further highlighted the effect of HosA and environmental conditions on the pathogenicity of E2348/69. Ruminant animals, in particular cattle, are the main reservoir of enterohaemorrhagic *E. coli* O157:H7 with infection remaining asymptomatic. By comparison infection in humans can result in a range of sequelae from mild to life-threatening. *E. coli* O157:H7 is derived from an EPEC progenitor and as expected, dissemination was affected by specific AHLs in a similar manner to E2348/69. However, no aggregation was observed in the presence or absence of signal. This suggested a difference in the genes affected by quorum sensing between enteropathogenic and enterohaemorrhagic *E. coli*. Development of biocontrol strategies targeting AHL-dependent quorum sensing regulated processes, such as aggregation to reduce *E. coli* O157:H7 contamination of meat products is possible, based on the data presented in this thesis.

## **Acknowledgments**

A heartfelt thank you goes to my supervisors, Dr. Helen Withers and Prof. Nigel French for the help, encouragement and unfailing support throughout the length of my project and the writing of my thesis.

Thanks also go to Dr. Jonathan Marshall for his help during this project, particularly for the statistics advice, the help with developing the aggregation method and for providing information on the IPS model.

My thanks also go to the Food Assurance and Meat Quality team both past and present for their support and understanding. Special thanks go to Shelley Ulrich, who provided a figure for this thesis, and Ben Bright and Justine Couper for teaching and providing advice during my project.

Extra special thanks go to Dr. Tanushree Gupta for the unending support both professionally and personally, all the advice provided over the years, for being there when I needed support and for making sure I got time out once a week.

Thanks also go to Leanne Hall, Jess Owens, Lynsay Morgan, Tobi Sawdon and Cate Davis for the de-stressing distractions, non-science based conversations and helping me keep perspective.

Huge heartfelt thanks go to my family for the love and support, for being a shoulder to cry on and for listening to me at all hours of the day or night. Special thanks go to Frank Turnbull for being there, for being you and without whom I would not have been able to finish this thesis.

Finally, thanks go to the Ministry of Business, Innovation and Employment for funding my project.

# **Contents**

	<b><u>Page</u></b>
<b>Chapter One - Introduction</b>	<b>1</b>
1.1 <i>Escherichia coli</i>	1
1.1.1 <i>Escherichia coli</i> pathotypes DAEC, ETEC, EAEC and EIEC	1
1.1.2 Enteropathogenic <i>E. coli</i>	3
1.1.3 Enterohaemorrhagic <i>E. coli</i>	5
1.1.3.1 <i>E. coli</i> O157:H7 in cattle	6
1.1.3.2 Epidemiology of EHEC on foodstuffs	9
1.1.4 EPEC and EHEC pathogenesis	13
1.1.4.1 Attaching/Effacing Lesions	13
1.1.4.2 Transcriptional Regulator, HosA	19
1.1.4.3 Motility and Aggregation	20
1.1.4.4 EPEC-specific virulence factors	21
1.1.4.5 EHEC-specific virulence factors	23
1.2 Quorum Sensing (QS)	26
1.3 <i>N</i> -Acylhomoserine Lactones (AHLs)	32
1.3.1 LuxI and LuxR	32
1.3.1.1 SdiA and other Orphan LuxR Homologues	36
1.3.2 AHL Structure and Function	39
1.3.2.1 Phenotypic Switching	42
1.3.3 <i>Pseudomonas aeruginosa</i> – a complex example of a QS hierarchy	44
1.3.3.1 LasRI and RhIRI	46
1.3.3.2 PQS, QscR and VqsR	47
1.4 Autoinducer-2 (AI-2)	48
1.4.1 AI-2 Synthesis	48
1.4.2 LuxS	51
1.4.3 Phenotypic Switching	52
1.4.4 <i>Vibrio</i> spp. – an example of the similarities of function in two QS systems	53
1.4.4.1 <i>Vibrio harveyi</i>	54
1.5 Quorum Sensing and Food Safety	56
1.6 Infection Models of Pathogenicity	57
1.7 Research Hypotheses	57
<b>Chapter Two - Materials and Methods</b>	<b>60</b>
2.1 Growth Media, Diluents and Supplements	60
2.1.1 Luria Broth (LB)	60
2.1.2 Luria Agar (LA)	60
2.1.3 Marine Agar	60
2.1.4 Autoinducer Bioassay Media (AB)	60

		<b>Page</b>
	2.1.5 Autoinducing Bioassay Agar	61
	2.1.6 Phosphate Buffered Saline (PBS)	61
	2.1.7 Antibiotic Solutions	61
	2.1.8 <i>N</i> -acylhomoserine Lactones (AHLs)	62
2.2	Bacterial Strains and Plasmids	62
2.3	Autoinducer-2 Bioassays	62
	2.3.1 Conditioned Media (CM) Production	62
	2.3.2 <i>Vibrio harveyi</i> BB170-based Assay	65
	2.3.3 <i>Vibrio harveyi</i> MM32-based Assay	65
	2.3.4 Plate Diffusion-based AI-2 Assay	65
2.4	AHL Detection Methods	66
	2.4.1 T-streaks for the Detection of AHL Production	66
	2.4.2 T-streaks for the Detection of AHL Production using CM	66
	2.4.3 Plate Diffusion assay	67
	2.4.4 Thin Layer Chromatography (TLC)	67
	2.4.4.1 TLC Plate Preparation	67
	2.4.4.2 Extraction of AHLs from Rumen Fluid	68
2.5	Phenotypic Assays	69
	2.5.1 Motility Assays	69
	2.5.2 Promoter Expression Assay	69
	2.5.3 Aggregation Indices (AI)	70
	2.5.4 Aggregation Phase Contrast Microscopy Assay	70
	2.5.4.1 Analysis of Aggregation	71
	2.5.5 Curli Expression Plate Assay	71
	2.5.6 Cellulose Expression Assay	73
	2.5.7 Exopolysaccharide Production Assay	73
	2.5.8 Antigen 43 Assay	73
	2.5.9 Proteins	74
	2.5.9.1 Total Cell Protein Extraction	74
	2.5.9.2 Protein Gels	74
	2.5.9.3 Protein Visualisation using Coomassie Blue	75
	2.5.10 Uronic Acid Assay	75
2.6	Genetic Methods	77
	2.6.1 DNA Agarose Gels	77
	2.6.2 Polymerase Chain Reaction (PCR)	77
	2.6.3 Pulsed Field Gel Electrophoresis (PFGE)	79
	2.6.3.1 Reagents	79
	2.6.3.2 Plug Preparation	79
	2.6.3.3 Restriction Enzyme Digest	80

		<b>Page</b>
	2.6.3.4 PFGE	81
2.7	Tissue Culture	82
	2.7.1 Growth Medium	82
	2.7.2 HT-29 Cell Line	82
	2.7.3 Fluorescence Actin Staining (FAS test)	83
	2.7.3.1 HT-29 Cell Preparation	83
	2.7.3.2 Bacterial Preparation	83
	2.7.3.3 FAS Test	84
2.8	<i>Galleria mellonella</i> Infection Studies	84
	2.8.1 Bacterial Preparation	85
	2.8.1 Inoculation of <i>Galleria mellonella</i> Larvae	85
2.9	Statistics	85
2.10	Approvals	87
<b>Chapter Three - Effect of Quorum Sensing on Motility and the Influence of HosA</b>		<b>89</b>
	3.1 Introduction	89
	3.2 Results	90
	3.2.1 Role of AHL and Temperature on the Population Expansion of E2348/69	90
	3.2.2 Role of HosA on the Population Expansion of E2348/69	98
	3.2.3 Effect of HosA and AHL on Aggregation by E2348/69	105
	3.2.4 Development of a Phase Contrast Microscopy Method for Aggregation Analysis	109
	3.2.5 Effect of HosA on Cell Aggregation of E2348/69	116
	3.2.6 Role of AHL in Cell Aggregation of E2348/69 and E2348/69 <i>hosA</i> <sup>-</sup>	116
	3.2.7 <i>hosA</i> Promoter Expression as a Response to Temperature and AHL	125
	3.3 Discussion	130
<b>Chapter Four – Identification of Cell Surface Macromolecules Affected by AHLs in E2348/69</b>		<b>140</b>
	4.1 Introduction	140
	4.2 Results	141
	4.2.1 Effect of AHL on Aggregation and Population Expansion in a LuxS/AI-2 Negative Background	141
	4.2.2 Effect of AHL on Polysaccharide Expression in E2348/69 and the HosA mutant	153
	4.2.3 Effect of Protease on the Aggregation of E2348/69 <i>hosA</i> <sup>-</sup>	155
	4.2.4 Effect of AHL on Cell Surface Factors in E2348/69 and E2348/69-derived strains	159

		<b><u>Page</u></b>
4.2.5	Role of the EAF plasmid in the Aggregation and Population Expansion of E2348/69	162
4.2.6	Association Between the EspA Filament and Cell Aggregation in E2348/69	176
4.2.7	Effect of AHL on the Formation of Attaching-effacing Lesions by E2348/69 and E2348/69-derived strains	179
4.3	Discussion	187
<b>Chapter Five - Effect of AHL on the motility and aggregation of <i>E. coli</i> O157:H7</b>		<b>198</b>
5.1	Introduction	198
5.2	Results	199
5.2.1	Presence of AHL in Complex Biological Matrices	199
5.2.2	Genetic Relatedness of a Selection of <i>E. coli</i> O157:H7 Isolates	203
5.2.3	Role of AHL and Temperature on the Population Expansion of <i>E. coli</i> O157:H7	205
5.2.4	Cell Aggregation of <i>E. coli</i> O157:H7	210
5.2.5	Effect of AHL on the Expression of Exopolysaccharide in <i>E. coli</i> O157:H7	212
5.2.6	Effect of AHL on the Attachment of <i>E. coli</i> O157:H7 to Mammalian Cells	216
5.2.7	Effect of Experimental Controls on <i>Galleria mellonella</i>	218
5.2.8	Effect of AHLs on <i>E. coli</i> O157:H7 Pathogenicity using the <i>Galleria mellonella</i> Model	223
5.2.10	Role of Signalling and Environment on E2348/69 Pathogenicity using the <i>Galleria mellonella</i> Model	226
5.3	Discussion	230
<b>Chapter Six - General Discussion</b>		<b>239</b>
<b>Chapter Seven - References</b>		<b>252</b>



## **Abbreviations**

(v/v)	volume/volume ratio
(w/v)	weight/volume ratio
A/E Lesions	Attaching-effacing lesions
AB	Autoinducing Bioassay medium
AHL	N-acylhomoserine lactone
AI	Aggregation Indices
AI-2	Autoinducer-2
AIP	Autoinducing Peptide
AMC	Activated Methyl Cycle
ANOVA	Analysis of Variance
Bfp	Bundle forming pili
BSA	Bovine serum albumin
DAEC	Diffusely adherent <i>Escherichia coli</i>
dDHL	N-dodecanoyl-L-HSL
dH <sub>2</sub> O	de-ionised water
DMEM	Dulbecco's Modified Eagles Medium
DMSO	Dimethyl Sulphoxide
D-OdDHL	N-(3-oxododecanoyl)-D-HSL
D-OHHL	N-(3-oxohexanoyl)-D-HSL
DPD	4,5-hydroxy-2,3-pentanedione, the AI-2 precursor
EAEC	Enteraggregative <i>Escherichia coli</i>
EAF	EPEC adherence factor
EHEC	Enterohaemorrhagic <i>Escherichia coli</i>
EIEC	Enteroinvasive <i>Escherichia coli</i>
EPEC	Enteropathogenic <i>Escherichia coli</i>
ETEC	Enterotoxigenic <i>Escherichia coli</i>
FAS	Fluorescence Actin Staining
FBS	Foetal Bovine Serum
HosA	Homologue of SlyA

HUS	Haemolytic Uraemic Syndrome
K-S	Kolmogorov-Smirnov test
LA	Luria Agar
LB	Luria Broth
LEE	Locus of Enterocyte Effacement
OD <sub>600</sub>	Optical Density (600nm)
OHHL	<i>N</i> -(3-oxohexanoyl)-L-HSL
PBS	Phosphate Buffer Saline
PFGE	Pulsed Field Gel Electrophoresis
QS	Quorum Sensing
RLU	Relative Light Units
RT	Room Temperature
SAH	S-adenosylhomocysteine
SAM	S-adenosylmethionine
SdiA	Suppressor of division
SRH	S-ribosylhomocysteine
STEC/VTEC	Shiga-toxin containing/ verocytotoxin-producing <i>Escherichia coli</i>
Stx	Shiga toxin
sv.	serovar
VFA	volatile fatty acids

## **Figures**

		<b><u>Page</u></b>
<b>Figure 1</b>	Development of the gastric system in cattle from birth to maturity	7
<b>Figure 2</b>	Recorded cases of intestinal infections in New Zealand	12
<b>Figure 3</b>	Attaching/effacing lesion morphology of enteropathogenic <i>E. coli</i> on human epithelial cells	14
<b>Figure 4</b>	Locus of enterocyte effacement (LEE) in <i>E. coli</i>	16
<b>Figure 5</b>	Attaching/effacing lesion formation by enteropathogenic <i>E. coli</i>	18
<b>Figure 6</b>	Schematic diagram illustrating the basis of quorum sensing	28
<b>Figure 7</b>	Chemical structures of non-modified and modified AHLs	40
<b>Figure 8</b>	AHL synthesis in relation to changing population density in <i>Euprymna scolopes</i> , the Hawaiian bobtail squid	43
<b>Figure 9</b>	Quorum sensing regulatory pathways in <i>Pseudomonas aeruginosa</i>	45
<b>Figure 10</b>	Schematic of the activated methyl cycle and synthesis of AI-2	49
<b>Figure 11</b>	Schematic of QS regulation in <i>Vibrio harveyi</i> leading to bioluminescence	55
<b>Figure 12</b>	Inoculation of <i>Galleria mellonella</i> larvae	86
<b>Figure 13</b>	Effect of temperature on E2348/69 population expansion	91
<b>Figure 14</b>	Effect of AHLs on E2348/69 population expansion at 25°C	93
<b>Figure 15</b>	Variation in the diameter of the motility zones produced by E2348/699 in the presence and absence of different AHLs at 25°C	94
<b>Figure 16</b>	Variation in the diameter of the motility zones produced by E2348/69 in the presence and absence of different AHLs at 37°C	97
<b>Figure 17</b>	Effect of temperature on E2348/69 <i>hosA</i> <sup>-</sup> population expansion	99
<b>Figure 18</b>	Effect of AHLs on E2348/69 <i>hosA</i> <sup>-</sup> population expansion at 25°C	100
<b>Figure 19</b>	Variation in the diameter of the motility zones produced by E2348/69 <i>hosA</i> <sup>-</sup> in the presence and absence of different AHLs at 25°C	101
<b>Figure 20</b>	Comparison of variation of E2348/69 and E2348/69 <i>hosA</i> <sup>-</sup> population expansion at 25°C in the presence and absence of <i>N</i> -(3-oxohexanoyl)-L-HSL and <i>N</i> -dodecanoyl-L-HSL	103
<b>Figure 21</b>	Variation in the diameter of the motility zones produced by E2348/69 <i>hosA</i> <sup>-</sup> in the presence and absence of different AHLs at 37°C	104
<b>Figure 22</b>	Comparison of cell aggregation by E2348/69 and E2348/69 <i>hosA</i> <sup>-</sup> using aggregation indices and incubation at 25°C	106
<b>Figure 23</b>	Effect of <i>N</i> -(3-oxohexanoyl)-L-HSL on cell aggregation by E2348/69 <i>hosA</i> <sup>-</sup> at 25°C	108
<b>Figure 24</b>	Aggregates formed by E2348/69 and E2348/69 <i>hosA</i> <sup>-</sup> in three independent biological replicates	110
<b>Figure 25</b>	CellProfiler™ outputs produced during analysis of the microscopy images illustrating the aggregation of E2348/69 and E2348/69 <i>hosA</i> <sup>-</sup>	111
<b>Figure 26</b>	Aggregation profiles of biological replicates of E2348/69 and E2348/69 <i>hosA</i> <sup>-</sup> at 25°C	113
<b>Figure 27</b>	Graphical representations of variation between the aggregation profiles of two independent replicates of E2348/69	115

	<b><u>Page</u></b>
<b>Figure 28</b>	Comparison of the aggregation profiles produced by E2348/69 and E2348/69 <i>hosA</i> <sup>-</sup> at 25°C 117
<b>Figure 29</b>	Aggregates formed by E2348/69 in the presence and absence of AHL at 25°C 119
<b>Figure 30</b>	Aggregation profile of E2348/69 in the presence and absence of <i>N</i> -(3-oxohexanoyl)-L-HSL and <i>N</i> -dodecanoyl-L-HSL at 25°C 120
<b>Figure 31</b>	Aggregation profile of E2348/69 in the presence and absence of <i>N</i> -(3-oxo-hexanoyl)-D-HSL and <i>N</i> -(3-oxododecanoyl)-D-HSL at 25°C 122
<b>Figure 32</b>	Aggregates formed by E2348/69 <i>hosA</i> <sup>-</sup> in the presence and absence of AHL at 25°C 123
<b>Figure 33</b>	Aggregation profile of E2348/69 <i>hosA</i> <sup>-</sup> in the presence and absence of <i>N</i> -(3-oxohexanoyl)-L-HSL and <i>N</i> -dodecanoyl-L-HSL at 25°C 124
<b>Figure 34</b>	Aggregation profile of E2348/69 <i>hosA</i> <sup>-</sup> in the presence and absence of <i>N</i> -(3-oxo-hexanoyl)-D-HSL and <i>N</i> -(3-oxododecanoyl)-D-HSL at 25°C 126
<b>Figure 35</b>	Comparison of the aggregates formed by E2348/69 and E2348/69 <i>hosA</i> <sup>-</sup> in the presence and absence of <i>N</i> -(3-oxohexanoyl)-L-HSL and <i>N</i> -dodecanoyl-L-HSL at 25°C 127
<b>Figure 36</b>	Effect of temperature and active AHL on <i>hosA</i> promoter activity in E2348/69 and E2348/69 <i>hosA</i> <sup>-</sup> 129
<b>Figure 37</b>	Comparison of E2348/69 population expansion with that of the <i>HosA</i> and <i>LuxS</i> mutants at 25°C 142
<b>Figure 38</b>	Variation in the diameter of the motility zones produced by AE2348/69 <i>luxS</i> <sup>-</sup> in the presence and absence of different AHLs at 25°C 143
<b>Figure 39</b>	Aggregates formed by AE2348/69 <i>luxS</i> <sup>-</sup> in the presence and absence of exogenous AI-2 at 25°C 145
<b>Figure 40</b>	Aggregation profile of AE2348/69 <i>luxS</i> <sup>-</sup> and the effect of exogenous AI-2 at 25°C 146
<b>Figure 41</b>	Aggregates formed by AE2348/69 <i>luxS</i> <sup>-</sup> in the presence of AHL at 25°C 149
<b>Figure 42</b>	Aggregation profile of AE2348/69 <i>luxS</i> <sup>-</sup> in the presence and absence of <i>N</i> -(3-oxohexanoyl)-L-HSL and <i>N</i> -dodecanoyl-L-HSL at 25°C 151
<b>Figure 43</b>	Aggregation profile of AE2348/69 <i>luxS</i> <sup>-</sup> in the presence and absence of <i>N</i> -(3-oxo-hexanoyl)-D-HSL and <i>N</i> -(3-oxododecanoyl)-D-HSL at 25°C 152
<b>Figure 44</b>	Comparison of exopolysaccharide production by E2348/69 and E2348/69 <i>hosA</i> <sup>-</sup> 154
<b>Figure 45</b>	Cellulose expression by E2348/69 and E2348/69 <i>hosA</i> <sup>-</sup> 156
<b>Figure 46</b>	Aggregates formed by E2348/69 <i>hosA</i> <sup>-</sup> in the presence and absence of protease at 25°C 157
<b>Figure 47</b>	Aggregation profile of E2348/69 <i>hosA</i> <sup>-</sup> in the presence and absence of protease at 25°C 158
<b>Figure 48</b>	Effect of <i>N</i> -(3-oxohexanoyl)-L-HSL on antigen 43 expression in E2348/69 and E2348/69 <i>hosA</i> <sup>-</sup> 161
<b>Figure 49</b>	Curli expression in E2348/69 and E2348/69-derived strains 163
<b>Figure 50</b>	Effect of AHL on curli expression in E2348/69, E2348/69 <i>hosA</i> <sup>-</sup> and AE2348/69 <i>luxS</i> <sup>-</sup> 164
<b>Figure 51</b>	Variation in the diameter of the motility zones produced by E2348/69 <i>bfpA</i> <sup>-</sup> in the presence and absence of different AHLs at 25°C 165
<b>Figure 52</b>	Aggregates formed by E2348/69 <i>bfpA</i> <sup>-</sup> in the presence and absence of AHL at 25°C 167

	<b><u>Page</u></b>
<b>Figure 53</b>	Aggregation profile of E2348/69 <i>bfpA</i> <sup>-</sup> in the presence and absence of <i>N</i> -(3-oxohexanoyl)-L-HSL and <i>N</i> -dodecanoyl-L-HSL at 25°C 168
<b>Figure 54</b>	Variation in the diameter of the motility zones produced by E2348/69 MAR001 in the presence and absence of different AHLs at 25°C 170
<b>Figure 55</b>	Aggregates formed by E2348/69 MAR001 in the presence and absence of AHL at 25°C 171
<b>Figure 56</b>	Aggregation profile of E2348/69 MAR001 in the presence and absence of <i>N</i> -(3-oxohexanoyl)-L-HSL and <i>N</i> -dodecanoyl-L-HSL at 25°C 172
<b>Figure 57</b>	Aggregation profile of E2348/69 MAR001 in the presence and absence of <i>N</i> -(3-oxohexanoyl)-D-HSL and <i>N</i> -(3-oxododecanoyl)-D-HSL at 25°C 174
<b>Figure 58</b>	Detection of the EAF plasmid by PCR 175
<b>Figure 59</b>	Variation in the diameter of the motility zones produced by E2348/69 <i>espA</i> <sup>-</sup> in the presence and absence of different AHLs at 25°C 177
<b>Figure 60</b>	Aggregates formed by E2348/69 <i>espA</i> <sup>-</sup> in the presence and absence of AHL 178
<b>Figure 61</b>	Aggregation profile of E2348/69 <i>espA</i> <sup>-</sup> in the presence and absence of <i>N</i> -(3-oxohexanoyl)-L-HSL and <i>N</i> -dodecanoyl-L-HSL at 25°C 180
<b>Figure 62</b>	Aggregation profile of E2348/69 <i>espA</i> <sup>-</sup> in the presence and absence of <i>N</i> -(3-oxohexanoyl)-D-HSL and <i>N</i> -(3-oxododecanoyl)-D-HSL at 25°C 181
<b>Figure 63</b>	FITC-Phalloidin staining of HT-29 cells in the presence and absence of AHL and solvent 183
<b>Figure 64</b>	A/E lesion formation by E2348/69 in the presence and absence of AHLs 184
<b>Figure 65</b>	Comparison of A/E lesion formation by E2348/69 and E2348/69 <i>bfpA</i> <sup>-</sup> 185
<b>Figure 66</b>	A/E lesion formation by AE2348/69 <i>luxS</i> <sup>-</sup> in the presence and absence of AHLs 186
<b>Figure 67</b>	A/E lesion formation by E2348/69 <i>hosA</i> <sup>-</sup> in the presence and absence of AHLs 188
<b>Figure 68</b>	Short chain AHLs produced by psychrotolerant Enterobacteriaceae isolated from the surface of meat 200
<b>Figure 69</b>	Separation of AHLs present in unfiltered rumen fluid by thin layer chromatography 202
<b>Figure 70</b>	Pulsed-Field Gel Electrophoresis separation of <i>E. coli</i> O157:H7 isolates 204
<b>Figure 71</b>	Effect of temperature on <i>E. coli</i> O157:H7 population expansion 206
<b>Figure 72</b>	Variation in the diameter of the motility zones produced by faecal isolates of <i>E. coli</i> O157:H7 in the presence and absence of different AHLs at 25°C 208
<b>Figure 73</b>	Variation in the diameter of the motility zones produced by hide and clinical isolates of <i>E. coli</i> O157:H7 in the presence and absence of different AHLs at 25°C 209
<b>Figure 74</b>	Aggregation profiles of <i>E. coli</i> O157:H7 isolates in the presence and absence of <i>N</i> -(3-oxohexanoyl)-L-HSL and <i>N</i> -dodecanoyl-L-HSL at 25°C 213
<b>Figure 75</b>	Comparison of exopolysaccharide production by <i>E. coli</i> O157:H7 in the presence and absence of AHL 215
<b>Figure 76</b>	A/E lesion formation by <i>E. coli</i> O157:H7 isolate N427 in the presence and absence of AHLs 217
<b>Figure 77</b>	A/E lesion formation by <i>E. coli</i> O157:H7 isolate N218 in the presence and absence of AHLs 219

		<b><u>Page</u></b>
<b>Figure 78</b>	A/E lesion formation by <i>E. coli</i> O157:H7 isolate N231 in the presence and absence of AHLs	220
<b>Figure 79</b>	A/E lesion formation by <i>E. coli</i> O157:H7 isolate N635 in the presence and absence of AHLs	221
<b>Figure 80</b>	A/E lesion formation by <i>E. coli</i> O157:H7 isolate N236 in the presence and absence of AHLs	222
<b>Figure 81</b>	<i>Galleria mellonella</i> pigmentation after injection with inoculation medium and supplements. Positive control is <i>Ps. aeruginosa</i>	224
<b>Figure 82</b>	Effect of AHL on <i>E. Coli</i> O157:H7 virulence and the impact on <i>Galleria mellonella</i> pigmentation	225
<b>Figure 83</b>	Effect of AHL on E2348/69 virulence and the impact on <i>Galleria mellonella</i> pigmentation	227
<b>Figure 84</b>	Effect of growth media on E2348/69 virulence and the impact on <i>Galleria mellonella</i>	229
<b>Figure 85</b>	Hypothetical model of the regulation of aggregation in enteropathogenic <i>E. coli</i>	243
<b>Figure 86</b>	Schematic summary of the key findings in this study	251

## Tables

	<u>Page</u>
<b>Table 1</b>	Examples of chemical structures of different classes of quorum sensing signals 31
<b>Table 2</b>	Phenotypic effects of known AHL systems in specific bacteria 35
<b>Table 3</b>	<i>Escherichia coli</i> isolates used during this study 63
<b>Table 4</b>	Strains used during this study 63
<b>Table 5</b>	Plasmids used during this study 64
<b>Table 6</b>	CellProfiler™ parameters used for the analysis of aggregation as part of the phase contrast microscopy method 72
<b>Table 7</b>	Reaction mix used for colony PCR reactions 78
<b>Table 8</b>	Primer sequences of <i>bfpA</i> and <i>perA</i> 78
<b>Table 9</b>	PCR cycling conditions used for all PCR reactions 78
<b>Table 10</b>	Statistical analysis of the effect of AHL on E2348/69 population expansion at 25°C 94
<b>Table 11</b>	Statistical analysis of the effect of AHL on E2348/69 population expansion at 37°C 97
<b>Table 12</b>	Statistical analysis of the effect of AHL on E2348/69 <i>hosA</i> <sup>-</sup> population expansion at 25°C 101
<b>Table 13</b>	Comparison of E2348/69 and E2348/69 <i>hosA</i> <sup>-</sup> population expansion at 25°C 103
<b>Table 14</b>	Statistical analysis of the effect of AHL on E2348/69 <i>hosA</i> <sup>-</sup> population expansion at 37°C 104
<b>Table 15</b>	Statistical comparison of the aggregation profiles produced by independent biological replicates of E2348/69 and E2348/69 <i>hosA</i> <sup>-</sup> 113
<b>Table 16</b>	Statistical comparison of the effect of active AHL on E2348/69 aggregation 120
<b>Table 17</b>	Statistical comparison of the effect of <i>D</i> -isomers on E2348/69 aggregation 122
<b>Table 18</b>	Statistical comparison of the effect of active AHL on E2348/69 <i>hosA</i> <sup>-</sup> aggregation 124
<b>Table 19</b>	Statistical comparison of the effect of <i>D</i> -isomers on E2348/69 <i>hosA</i> <sup>-</sup> aggregation 126
<b>Table 20</b>	Statistical comparison of the effect of active AHL on the aggregation of E2348/69 and E2348/69 <i>hosA</i> <sup>-</sup> 127
<b>Table 21</b>	Statistical analysis of the effect of AHL on AE2348/69 <i>luxS</i> <sup>-</sup> population expansion at 25°C 143
<b>Table 22</b>	Statistical analysis of the effect of exogenous AI-2 on AE2348/69 <i>luxS</i> <sup>-</sup> aggregation 146
<b>Table 23</b>	Statistical analysis of the effect of active AHL on AE2348/69 <i>luxS</i> <sup>-</sup> aggregation 151
<b>Table 24</b>	Statistical analysis of the effect of <i>D</i> -isomers on AE2348/69 <i>luxS</i> <sup>-</sup> aggregation 152
<b>Table 25</b>	Statistical analysis of the effect of protease on E2348/69 <i>hosA</i> <sup>-</sup> aggregation 158
<b>Table 26</b>	Statistical analysis of the effect of AHLs on E2348/69 <i>bfpA</i> <sup>-</sup> population expansion at 25°C 165
<b>Table 27</b>	Statistical analysis of the effect of active AHL on E2348/69 <i>bfpA</i> <sup>-</sup> aggregation 168
<b>Table 28</b>	Statistical analysis of the effect of AHL on E2348/69 MAR001 population expansion at 25°C 170
<b>Table 29</b>	Statistical analysis of the effect of active AHL on E2348/69 MAR001 aggregation 172
<b>Table 30</b>	Statistical analysis of the effect of <i>D</i> -isomers on E2348/69 MAR001 aggregation 174
<b>Table 31</b>	Statistical analysis of the effect of AHL on E2348/69 <i>espA</i> <sup>-</sup> population expansion at 25°C 177
<b>Table 32</b>	Statistical analysis of the effect of active AHL on E2348/69 <i>espA</i> <sup>-</sup> aggregation 180
<b>Table 33</b>	Statistical analysis of the effect of <i>D</i> -isomers on E2348/69 <i>espA</i> <sup>-</sup> in aggregation 181

		<b><u>Page</u></b>
<b>Table 34</b>	Statistical analysis of the effect of AHL on <i>E. coli</i> O157:H7 faecal isolate population expansion at 25°C	208
<b>Table 35</b>	Statistical analysis of the effect of AHL on <i>E. coli</i> O157:H7 hide and clinical isolate population expansion at 25°C	209
<b>Table 36</b>	Statistical analysis of the effect of AHL on <i>E. coli</i> O157:H7 population expansion at 37°C	211
<b>Table 37</b>	Statistical analysis of the effect of AHL on <i>E. coli</i> O157:H7 aggregation	214
<b>Table 38</b>	Fatality rates of <i>Galleria mellonella</i> after inoculation with the control samples	224
<b>Table 39</b>	Fatality rates of <i>Galleria mellonella</i> after inoculation with <i>E. coli</i> O157:H7	225
<b>Table 40</b>	Fatality rates of <i>Galleria mellonella</i> after inoculation with E2348/69 or E2348/69 <i>hosA</i> <sup>-</sup>	227
<b>Table 41</b>	Effect of <i>N</i> -(3-oxohexanoyl)-L-HSL on the fatality rates of <i>Galleria mellonella</i> after inoculation with E2348/69 and E2348/69 <i>hosA</i> <sup>-</sup> grown in LB	229



# **1 Introduction**

## **1.1 Escherichia coli**

*Escherichia coli* belong to the Enterobacteriaceae family of bacteria [1-3]. There are over 200 identified serogroups of *E. coli*, the majority of which are non-pathogenic [3]. The non-pathogenic strains of *E. coli* form the largest population of facultative anaerobes in the human gut, comprising approximately 1% of the mammalian intestinal microflora [4-6]. These commensal *E. coli* rarely cause disease, and some may be used as probiotics for therapeutic treatments of specific gastrointestinal ailments, such as Inflammatory Bowel Disease [3, 4, 6].

Pathogenic *E. coli* have acquired and adapted virulence genes from other bacteria, enabling infection of human hosts [4, 6]. There are 3 main clinical syndromes associated with infection by pathogenic *E. coli*: sepsis/meningitis, urinary tract or enteric/diarrhoeal infection [4, 6]. The research presented in this study will focus on diarrheagenic *E. coli*.

### **1.1.1 Escherichia coli pathotypes DAEC, ETEC, EAEC and EIEC**

Diarrhoea-causing *E. coli* can be divided into six broad pathotypes based on the pathogenic mechanism used during infection: Diffusely Adherent (DAEC), Enterotoxigenic (ETEC), Enteroaggregative (EaggEC), Enteroinvasive (EIEC), Enteropathogenic (EPEC) and Enterohaemorrhagic *E. coli* (EHEC) [4, 6].

Originally, any *E. coli* strain that attached to HEp-2 cells without forming micro-colonies was termed “diffusely adherent *E. coli*” (DAEC), a term now used to describe any *E. coli* strain forming the characteristic diffuse adherence patterns of attachment [4, 6]. Infection with DAEC is rarely found in children under the age of 12 months, but prevalence increases in those aged between 1 and 5 years [4, 6]. Studies suggest that infection with DAEC could be pro-inflammatory aiding induction of inflammatory bowel disease [4].

Enterotoxigenic *E. coli* (ETEC) are a major cause of diarrhoea in developing countries, causing two major clinical syndromes; childhood diarrhoea and traveller's diarrhoea. The disease can range from mild, self-limiting diarrhoea (mainly associated with the traveller's disease) to severe purging diarrhoea [4, 6]. Ingestion of contaminated food and water, or direct person-to-person contact are the main transmission routes for infection and spread of this type of *E. coli* [4, 6]. ETEC are classified by the production of one or more heat-labile (LT) or heat-stable (ST) enterotoxins [6]. LTs closely resemble the *Vibrio cholerae* enterotoxin in both structure and function. STs are small single-peptide toxins which can be divided into two subtypes, STa and STb [4, 6]. Both LTs and STs act by triggering an electrolyte imbalance in the intestinal lumen which results in diarrhoea.

Enteraggregative *E. coli* (EAEC) are purely human pathogens, resulting in an often persistent diarrhoeal infection in children in both developing and developed countries [4, 7]. No animal reservoir has been identified [7]. EAEC are defined as *E. coli* that adhere to HEp-2 cells in a stacked brick formation using aggregative adherence fimbriae, but do not produce either LT or ST [4]. EAEC release enterotoxins or cytotoxins such as *Shigella* enterotoxin 1 (ShET1) or the enteraggregative *E. coli* enterotoxin EAST1, which has similar function to STa from ETEC [4, 6]. EAEC infection results in prolonged diarrhoeal-disease through continued epithelial cell destruction [4, 6]. Infection can be fatal in more susceptible individuals through the combined effects of continued water loss and cellular destruction of the intestinal mucosa [6]. Reported cases of EAEC infection are predominately sporadic, although some outbreaks have been reported [4, 6].

EAEC O104:H4, a shiga toxin expressing variant, was responsible for an outbreak in 2011 with cases reported in Germany, France and the UK [7-12]. Globally, a total of 4137 cases were recorded, 96.5% of these were in Germany. Of the 4137 recorded cases, 22% patients developed Haemolytic Uraemic Syndrome (HUS) with an overall mortality rate of 3.6%, while the

remaining 78% presented with severe gastroenteritis and had an overall mortality rate of 0.5% [12]. Haemorrhagic diarrhoea and abdominal pain were the most common symptoms, with some experiencing vomiting and low-grade fever [12]. Production of pathogenic traits, such as HUS, which have not been recorded in EAEC until now, suggested transfer and recombination of genetic material from enterohaemorrhagic *E. coli* in a common reservoir, such as the human gut [8, 11].

Enteroinvasive *E. coli* (EIEC) are closely related through biochemistry and genetics to *Shigella* spp. and are, at a species level, taxonomically indistinguishable [4]. The majority of EIEC cases result in watery diarrhoea [4, 6]. EIEC pathogenesis differs from other *E. coli* strains as they actively invade host epithelial cells and macrophages in more severe cases, resulting in invasive inflammatory colitis and secretory small bowel syndrome [4, 6].

#### **1.1.2 Enteropathogenic *E. coli***

Enteropathogenic *E. coli* (EPEC) is a human pathogen responsible for over 2 million deaths per annum, particularly among children under the age of 2 years [4, 6, 13-15]. EPEC was the first pathotype to be described following a large outbreak of diarrhoea in young children in the United Kingdom during 1945 [4]. The serologically distinct *E. coli* were isolated from children under 6 months of age suffering from diarrhoea, but were not found in the stools of healthy children of equivalent age [4, 6]. In children over 2 years, EPEC was isolated from the stools of both healthy and sick children [4, 6]. EPEC can cause diarrhoea in adults if a high inoculum is ingested (approximately  $10^8$  to  $10^{10}$  bacteria), coupled with neutralisation of gastric acid [6]. Adults with compromising factors such as immunosuppression or diabetes, and the elderly are more susceptible to diarrhoea caused by EPEC [6]. Infection with EPEC results in watery diarrhoea with vomiting and low-grade fever in more severe cases [4, 6].

EPEC can be divided into typical and atypical EPEC depending on the presence or absence of specific genetic elements [16]. Outbreaks of infantile diarrhoea induced by typical EPEC is now relatively uncommon in developed countries, although cases have been associated to contact with child day care centres, hospitals and nurseries [4, 6].

In less developed countries typical EPEC is a major cause of infantile diarrhoea [4, 6]. EPEC is often the most isolated diarrheagenic bacteria from stools of children aged under 6 months [6]. Studies in Brazil, Mexico and South Africa have attributed 30-40% reported cases of infantile diarrhoea to infection by EPEC, with mortality rates of 30% in some less socioeconomically developed areas of these countries [6, 17-19].

Typical EPEC is transmitted predominantly via the faecal-oral route on contaminated hands, foodstuffs or fomites [6]. EPEC has been isolated from dust and other aerosols, suggesting a potential airborne transmission [6]. Carriage can be both symptomatic and asymptomatic with some studies showing 17-20% of healthy infants under the age of 2 years shedding EPEC in their stool [6] (reviewed in [20]).

Atypical EPEC (aEPEC) has come to dominate in EPEC-related diarrhoeal disease in developed countries, such as the USA. For example, in the UK aEPEC accounts for 90% of all recorded EPEC strains [21]. It has been shown that the emergence of these aEPEC strains is through genetic recombination events similar to those involved in the emergence of some toxigenic strains, such as *E. coli* O157:H7 [16, 21]. No animal reservoir has been identified in typical EPEC, however aEPEC has been isolated from different animal species, such as dogs [21, 22]. Atypical EPEC is more closely related genetically to some enterohaemorrhagic *E. coli* [16, 21].

### **1.1.3 Enterohaemorrhagic *E. coli***

Enterohaemorrhagic *E. coli* (EHEC) are a group of zoonotic pathogens defined as a distinct pathotype due to epidemiological observations in the early 1980s [4, 6, 23]. Two outbreaks of a distinctive gastrointestinal infection characterised by acute abdominal cramps and watery diarrhoea, which was closely followed by haemorrhagic, or bloody, diarrhoea with little or no fever [6]. This illness was termed haemorrhagic colitis and was linked to ingestion of undercooked beef burgers at a fast-food restaurant [6]. Serological testing of stool samples from infected patients yielded the serotype *E. coli* O157:H7 [6]. Another key factor for disease progression was the association between *E. coli* O157:H7 infection and cases of haemolytic uraemic syndrome (HUS). Resulting in renal failure, HUS has also been linked with other serious sequelae such as thrombocytopenia and microangiopathic haemolytic anaemia, all of which can be fatal [3, 4, 6, 23-26].

*E. coli* O157:H7 is mainly transmitted via food and contact with an infected individual, either human or animal. This pathogen has a low infectious dose in the human host, reported as <100 bacteria [4, 6]. During these outbreaks, the most at risk of severe EHEC disease are children under 5 years of age, immune-compromised and the elderly [4, 6]. Although reported cases have been predominately associated with consumption of contaminated foodstuffs, contaminated municipal drinking water, visits to petting zoos or farms and person-to-person transmission have also been identified as sources of infection [2-4, 6, 25, 27, 28].

Shiga-toxin containing *E. coli* (STEC) or verocytotoxin-producing *E. coli* (VTEC), of which *E. coli* O157:H7 is the most high profile strain, are all equally pathogenic to humans [29]. In the USA non-O157 serotypes O26, O111, O103, O121, O45 and O145 have been identified as causing 71% of non-O157 EHEC infections [29, 30]. The USA has recently added these serotypes to the list of adulterants, meaning if any of them are isolated from red meat imported into the USA it could result in a cessation of trade with the country of origin. Cattle remain a

recognised reservoir for these serotypes [29]. It is hypothesised that sufficient homology between these serotypes and *E. coli* O157:H7 remains so that any mitigation targeting one will affect the others. Although these non-O157:H7 EHEC strains are becoming more important in both human health and food processing, this research project will focus on *E. coli* O157:H7.

#### 1.1.3.1 *E. coli* O157:H7 in cattle

The main animal reservoir for EHEC are the ruminants, particularly cattle where it is found as a commensal in the lower gastrointestinal tract, and infection is asymptomatic [6, 23, 27, 31]. *E. coli* O157:H7 has also been found in calves, and transmission between calves housed in the same pen has been observed suggesting faecal-oral transmission within the bovine reservoir [32]. Human disease-causing EHEC can be found in various locations throughout the cattle digestive tract, with up to 26 individual serotypes existing concomitantly [33]. The principal EHEC colonisation site in cattle is the rectal-anal junction as the reduced oxygen concentration and available nutrients make this the ideal environment [23, 34, 35]. As digested food moves through the intestine the *E. coli* may be carried in or with the intestinal contents and shed to the environment in faeces. Newborn calves are monogastric, compared to adult cattle which are ruminants with four separate stomach compartments used to digest plant material prior to entry into the intestines (Figure 1). Differences in carriage rates of *E. coli* O157:H7 between monogastric and ruminant animals have been observed by scientists (Personal Communication, AgResearch Ltd). This finding is important for the development of strategies to reduce the bacterial load in cattle.

A longitudinal study by Edrington *et al* proposed that shedding levels of *E. coli* O157:H7 by cattle in the USA varied depending on the season where less shedding occurred in the winter and spring months, with higher bacterial counts recorded during the summer and autumn [35]. A

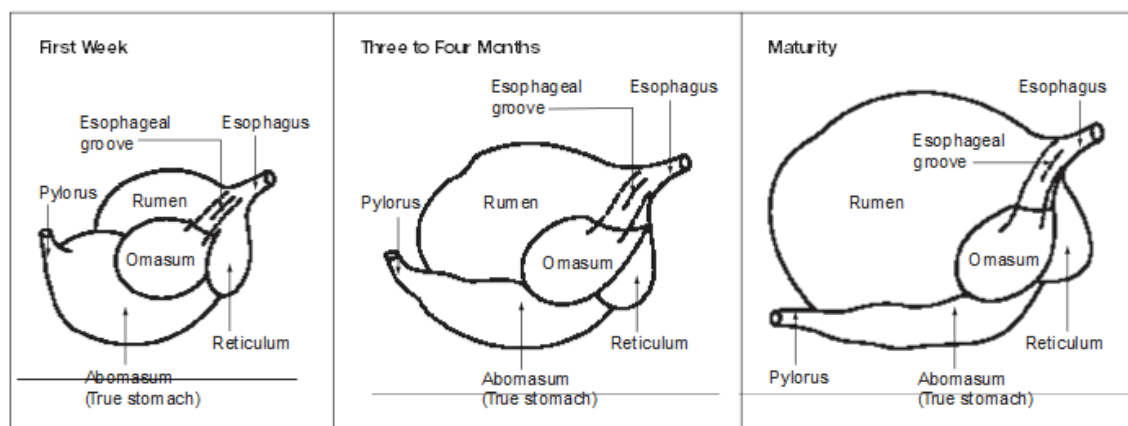


**Figure 1 – Development of the gastric system in cattle from birth to maturity.**

Image provided by and reproduced with permission from A.J Heinrichs and C.M Jones (Penn State University) [36]. Following birth the calf is monogastric, utilising only one of the four stomach compartments for the digestion of milk. The rumen, reticulum and omasum are undeveloped, so milk moves through the abomasum which functions like a human stomach and comprises approximately 60% of the stomach volume in an unweaned calf [36]. During growth the size of the remaining 3 compartments changes as they develop and mature with the rumen and reticulum combined comprising 70% of the total stomach volume, the omasum 10% and the abomasum reduced to 20% of the total volume by 12 weeks [36]. Although the abomasum appears to reduce in size, in actuality it increases, merely constituting a smaller proportion of the overall stomach in comparison to the other compartments. The function of the abomasum remains similar to that of a human stomach throughout the life of the cow. As the calf matures the use of oesophageal groove decreases and grass and solid foodstuffs move primarily into the rumen where it is exposed to microbial breakdown [36]. From the rumen the semi-digested food moves through the reticulum to the omasum before entering the abomasum, undergoing enzymatic digestion before moving into the intestines, much like in the human gastro-intestinal tract [36].

similar study in Scotland has also indicated a seasonal shedding rate of *E. coli* O157:H7 [31]. The seasonally controlled shedding of *E. coli* O157:H7 has long been thought to be related to temperature and weather conditions; however links between day length and melatonin levels have recently been identified [5].

Diet is a major influence on shedding rates of *E. coli* O157:H7 by cattle. Volatile fatty acids (VFA) are produced as by-products of the fermentation within the rumen and can have bactericidal effects. VFA are toxic to *E. coli* and affect the pH within both the rumen and the intestinal tract [5]. Fasting prior to slaughter has been shown to decrease VFA concentrations increasing the rumen pH to be more alkaline resulting in a higher population of *E. coli* O157:H7 in the rumen [5]. A higher *E. coli* population in the rumen would lead to a higher overall population throughout the gastrointestinal tract, which would potentially increase the bacterial load shed to the environment. Probiotics such as *Lactobacillus gallinarum* have been shown to reduce the *E. coli* O157:H7 population in the cattle rumen [5].

Barley-fed animals have a higher faecal pH compared to corn-fed cattle, and a lower concentration of VFA [5]. Waste corn from ethanol production and steam-flaked grains have been shown to increase *E. coli* O157:H7 shedding in cattle [5]. Callaway *et al* showed that the higher starch content in the hindgut, where the corn is fermented to produce VFA, lowers the pH causing acid-shock bacterial cell death [5]. A study in the USA has shown the use of orange peel (at a concentration of 2% of the total volume of feed) reduced the *E. coli* O157:H7 population resulting in lower shedding rates as a result of anti-microbial action by chemicals, such as the essential oil limonene found in the peel of citrus fruits [37, 38].

Shedding rates of *E. coli* O157:H7 of between  $10^2$  and  $10^5$  CFU/g cattle faeces have been identified from cows [27]. These bacteria can persist in the environment leading to contamination of the hide and colonisation of cattle [27, 39-41]. Cattle with high levels of *E. coli* O157:H7 can be divided into super-shedders and super-spreaders. A super-shedder is an animal



who excretes a higher number of bacteria than most other individuals of the same species, for a defined period of time [23, 27, 39-41]. In contrast a super-spreader is defined as an individual animal that has increased opportunity to infect others, i.e. is more connected in the social network thereby increasing the probability of other animals in close proximity becoming infected [23]. Incidence of *E. coli* infection in cattle could potentially be controlled if colonisation were to be prevented in these super-shedders [39-41]. Common sources of transmission for super-spreaders include markets and auctions, or during lairage and transport. Super-shedder therefore describes the host-bacteria relationship, while super-spreader relates to host-host interactions [23].

Bacteria are commonly found on the hide of cattle at the abattoir through contact with soil, water and/or vegetation contaminated with faeces containing *E. coli* O157:H7. Transfer to carcass surfaces from the hide can occur during processing [27, 42, 43].

#### 1.1.3.2 Epidemiology of EHEC on foodstuffs

In the USA it has been estimated that infection with *E. coli* O157:H7 through consumption of contaminated and undercooked red meat accounts for approximately 20,000 cases of illness with 250 deaths each year [44]. Several major outbreaks were recorded in the USA between 1992 and 1997 which were linked with consumption of meat products [25, 44]. In Scotland between 1990 and 1996 there were 25 recorded outbreaks with over 700 reported cases in total [44]. The largest national outbreak of foodborne disease in the UK was recorded in Scotland in 1996 where consumption of contaminated meat caused 120 people to become ill with 34 developing HUS. Of these 34 cases 82% were adults and the mortality rate from HUS reached 47% overall [31, 44]. Recorded incidences appear to have a seasonal trend with numbers peaking in summer and early autumn in the UK and USA [44].

The most common route of *E. coli* O157:H7 carcass contamination is from the hide of the animal during processing. Some leakage of intestinal contents can also occur during processing [39, 41, 45, 46]. Exposed muscle tissue during slaughter, dressing, chilling and cutting provides a path for environmental contamination of meat products [46].

The reduction of *E. coli* O157:H7 counts on meat is a major influence on manufacturing practice due to the economic impact of confirmed infections associated with consumption of meat or meat products, in addition to the severity of human infection [46]. Good manufacturing practices as well as interventions have been put in place to reduce the EHEC load on meat during processing [46]. In the USA these include decontamination procedures such as chemical carcass rinses, chemical de-hairing, carcass trimming of contaminated areas and steam vacuuming in addition to immersion, flooding, deluging, rinsing, cascading or spray-washing with either chemicals or water pre- and post-evisceration [46].

Cases of *E. coli* O157:H7 have been linked with consumption of contaminated vegetables and water supplies. The bacteria are transferred to plant surfaces through contact with either contaminated water or manures/soil, and result in human infection through poor food hygiene practices by the consumer [2-4, 6, 25, 27, 28, 47]. An outbreak of *E. coli* O157:H7 in Japan in 1996 resulted in 9500 individuals becoming ill after consuming contaminated radish sprouts, while in the USA there have been reports of infection from consumption of unpasteurised apple juice/apple cider [6]. In 2000 a total of 5 people died and 27 were hospitalised from an *E. coli* O157:H7 infection in Ontario, Canada after drinking contaminated water [25].

Non-O157:H7 Shiga toxin-containing EHEC (STEC) or verotoxin *E. coli* (VTEC) have also been reported to cause HUS. In Norway in 2006 EHEC O103:H25 was identified as the causal agent in a national disease outbreak resulting in 17 cases of infection, with 94% reporting diarrhoea, 59% developing HUS and a recorded mortality rate of 6%. The transmission route was identified as fermented sausage meat [10]. Genetic comparisons have shown the phage

carrying the toxin genes in EHEC O103:H25 very closely resemble EAEC O104:H4 from the German outbreak in 2011 [10].

In the 2011 EAEC O104:H4 outbreak, the majority of cases were recorded in adult females, contrary to *E. coli* O157:H7 infection which primarily affects children [9, 12]. Epidemiological studies have suggested that, as the transmission vehicle was identified as fenugreek seeds, the predominance of adult female cases reflects the exposure distribution rather than specific virulence properties of the bacterium [9]. This outbreak of HUS represents the largest ever described, illustrating how genetic recombination can result in the evolution of novel pathogens [7, 12].

In New Zealand, more than 95% of reported VTEC clinical infections are caused by *E. coli* O157:H7, although some non-O157:H7 infections have been identified [48]. Since there is currently no consistent method available for medical laboratories to use for the identification of non-O157:H7 infection, the incidence may be under-reported [48, 49]. Furthermore, cases of mild diarrhoea are unlikely to be tested for the presence of *E. coli* O157:H7, thereby increasing the likelihood of under-reporting [49]. The majority of cases of *E. coli* O157:H7 are reported during the autumn and spring, but little information is available regarding the epidemiology of carriage of this bacterium in humans [49-51].

Several intestinal infections are notifiable in New Zealand, requiring any cases to be reported. These include *E. coli* O157:H7, *Campylobacter* and *Salmonella* infections (Figure 2A). *Campylobacter* spp. have the highest incidence with up to 15873 cases recorded in 2006 [51]. By comparison, *Salmonella* has a much lower recorded incidence where the number of cases in 2006 was 1335 [51]. General gastroenteritis was lower with a maximum of 937 cases recorded in 2006 [51]. *E. coli* O157:H7 infection is markedly lower than all of these other notifiable infections, with the maximum number of cases recorded in 2006 measuring 87 [51].

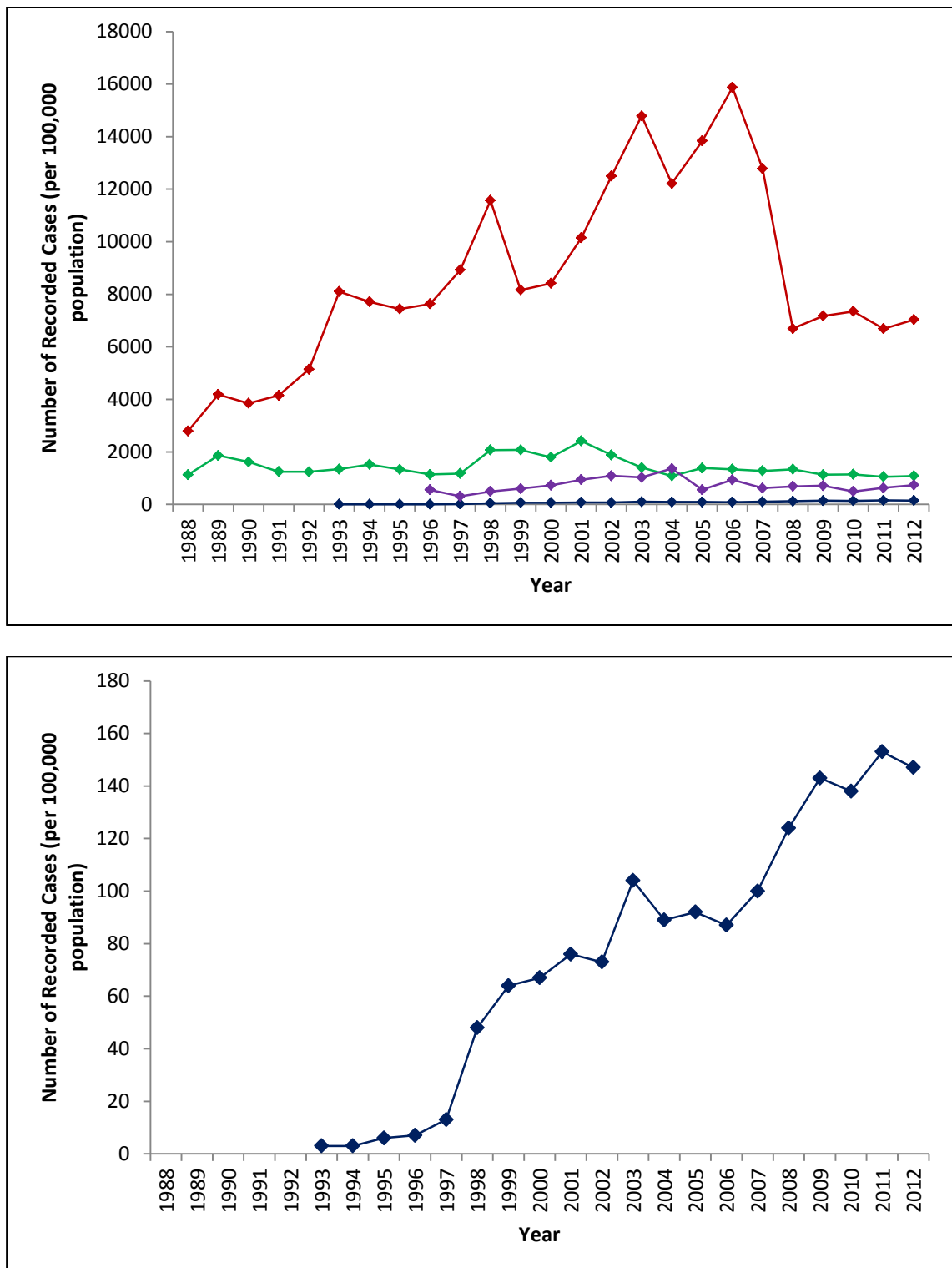


**Figure 2 - Recorded cases of intestinal infections in New Zealand**

(A) Gastrointestinal infections

(Blue) *Escherichia coli* O157:H7

(Red) *Campylobacter* spp.

(Green) *Salmonella* spp.

(Purple) Gastroenteritis

(B) *Escherichia coli* O157:H7

Data sourced from ESR Public Health Surveillance Annual Reports [51].

For *E. coli* O157:H7, cases in NZ were first recorded in 1993, with only 3 cases recorded [51]. Between 1993 and 2011, this number increased 50-fold, with the incidence of confirmed *E. coli* O157:H7 cases in New Zealand doubling over the 10 year period between 2001 and 2011 (Figure 2B). Part of this observed increase may be the result of improvements to testing protocols in the early period of testing, however with standardised methods now available it is likely that there has been a real increase in the number of cases being reported. Among the most common exposures identified from case data supplied by the surveillance system were contact with pets, farm animals or animal manure, with consumption of dairy products or raw fruit and vegetables consistently higher than beef or beef products [50, 51]. There have been no major food-related outbreaks reported in New Zealand, with the majority of cases recorded occurring sporadically or within a family, having been environmentally derived from contact with animals and contaminated faeces and/or water [49-51].

#### **1.1.4 EPEC and EHEC pathogenesis**

##### **1.1.4.1 Attaching/Effacing Lesions**

Histopathological investigations have shown an important pathogenicity mechanism of EPEC and EHEC is the formation of A/E lesions [4, 6, 13, 14, 52-54]. Attaching-effacing lesions, or pedestals, are produced by both EPEC and EHEC and are characterised by localised destruction of the microvilli in the intestine (Figure 3).

There are three main stages to A/E lesion formation; localised adherence, signal transduction and intimate adherence [6]. In typical EPEC bundle forming pili (Bfp) are important for localised adherence to host cells, while in atypical EPEC and EHEC this role may be carried out by a different pilus if it occurs at all [21, 22].

The formation of A/E lesions and the attachment of EPEC and EHEC to host epithelial cells require signal transduction within the eukaryotic cell, which leads to cytoskeletal

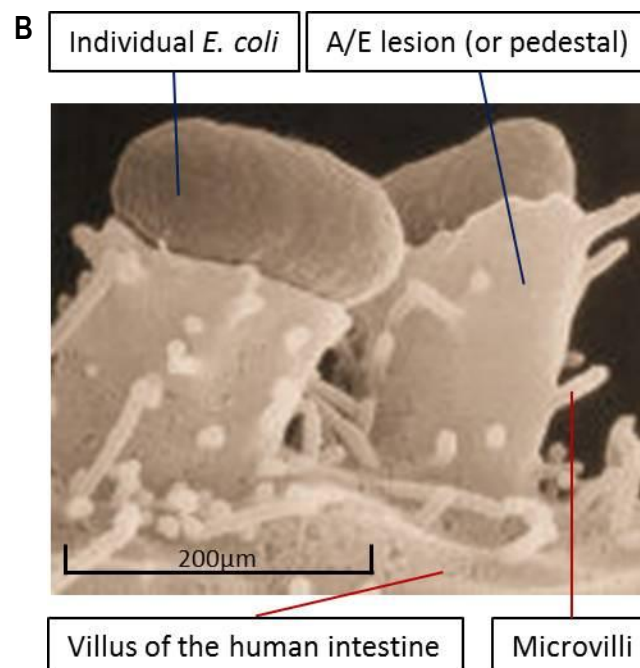
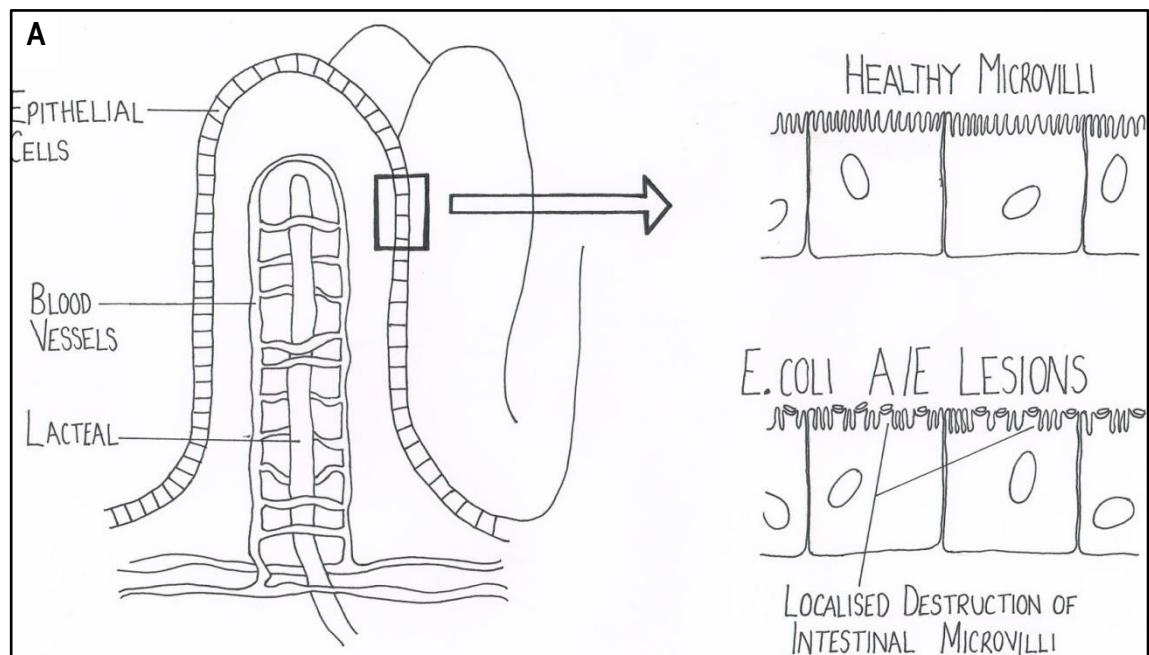


**Figure 3 – Attaching/effacing lesion morphology of enteropathogenic *E. coli* on human epithelial cells**

A/E lesion formation on intestinal cells in the human host, illustrating the flat pedestal-like structure formed on the microvilli during the subversion of the host cell cytoskeleton. Each A/E lesion surrounds a single *E. coli*.

(A) Diagram from B. Govan undergraduate study notes, circa 2003-2007. Schematic shows the structure of a healthy villus of the small intestine, with a closer view of the microvilli in the presence and absence of EPEC or EHEC representing the localised destruction characteristic of A/E lesions

(B) Adapted from <http://www.bioteach.ubc.ca/>, SEM micrograph of A/E lesions formed on the microvilli in the presence of EPEC or EHEC

rearrangement. The genes responsible for this signal transduction are encoded on the 35kb pathogenicity island, named the Locus of Enterocyte Effacement (LEE) [6, 34, 53]. LEE is composed of 41 genes which is divided into five polycistronic operons; LEE1, LEE2, LEE3, TIR and LEE4 (Figure 4).

Regulation of LEE is dependent on multiple factors including environmental conditions and the activity of multiple regulators, including Per, and the LEE-encoded GrlA, GrlR and Ler (Figure 4) [4, 6, 53, 55, 56].

The type three secretion system (TTSS) used by *E. coli* to translocate virulence factors, is located at the 5 prime (5') end of the LEE operon encoded by approximately 20 genes, including *sep* and *esc* [6, 53, 55-58]. EPEC and EHEC both produce a needle-like TTSS. Membrane-bound proteins are exported to form the foundation of the needle-like complex via the *sec* pathway [56]. EscC and EscV, located in LEE2 and LEE3 respectively, are the major components of both inner and outer membrane ring structures in the *E. coli* TTSS [56]. EscJ from LEE2 forms the periplasmic bridge between the inner and outer membrane components of the TTSS [56]. The needle structure of the TTSS is formed of EscF, providing a 'projection channel' for secreted proteins [56]. In EPEC and EHEC a hollow tube-like filament formed of EspA protein binds the EspF needle structure, providing a means of transportation for effector proteins and signals from the bacterial cell to the host [6, 14, 53, 55-58]. Translocator proteins EspB and EspD, both encoded in LEE4, are the first proteins translocated via the EspA filament to the epithelial cell membrane where they form a transmembrane pore into the host cell allowing free movement of proteins into the cytosol [6, 14, 55-58]. EspD may have dual function as it is also required for the generation of the EspA filament itself [56]. A mutation in any of the TTSS genes, or EspA, B, or D causes translocation and transduction of proteins to be abolished [6, 59, 60]. Chaperones, essential for successful translocation of proteins, are encoded by *ces* [56].

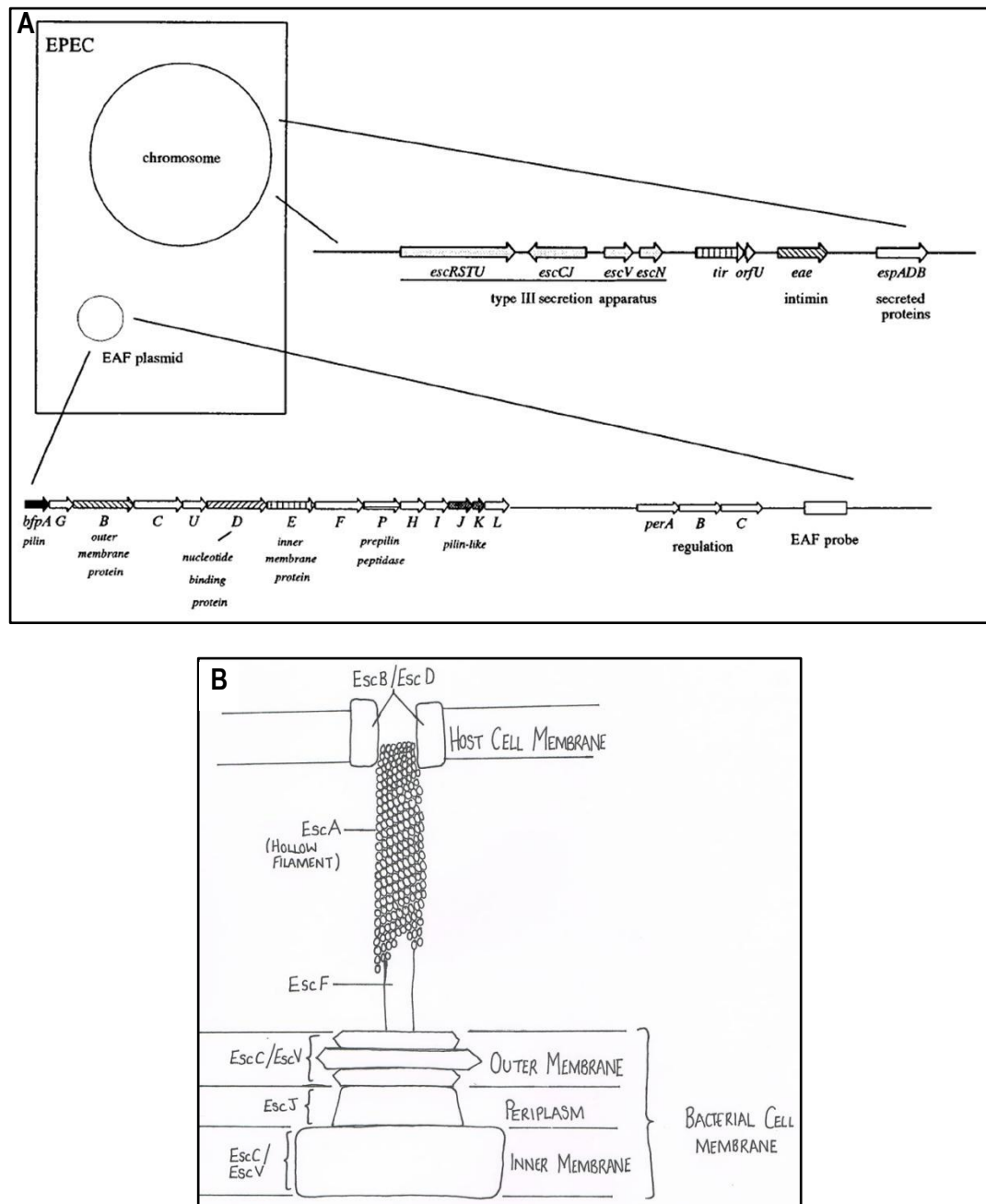


**Figure 4 – Locus of enterocyte effacement (LEE) in *E. coli***

- (A) Genetic organisation of LEE in *E. coli*. Chromosomal virulence genes involved in the formation of attaching/effacing lesions by EPEC and EHEC are clustered within a region called LEE, which encode a type 3 secretion system, *tir/intimin* and other secreted proteins. The EAF plasmid is present in EPEC only and encodes the BFP operon, a gene cluster responsible for the expression of BFP. Furthermore *Per*, a transcriptional regulator important for LEE gene expression is encoded on EAF. Image has been reproduced from Nataro and Kaper (1998) [6] with permission from the American Microbiological Society.
- (B) Structure of the type 3 secretion system formed by *E. coli* as a result of LEE transcription. Image was adapted from B. Govan undergraduate study notes circa 2003-2007.



Once the link between host and bacteria has been formed, other proteins responsible for the intimate attachment and cytoskeletal rearrangements associated with A/E lesions can be translocated into the host cell. Important proteins for cytoskeletal rearrangement include intimin and Tir. Upon translocation of the effector proteins, both the EspA filament and the needle-like TTSS structure are removed from the bacterial cell surface [56]

Intimin, encoded by *eae* in the TIR region of the LEE operon (Figure 4), is a 94kDa adhesion protein located in the outer membrane of both EPEC and EHEC [4, 6, 55, 57, 58, 61]. The main function of intimin is as a ligand for host epithelial cell binding via a translocated receptor protein, Tir, which is also encoded on the LEE locus (Figure 4) [4, 6, 55-58, 61]. *E. coli* O157:H7 Tir contains an amino acid change, which prevents a phosphorylation step involved in pedestal formation. Due to this mutation *E. coli* O157:H7 requires transcription of *tccP*, which encodes the Tir cytoskeleton coupling protein to produce A/E lesions [62, 63].

Tir translocates into the host cell and localises in the host plasma membrane following modification by host protein kinases with both extracellular and cytosolic domains [4, 6, 55, 56, 61]. The extracellular region of Tir binds with intimin, forming the intimate attachment characteristic of A/E lesions [4, 6, 34, 55, 56]. The intracellular region of Tir binds to Nck, an adaptor protein in host cells [4]. Nck recruits N-WASP, binding to the N-terminus of this protein, and the actin-related protein 2/3 (Arp2/3) complex [4]. Activation of Arp2/3 allows the bacterium to subvert the host cell structure initiating rearrangement of the actin cytoskeleton [4]. This results in production of the characteristic actin-rich pedestals beneath the bacteria (Figures 3 and 5). By altering the surface area of the host cells within the intestine, the bacteria reduce the absorptive capacity of the colon resulting in diarrhoea [4, 24, 64]. Although similar, EHEC lacks the ability to complete the localised adherence step due to the lack of Bfp and the EAF plasmid. EHEC, as with aEPEC, retains the ability to form pedestals but a lower number are observed under laboratory conditions [6]. This suggests Bfp is important but not essential in the formation

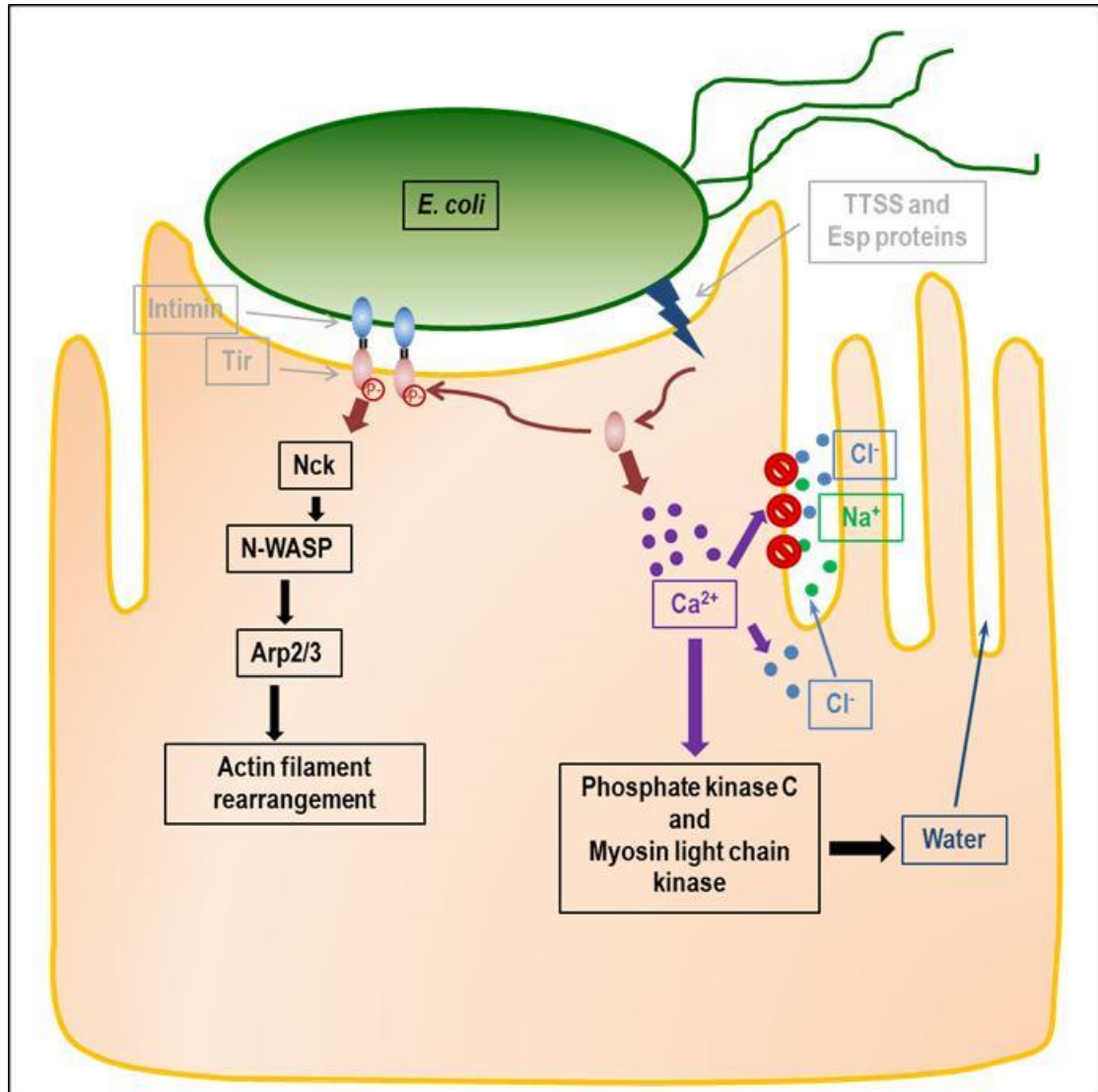


**Figure 5 – Attaching/effacing lesion formation by enteropathogenic *E. coli*.**

Bacterial proteins or effectors are indicated in grey with open arrow heads

Block arrows show the processes activated by the activity of Tir and other effector proteins leading to actin rearrangement within the host cell

Thin arrows with closed heads indicate the direction of movement of molecules around the cell or to the external environment

of A/E lesions and the successful infection of a host. In order to produce the TTSS and initiate subversion of the host cell cytoskeleton, other adhesins present in the *E. coli* genome may be used by EHEC and aEPEC.

Adherence of either EPEC or EHEC to the human intestinal epithelia induced the activity of the myosin light chain kinase and protein kinase C [6]. Through the activities of these enzymes, intracellular calcium ion levels within the host cell have been observed to increase, which not only inhibit sodium and chloride ion absorption, but also stimulate movement of chloride ions out of the host cell into the intestinal lumen (Figure 5) [6]. This electrolyte imbalance initiates diarrhoea through water secretion into the intestinal lumen, in an attempt to equalise ion concentrations [6]. The increased ion and water secretion rates are coupled with increased permeability of the intestinal epithelial cells [4].

#### 1.1.4.2 Transcriptional regulator, HosA

The MarR family of transcriptional regulator proteins has been shown to facilitate adaption by bacteria, and some Archaea, to environmental stress. SlyA, a member of this family, was found to regulate heat resistance and acid shock genes in EIEC [65]. Homologues of SlyA have been linked with invasion regulation in some *Yersinia* spp., antibiotic resistance in *Serratia marcescens* and virulence in *Erwinia carotovora* [65-67].

In addition to SlyA, which is present in both EPEC and EHEC, a SlyA homologue has been identified in pathogenic strains of *E. coli*, known as HosA. Ferrándiz *et al* showed that although structurally similar to the other SlyA homologues, HosA targets and binds different genes due to diversity in the amino acid sequence of the DNA binding domain [68]. In the same study HosA expression was shown to be affected by external factors such as temperature and pH as well as the growth phase of the bacterium.

#### 1.1.4.3 Motility and Aggregation

The ability to swim has been shown to be an important capability for the survival and virulence of both gram positive and gram negative bacteria [69]. Release and detection of small chemical signals, such as autoinducers and cyclic di-GMP, have been shown to play an important role in the expression of flagellin genes, surface factors and DNA transcription in *Ps. aeruginosa* and *Yersinia* spp [69, 70]. These effectors have been shown to affect population motility by changing the affinity of the bacteria to interact and form aggregates [69, 70].

The formation of bacteria-bacteria interactions and the resultant bacterial aggregates is a form of cellular agglutination, where clumps or floccules of cells are formed - either spontaneously or following specific treatments [71]. Auto-agglutination occurs in response to a self-derived signal or chemical [71]. An example of bacterial aggregation is biofilms, which are matrix-enclosed populations of bacteria adhering to a surface. A number of different clinically relevant bacteria are capable of producing biofilms, of which *Ps. aeruginosa* is the most well studied. *Ps. aeruginosa* is a common producer of bacterial biofilms on medical devices such as patient catheters, cannulas and other implants, which can result in serious sequelae in immune-compromised patients [70, 72-78]. In addition *Ps. aeruginosa* biofilms have been linked to difficulties in industrial and environmental settings including microbial corrosion in engines following successful growth in diesel and jet fuel [70]. As part of an aggregate the bacteria can persist due to potential increases in resistance to bactericidal agents or mechanical cleaning when compared to individual bacteria [70, 72-78].

*Ps. aeruginosa* forms aggregates during exponential phase growth, adhering to each other using a matrix, a component of which is environmental DNA - genetic material shed to the environment [70]. During stationary phase the proportion of the population present within aggregates in relation to the total biomass decreased significantly from 90% to 10% [70]. This dispersal event forms a transition from a sessile complex to an individual planktonic lifestyle and

has been linked to depleted levels of carbon and oxygen within the matrix. In addition, the concentration of the intracellular secondary messenger cyclic di-GMP has also been shown to decrease during this transition [70].

In *Yersinia* spp. aggregates were shown to be held together by protein interactions. SDS-PAGE analysis and N-terminal sequencing suggested that flagellin may be up-regulated in aggregating cells compared to planktonic [69]. Rowe *et al* showed cellulose to be an important component of uropathogenic *E. coli* aggregates [79]. Expression of cellulose was linked to iron chelation and the ability to form attachments with the bladder wall [79]. Dunny *et al* showed aggregation to be important in the mating of donor and recipient cells of *Streptococcus faecalis* [80]. These bacteria release a substance hypothesised to be a small peptide or protein responsible for inducing the donor cells to become adherent, thereby encouraging clumping [80].

For EPEC, Ferrándiz *et al* showed population motility was linked with aggregation and HosA [68]. During the study they showed that HosA bound upstream of *fliC*, which encodes the structural component of the flagella [68]. As a result of this binding FliC expression was higher in the wildtype when compared to the *hosA* deletion mutant. Further temperature changes did not affect the ability to produce flagella as individual bacteria were still motile, but rather the reduction in temperature increased the propensity of the population to form aggregates, which had an adverse effect on population motility. Over-expression of HosA in the parent strain resulted in the inhibition of population motility. Ferrándiz *et al* hypothesised that HosA acted as a positive control element in flagellum-driven motility in pathogenic *E. coli*, modulating expression of specific genes in relation to temperature and other environmental cues [68].

#### 1.1.4.4 EPEC-specific virulence factors

Some EPEC strains encode a 110-kDa enterotoxin, EspC [81]. EspC belongs to the serine protease family of autotransporters, which are found in both diarrheagenic and uropathogenic *E.*

*coli* [4, 81]. Unlike the toxins of other pathotypes, EspC is an autotransporter forming a  $\beta$ -barrel of proteins in the outer membrane [4, 81]. This pore allows the other part of the toxin access to the extracellular milieu [4]. Expression of EspC has been found to be under Ler regulation [4]. The target of the toxin remains unknown, but *in vitro* experiments have shown EspC to increase the short circuit current in Ussing chambers which are used to monitor the net movement of ions across a membrane [81]. This observation suggests EspC may be a mechanism for diarrhoea production through initiation of electrolyte imbalance.

Typical EPEC contain the 60-MDa (80kb) EPEC Adherence Factor (EAF) plasmid, while atypical EPEC and *E. coli* O157:H7 do not [4, 6, 13, 14, 21, 22, 52-54, 57]. This plasmid carries genes important for the regulation of the Locus of Enterocyte Effacement (LEE), a virulence operon found in both EPEC and EHEC [22]. Although not essential for successful colonisation by EPEC, the EAF plasmid increases the efficiency of production of the characteristic Attaching/Effacing (A/E) lesions [21]. A cluster of three EAF plasmid-borne genes, PerA, B and C, regulate expression of Ler, a protein responsible for regulation of LEE expression [15, 16, 21, 58].

Girón *et al* describe 7nm diameter fimbriae produced by those EPEC strains able to aggregate [52]. These fimbriae, known as bundle forming pili (Bfp), are encoded by 14 genes on the EAF plasmid, and have been shown as an important factor in the production of diarrhoea by typical EPEC [4, 6, 13, 14, 52-54, 57]. Bfp are composed of rope-like bundles of filaments of repeating 19.5 kDa polypeptide subunits, which mediate initial contact between bacteria and host cell, interconnect bacteria to form micro-colonies and thereby increase the stability once adhered to the host [21, 22, 82, 83]. These pili are only produced under conditions that mimic the intestine with maximal production occurring in the presence of calcium [4, 14, 52, 64]. Studies have shown atypical EPEC, which lack all *bfp* genes are still able to adhere, albeit less efficiently, to host cells [21, 22].

Typical and atypical EPECs belong to two different sets of serotypes. The typical EPEC rely on EAF regulation of LEE expression to produce the characteristic localised adherence pattern of A/E lesions mediated by  $\alpha$ -,  $\beta$ - and  $\delta$ -type intimin [21, 84]. Atypical strains frequently produce EAST1 and other potential virulence factors not encoded in the LEE operon. There are 3 types of adherence observed in atypical EPEC strains, each mediated by a different adhesin. Localised-like adherence, which is most similar to the standard adhesion pattern of typical EPEC, is mediated by  $\alpha$ -,  $\beta$ - and  $\gamma$ -type intimin, diffuse adherence is mediated by the Afa adhesin, and aggregative adherence mediated by the aggregative adhesion [21, 84]. Although theoretically the loss of the EAF plasmid may result in a decrease in virulence, this has not been observed in the statistics of reported cases suggesting atypical EPEC may compensate for this loss by expressing other virulence factors [21, 84].

Inactivation of BfpA by substitution of serine 129 for a cysteine resulted in a non-adherent phenotype [14, 57]. However, mutation in *bfpF* resulted in increased localised adherence and increased bacterial aggregation.

#### 1.1.4.5 EHEC-specific virulence factors

EHEC encodes a potent shiga-like toxin. The structural genes for this toxin are encoded by two genes *stx1* and *stx2*, which are located on separate lysogenic lambdoid bacteriophages and are expressed either in combination or individually [6, 26]. Stx1, when expressed on its own, has rarely been associated with human disease as expression is reduced by lower temperature and increased iron availability [6, 26, 85]. The Stx2 variants pathogenic to humans are unaffected by these factors and are responsible for the severe sequelae characteristic of an *E. coli* O157:H7 infection when expressed either individually or in combination with Stx1 [6, 26].

The primary site of localised damage by the Stx toxin is the colonic epithelia resulting in haemorrhagic diarrhoea, haemorrhagic colitis, colonic epithelia necrosis and/or intestinal

perforation [4]. Stx toxin is produced in the human colon but moves, purportedly through the bloodstream, to the kidneys, although no toxin has been found in the bloodstream of HUS patients [4].

Once the toxin reaches the kidneys Stx causes damage to the renal endothelial cells obstructing the microvasculature through direct toxicity and induction of local chemokine and cytokine production [4, 6]. This results in renal inflammation which can lead to HUS [4].

Stx1 is highly conserved and genetically identical to the Shiga toxin from *Shigella dysenteriae* [6, 30]. There are multiple forms of Stx2 due to a high level of sequence variation [6]. All members of the shiga toxin family encode a simple AB toxin, with five B subunits each of 7.7kDa forming a pentamer that binds to globotriaosylceramide (Gb<sub>3</sub>) – a glycolipid receptor found predominantly on the surface of eukaryotic cells in the kidneys and human intestine epithelia, but can also be found throughout other organs [6, 86]. While Gb<sub>3</sub> is the predominant receptor for Stx1 in human infections, Stx2 is most likely to bind Gb<sub>4</sub> [6]. Cattle do not have either Gb<sub>3</sub> or Gb<sub>4</sub> receptors and so are unaffected by the toxin [86]. The single 32kDa A subunit is proteolytically cleaved into two smaller units, a 28kDa A<sub>1</sub> peptide and a 4kDa A<sub>2</sub> peptide [6]. The A<sub>2</sub> subunit remains extracellular binding the A subunit to the B pentameric protein, while A<sub>1</sub> becomes internalised into the host cell [6]. The A<sub>1</sub> subunit is an *N*-glycosidase that is translocated into the host cytoplasm where it removes a single adenine base from the 28S ribosomal RNA causing inhibition of protein synthesis [6]. This results in necrosis of renal endothelial cells, intestinal epithelia cells and any other host cells containing either the Gb<sub>3</sub> or Gb<sub>4</sub> receptors within the membrane [6]. It has been hypothesised that the absorptive intestinal epithelial cells have a greater number of Gb receptors compared to the secretory intestinal epithelial cells. The higher number of receptors make the absorptive cells more susceptible to toxin binding leading to an imbalance in the secretion: absorption ratio causing diarrhoea [6].



*E. coli* O157:H7 is not the only strain of *E. coli* to carry the *stx* genes. The other strains are commonly termed non-O157:H7 shiga-toxin containing *E. coli* (STEC) [29]. Some atypical EPEC have also been found to carry *stx* genes [16, 21]. EAEC O104:H4 responsible for the German outbreak carried only *stx2* [10-12]. In the Norwegian O103:H25 outbreak in 2006, again the *stx2* gene was identified in some of the clinical isolates from patients suffering from HUS [10]. Of the other food-related non-O157 Shiga Toxin-containing *E. coli* (STEC), six serotypes all carrying the *stx* genes have been identified as responsible for 71% of the recorded non-O157 STEC-related disease in the US: O26, O45, O103, O111, O121 and O145 [29]. The similarity between the *E. coli* Stx toxin and the *Shigella* Shiga toxin, suggest historic horizontal transfer of mobile genetic elements [6, 30]. The presence of the *stx2* gene in non-O157:H7 STEC, including EAEC O104:H4 indicate recombination and genetic transfer is a significant influencing factor for *E. coli* populations and sequence divergence [8].

In addition to Stx and the LEE locus, EHEC produce EAST1, the enterotoxin found in EAEC [6]. The function of EAST1 in EHEC pathogenicity is unclear, but may be responsible for the non-haemorrhagic diarrhoea sometimes associated with infection by EHEC [6].

EHEC also carry the pO157 plasmid, a 94-104kDa plasmid encoding enterohaemolysin, catalase-peroxidase and other adherence factors [6]. Again, the significance of the enterohaemolysin has not been conclusively determined, but it has been shown to cause lysis of human erythrocytes and bovine leukocytes. The lysis of erythrocytes would release haem and iron into the bloodstream, which would increase the growth and proliferation of *E. coli* O157:H7 [6]. By lysing leukocytes EHEC would be able to evade the bovine immune system to successfully colonise the hindgut. pO157 also encodes StcE, which inhibits the host complement pathway potentially contributing to cellular damage, intestinal swelling and thrombocytopenic changes [4].

A major virulence mechanism for EHEC is the adhesion to host cells through attaching/effacing lesions, which may be aided by the common pilus adherence factor encoded by *ecpA*, a highly conserved gene found throughout many commensal and pathogenic *E. coli* strains [87]. Curli, adhesive fimbriae-like structures, encoded by *csgA* are found on the cell surface of *E. coli* [88]. These proteins aid adherence to both epithelial cells and other surfaces by forming complex honeycomb-like structures utilising bacteria-bacteria interactions, and have been linked to biofilm production [88, 89]. The action of curli during attaching/effacing lesion production has not been well investigated [88].

Expression of virulence factors and survival of both EPEC and EHEC are affected by a complex combination of external environmental conditions, such as temperature and pH, and biochemical conditions, such as availability of nutrients and ions [4, 6, 56]. Survival on meat and the expression of certain virulence genes, such as the LEE locus, have been linked to cell-to-cell signalling and quorum sensing, which are discussed in sections 1.2 – 1.5 of this study [45, 56, 90, 91].

## **1.2 Quorum Sensing (QS)**

QS is often described as density-dependent cell-to-cell signalling. The definition of QS is a mechanism for the co-ordination of gene expression in a bacterial population which depends on the production and response to a self-generated signal [73, 92-94]. This allows individual bacteria to initiate social interactions and exhibit multicellular behaviour [93-95]. Diggle *et al* define a signal as “any act or structure that alters the behaviours of other organisms, which evolved owing to that effect, and which is effective because the receivers response has also evolved” [96].

Many bacteria synthesise QS signal molecules or autoinducers [93]. Within a defined area, such as an organ, as the bacterial cell density increases the concentration of autoinducer will rise

(Figure 6) [61, 93]. By detecting the concentration of signal molecule an individual bacterium 'senses' when a threshold signal concentration and thereby population level has been reached, leading to a response. These changes occur within a bacterium on an individual level, but occurs within multiple cells at the same time producing a concerted population response. QS is a multicellular behaviour modulating a range of physiological processes [95, 97]. Binding of a specific QS molecule with a receptor either directly or indirectly through a signal transduction cascade initiates repression or induction of target genes or regulons [73, 91, 93, 98, 99]. Examples of population-wide responses to QS include bioluminescence, sporulation, biofilm production, and expression of virulence factors including siderophores and adhesion molecules [91, 97, 100-103].

There is no defined quorum size as the QS effects are dependent on the rates of synthesis and consumption of the QS molecules, which are affected by external conditions [93, 94, 98, 103]. Some bacterial species require a relatively low amount of signal to activate the transduction cascade, other species need a much higher concentration and some require a variable concentration with responses activated in a dose-dependent manner [94].

QS has been shown to play a role in food spoilage and biofouling [90, 91, 104]. Biofouling describes growth of algae, bacteria and animals, such as crustaceans, on surfaces with prolonged exposure to water [104]. Such surfaces include pipes, tanks and the hulls and keels of ships [104]. Many opportunistic pathogens are able to utilise QS to aid biofilm formation on surfaces and increase specific virulence characteristics [104].

In addition, QS has been shown to be an important factor in the medical and dental areas. Opportunistic pathogens, such as *Pseudomonas aeruginosa* produce highly complex biofilms on medical catheters and other instruments. Research is currently underway to determine the effect of QS inhibitors on biofilm formation and degradation of different materials to reduce the risk of infection in susceptible patients [100, 104].

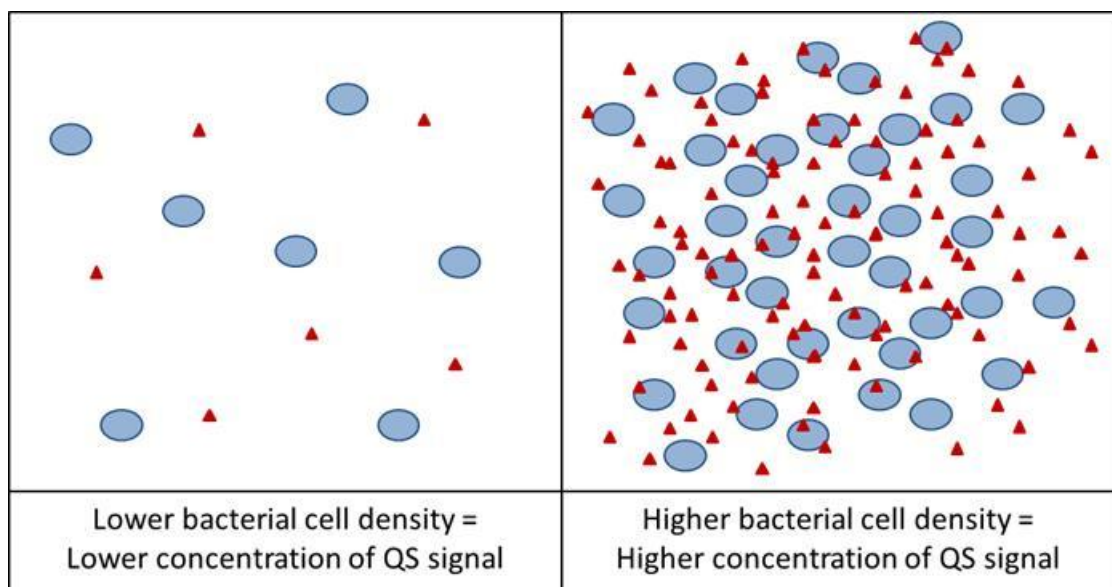


**Figure 6 – Schematic diagram illustrating the basis of bacterial quorum sensing**  
Blue ovals (●) represent the bacterial cells and the red triangles (▲) represent the QS signalling molecule.

In a true QS system there are four key components which must be present:

- 1) A signal synthase responsible for producing the specific signals, such as LuxI in *Vibrio fischeri* or LasI in *Pseudomonas aeruginosa* [61, 91, 93, 94, 98]
- 2) The signal, such as AHL or AI-2 [61, 91, 93, 94, 98]
- 3) A signal regulator, e.g. LuxR in *Vibrio fischeri*, LasR in *Ps. aeruginosa* and SdiA in *E. coli* [61, 91, 93, 94, 98]
- 4) A QS regulon, i.e. the genes to be regulated, for example the *lux* operon in *Vibrio fischeri* [61, 91, 93, 94, 98]

During the first half of the 20<sup>th</sup> Century it was determined that bacteria communicated via chemical signals [105]. By 1965 information on genes and gene regulation was widespread, but it was believed that changes were in response to chemical fluctuations within the individual bacterium, with no influence from other sources [105]. Kempner and Hanson suggested the bioluminescence produced by *Vibrio fischeri* was due to the removal of inhibitor found within the growth medium due to the late on-set of light production [106]. Nealson and Hastings suggested that bioluminescence was as a result of autoinduction and *V. fischeri* was communicating population-wide, introducing the idea of quorum sensing [107]. In 1981 Eberhard determined the structure of 3-oxo-C6-HSL, an *N*-acylhomoserine lactone responsible for communication in *Vibrio fischeri* [108]. Dunny *et al* identified bacterial 'sex pheromones', which in 1984 were redefined as autoinducing polypeptides affecting aggregation in *Enterococcus faecalis* [80, 105]. This type of chemical signalling was found to be density dependent, acting to coordinate the bacterial population as a whole. In 1994 Fuqua *et al* termed the bacterial unit affected by this type of chemical signalling as a quorum in order to recognise that the size of the population was critical to whether the signals had an effect. Later, this became known as quorum sensing (QS) [103, 105, 109-111].

Three main bacterial QS systems have been discovered so far, each relying on the production and release of different types of signal; *N*-acylhomoserine lactones (AHL), autoinducer-2 (AI-2) and auto-inducing peptides (AIP) (Table 1) [94, 110]. These molecules are chemically diverse, and different cognate regulators are often found in combination within a bacterial species working together in a hierarchical system [75, 93].

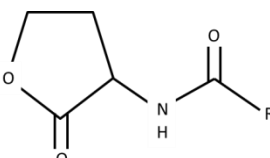
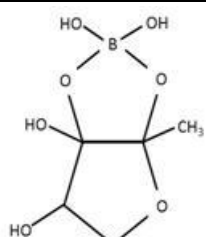
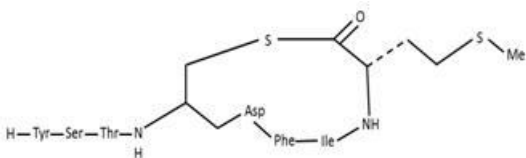
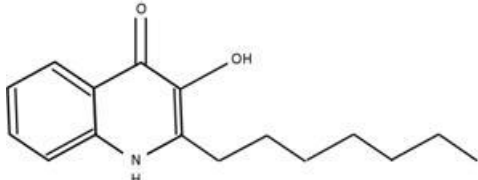
Briefly, AHLs are produced by some gram negative bacteria (Section 1.3) and AI-2 is often termed a universal signal as it is produced by some Gram negative and positive bacteria (Section 1.4). AIPs are only produced by Gram positive bacteria, such as *Staphylococcus aureus* [93]. These peptide signals, recognised by cell surface transmembrane histidine kinases, activate transcriptional regulators through a phospho-relay system [98, 110].

Other QS systems do exist, but appear to be found in a smaller range of bacterial species such as the *Pseudomonas* quinolone signal (PQS) and 2-heptyl-4-quinolone (HHQ), both of which are produced by *Pseudomonas aeruginosa* (Table 1) [93]. AI-3 is a controversial signalling molecule with a structure similar to mammalian catecholamines, the structure of which is still largely unknown. Recent research has suggested a role in metabolism rather than QS for AI-3 [24, 73, 112, 113]. Research showed AI-2 interacts with QseABC to regulate expression of the LEE locus [24, 113-118]. Other molecules such as indole and diamino acids have been suggested as quorum sensing signals, but the evidence suggests that these are more likely to be associated with cell status and age, although this hypothesis has yet to be confirmed [119-123].

Social networking is an expression utilised to describe the relationships between types of molecules produced by bacteria using economic terms such as “public goods” and “private goods”. Public goods are factors released by the bacteria into the external milieu constituting social products which can be beneficial to multiple species present in the QS niche [124]. By comparison, “private goods” remain within the cell, thereby constituting non-social products

**Table 1 - Examples of chemical structures of different classes of quorum sensing signals**

Structures taken from [93, 94, 125] and [125]

Signal family	Structure	Example of producers
<i>N</i> -acylhomoserine lactone (AHL)		Gram negative bacteria, e.g. <i>Pseudomonas</i> , <i>Vibrio</i> and <i>Yersinia</i>
Autoinducer-2 (AI-2)		Many species both gram positive and negative, e.g. <i>E. coli</i> , <i>Salmonella</i> and <i>Enterococcus faecalis</i>
Autoinducing Polypeptide (AIP)		Gram positive bacteria, e.g. <i>Staphylococcus aureus</i>
<i>Pseudomonas</i> Quinolone Signal (PQS)		<i>Pseudomonas aeruginosa</i> only

which are often required for metabolic processes [124, 126]. As these factors remain intracellular, concentration is not as important and therefore quorum sensing regulation is unlikely to be involved [124].

Although quorum sensing signals may be construed as public goods by voyeuristic bacteria such as *E. coli*, it is actually used to communicate and coordinate expression of external factors, and thereby control pathogenic phenotypes [96, 111, 124, 127]. These extracellular factors have been found to be utilised in the control of various biological processes, such as motility, biofilm production, nutrient acquisition and host immune evasion and/or suppression [124].

QS signals are rarely species specific, for example AHLs produced by one gram negative species can be detected and utilised by another species, thereby making the environment much more competitive and complex [93, 94, 110]. The interactions between bacterial species and QS signals can be accidental, antagonistic, agonistic or symbiotic in nature, thereby increasing the complexity of these systems further [110].

### **1.3 N-Acylhomoserine Lactones (AHLs)**

AHLs are quorum sensing signals produced by some gram negative species, such as *Pseudomonas*, *Vibrio*, and *Yersinia* [94]. It has been estimated that approximately 7% of gram negative bacteria belonging to the  $\alpha$ -,  $\beta$ - and  $\gamma$ -proteobacteria groups recognise and respond to AHLs [110]. The synthesis and structure of known AHLs will be discussed in addition to the function of and response to these chemical signals. The complexity of an AHL-dependent quorum sensing system will be illustrated using *Pseudomonas aeruginosa*.

#### **1.3.1 LuxI and LuxR**

Three protein families able to synthesise AHLs have been identified so far in gram negative bacteria: the LuxI family, the LuxM family and the lysophosphatidic acid acyltransferase protein



family [73]. The mechanism of biosynthesis utilised by the lysophosphatidic acid acyltransferase protein family is unknown, but the group includes Act protein of *Acidithiobacillus ferrooxidans* and HdtS in *Pseudomonas fluorescens* [73, 94, 95, 109, 128-130]. The LuxM family has so far only been found in *Vibrio* spp. and includes LuxM of *Vibrio harveyi*, VanM from *Vibrio anguillarum* and AinS from *Vibrio fischeri* [73, 94, 109, 131-133]. The LuxI family is the most common and is found in  $\alpha$ -,  $\beta$ - and  $\gamma$ -proteobacteria [73, 75, 94, 109, 130]. Once synthesised, AHLs interact and form complexes with transcriptional regulators [75, 93, 94, 98, 109, 110]. The majority of AHL regulators belong to the LuxR-AHL family, but other non-homologous transcriptional regulators such as LuxN in *Vibrio harveyi*, have the same function [73, 93, 94, 100, 109].

The LuxR protein has two functional domains - the N-terminus, a highly variable region known to interact and bind the AHL, and the C-terminus, a highly conserved transcriptional regulatory domain containing the DNA binding motif [73, 93, 94, 109, 134-137]. The specificity of LuxR proteins for specific AHL molecules appears to relate to the size of the hydrophobic binding pocket and the size and modification of the R group of the AHL (Table 1) [130]. LuxR proteins form a reversible bond with an AHL molecule utilising the stoichiometric ratio of 1:1 [130, 137]. By performing structural analysis of SdiA from *E. coli* and TraR from *Agrobacterium tumefaciens*, Nasser *et al* determined and characterised the structure of the AHL binding cavity of these two LuxR homologues, which are very similar [138-140]. A cluster of aromatic and hydrophobic amino acids form a cavity surrounded on both sides by a 5-stranded  $\beta$ -sheet adjacent to 3  $\alpha$ -helices [140]. Upon entering the cavity the AHL is stabilised by the formation of 4 hydrogen bonds around the lactone ring, with the fatty acid tail lying parallel to the  $\beta$ -sheets initiating further hydrophobic interactions. The specificity of the ligand binding pocket is determined by the amino acid composition and the affinity of an AHL to bind is affected by length of the fatty acid tail [130, 140]. Several synthetic QS inhibitors which mimic AHL structure but do not activate transcription

have been identified, suggesting that, although specific, molecules other than the cognate AHL are able to bind the LuxR protein [109, 110, 139, 141, 142].

Each LuxR protein has a cognate AHL ideally suited for the active site, for example LasR of *Pseudomonas aeruginosa* and CviR of *Chromobacterium violaceum* preferentially bind *N*-(3-oxododecanoyl)-L-HSL and *N*-hexanoyl-L-HSL respectively, whilst TraR of *Agrobacterium tumefaciens* optimally binds *N*-(3-oxo-octanoyl)-L-HSL (Table 2) [73, 75, 93, 94, 98, 109, 127, 137, 143, 144].

Direct binding of the AHL to the active site of the LuxR *N*-terminus results in a conformational change in the LuxR protein, leading to the DNA binding motif of the C-terminus becoming accessible, initiating binding to DNA [73, 75, 93, 94, 98, 109, 127, 137, 138, 145-147]. Once bound the AHL/LuxR complex interacts with the C-terminal of the  $\alpha$ -subunit of the RNA polymerase regulating the initiation of transcription [73, 75, 93, 94, 98, 109, 127, 145-150]. When the LuxR C-terminus binds the DNA upstream of the promoter it is able to initiate direct contact with the RNA polymerase, thereby acting as a transcriptional activator [136, 151].

One particular region of DNA bound by some AHL/LuxR complexes is the *lux* box, although not all LuxR-type proteins bind this motif. In *Pseudomonas aeruginosa* the *las* box functions in the same manner as the *lux* box in other bacteria [136]. Some orphan LuxR proteins bind the *lux* box in the absence of AHL, thereby acting as a repressor and blocking the access by RNA polymerase to the promoter [136]. In the presence of AHL, a repressor LuxR/signal complex is formed, resulting in a conformational change and dissociation of the complex. This allows access to the RNA polymerase [136]. An example of a repressor LuxR homologue is QscR in *Pseudomonas aeruginosa*.

Neither *Escherichia coli* nor *Salmonella enterica* sv. Typhimurium have the genes for any of the AHL synthases, but retain an orphan LuxR homologue known as SdiA [73, 75, 93, 94, 98, 109, 127, 137, 143, 144]. Since *E. coli* is unable to produce *N*-acylhomoserine lactones, the

**Table 2 - Phenotypic effects of known AHL systems in specific bacteria**

Bacterium	AHL	Synthase/Regulator system	Regulon phenotype	References
<i>Ps. aeruginosa</i>	<i>N</i> -butanoyl-L-HSL	RhlRI	Multiple extracellular enzymes Secondary metabolites Biofilm maturation Adhesion	[75, 93, 143, 144, 152]
	<i>N</i> -(3-oxododecanoyl)-L-HSL	LasRI	Multiple extracellular enzymes Biofilm formation Virulence Production	[75, 93, 143, 152]
<i>Serratia</i> spp.	<i>N</i> -butanoyl-L-HSL	SwrRI	Extracellular protease Swimming/Swarming	[75, 93, 143, 152]
<i>Yersinia</i> spp.	<i>N</i> -(3-oxohexanoyl)-L-HSL	YtbRI ( <i>Y. pseudotuberculosis</i> ) YpeRI ( <i>Y. pestis</i> )	Regulation of motility and clumping	[75, 93, 94, 137, 143, 153]
	<i>N</i> -hexanoyl-L-HSL	YtbRI	Regulation of motility and clumping	[75, 93, 94, 137, 143, 153]
	<i>N</i> -(3-oxodecanoyl)-L-HSL	YspRI	Regulation of motility and clumping	[75, 93, 94, 137, 143, 153]
<i>Erwinia</i> spp.	<i>N</i> -(3-oxooctanoyl)-L-HSL	ExpRI ( <i>E. caratovora</i> ) EsaRI ( <i>E. stewartii</i> )	Exo-enzymes Carbapenem antibiotics Exopolysaccharide Virulence Factors	[75, 93, 99, 109, 143, 154]
	<i>N</i> -(3-oxohexanoyl)-L-HSL		Carbapenem production	[154]
<i>Vibrio</i> spp.	<i>N</i> -(3-oxohexanoyl)-L-HSL	LuxRI ( <i>V. fischeri</i> )	Bioluminescence	[75, 93, 143]
	<i>N</i> -(3-hydroxybutanoyl)-L-HSL	LuxMN ( <i>V. harveyi</i> )	Bioluminescence Biofilm production	[75, 143, 144, 152]
<i>C. violaceum</i>	<i>N</i> -hexanoyl-L-HSL	CviRI	Violacein Antibiotics Exo-enzyme production Cyanide	[75, 93, 109, 143, 152]

response to exogenous quorum sensing molecules by the bacterium is not true quorum sensing. However, for the purposes of this study any comments regarding AHL-dependent QS by *E. coli* are in response to the observed effect of exogenous signal on the phenotypic behaviour of the population as a whole.

#### 1.3.1.1 SdiA and other Orphan LuxR Homologues

Orphan LuxR homologues are transcriptional regulators able to bind AHLs that do not have a cognate LuxI [136, 155]. These proteins retain the functional domains of a typical LuxR protein, enabling the bacterium to eavesdrop on signalling in the external milieu and co-ordinate their own behaviour [136, 140, 155, 156]. QscR of *Pseudomonas aeruginosa* and SdiA of *E. coli* and *S. enterica* sv. Typhimurium are examples of orphan LuxR homologues [136, 157].

The Suppressor of cell Division Inhibitor (SdiA) is a protein composed of 240 amino acids which can bind short chain AHLs [122, 138, 158, 159]. The two most potent AHLs tested, and potentially the cognate signal for SdiA, are *N*-(3-oxohexanoyl)-L-HSL and *N*-(3-oxo-octanoyl)-L-HSL, both of which are known to be produced by several bacteria (Table 3) [136, 155, 158].

In addition, Dyszel *et al* have determined that plasmid-encoded SdiA is able to detect *N*-(3-oxodecanoyl)-L-HSL and *N*-octanoyl-L-HSL [160].

Although the AHLs they detect may be different, Lindsay and Ahmer determined RhIR of *Ps. aeruginosa* and SdiA are closely related through similarities in their DNA binding site specificity [138, 158]. Upstream of *sdiA* is *yecC*, encoding an ATP binding component similar to that of an ABC transporter [155]. Downstream is *uvrY* in *E. coli* or *sirA* in *S. enterica* sv. Typhimurium, which are both transcription factors controlling virulence functions in all  $\gamma$ -proteobacterial pathogens, such as *Pseudomonas* spp. [155, 161].

SdiA has been better characterised in *Salmonella* spp. but there is 69% homology at amino acid level between SdiA in *Salmonella* and *E. coli* [136, 162]. In *Salmonella* spp. SdiA was

found to regulate the *rck* operon, which encodes a small outer membrane protein conferring resistance to complement killing whilst in a human host [136, 156, 158, 159, 163]. Encoded on a plasmid, the *rck* operon affects the ability of the bacteria to bind to extracellular proteins and epithelial cells [136, 164]. The *rck* operon encodes *srgC* and *srgD*, both of which are transcription factors involved in bacterial fitness. SdiA may thereby be associated with bacterial fitness in *Salmonella* spp. [161].

SdiA is the only known LuxR homologue in *E. coli* and was originally identified as a transcriptional activator of the *ftsQAZ* operon, encoding proteins essential for cell division [61, 101, 122, 165, 166]. By affecting this gene cluster, SdiA and therefore QS may regulate other cellular systems, specifically the cell cycle [134]. Overexpression of SdiA from a plasmid resulted in changes in pathogenic traits such as antibiotic resistance and appeared to have a negative regulatory effect on adhesion genes. However, when expressed from the chromosome these effects were not observed [138, 161, 167]. Clear differences exist between plasmid- and chromosomally-expressed *sdiA*. In the plasmid form, multiple copies of the gene were present in the cell, which would potentially increase the cellular level of SdiA. This in turn could result in differences in binding of co-factors due to the availability required for regulation of gene expression, resulting in a change in the expression profiles and resulting phenotypes. There may also be variation in the regulation of transcription between plasmid- and chromosome-expressed genes.

In *E. coli* *sdiA* is conserved between different strains [61]. Overexpression of SdiA in *E. coli* O157:H7 was found to negatively regulate transcription of both EspD and intimin, both of which are essential for intimate attachment to host epithelial cells [61, 134, 161, 168]. Hughes *et al* (cited in [138]) showed that SdiA binds the *ler* promoter, repressing LEE expression [138, 163, 169]. Sharma *et al* found a single chromosomal copy of *sdiA* in *E. coli* O157:H7 repressed flagellation, motility, adherence and fimbriation [170]. Dziva *et al* showed that a functional SdiA

is required for attachment to and colonisation of the gastrointestinal tract of 10-14 day old calves by *E. coli* O157:H7 [171].

Yakhnin *et al* determined that SdiA is regulated by CsrA, a conserved carbon storage regulator in *E. coli* which binds two sites within the *sdiA* promoter, thereby repressing translation [172]. Production of CsrBC as a response to increased CsrA levels would alleviate repression of *sdiA* by CsrA, thereby allowing expression of SdiA [172].

Active AHLs have only been found in the rumen of cattle, suggesting *E. coli* O157:H7 will only be exposed to QS signals early during their passage through the gut [169, 173]. Expression of AHLs and the composition of the bacterial population within the rumen of cattle were shown to be dependent on the time of year and diet [35, 163]. The effects of QS in the rumen remain largely unknown, although if the AHLs that are present do have a negative effect on the expression of the LEE genes, *E. coli* may utilise QS as an energy saving mechanism [35, 169, 173, 174]. By only up-regulating LEE in the hindgut where there is an absence of AHL, the bacterium would ensure successful colonisation of the optimal site, the hindgut [163, 169].

Cognate AHLs for SdiA in *E. coli* are still unidentified, although are most likely to be the same as those bound by SdiA in *Salmonella* spp. [140, 158]. As with other LuxR homologues, SdiA in *E. coli* undergoes a conformational change upon binding a cognate AHL. When *sdiA* is overexpressed binding of the cognate AHL was found to result in a switch from insoluble inclusion bodies to a soluble 3-dimensional folded structure [138, 140]. An SdiA box for targeted DNA binding has been identified in *E. coli* in the absence of AHL [159]. However, Zhou *et al* determined the same SdiA box was not present in *Salmonella* [162]. This suggested that other factors or proteins may be involved in determining the binding specificity of SdiA as a transcriptional activator [159, 162]. Links between SdiA function and biofilm formation have been reported for some strains of *E. coli* [121, 162].

### **1.3.2 AHL Structure and Function**

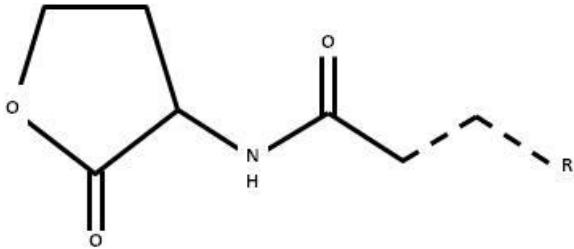
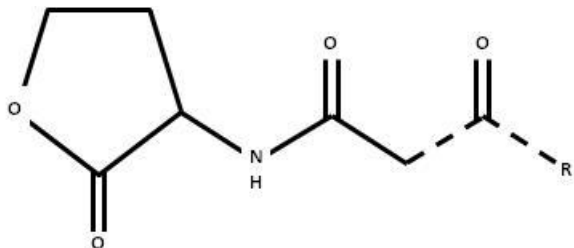
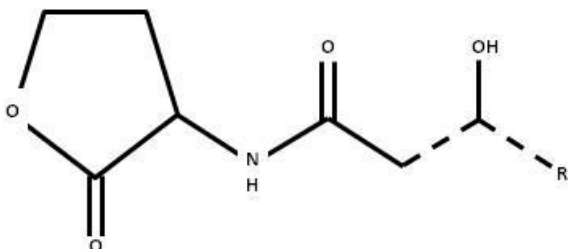
AHLs are composed of a homoserine lactone ring and a fatty acid side chain and are synthesised primarily through the actions of a LuxI synthase or homologue [73, 75, 93, 94, 98, 99, 109, 127, 146]. Acyl-acyl carrier proteins, such as acyl-CoA provide the fatty acid hydrocarbon tail, while S-adenosylmethionine (SAM) from the activated methyl cycle (AMC) is the source of the homoserine lactone ring [94, 109, 146]. LuxI acts as the catalyst for the formation of an amide bond between these two molecules [94, 110, 146]. Once the amide bond has been formed, lactonisation of the reaction intermediate and the release of methylthioadenosine lead to the formation of the AHL signal molecule [75].

All AHLs have the same homoserine lactone ring structure, but can vary in the length and structure of the fatty acid chain [73, 91, 143, 155, 175]. The side chain, or R-group, can be between 4 and 18 carbons in length, and can be unmodified, or may have a hydroxyl, oxygen or a fully reduced alkyl group on the third carbon (Figure 7) [91, 93, 94, 109, 127, 143, 155, 175].

In addition there are two stereoisomers of AHL, differing in orientation at the  $\alpha$ -centre of the lactone ring; the *L*-isomer and the *D*-isomer. The *L*-isomer is able to activate the ligand-binding domain of the LuxR protein, while the *D*-isomers are not [93].

Using radiolabelled *N*-(3-oxohexanoyl)-L-HSL both Kaplan and Greenberg and Pearson *et al* showed the AHL readily diffused across the membranes of *V. fischeri* and *E. coli* as both influx and efflux [176, 177].

Pearson *et al* compared the internalisation of *N*-butanoyl-L-HSL and *N*-(3-oxododecanoyl)-L-HSL in *Ps. aeruginosa* [178]. Both AHLs were found to diffuse into and out of the bacteria during the study. Using changes in concentration of the AHL, internal concentrations of *N*-butanoyl-L-HSL were observed to reach a steady level quickly which nearly equalled the external concentration of the AHL. This result suggested passive diffusion of the signal across the cell membrane. In contrast, *N*-(3-oxododecanoyl)-L-HSL took longer to reach a steady

Non-modified AHL	
<i>N</i> -(3-oxo)-DL-HSL	
<i>N</i> -(3-hydroxy)-DL-HSL	

**Figure 7 - Chemical structures of non-modified and modified AHLs**

Adapted from [93, 94, 127]. The dotted lines represent the R-groups which differ in length and modification.



concentration, which was higher inside the cell compared to the external milieu. Further investigation suggested active efflux of the long chain AHL out of *Ps. aeruginosa* required the MexAB-OprM efflux pump [178]. These observations in *Ps. aeruginosa* suggest mechanistic differences in AHL uptake depending on chain length, which is likely to be conserved across bacterial species [98, 109, 178].

The length of the fatty acid chain affects the physical characteristics of the signals, such as solubility, mobility and hydrophobicity [175]. An AHL with a side chain of between 4 and 8 carbons in length, classed as short chain AHLs, are highly soluble in water and readily diffuse across the bacterial cell membrane [175]. The AHLs with the longer R-groups become progressively less soluble as the number of carbons increases, and the ability to diffuse across the cell membrane decreases in relation to the size of the molecule [98, 175]. When modified, for example addition of an oxo-group to the third carbon, the molecule becomes more hydrophilic and solubility in water increases, however the diffusion across the membrane is unchanged from the non-modified form [143, 175].

The structure and thereby activity of AHLs can also be affected by pH and enzyme activity [103]. In order to maintain the structure of the homoserine lactone ring, a more acidic pH is required [73, 93]. Exposure to a pH of more than 6.5 for an extended period resulted in the opening of the lactone ring, thereby rendering the AHL inactive [93]. By decreasing the pH to between pH1 and 2 for up to 24 hours the lactone ring can be reformed, activating the AHL molecule [93, 94] (Personal Communication, Williams. P, February 2010). The long chain AHLs are more resistant to alkaline hydrolysis compared to the short chain and modified AHLs, but prolonged exposure also caused adverse changes in structure of these longer signal molecules [103, 175].

Enzymes produced by some gram positive and gram negative bacteria can inactivate the AHLs. Lactonases open the lactone ring by hydrolysing the ester bond, whilst acylases cleave

the side chain by hydrolysis of the amide bond between the fatty acid and the lactone ring [73, 100, 110]. These enzymes decrease the amount of gram-negative specific signal in the external milieu, thereby reducing the potential for interspecies competition within a given niche [110].

#### 1.3.2.1 Phenotypic switching

AHL synthesis occurs constitutively at a low level, maintaining a background concentration of the signal in the external milieu [139, 179]. The concentration of signal has been shown to increase relative to cell density [75]. Upon achieving a critical signal concentration threshold which reflects the size of the population, synthesis of specific AHL signals would rapidly increase as a result of a positive transcription feedback loop. The signals bind the cognate LuxR protein resulting in a phenotypic change in the bacterial population (Figure 8) [61, 75, 98, 155, 165]. As the signal is internalised or the bacterial population is reduced through translocation from the defined QS area, the concentration of AHL would decrease giving rise to an oscillating pattern of AHL production [61, 75, 98, 155, 165].

The phenotypic switch in the bacterial population is a result of up- or down-regulation of transcription [75, 94, 110]. These changes alter the regulation of pathogenic traits, such as production of toxins, or of secondary metabolites such as antimicrobials, proteases or siderophores (Table 2) [143, 155]. An important target for regulator binding is the *luxI* promoter as this increases signal production further [155].

#### 1.3.3 *Pseudomonas aeruginosa* – a complex example of a QS hierarchy

QS regulation has been extensively studied in *Ps. aeruginosa*. In addition, this bacterium is also one of the most complex examples as it utilises a multi-level hierarchy involving 2 interconnected QS operons and regulons, which are tied into cell behaviour via an extensive network of orphan LuxR homologues and other transcriptional regulators [77, 177, 180-182]. This provides a good

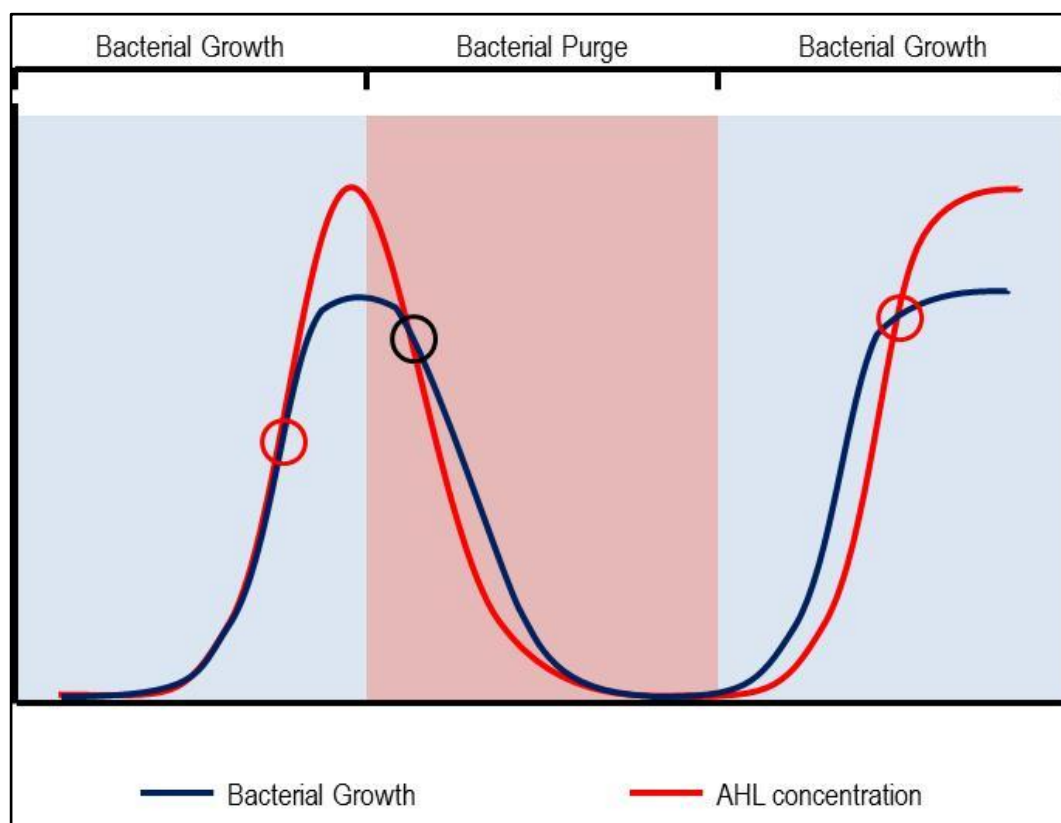


**Figure 8 - AHL synthesis in relation to changing population density in *Euprymna scolopes*, the Hawaiian bobtail squid**

Schematic representation of the AHL concentration in relation to population density produced using information from [75, 144, 183, 184]. The red circle represents the rapid increase in AHL biosynthesis and the phenotypic switch in population behaviour, and the black circle represents the point at which the synthase is inhibited and the population switches back to the original phenotype.

model for studying the role of quorum sensing in the regulation of gene transcription and pathogenicity traits.

This opportunistic pathogen is associated with infection of immune-compromised human hosts resulting in bronchial and respiratory problems [73]. *Ps. aeruginosa* is the primary pathogen in the lungs of cystic fibrosis patients where it produces dense and complex biofilms [72, 74-78]. By secreting extracellular virulence factors such as toxins, pyocyanin, haemolysins and proteases, this pathogen can cause extensive damage to host tissues [73, 77]. Regulation of these pathogenic traits is via at least 3 QS systems, the combination of which increases the flexibility of coordinating phenotypic changes through the use of multiple signals [73, 98]. Gobetti *et al* estimate 6-10% of *Ps. aeruginosa* chromosomal genes are regulated by AHL-controlled QS [91, 96, 185, 186]. In addition to these 'true' QS systems, an orphan LuxR homologue, QscR, and other unrelated QS factors have been identified as part of the pathogenicity regulon [73, 75, 109]. Furthermore, QS signals from *Ps. aeruginosa* have been isolated from the sputum of cystic fibrosis patients [77, 78].

A hierarchical quorum sensing cascade of AHL-based systems exists within *Ps. aeruginosa* linking LasRI, RhIRI, 4-quinolone (PQS) signalling, QscR and VqsR [98, 110]. A schematic of the interconnections between the AHL-systems in *Ps. aeruginosa* strain PA01 is shown in Figure 9.

#### 1.3.3.1 LasRI and RhIRI

LasI and RhII are LuxI homologues which produce *N*-(3-oxododecanoyl)-L-HSL and *N*-butanoyl-L-HSL respectively [73, 75, 77, 93, 94, 109, 182, 185]. Although these are the cognate signals, the transcriptional regulators LasR and RhIR can bind molecules with a similar structure [76, 77, 109, 110, 139, 141]. Most importantly in the hierarchical scheme, activation of LasR by the cognate AHL initiates up regulation of RhII, thereby resulting in production of *N*-butanoyl-L-HSL

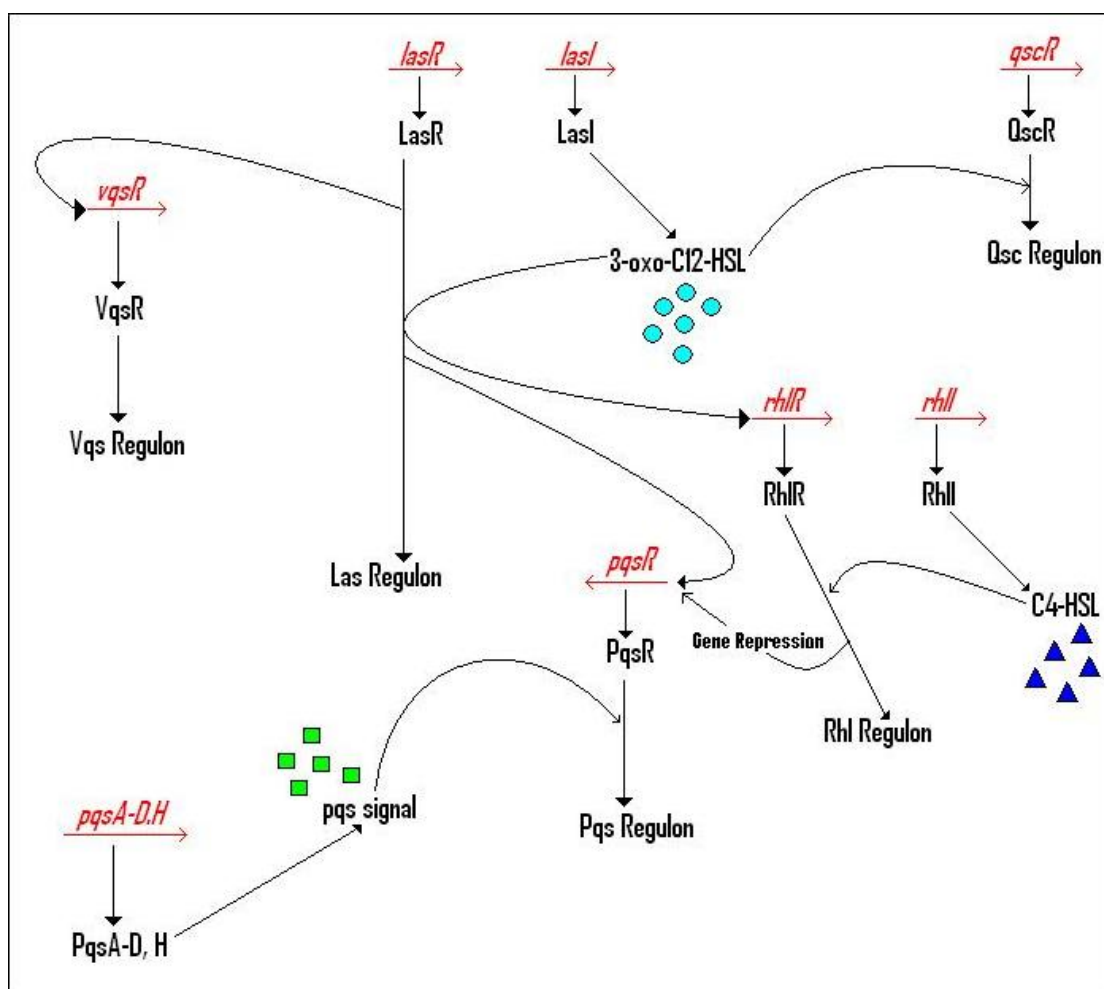


**Figure 9 – Quorum sensing regulatory pathways in *Pseudomonas aeruginosa***

This illustration is adapted from [98].

(Red) Genes

(Black) Proteins and phenotypes

(▲ ■ ●) Different signals differentiated by shape and colour

and the activation of RhIR [185]. Although generally observed working concurrently, it has been observed that these systems can work independently [185]. LasR primarily binds *N*-(3-oxododecanoyl)-DL-HSL, but *N*-(3-oxohexanoyl)-DL-HSL has also been shown to initiate phenotypic switching, albeit generating a weaker response than with the cognate AHL [75, 143, 187].

RhIR and LasR modulate a quorum sensing regulon comprising an overlapping set of genes equivalent to 6% of the genome [96, 182, 186]. These two systems regulate production of elastase (LasB), LasA protease (*lasA*), alkaline protease (*apr*), exotoxin A (*toxA*), cytotoxic PA-IL/LecA lectin (*pa-IL/lecA*), chitinase, hydrogen cyanide, pyocyanin, rhamnolipids and siderophores [73, 75, 77, 94, 97, 109, 182, 185, 188, 189].

QS was found to affect lectin production, a form of adhesin, in *Ps. aeruginosa* [73, 75, 77, 94, 97, 109, 182, 185, 188]. Winzer *et al* identified a putative *lux* box upstream of *lecA* [97]. The LasRI system activated expression of *lecA* at a background level only, whereas RhIRI up-regulated gene expression leading to increased lectin production [97]. Since LasRI is the main QS system in *Ps. aeruginosa*, lectin production, although controlled by RhIRI, is under hierarchical regulation of LasRI. Other growth factors may be required in addition to RhIRI and the associated AHLs for successful and prolonged up-regulation of lectin production, including RpoS, a regulator of general stress responses to heat, low pH, high osmolarity, hydrogen peroxide and ethanol [97].

#### 1.3.3.2 PQS, QscR and VqsR

The *Pseudomonas* quinolone signal (PQS) [2-heptyl-3-hydroxy-4(1*H*)-quinolone] has been found to regulate secondary metabolites such as elastase, pyocyanin, LecA (a galactophilic lectin), and rhamnolipids. In addition PQS is also involved in the regulation of biofilm production and iron chelation [94, 96, 186, 189, 190]. PQS and *N*-(3-oxododecanoyl)-L-HSL have host immune

modulation actions [94]. Although a QS signal in its own right, PQS is under hierarchical control of LasRI and RhIRI through regulation of the conversion of the precursor HHQ to PQS [94, 96, 186, 189, 190].

Two other putative QS systems in *Ps. aeruginosa*, QscR and VqsR, are genetically unlinked to any of the other 3 systems identified above [185].

QscR, or the quorum sensing control regulator, is an orphan LuxR homologue [136]. A mutation in *qscR* resulted in a hypervirulent strain of the bacterium producing excess phenazine pigment indicated by the formation of blue colonies [136, 191]. QscR has been shown to respond to *N*-(3-oxodecanoyl)-L-HSL, *N*-dodecanoyl-L-HSL and *N*-(3-oxododecanoyl)-L-HSL, suggesting that QscR may respond to signals produced by other bacteria in addition to those produced through the LasRI system [136, 157, 180]. LuxR proteins have been shown to function as active homodimers, which become inactive upon formation of heterodimers [136, 157, 185]. By initiating production of heterodimers QscR represses *lasR* expression during the early stages of bacterial growth, thereby allowing the concentration of *N*-(3-oxododecanoyl)-L-HSL to increase in the external milieu [185]. A main function of QscR is as a repressor of *lasI* during early growth of the bacterium by forming inactive heterodimers with LasR and RhIR [185, 191]. Once the threshold concentration of AHL has been exceeded the signals compete with QscR for binding to other LuxR homologues, initiating disassociation of the heterodimers back into homodimers thereby lifting the repression of the regulator proteins [185].

VqsR, the virulence and quorum sensing regulator, is a LuxR-type regulator, which contains the DNA-binding motif found in all LuxR proteins, but lacks the autoinducer-binding domain [136]. Raina *et al* state that *vqsR* knockout mutants exhibit a reduction in AHL production due to lower expression of *LasI*, virulence determinant production decreases as a result, and lower pathogenicity in some infection models has been noted [185] [73]. The expression of *vqsR* is controlled by LasR [73, 181].

## **1.4 Autoinducer-2 (AI-2)**

*E. coli* utilise both the AHL-dependent signalling and the AI-2 systems. Autoinducer 2 is a small signalling molecule released by many bacterial species such as *V. harveyi*, *E. coli* and *S. enterica* sv. Typhimurium [73, 75, 94, 95, 192]. As this molecule can be produced and utilised by some Gram-positive and Gram-negative bacteria, it is often described as a 'universal' signal, sometimes nicknamed 'Bacterial Esperanto' [75, 91, 94, 193, 194]. The precursor to AI-2, known as DPD, is produced by most bacteria as a metabolic by-product of the activated methyl cycle (AMC), but not all bacteria use the resultant AI-2 molecule as a QS signal [94, 194].

### **1.4.1 AI-2 Synthesis**

The umbrella term 'AI-2' is used to describe all autoinducing molecules derived as a by-product of the AMC (Figure 10) [110, 195]. The structure and function of AI-2 is conserved, but the stabilising cation can be different. This variation is a result of the number of bacteria producing a different form of the signal, in addition to the different environments and available ions. AI-2 molecules are proposed to be a mixture of boronated, hydrated and cyclic complexes [192, 196]. Although varied, there remains sufficient similarity for AI-2 produced by one species of bacteria to be recognised by the ligand binding domains of another [197]. For example, *V. harveyi* produces a furanosyl borate diester ([2S, 4S]-2-methyl-2,3,3,4-tetrahydroxytetrahydrofuran-borate [S-THMF-borate]), while *S. enterica* sv. Typhimurium produces a non-boronated form ([2R,4S]-2-methyl-2,3,3,4-tetrahydroxytetrahydrofuran [R-THMF]) [98, 192, 198].

The AMC utilises methionine to generate homocysteine, adenine and adenosine through a series of enzymatic activities (Figure 10). S-adenosylmethionine (SAM) is essential for synthesis of cellular components as well as for regulation, and is the main methyl donor in eukaryotic, archaeobacterial and eubacterial cells [91]. Methyl is important in bacterial systems for activation of enzymes, production of amino acids and protection of its own DNA against enzymes



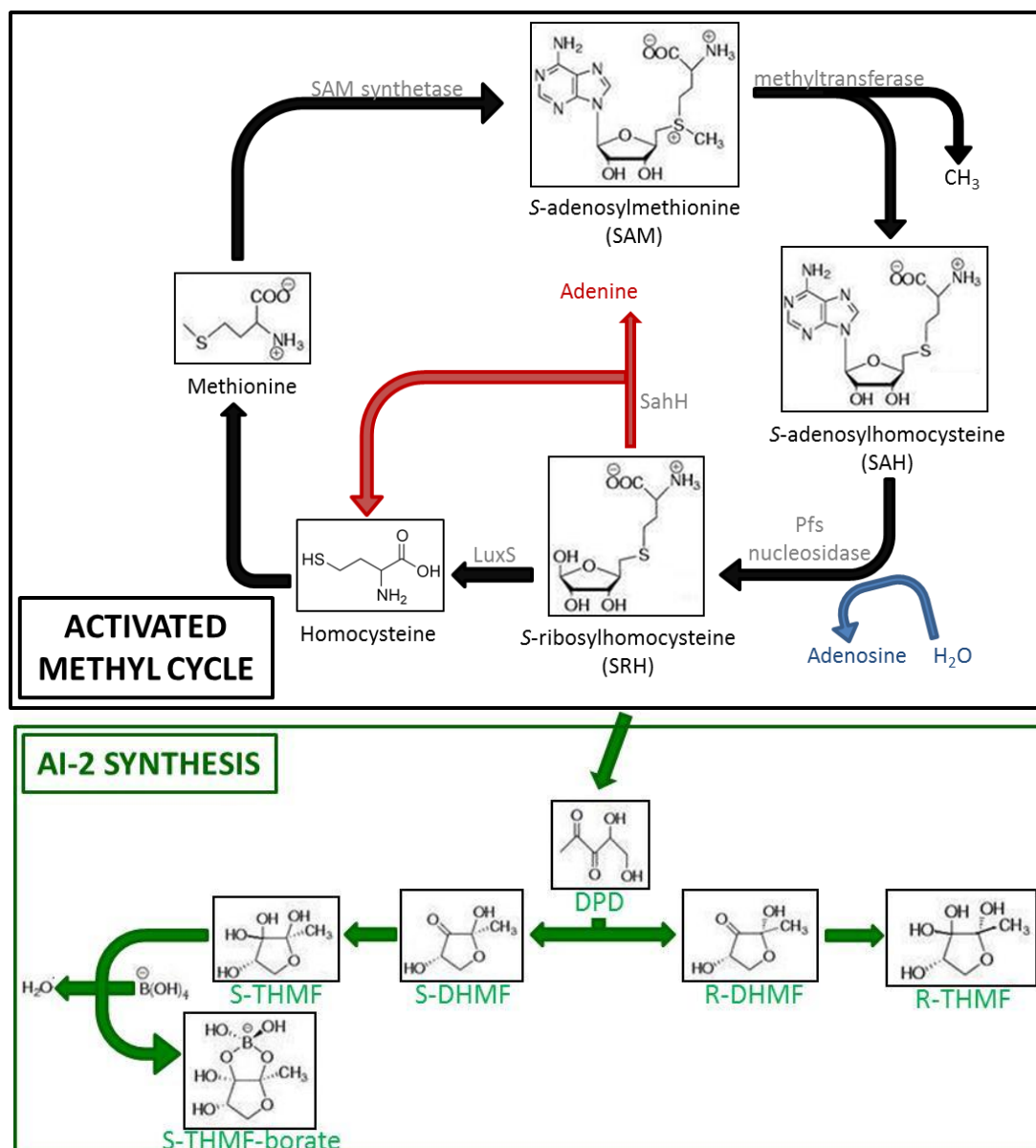


**Figure 10 - Schematic of the activated methyl cycle and synthesis of AI-2**

S-THMF-borate is produced by *Vibrio* spp. and R-THMF is produced by *Salmonella enterica* sv. Typhimurium and *E. coli*.

which remove foreign DNA. The AI-2 precursor 4,5-hydroxy-2,3-pentanedione (DPD) is a metabolic by-product of enzymatic cleavage by LuxS of S-ribosylhomocysteine (SRH) to regenerate homocysteine [73, 91, 94, 110, 162, 192, 195, 199].

DPD is a single molecule derived from S-ribosylhomocysteine and the synthesis pathway has been shown to be identical in several bacterial species, including *Vibrio*, *E. coli* and *Salmonella* [91, 192]. The exact mechanism of conversion from DPD to an AI-2 molecule is unknown, however Miller *et al* proposed the conversion of DPD to either (2*R*, 4*S*) - or (2*S*, 4*S*)-2, 4-dihydroxy-2-methyldihydrofuran-3-one (*R*- and *S*-DHMF respectively) initially, prior to conversion to either *R*- or *S*-THMF [110, 198]. *V. harveyi* produces a furanosyl borate diester. Borate is available in high concentrations in the marine environment of these bacteria, and readily reacts with hydroxyl groups on the furanosyl rings acting to stabilise the molecule. This suggests S-THMF-borate is created as a spontaneous chemical reaction due to the highly reactive state of the molecules [94, 98, 198].

Swift *et al* hypothesised the variation in structure of the AI-2 signalling molecules implied alternative function, for example a role purely in metabolism as opposed to QS involvement [98].

As a QS molecule, AI-2 concentrations proportionally increase extracellularly as the cell density rises [91, 183, 184, 200]. For each SRH molecule used a single DPD molecule is produced. This 1:1 ratio continues as the bacterial population continues to increase [91]. If the bacterial population decreases then DPD and therefore AI-2 production will reduce in proportion to the slowing of the AMC [91]. Binding of AI-2 to a periplasmic protein with subsequent interaction with a transporter results in activation of a phosphorylation cascade ultimately resulting in a change in gene expression [201].

### **1.4.2 LuxS**

Highly conserved homologues of *luxS* have been identified in over 30 species of bacteria, including *Salmonella*, *Campylobacter*, *Staphylococcus* and *Clostridium* [91]. Deletion or mutation of LuxS eliminates AI-2 production [202]. Regulation of motility genes and flagella expression has been linked to LuxS and AI-2 signalling in *E. coli* K-12 and EHEC [98, 203].

LuxS is a small metalloenzyme of approximately 170 amino acids in size, existing as a homodimer with two identical active sites [195]. The active sites each contain an Fe<sup>2+</sup> ion which catalyses a redox reaction within the protein [195]. Within the LuxS sequence is a tyrosine kinase phosphorylation site [195]. Activation of this phosphorylation site has been associated with exopolysaccharide production, and has also been linked to biofilm formation in *Salmonella enterica* sv. Typhimurium [102, 195]. It is unclear whether this is through LuxS expression or as a direct result of AI-2.

The role of AI-2 and LuxS is a source of scientific debate. One school of thought suggests a global regulatory system, while the other primarily a metabolic function [94]. LuxS is vital for the AMC, producing AI-2 as a metabolic by-product [195]. To strengthen this metabolic theory *luxS* and *pfs* (encoding the Pfs nucleosidase enzyme) are located adjacent to other genes exerting metabolic activity on the AMC [194]. This suggested LuxS is the enzyme primarily responsible for the detoxification of S-adenosylhomocysteine (SAH) [195]. AI-2 has therefore been associated more with growth and cell proliferation rather than strictly to high cell density and QS [194, 195].

### **1.4.3 Phenotypic Switching**

In *E. coli* and *Salmonella enterica* sv. Typhimurium DPD is converted to R-THMF [98, 192, 198]. AI-2 binds the LuxS-regulated protein B (LsrB), a periplasmic binding protein that is part of the ABC transporter encoded by the *lsrACDBFGE* operon which transports AI-2 into *Salmonella* [73,

192, 200]. The *lsr* operon of *Salmonella* spp. and the *b1513* operon in *E. coli* are homologous [195, 200].

In both *E. coli* and *Salmonella* once the threshold concentration of AI-2 in the external milieu has been reached, the signal is transported into the cell by LsrCD, two transmembrane proteins. LsrA, a cytoplasmic protein responsible for ATP hydrolysis is also required for transport. Once in the cytosol LsrK, a protein kinase, phosphorylates the AI-2 molecule [162, 204-206]. Phospho-AI-2 binds a suppressor of the *lsrACDBFGE* operon, LsrR [73, 162, 179, 200, 204]. By binding LsrR repression of the Lsr transporter is lifted initiating active transport of higher concentrations of AI-2 into the cell [73, 162, 179, 200, 204]. During the stationary phase of growth by both *E. coli* and *Salmonella* a rapid decline in the concentration of available AI-2 was observed. This decrease in AI-2 concentration in the external milieu was proposed to be as a result of the transport of high concentrations of the signal into the cells via the LsrCDA transporter during late exponential phase of growth [195, 206]. Prolonged production of AI-2 requires a carbon source, for example glucose to maintain the AMC and continued SRH production [102, 195].

AI-2 signalling in diarrheagenic *E. coli* has been linked to a change in virulence gene expression [58, 99, 109]. LuxS, and thereby AI-2, was shown to affect the expression of the LEE locus [58, 95, 201]. Raina *et al* identified 242 genes, comprising between 5-10% of the *E. coli* genome that were associated with virulence or cell division and expression was affected by the presence of AI-2 [185]. Cell division, rRNA and tRNA genes were found to be down-regulated by the AI-2/regulator complex, while flagella biogenesis, chemotaxis and motility genes were found to be up-regulated [185, 207]. Zhu *et al* showed that LuxS was required for initiation of a signal transduction cascade resulting in the expression of the LEE operon in *E. coli* [208]. Over-expression of LuxS resulted in up-regulation of the LEE genes, while concurrent down-regulation of attachment genes caused the bacteria to become less virulent than the wild type [58, 208].

The most studied example of AI-2 signalling is in *Vibrio* spp. which produce bioluminescence in response to QS. This bacterium also provides a good example of AI-2 and AHL systems working in conjunction to produce a response.

#### **1.4.4 *Vibrio* spp. – an example of the similarities of function in two QS systems**

*Vibrio fischeri* and *Vibrio harveyi* produce bioluminescence, the expression of which is under QS regulation. *V. fischeri* are responsible for the light produced by *Euprymna scolopes* (Hawaiian bobtail squid) and *Ceratiidae* spp. (Deep sea angler fish). In these creatures, the bacteria exist in symbiosis with the host in the light organ where they produce bioluminescence when at a sufficient cell density [209]. The bacteria do not enter the host cells, but rather remain in high concentrations within the tubules and canals of the light organ [209].

Bioluminescence production by *V. fischeri*, previously known as *Photobacterium fischeri*, was linked to growth in the late 1960s, when a period of variable, but low level bioluminescence was observed during the lag phase of growth but which increased during exponential phase [106]. Inoculation of exponential phase *V. fischeri* cells into fresh medium resulted in an initial loss of bioluminescence production, which was reinitiated once the new culture reached exponential growth phase [107]. This highlighted the link between cell density and bioluminescence production, suggesting regulation via autoinduction [107]. It took many more years to determine AI-2 was an important factor in cell-density-mediated phenotypes, after a similar phenomenon was observed with a specific AHL signal and the trait termed quorum sensing.

Quorum sensing, as a mechanism, was first described in *V. fischeri* [91, 110]. *Vibrio* spp. utilise three QS systems; Autoinducer-1 (AHL), AI-2 and CA-1. CA-1 is a long chain  $\alpha$ -hydroxyketone, and together with these other signals functions through LuxO [94]. High concentrations of either a specific AHL or AI-2 resulted in either a change in colony morphology

or in the production of bioluminescence and iron-chelating siderophores [197]. Both AHL and AI-2 signals are dependent on the metabolism of methionine through the AMC for synthesis [197]. SAM and an acyl-acyl carrier protein are required for AHL synthesis [91]. AHL and AI-2 in *Vibrio* spp. activate a phosphorylation cascade which terminates with DNA binding by a phosphorylated transcriptional regulator [100].

The principle AHL molecule used by *V. fischeri* is *N*-(3-oxohexanoyl)-L-HSL, produced by the signal synthase LuxI [149]. At low cell density the signal molecule diffuses out of the cell into the external milieu, but as the cell density increases the concentration of the signal inside and outside the cell equalises, resulting in activation of transcription [111]. The genes responsible for bioluminescence production are located in the *luxCDABEGH* operon, alongside *luxI* [149]. The AHL molecule forms a complex with LuxR, which binds to the *lux* box activating DNA transcription and ultimately bioluminescence production [91, 149].

#### 1.4.4.1 *Vibrio harveyi*

The AHL and AI-2 systems are interconnected in *Vibrio* spp. with sensory information shared and integrated through a regulatory network controlling bioluminescence (Figure 11) [202]. In *V. harveyi* the predominant AHL signal is *N*-(3-hydroxybutanoyl)-L-HSL produced via LuxM, a LuxI homologue [94]. The AHL activates the periplasmic sensor kinase LuxN when at high concentrations [165, 210]. LuxN phosphorylates LuxU, a signal regulator (Figure 11) [98]. If *N*-(3-hydroxy-butyryl)-L-HSL is absent, induction of LuxN does not occur and the signal therefore undergoes autophosphorylation [98]. This triggers a phosphorylation cascade involving LuxU and LuxO resulting in expression of a series of small RNA molecules destabilising the messenger RNA encoding LuxR, thereby inhibiting bioluminescence production [94, 98]. Exogenous AI-2 binds LuxP, a periplasmic protein belonging to a large family of binding proteins including LsrB in *Salmonella* spp., although these two proteins share low homology [73, 192, 201, 205].



The formation of the LuxP/AI-2 complex initiates dephosphorylation of LuxQ, a sensor kinase responsible for detecting AI-2 in *Vibrio* spp. [98, 99, 201, 212]. The phosphate is transferred to LuxU. At low cell density LuxQ is autophosphorylated in a similar way to LuxN in the AHL system [94, 98, 212].

In both systems phospho-LuxU inactivates LuxO by phosphorylation [94, 212]. Once LuxO has been inactivated, expression of the transcriptional activator LuxR is initiated. LuxR activates the *luxCDABEGH* operon resulting in bioluminescence production (Figure 11) [98, 165, 213].

## **1.5 Quorum Sensing and Food Safety**

Aerobically-packed meat contains microbiota on the surface composed largely of *Ps. aeruginosa* and Enterobacteriaceae spp. [42, 45, 91, 153, 214, 215]. The majority of these bacteria are able to produce AHLs [91, 214, 216]. *Ps. aeruginosa* is able to utilise quorum sensing in the production of biofilms on meat surfaces thereby acting to increase spoilage (Table 2) [91, 153, 215, 217]. While not directly affecting spoilage the AHL signals stimulate increased enzyme production in Enterobacteriaceae spp. at particular cell densities, contributing to changes in meat quality even when at relatively low bacterial loads [91, 138, 214, 215]. In vacuum-packed meat some species of *Hafnia* and *Serratia* have been recorded, both of which are known to produce AHLs [91, 214, 218].

Varying concentrations of AI-2 on or in foodstuffs may explain differences in shelf life and changes in virulence of enteric bacteria [219]. Low levels of AI-2 have been observed in meat products, with higher concentrations derived from milk and yoghurt [219]. It has been reported that AI-2 affects the survival of *E. coli* O157:H7 cells *in vivo*, increasing their ability to replicate and persist [220, 221]. However, in ground beef extract an inhibitory effect on survival was observed [220, 221]. Exposure of *E. coli* K-12 to sodium acetate decreased AI-2 production while



other substrates such as acetic acid increase *luxS* expression, both of which are used in food production [219].

## **1.6 Infection Models of Pathogenicity**

*Galleria mellonella*, the greater wax moth larvae are found in most inhabited parts of the world. These insects are an excellent model organism for *in vivo* investigation of pathogenicity and toxicology testing [222-225]. *G. mellonella* share some innate immune responses in common with mammals. These include cellular responses, such as phagocytes, plasmocytes and granulocytes, and humoral responses such as lysozyme, lectins, protease and carbohydrases, in addition to simple structural and passive barriers [222-225]. The presence of these immune responses allows the use of these larvae as an infection model, monitoring death rate after injection of pathogenic bacteria as a method of comparing virulence [222-225]. Melanin is produced by these larvae in response to stress, turning the naturally beige larvae to varying shades of brown/black. If the larvae expire as a result of natural causes such as asphyxiation, or if death is instantaneous following application of chemicals such as insect spray during euthanasia the larvae do not produce melanin. The hue of the pigment is relative to the pathogenicity of the injected bacteria [222-225].

## **1.7 Research Hypotheses**

Quorum sensing can be part of a complex regulatory network of interconnecting signals and regulatory proteins as is the case with *Pseudomonas aeruginosa*, or an individual protein allowing selective advantage by eavesdropping on signals from other bacteria, such as SdiA in *E. coli*. By utilising these cell-density-dependent systems bacteria can initiate phenotypic changes at the optimal time, thereby reacting to selective pressure and persisting within a specific niche.

Although non-pathogenic to cattle, *Escherichia coli* O157:H7 remains a major concern for human health and food safety. Transference of this pathogen from faeces and hide onto the carcass at the time of slaughter poses a serious risk for infection and will have economic consequences for red meat industries in some countries, including New Zealand.

This project is part of the Improved Pathogen Control Technologies (IMPACT) programme which aims to identify whether quorum sensing could be used as a mitigation strategy for reducing *E. coli* O157:H7 on New Zealand cows. The overall aim of this project is to identify the role of quorum sensing and environment on phenotypic traits within *E. coli*, and produce biological data that can be used to develop a model *in silico* of the regulatory effects.

The project has four hypotheses:

1. Do AHLs affect the motility and aggregation phenotypes of EPEC and EHEC strains?

Motility and aggregation are important phenotypes in the infection model utilised by both EPEC and EHEC. *E. coli* cannot produce AHL, and so by adding specific exogenous signals at physiological concentrations, the effects on these behaviours can be evaluated.

2. Do complex regulatory pathways exist in *E. coli* controlling motility and aggregation?

Bacteria utilise interconnecting regulatory pathways to control expression of phenotypic traits. Due to the dual lifestyle of both EPEC and EHEC, it is likely part of this regulation is in response to environmental cues. Using knockout mutants and changes in growth conditions the regulatory pathways and effectors can be identified.

3. Does AHL affect the virulence of EPEC and EHEC strains?

If AHL is shown to affect aggregation, it is likely changes in virulence will be observed. This would result from changes in physical characteristics and expression of virulence genes. Infection of tissues *in vitro* and *in vivo* would allow confirmation of this hypothesis.

4. Do all EHEC isolates behave the same way?

*E. coli* O157:H7 exist in high numbers in the bovine reservoir and must survive both internal and external to the host. There is a high probability that DNA transfer occurs under these conditions, leading to a genetically diverse population. By monitoring a small subset of isolates for differences in phenotypic behaviour, it would be possible to determine if this is likely.

## **2 Materials and Methods**

### **2.1 Growth Media, Diluents and Supplements**

#### **2.1.1 Luria Broth (LB)**

1.0% tryptone (w/v), 0.5% yeast extract (w/v), 0.5% sodium chloride (w/v) was dissolved in deionised water. The pH was adjusted to between 6.9 and 7.1 using NaOH or HCl. Media was sterilised by autoclaving at 121°C for 20 minutes and stored at 4°C until required.

#### **2.1.2 Luria Agar (LA)**

1.5% (w/v) BD Bacto™ agar (Becton, Dickinson and Co.) was added to LB prior to autoclaving. Media was boiled for 1-2 minutes to dissolve the agar prior sterilisation. After autoclaving molten agar was tempered to 48°C in a waterbath prior to pouring.

Semi-solid LA was produced by the addition of 0.6% (w/v) or 0.3% (w/v) agar as required.

#### **2.1.3 Marine Agar**

Marine broth (BD Difco™; Becton, Dickinson and Co.) was prepared according to the manufacturer's instructions. 1.5% (w/v) BD Bacto™ agar (Becton, Dickinson and Co.) agar was added and the mixture boiled for 2 minutes prior to autoclaving.

#### **2.1.4 Autoinducer Bioassay Media (AB)**

AB media was produced as described by Greenberg *et al* [226]. 1.75% (w/v) sodium chloride, 0.6% (w/v) magnesium sulphate (Sigma-Aldrich) and 0.2% (w/v) vitamin-free casamino acids (BD Difco™; Becton, Dickinson and Co.) were dissolved in deionised water to produce the AB base. The pH was adjusted to 7.5 prior to autoclaving at 121°C for 20 minutes. 384 ml AB base was supplemented with 4 ml 1M potassium phosphate buffer. The buffer was composed of 6.15 ml

1M di-potassium phosphate and 3.85 ml 1M mono-potassium phosphate. 4 ml 0.1M *L*-arginine stock and 8 ml of a 50% glycerol stock solution were also added. All supplements were filter-sterilised using a 0.22 µm syringe-filter (Millex GP, filter type PES) prior to addition. Both AB base and the supplemented AB media were stored at 4°C until required.

#### **2.1.5 Autoinducing Bioassay Agar**

1.5% (w/v) BD Bacto™ agar (Becton, Dickinson and Co.) was added to AB base and boiled for 1 minute prior to sterilisation by autoclaving. The pH was adjusted to 7.5 prior to autoclaving at 121°C for 20 minutes. The agar was tempered to 48°C in a waterbath. 384 ml AB base was supplemented with 4 ml 1M potassium phosphate buffer. The buffer was composed of 6.15 ml 1M di-potassium phosphate and 3.85 ml 1M mono-potassium phosphate. 4 ml 0.1M *L*-arginine stock and 8 ml of a 50% glycerol stock solution were also added. All supplements were filter-sterilised using a 0.22 µm syringe-filter (Millex GP, filter type PES) prior to addition.

#### **2.1.6 Phosphate Buffered Saline (PBS)**

1 tablet (Lorne Laboratories, UK) was dissolved in 1 litre deionised water and sterilised by autoclaving at 121°C for 20 minutes. PBS was stored at 4°C until required.

#### **2.1.7 Antibiotic Solutions**

50 mg/ml carbenicillin stock solutions were prepared in 50% ethanol and stored at -20°C until required. Carbenicillin was used at a final concentration of 50 µg/ml unless otherwise stated.

50 mg/ml kanamycin stock solutions were prepared in sterile water and stored at -20°C until required. Kanamycin was used at a final concentration of 50 µg/ml final concentration unless otherwise stated.

5 mg/ml tetracycline stock solutions were prepared in 50% ethanol. Tetracycline was used at a final concentration of 5 µg/ml unless otherwise stated.

### **2.1.8 N-acylhomoserine Lactones (AHLs)**

All AHLs were resuspended in ethyl acetate (BDH Ltd) and stored at room temperature (Table 5). Stock solutions were prepared at concentrations of 10 µM, 1 mM and 100 mM. AHLs were used at a final concentration of 5 nM, unless otherwise stated. *L*-isomers of the AHLs were obtained from Sigma-Aldrich (New Zealand) and the *D*-isomers were obtained from the School of Molecular Medical Sciences, Nottingham (UK).

## **2.2 Bacterial Strains and Plasmids**

Bacteria species and strains used in this work are summarised in Tables 3 and 4. Plasmids used during this study, and the bioreporter specificity are shown in Table 5.

## **2.3 Autoinducer-2 Bioassays**

### **2.3.1 Conditioned Media (CM) Production**

All strains used to prepare CM were grown for 8 hours with shaking at 100 rpm. *Vibrio harveyi* BB120 was grown in AB broth at 30°C, *E. coli* and *Pseudomonas aeruginosa* were grown in LB at 37°C. Psychrotolerant Enterobacteriaceae *Hafnia alvei*, *Rahnella aquatilis* and *Serratia* were grown at 25°C. Bacterial cultures were centrifuged at 5310 x *g* for 10 minutes (Heraeus Multifuge 3 S-R, Rotor 6335) to pellet the cells. The resulting supernatant was filter-sterilised using a 0.22 µm syringe filter (Millex GP, filter type PES)[101, 227]. CM was stored at -20°C until required.

**Table 3 – *Escherichia coli* isolates used during this study**

Strain	Scientific Code	Distinguishing Characteristics**	Source or reference	Growth Conditions
E2348/69		O127:H6 EPEC	Levine <i>et al</i> [228]	37°C on LA/LB
E2348/69 SS*		O127:H6 EPEC	Levine <i>et al</i> [228]	
E2348/69 <i>hosA</i>	II150	$\Delta$ <i>hosA</i>	Ferrándiz <i>et al</i> [68]	
E2348/69 <i>bfpA</i>	UMD901	<i>bfpA</i>	Zhang and Donnenberg [229]	
E2348/69 MAR001	MAR001	$\Delta$ EAF plasmid	Baldini <i>et al</i> [230]	
E2348/69 <i>espA</i>	UMD872	$\Delta$ <i>espA</i>	Kenny <i>et al</i> [231]	
AE2348/69 <i>luxS</i>	SES03	<i>luxS::Tn5</i>	S. Snape [232]	
NCTC12900		O157:H7 $\Delta$ <i>stx</i>	Reference Culture	35°C on LA/LB or CT-SMAC
N427		O157:H7	Very young calf (Faecal)	
N218		O157:H7	Very young calf (Faecal)	
N231		O157:H7	Very young calf (Faecal)	
N635		O157:H7	Very young Calf (Hide)	
N236		O157:H7	Very young Calf (Hide)	
NZRM3441 (E87)		Human clinical O157:H7	Environmental Science and Research (ESR), NZ	

\*SS refers to a specific parental strain

\*\* Distinguishing characteristics refers to the genotype, phenotype or serotype as an identifying feature

**Table 4 –Strains used during this study**

	Scientific Code	Genotype	Phenotype	Source or Reference	Growth conditions
<i>Vibrio harveyi</i> BB120				Bassler <i>et al</i> [183]	30°C, marine agar/AB medium
<i>Vibrio harveyi</i> BB170		<i>luxN</i>	Bioluminescence produced in the presence of exogenous AI-2	Bassler <i>et al</i> [184]	
<i>Vibrio harveyi</i> MM32		<i>luxN luxS</i>	Bioluminescence produced in the presence of exogenous AI-2	Miller <i>et al</i> [198]	
<i>Chromobacterium violaceum</i>	CV026	$\Delta$ <i>cvil</i>	Pigment produced in the presence of C4-C8 AHLs	McClellan <i>et al</i> [233]	30°C, LA/LB
<i>Pseudomonas aeruginosa</i>	PA01			Reference Culture	37°C, LA/LB
<i>Hafnia alvei</i>			Psychrotolerant Enterobacteriaceae	Meat-acquired isolates	25°C, LA/LB
<i>Rahnella aquatilis</i>					
<i>Serratia marcescens</i>					

**Table 5 – Plasmids used in this study**  
Key distinguishing features are indicated.

Plasmid	Genotype	Phenotype	Source or Reference
pSB377	Promoterless <i>luxCDABE</i> reporter operon		Winson <i>et al</i> [234]
pMJFA18	PCR-amplified <i>hosA</i> promoter and <i>gfp</i> cloned into pSB377	Bioluminescence produced relative to promoter activity	Ferrándiz <i>et al</i> [68]



### **2.3.2 *Vibrio harveyi* BB170-based Assay**

This method was adapted from Surette and Bassler [227]. The biosensor, *Vibrio harveyi* BB170 was grown in AB broth at 30°C to an optical density (OD<sub>600</sub>) of 1.6 - 1.8. For the assay, the culture was diluted 1:1000 in fresh AB broth and 10% (v/v) CM added. The mixture was incubated at 30°C with shaking at 200 rpm and hourly samples of 200 µl removed into a 96-well microtitre plate. Bioluminescence emission was measured using a luminometer (POLARstar Galaxy; BMG) and analysed using the FLUOstar Galaxy software version 1.31.0. Bioluminescence was reported as Relative Light Units (RLU) and where appropriate as RLU/OD<sub>600</sub>.

### **2.3.3 *Vibrio harveyi* MM32-based Assay**

This method was adapted from Miller *et al* [198]. *Vibrio harveyi* MM32 was grown in AB broth overnight at 30°C to an OD<sub>600</sub> of 1.7. The culture was diluted 1:5000 in fresh AB media and 10% (v/v) test CM added. Samples were incubated at 30°C with shaking at 200rpm and hourly samples of 200µl removed into a 96-well microtitre plate. Bioluminescence emission was measured using a luminometer (POLARstar Galaxy; BMG). Analysis was completed using the FLUOstar Galaxy software version 1.31.0 and the bioluminescence reported as Relative Light Units (RLU), or where appropriate as RLU/OD<sub>600</sub>.

### **2.3.4 Plate Diffusion-based AI-2 Assay**

A modified agar plate diffusion method was developed for use in this plate based assay [235, 236]. Overnight *V. harveyi* BB170 or MM32 cultures were used to seed a bacterial lawn. A 4.5 mm diameter well was cut into the centre of each plate and filled with 20 µl CM. Plates were incubated at 30°C and monitored for bioluminescence. Light emission was photographed using the Chemiluminescence Imaging System (Alliance 4.7; UviTech, Cambridge, UK) with an

exposure time of 6.5 seconds. Analysis of both light intensity and emission diameter was carried out using the ImageJ™ (Research Services Branch, National Institute of Mental Health, USA). A control image of *V. harveyi* only was used to remove background light from all images prior to analysis with ImageJ™.

## **2.4 AHL Detection Methods**

### **2.4.1 T-streaks for the Detection of AHL Production**

Bioreporter was streaked in a straight line down the centre of an LA plate. Test cultures were streaked perpendicular to the bioreporter, ensuring the culture was close but not touching the bioreporter [237]. Plates were incubated at optimum temperatures for the test strain(s) for 24 hours. Presence of AHL was monitored using either colour changes or bioluminescence production. Appropriate controls were used and these are *Pseudomonas aeruginosa* for the presence of both short and long chain AHLs, and *E. coli* MG1655 as a negative control.

*Chromobacterium violaceum* CV026 produced violacein, a purple pigment, in the presence of short chain AHLs [233, 238]. CV026 has been genetically modified to no longer produce AHLs by a transposon insertion in *luxI*, the LuxI synthase. Thus CV026 only produces violacein in the presence of exogenous AHL. Basic quantification was achieved using depth of colour and size of coloured area.

### **2.4.2 T-streaks for the Detection of AHL Production using CM**

A 20 µl drop of filtered test CM was spotted onto a standard LA plate and allowed to dry at room temperature. A colony of bioreporter was streaked through the centre of the CM spot. The plate was incubated at the optimum temperature for the bioreporter for 24 hours and assessed for either colour or bioluminescence production.

### **2.4.3 Plate Diffusion Assay**

The standard plate diffusion method was used for this assay [235, 236]. Briefly, an LA plate was dried using a laminar flow cabinet to remove excess moisture. *C. violaceum* CV026 was seeded onto the plate using an overnight culture and a sterile swab to form a bacterial lawn. Multiple 4.5 mm diameter wells were cut into the plate and each filled with 20 µl of test CM or control CM. Plates were incubated at 30°C overnight. Pigment halos were analysed for intensity of colour and diameter using a ruler.

### **2.4.4 Thin Layer Chromatography (TLC)**

#### **2.4.4.1 TLC Plate Preparation**

Silica gel RP18 F<sub>254</sub>S with aluminium backing (Merck) chromatography plates were used for the separation of short chain AHL separation. The TLC plates were set up using a modified version of Fletcher *et al* [239]. A pencil line was drawn 2.5 cm from the bottom of the TLC plate and evenly spaced pencil dots applied for positioning of samples. A 10 µl sample was applied to each spot on the plate at the designated places. AHL markers were prepared and 5 µl of each loaded at the following concentrations: 100 µg/ml *N*-butanoyl-DL-HSL, 10 µg/ml *N*-hexanoyl-DL-HSL and 1 µg/ml *N*-(3-oxohexanoyl)-L-HSL. The plate was left at room temperature to allow the spots to dry. The plate was placed into a TLC tank, which contained methanol:water 60:40 to a depth of approximately 1 cm up from the base of the plate. The run was completed when the mobile phase was within 1 to 2 cm from the top of the plate. The plate was removed from the tank and allowed to dry at room temperature. Tape was applied to the edge of the plate on the base, and folded to create a well with a depth of no less than 0.5 cm. A 1:10 dilution of an overnight culture of *C. violaceum* CV026 was prepared in 100 ml 0.6% LA and poured over the TLC plate. Once set the plate was incubated at 30°C overnight. Plates were visualised using a digital camera (Nikon Coolpix S600).

#### 2.4.4.2 Extraction of AHLs from Rumen Fluid

Rumen fluid was kindly donated by the Rumen Microbiology team of AgResearch Ltd at Grasslands Research Centre, Palmerston North (New Zealand). The rumen fluid was collected from fistulated cows at the Ruakura Research Centre in Hamilton (Ruakura animal ethics permit number AE 11483), or Grasslands Research Centre in Palmerston North (New Zealand) (Grasslands animal ethics permit number AE12174). Upon collection the fluid was centrifuged at 5310 x *g* for 10 minutes to remove large particulate matter, such as grass. The rumen fluid was filtered through a 0.22 µm syringe filter (Millex GP, filter type PES) to remove fine particulate material and any microbial cells, including bacteria. The filtered rumen fluid was either stored at -20°C until required, or acidified to pH 1-2 using concentrated HCl and refrigerated at 4°C for 24 hours. The pH of rumen fluid ranges from 5.5 to 7 depending on diet and the concentration of volatile fatty acids. Extraction of AHLs was carried out using the method by Erickson *et al* with modifications [173, 240]. Briefly, rumen fluid was mixed with dichloromethane at a ratio of 2:1 and shaken at 100 rpm for one hour, after which the organic phase was removed using a separating flask. Anhydrous sodium sulphate was added to the organic phase to remove any residual aqueous phase and was subsequently removed by filtering through a Whatman 1 Filter paper. The resulting extract was rotary evaporated to dryness (Vacuum Pump V-700, Buchi Switzerland; Vacuum Controller V-850, Buchi Switzerland; Rotary Evaporator R-210, Buchi Switzerland). The resulting extract was washed 3 times with 500 µl methanol and the solvent evaporated using nitrogen gas (Fletcher, M., Personal Communication, 2010). The rumen extract was resuspended in acetonitrile and stored at 4°C until required [241].

## **2.5 Phenotypic Assays**

### **2.5.1 Motility Assays**

Population expansion, or swimming motility assays were performed using the method of Atkinson *et al* [242]. Motility agar (1% (w/v) tryptone, 0.5% (w/v) sodium chloride, 0.3% BD Bacto™ agar (Becton, Dickinson and Co.), MilliQ water) was prepared and boiled for 1 minute [243]. The pH was adjusted to 6.9 - 7.1 prior to sterilisation. The agar was sterilised by autoclaving and tempered to 48°C prior to pouring. Agar was poured into plates (25 ml per 95 x 95 mm plate, or 50 ml per 145 x 145 mm plate) and left at room temperature for 20 minutes to cool. The plates were incubated at 25°C for 2 hours prior to inoculation to ensure the agar was set properly [244]. Overnight cultures grown in LB were used to stab inoculate the centre of each plate ensuring the agar was not pierced completely [245]. Plates were incubated at both 25°C and 37°C for 18 hours [244]. Positively motile populations produce an opaque ring around the point of inoculation, termed a motility zone or zone of motility. Negatively motile populations are characterised by a small dense area of bacterial growth around the point of inoculation, with no 'diffusion' into the media. The diameter of the motility zone was measured using a ruler and images taken using the Chemiluminescence Imaging System (Alliance 4.7; UviTech, Cambridge, UK).

### **2.5.2 Promoter Expression Assay**

Using the method from Ferrándiz *et al* a bioluminescence assay was used to measure *hosA* promoter activity [68]. A single bacterial colony was suspended in 100 µl LB and diluted 1:1000 in fresh media. Cultures were incubated at 37°C or 25°C with shaking at 200 rpm. At each sampling point 200 µl was removed and placed in a sterile, high-binding 96-well half area black microplate with µclear base (Grenier Bio-One). The OD<sub>620</sub> was measured using Lucy2 (Anthos Microplate Luminometer, with Anthos ADAP software), and the bioluminescence measured using VICTOR (Wallac™ Victor<sup>2</sup> 1420 Multilabel Counter with Wallac™ 1420 Manager Software). To

express *hosA* promoter activity as a function of bacterial growth bioluminescence readings were divided by the OD<sub>620</sub> readings, and the results given as RLU/OD<sub>620</sub>.

### **2.5.3 Aggregation Indices (AI)**

Analysis of aggregation was performed using the methodology of Rowe *et al* but with shaking at 100 rpm instead than 200 rpm [79]. Briefly, overnight cultures were diluted 1:100 in fresh LB and divided into 10 ml aliquots in sterile 50 ml V-bottomed polypropylene falcon tubes. One tube was used for each time point and then discarded. At each time point a single culture was centrifuged at 610 x *g* (Heraeus Multifuge 3 S-R Rotor 6335) for 2 minutes to pellet the aggregates, and the OD<sub>600</sub> of the planktonic cells, located in the top 5ml of the culture was measured (Implen NanoPhotometer 7122 v2.3.1). The planktonic cells were returned to the tube and the samples centrifuged at 2450 x *g* for 5 minutes to pellet the cells (Heraeus Multifuge 3 S-R Rotor 6335). The supernatant was discarded and the pellet resuspended in 10 ml fresh media. Total OD<sub>600</sub> for the sample was measured. Aggregation indices (AI) were calculated as follows:

$$AI = \frac{(OD_{600[total]} - OD_{600[planktonic]})}{OD_{600[total]}}$$

### **2.5.4 Aggregation Phase Contrast Microscopy Assay**

This method is based on the Rowe *et al* protocol which was adapted to allow analysis of more weakly aggregating bacterial cells [79]. Overnight cultures were grown in 5 ml LB and diluted 1:100 into fresh media. The cultures were divided into 10 ml aliquots in sterile 50ml V-bottomed polypropylene falcon tubes. The samples were incubated at 25°C with shaking at 100 rpm. At 5 hours incubation, samples were centrifuged at 610 x *g* for 2 minutes (Heraeus Multifuge 3 S-R Rotor 6335). The top 6 mls were removed from each culture and transferred to a sterile 15 ml centrifuge tube. The aggregates were gently resuspended by swirling in the remaining 4 ml media. 10 µl samples were removed from the aggregated cell suspension, spotted onto a pre-

cleaned microscope slide and covered with a 22 x 22 mm glass coverslip. Aggregates were imaged using 100x and 1000x magnification phase contrast microscopy (Olympus BX60 microscope). Three slides were set up per culture, and 2 fields of view were captured per slide using a Nikon DS-5Mc camera and Nikon NIS-Element Basic Research software. To get the total cell density, planktonic cells were returned to the aggregated cells and 0.3mM (final concentration) sodium chloride was added to break the aggregates apart. The samples were vortexed for 5 minutes and the optical density measured at 600 nm (Implen NanoPhotometer 7122 v2.3.1).

#### 2.5.4.1 Analysis of Aggregation

Analysis of microscopy images was completed using CellProfiler™ (Broad Institute; affiliated with MIT and Harvard universities, USA) to automatically identify, count and characterise each aggregate within an image. Each image was converted to greyscale and aggregates identified using the parameters in Table 6.

Data from CellProfiler™ was exported to Microsoft™ Excel for analysis. Statistical analyses were performed using the Kolmogorov-Smirnov test in R™ (R Foundation for Statistical Computing, Vienna, Austria).

#### 2.5.5 Curli Expression Plate Assay

Congo Red is a red dye that binds to amyloid fibrils, such as curli and other cell surface pili. If these structures are present within a sample a red colour is observed within the culture. Congo Red, dissolved in 50% ethanol, was added to molten LA tempered to 48°C to a final concentration of 3.7% (w/v). Additional supplements of 5nM AHLs and/or 0.4% glucose were added to the agar prior to pouring as required. Plates were inoculated with 20 µl drops of overnight cultures grown in LB, and incubated at 37°C overnight. Images were taken using a

**Table 6 – CellProfiler™ parameters used for the analysis of aggregation as part of the phase contrast microscopy method**

	Parameter	Settings
<b>Diameter</b>	Minimum	1
	Maximum	1000
<b>Thresholding</b>	Method	Otsu Global
	Class	Two class thresholding
	Variance	Minimise weighted variance
	Threshold correction factor	1
	Bounds on threshold	Lower = 0.2
		Upper = 1.0
	Distinguishing method	Distinguish objects by intensity



Nikon Coolpix S600 digital camera or a ProtoCOL 2 Count imaging system (Synbiosis™).

### **2.5.6 Cellulose Expression Assay**

Calcofluor White™ stain produces a blue fluorescent pigment in the presence of cellulose. A stock solution of Calcofluor White™ stain (1 g/L) was diluted 1:1 (v/v) in PBS. 10 µl of the diluted stain was used to resuspend a single colony on a pre-cleaned microscope slide and a coverslip applied. Where overnight broth cultures were used the stain was diluted 1:1 with the culture on each slide. Slides were left at room temperature for 1 minute. Images were taken by microscopy using a UV filter (Olympus BX60 microscope, Nikon DS-5Mc camera and Nikon NIS-Element Basic Research software).

### **2.5.7 Exopolysaccharide Production Assay**

Addition of glucose to standard agar can stimulate production of exopolysaccharide, characterised by shiny, mucoid colonies. Standard LA was tempered to 48°C and glucose added to a final concentration of 0.4% (v/v). Plates were inoculated with individual colonies and left at room temperature for 7 days. The plates were monitored daily for differences in colony morphology. Images were taken using the Chemiluminescence Imaging System (Alliance 4.7; UviTech, Cambridge, UK).

### **2.5.8 Antigen 43 Assay**

Antigen 43 is a cell surface protein which provides some resistance to hydrogen peroxide. The presence of colonies within the clear zone of growth inhibition indicate the presence of Antigen 43. *E. coli* strain 536, as a positive control, produced visible colonies within this zone. 20 ml aliquots of LA tempered to 48°C were seeded with overnight cultures at 1:100 dilution. Inoculated agar was poured into plates and allowed to set. A 5 µl drop of 30% hydrogen

peroxide solution was placed in the centre of each plate. Plates were incubated overnight at 37°C and imaged using the Chemiluminescence Imaging System (Alliance 4.7; UviTech, Cambridge, UK).

## **2.5.9 Proteins**

### **2.5.9.1 Total Cell Protein Extraction**

Overnight cultures grown in LB were diluted 1:100 in fresh LB and grown at 25°C for 5 hours with shaking at 100rpm. The OD<sub>600</sub> was recorded for each culture prior to centrifuging at 5310 x *g* for 10 minutes. The supernatant was removed and the pellet stored at -20°C until required. The pellets were normalised to an OD<sub>600</sub> of 1.0 by resuspending in sterile water. The samples were sonicated 3 times on ice for 30 seconds each time. Methanol was added to the sample at 4x the volume and vortexed for 30 seconds. Chloroform at 1x original sample volume was added and the sample vortexed. The extracts were centrifuged at 13150 x *g* for 1 minute (MiniSpin plus, Global Science) and the liquid phase discarded. Three volumes of sterile water was added and the sample vortexed. The aqueous layer was discarded and a further 4 volumes of methanol added with vortexing. The samples were centrifuged at 13150 x *g* for 2 minutes and the liquid phase discarded. The pellets were dried using nitrogen gas and resuspended in sterile water to the original volume. 50 µl β-mercaptoethanol, or 0.5M (final concentration) DL-Dithiothreitol was added to 950 µl Laemelli sample buffer (BioRad™). 65 µl Laemelli sample buffer was added to 65 µl sample and heated to 100°C for 10 minutes. Samples were stored at -20°C until required.

### **2.5.9.2 Protein Gels**

Protein samples were separated on Ready Gel Tris-HCl 4-15% precast linear gradient polyacrylamide 10 well gels (Bio-Rad™ Ltd) using the Mini-PROTEAN 3 electrophoresis system. The reservoir tanks were filled with 1x Tris/Glycine/SDS buffer. Well spacers were repositioned

using an 18 or 23 gauge needle and the wells washed thoroughly with buffer to remove any unpolymerised acrylamide. 10-20 µl protein sample was loaded per well. 10 µl of two ladders were added to each gel; Colourburst™ electrophoresis marker of molecular weights 8000-220,000 D from Sigma-Aldrich, and Precision Plus Protein™ standards (unstained) of molecular weight 10,000-250,000 D from BioRad™ Ltd. Gels were run at 175 V until the Bromophenol Blue dye reached the bottom of the gel.

#### 2.5.9.3 Protein Visualisation using Coomassie Blue

Proteins were visualised using coomassie blue stain. The staining solution was prepared by dissolving 250mg Brilliant Blue (coomassie) in 40% (v/v) methanol, 10% (v/v) glacial acetic acid and 50% (v/v) Milli-Q water. Polyacrylamide gels were placed in stain for 30 minutes with gentle agitation at 56rpm. The stain was removed and replaced with destain (10% (v/v) acetic acid, 7% (v/v) methanol and 83% Milli-Q water). The destain was replaced as required. Gels were washed with filtered water prior to imaging. Photography was carried out using either a Nikon Coolpix S600 digital camera, or an HP Scanjet 7400C with HP PrecisionScan Pro 3.1 software.

#### 2.5.10 Uronic Acid Assay

Quantification of uronic acid was based on the methods of Van den Hoogen *et al* [246]. Strains, grown on LA, were subcultured into 5 ml LB and grown at 37°C statically overnight. Cultures were diluted 1:100 in fresh LB and grown at 25°C with shaking at 100 rpm in a sterile 50 ml conical bottomed falcon tube. After a total of 5 hours incubation, 2 ml of the sample was taken from the bottom third of the culture and 1 ml of this was transferred to a 1.5 ml eppendorf. Samples were centrifuged at 6708 x g in a microfuge (MiniSpin plus, Global Science). The supernatant was discarded and cells resuspended in 1 ml 0.15M NaCl and vortexed. The

samples were centrifuged at  $11340 \times g$  in the microfuge for 10 minutes. 500  $\mu$ l of the supernatant was removed and frozen at  $-20^{\circ}\text{C}$  until required for the uronic acid assay.

18M sulphuric acid (ThermoFisher Scientific)/120 mM sodium tetraborate (Sigma-Aldrich) was heated to  $80^{\circ}\text{C}$  to dissolve the sodium tetraborate in a glass vial. 150  $\mu$ l of the solution was pipetted into each well of a 96-well microtitre plate and supplemented with 50  $\mu$ l of prepared cell supernatant with subsequent gentle mixing by pipetting. All analyses were carried out in duplicate. The plate was incubated at  $80^{\circ}\text{C}$  for 1 hour with gentle rocking in a hybridisation oven (Hybridization oven/shaker, Amersham Pharmacia Biotech, UK). Once completed the plate was allowed to cool, before being read at 540 nm using a plate reader (Versamax tunable microplate reader, Molecular Devices Corp., US with SOFTmax Pro version 3.0 software). This provided the blank for each of the test wells. Detection reagent was prepared by dissolving 100 mg 3-phenylphenol (Sigma-Aldrich) dissolved in 1 ml dimethyl sulphoxide (DMSO) (Sigma-Aldrich), and was stored in the dark until required. 100  $\mu$ l of detection reagent was added to 4.8 ml 80% (v/v) sulphuric acid immediately prior to use. 40  $\mu$ l of this mixture was added to each well and mixed by gently pipetting and the plate left for 15 minutes at room temperature. A second reading was taken at 540 nm. Background absorbance was removed by subtracting the first reading from the second. A standard curve was prepared using D-glucuronic acid (Sigma-Aldrich) at concentrations ranging from 0.1  $\mu$ g to 100  $\mu$ g which was used to quantify uronic acid levels present in the samples.

To determine the protein concentration within the cultures used for the uronic acid assay, the cell density of the remaining 1 ml of sample was recorded (Implen NanoPhotometer 7122 v2.3.1) and the sample centrifuged at  $5310 \times g$  for 10 minutes to pellet the cells (Heraeus Multifuge 3 S-R Rotor 6335). The supernatant was discarded and the pellet normalised to a cell density of an  $\text{OD}_{600}$  of 1.0 by resuspending in sterile water. The samples were sonicated 3 times on ice for 30 seconds each time to lyse the cells and release cellular proteins within the sample.

Bradford reagent (Sigma-Aldrich) was used to measure the protein concentration in each sample [247]. A standard curve was prepared using bovine serum albumin (BSA) (Sigma-Aldrich) at concentrations ranging between 10 – 100 µg/ml. Uronic acid concentrations present in the samples were expressed as µg of uronic acid per mg of protein.

## **2.6 Genetic methods**

### **2.6.1 DNA Agarose Gels**

A 1% (w/v) agarose/TBE gel was prepared and 2.5 µl 10 mg/ml ethidium bromide added prior to pouring into a mould. A comb was inserted and the gel allowed to set for 15 minutes at room temperature. 1 µl loading dye was combined with 5 µl DNA sample on petrifilm and loaded into the gels. A 1kB+ DNA ladder was used as a marker (Invitrogen™). The gels were run at 110-115 V and visualised using the GelDoc™ XR+ molecular imager (BioRad™) and ImageLab version 3.0 software system.

### **2.6.2 Polymerase Chain Reaction (PCR)**

Reaction mastermix was produced using the ratios provided in Table 7. A negative control was prepared where 1 µl DAPQ water replaced the cells. Primer sequences used during this study are provided in Table 8.

The PCR cycling conditions used to amplify both genes is given in Table 9. The reactions were performed using an MJ Research PTC-100 programmable thermo cycler (MJ Research Inc).

PCR products were visualised using a 1% (w/v) agarose:TBE buffer gel.

**Table 7 – Reaction mix used for colony PCR reactions**

	Stock Concentration	Volume (μL)
DNA	-	Cells
Buffer	10x	5
MgCl <sub>2</sub>	25 mM	3
dNTPs	200 μM	1
Recombinant TAQ polymerase (Invitrogen™)	-	0.5
Primer A	1 mg/ml	0.5
Primer B	1 mg/ml	0.5
dH <sub>2</sub> O	-	39.5
Final Volume		50.0

**Table 8 – Primer sequences of *bfpA* and *perA***

Target Gene	Primer Sequence
<i>bfpA</i>	(F) 5' – TTTTCTTGGTGCTTGCGTGTCT – 3'
	(R) 5' – CATATAATACGCCCAAAACAG – 3'
<i>perA</i>	(F) 5' – TCTGAAAATAAACAAGAG – 3'
	(R) 5' – TGTGTAATAGAATAAACG – 3'

**Table 9 – PCR cycling conditions used for all PCR reactions**

Stage	Temperature (°C)	Time	Number of cycles
Initial Denaturing	95	10 minutes	1
Denaturing	95	1 minute	25
Annealing	48	1 minute	
Extension	72	1 minute 15s	
Final Extension	72	7 minutes	1

### **2.6.3 Pulse Field Gel Electrophoresis (PFGE)**

Production and processing of plugs was based on the methods described in Smith *et al* and Brett *et al* [248, 249].

#### **2.6.3.1 Reagents**

##### **20x TE Buffer**

4.22 g Tris-base (Sigma-Aldrich) was dissolved in 4 ml 0.5M EDTA, and made up to a final volume of 1 litre using distilled water. The pH was adjusted to 8.0 and the buffer was sterilised by autoclaving.

##### **Pett IV Buffer**

58.44 g sodium chloride was mixed with 10 ml 1M Tris-HCl (pH 7.6) and made up to a total volume of 1 litre using distilled water. Pett IV buffer was sterilised by autoclaving and stored at 4°C.

##### **ESP Buffer**

4 g *N*-lauroylsarcosine (Sigma-Aldrich) was shaken vigorously with 400 ml 0.5M EDTA. 200 mg Proteinase K was added and incubated at 37°C for 2 hours. ESP buffer was stored at -20°C in 20ml aliquots until required.

##### **Agarose for Plugs**

A 1.6% agarose solution was prepared using InCert agarose (Alphatech) and distilled water. Molten agarose was tempered to 50°C in a waterbath prior to use.

##### **DNA Staining Solution**

7.5 µl ethidium bromide (10mg/ml) was added to 150 ml 0.5% TE buffer.

#### **2.6.3.2 Plug Preparation**

Using a fresh culture grown overnight on LA, sufficient growth was resuspended in 1 ml Pett IV buffer to a density of 1 McFarland Standard. Cells were pelleted by centrifugation at 6710 x g for

2 minutes in a microcentrifuge (MiniSpin plus, Global Science). The supernatant was discarded and the cells resuspended in 150 µl fresh Pett IV buffer with 2 µl Proteinase K (Invitrogen™). 150 µl molten 1.6% InCert agarose was added and mixed gently to avoid the formation of air bubbles. The mixture was transferred to the plug mould and left at 4°C for 15 minutes to 1 hour until the agarose had set. Plugs were removed from the mould and manipulated into sterile polycarbonate bijoux tubes using a sterile plastic inoculation loop. 1-2 ml ESP buffer was added to each tube and the samples incubated in a waterbath at 50°C for 18 hours. The buffer was removed and replaced with 50 ml 1x TE buffer in a sterile conical bottomed falcon tube, with incubation at 4°C overnight. Using a screw-on sieve cap the buffer was drained and replaced with 50 ml fresh 1x TE buffer with a further overnight incubation at 4°C. The buffer was discarded and replaced with 30 ml 1x TE buffer, with incubation for at least 3 hours at 4°C. Prepared plugs can be stored for up to 5 years at 4°C conditions in 1x TE buffer [248, 249].

### 2.6.3.3 Restriction Enzyme Digest

The plugs were removed from TE buffer and transferred onto parafilm. Each plug was cut to the desired size using a glass coverslip with the comb as a size guide. Using a plastic inoculation loop the plug fragment was manipulated into a sterile eppendorf tube. 100 µl of enzyme reaction mix was added to each tube and incubated overnight at 37°C. An example of the reaction mix calculation is provided below:

$$\text{Total volume (buffer and dH}_2\text{O)} = 100\mu\text{L (volume per plug)} \times \text{Number of plugs}$$

Using the total volume, the required volumes of specific reagents were calculated as follows:

$$\text{Buffer volume} = \frac{\text{Total volume}}{10} \quad \div \quad 10 \text{ (dilution factor)}$$

$$\text{dH}_2\text{O volume} = \text{Total volume} - \text{Buffer volume}$$

$$\text{Enzyme volume} = \frac{\text{Number of plugs} \times \text{Units per plug}}{\text{Concentration of enzyme (Units per } \mu\text{L)}}$$



#### 2.6.3.4 PFGE

Two litres of 0.5x TBE buffer was prepared using distilled water and chilled. 100 ml 1% (w/v) SeaKem agarose was prepared using 0.5x TBE. 0.8% (w/v) InCert agarose was prepared in sterile water. Both the InCert and SeaKem agarose were tempered to 50°C in a waterbath. The comb was placed horizontally on the casting block and the digested plugs loaded onto the teeth using disposable plastic inoculation loops. Excess buffer was removed using a piece of tissue and the plugs manoeuvred to the bottom of the teeth. The plugs were stuck to the comb using a few drops of the 0.8% InCert agarose, ensuring no air bubbles formed. The agarose was allowed to set at room temperature for 15 minutes. The comb was placed vertically into the casting stand, ensuring the bottom of the teeth was tight against the base of the casting stand. The SeaKem agarose was poured in carefully, avoiding production of air bubbles. The gel was allowed to set for 30 minutes and the comb removed, ensuring the plugs remained at the base of the wells. The wells were filled using the remaining 0.8% InCert agarose. The agarose was allowed to set for 10 minutes before the gel and platform were loaded into the running chamber. Prior to the gel transfer, the chamber of the CHEF-DRII (BioRad™) had been rinsed with distilled water and filled with 2 litres of pre-chilled 0.5x TBE buffer. The mini-chiller was turned on and the buffer chilled to 14°C ensuring no air bubbles were running through the equipment. Once the gel was placed in the chamber frame the pump was turned to a speed setting of 90, to ensure a constant buffer flow that did not displace the gel. The following parameters 4 V/cm, 30 hours, 5-35 seconds were used to separate the DNA fragments. Once completed, the gel was placed in the ethidium bromide stain solution and left at room temperature in the dark for 30 minutes. The gel was then transferred to 0.5x TBE buffer to destain and left at 4°C for 30 minutes. Images were taken using the GelDoc™ XR+ molecular imager (BioRad™) and ImageLab version 3.0 software system.

Analysis of the images was completed using BioNumerics 4.0 software.

## **2.7 Tissue Culture**

### **2.7.1 Growth Medium**

10% (v/v) foetal bovine serum (FBS) was added to Dulbecco's modified eagle medium (DMEM) (Gibco®) and stored at 4°C in pre-sterilised glass bottles. 50 µL 1M HCl was added to 200 ml media once a week to maintain pH.

### **2.7.2 HT-29 Cell Line**

HT-29 cells are cancer cells from the human colon which have been immortalised for laboratory use (European Collection of Cell Cultures number 91072201). HT-29 cells were kept in 95% complete growth media/5% DMSO at  $2 \times 10^6$  cells per ml at -80°C until required.

The initial cell culture was achieved by pre-warming 20-30 ml DMEM/FBS to 37°C. 5 ml pre-warmed media was transferred to a sterile 15 ml centrifuge tube. The cells were removed from the freezer and thawed quickly in a 37°C waterbath. The cells were gently pipetted into the 5 ml DMEM/FBS. The cells were seeded into the remaining pre-warmed media in a 75 cm<sup>2</sup> tissue culture treated canted neck flask with filter cap (Corning®). The flask was incubated at 37°C in 5% CO<sub>2</sub> overnight. After 24 hours, 50% of the culture medium was replaced with fresh media and the flask returned to the incubator.

Cells were subcultured when approximately 60-80% monolayer confluency was reached. Confluency was monitored by microscopy (Nikon Eclipse TS100). For subculturing, the monolayer was washed twice with a small volume of PBS, for approximately 30 seconds per wash. 2 ml of 1x TrypLE (Gibco®) was added to the flask and the flask returned to the incubator for approximately 5 minutes, or until the majority of the cells had rounded up and were detached from the surface of the flask. When necessary the cells were displaced from the base of the flask by gentle tapping, and 10ml fresh DMEM/FBS added. The cells were transferred to a sterile 15 ml centrifuge tube and spun at 200 x g for 5 minutes. The supernatant was discarded and the

cells resuspended in 10ml fresh pre-warmed DMEM/FBS. A volume of 450-1000  $\mu$ l, depending on cell density, was added to 20-30 ml pre-warmed media in a sterile canted neck flask. Cell density was measured using observations of confluency in the canted neck flask, or microscopically using Gibco® 0.4% Trypan Blue solution and counting. 50% of the culture medium was replaced after 2-3 days incubation.

### **2.7.3 Fluorescence Actin Staining (FAS test)**

This method was adapted from Ferrándiz *et al* and Carlson *et al* [68, 250].

#### **2.7.3.1 HT-29 Cell Preparation**

Circular 16x16 mm glass coverslips were sterilised using 70% ethanol and 2-3 coverslips were placed in each well of a 6-well plate (Corning®). 3 ml DMEM/10% FBS added to each well and the plate incubated at 37°C to pre-warm the medium. 100  $\mu$ l HT-29 cell suspension was seeded in each well and the plate incubated at 37°C in 5% CO<sub>2</sub> for 2-3 days, or until 50% confluency had been achieved. For the sterile 2-well Lab-Tek chamber slide (with cover) composed of permanox (Nunc®) 2 ml media and 85  $\mu$ l cell suspension were added. Slides were incubated at 37°C in 5% CO<sub>2</sub> for 2-3 days, or until 50% confluency had been achieved.

#### **2.7.3.2 Bacterial Preparation**

Bacteria were grown in 10 ml LB overnight at 37°C with shaking at 100 rpm. The cultures were centrifuged at 3400 x *g* for 10 minutes and the pellet resuspended in pre-warmed DMEM. Resulting cultures were diluted 1:20 into fresh pre-warmed DMEM and incubated at 37°C for 3 hours with shaking at 200 rpm. OD<sub>600</sub> was measured using the spectrophotometer (Implen NanoPhotometer 7122 v2.3.1) and normalised to 0.3 using pre-warmed DMEM prior to inoculation.

### 2.7.3.3 FAS Test

Growth medium was removed from the wells and 3ml of bacterial cell suspension added to each well. The plates were incubated at 37°C in 5% CO<sub>2</sub> for 3 hours to allow bacterial attachment. Each well was washed 3 times with 3ml PBS with gentle rocking of the plate for 5 minutes during each wash. The PBS was discarded after each wash. 1 ml 3% (v/v diluted from a 40% w/v stock solution) formaldehyde (Sigma-Aldrich) in PBS was added to each well and the plate incubated for 14 hours at 4°C. The formaldehyde was discarded and the wells washed 3 times with PBS. 1 ml 1% (v/v) Triton X-100 (Sigma-Aldrich) in PBS was added to each well and the plate left at room temperature for a maximum of 30 minutes. The Triton X-100 solution was removed and the wells washed twice with PBS. Each coverslip in the wells was flooded with 20 µl 50 µg/ml solution of FITC-Phalloidin in PBS and the plate was placed in a humidified box with no light at room temperature for 2 hours. The wells were washed 3 times with PBS. A 10 µl drop of Antifade™ (Sigma-Aldrich) was placed onto a microscope slide and a coverslip inverted over the top. The coverslip was sealed with nail varnish and stored in the dark. Coverslips were analysed using the WIB filter on an Olympus BX-60 microscope, a Nikon DS-5Mc camera and Nikon NIS-Element Basic Research software.

## **2.8 *Galleria mellonella* Infection Studies**

*Galleria mellonella* larvae were used as an infection model. Larvae were obtained from BioSuppliers Ltd (Auckland, NZ) and stored at 15°C and monitored daily for signs of pupation until required. Larvae used during the infection were all in stage 5 of the lifecycle, and weighed between 1 g and 1.5 g each.

### **2.8.1 Bacterial Preparation**

Overnight cultures were diluted 1:100 in 10 ml fresh LB and incubated at 25°C with shaking at 100 rpm for 5 hours. Cells were pelleted by centrifugation at 3400 x g for 10 minutes and the pellets resuspended in 10 ml pre-warmed DMEM with no foetal bovine serum. The cells were incubated at 37°C in 5% CO<sub>2</sub> for 3 hours. The cells were centrifuged at 3400 x g for 10 minutes and the pellets washed twice in PBS. Pellets were resuspended in PBS and normalised to a McFarland standard 4.0 (OD<sub>600</sub> 0.66). Bacterial viability prior to injection was determined by plate count. The bacterial suspension was loaded into a 1 ml syringe (Terumo™) with a 27 gauge needle.

### **2.8.2 Inoculation of *Galleria mellonella* Larvae**

Each larvae was mounted on a specially constructed inoculation platform to immobilise them during the injection procedure (Figure 12). The larvae were each injected with 10 µl bacterial cell suspension and incubated for a maximum of 72 hours at 37°C. The *Galleria* larvae were monitored daily for colour changes and loss of movement. After 72 hours any remaining living larvae were euthanized using fly spray. Use of fly spray ensured the larvae were dead, and sterilisation by autoclaving ensured the inoculated bacteria had been killed. Differences in fatality rate were analysed for significance using a Fishers Exact 2-sided test.

## **2.9 Statistics**

Comparison of the effects of a given treatment on population expansion was performed by analysing the diameter of the motility zones using a 2-way analysis of variance (ANOVA) against the presence and absence of AHL, taking into account variation due to biological replicates. The ANOVA provides F-statistics and p-values for both the treatment effect of AHL, and the effect of

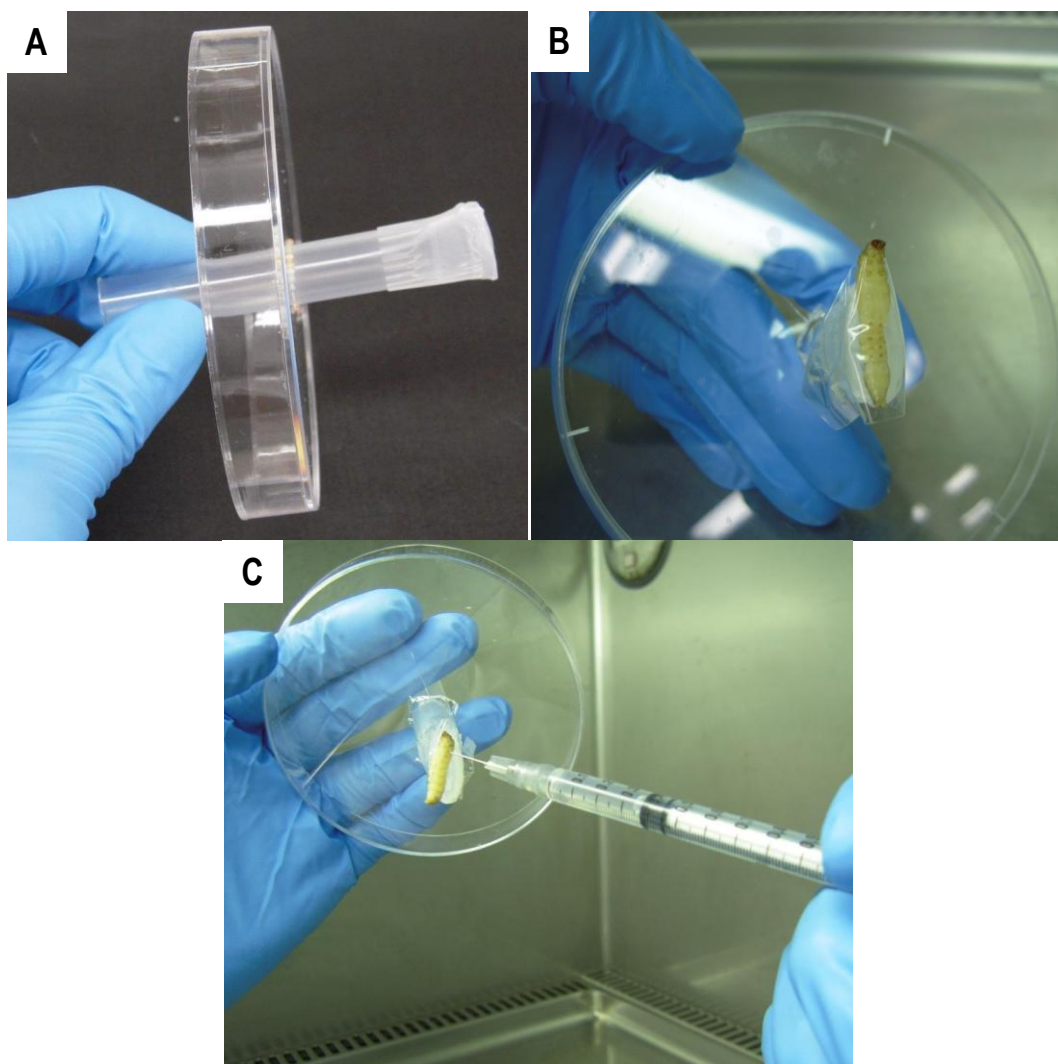


**Figure 12 –Inoculation of *Galleria mellonella* larvae**

(A) Inoculating platform comprising of a re-shaped 5ml pipette tip inserted through the lid of a standard 95 x 95mm agar plate

(B) Larvae were placed onto the inoculation platform face-up to allow identification of the lower left pro-leg, and held in place by Sellotape™

(C) Injection of larvae was carried out using a 1ml sterile disposable syringe fitted with changeable luer lock 27 gauge needles to reduce contamination. Accuracy of inoculation technique was regularly checked using a calibrated balance and PBS

biological variation[251]. The p-value describes the probability that the differences between the groups means would arise by chance under the assumption that all group means were the same. A small *p*-value suggests that it is unlikely the observed differences arose by chance, and that the groups therefore differ [251].

Changes in the propensity of a bacterial population to form aggregates was analysed using the Kolmogorov-Smirnov (K-S) test. The phase contrast microscopy images were analysed using CellProfiler™, which provided numerical values describing various physical characteristics of the aggregates produced by a bacterial population. Of the data exported for each image, the distribution of aggregate sizes was analysed to determine whether the addition of a given treatment had an effect on the propensity of the population to aggregate.

The K-S test is a non-parametric pair-wise test that was used to determine the equality of the aggregation profiles produced for two treatment groups [252]. The D-value produced is calculated from the continuous one-dimensional aggregation profiles provided by the CellProfiler™ data, and represents the distance between the empirical distribution functions of the two samples [252]. Therefore, a higher D-value shows a greater difference between the population distributions, indicating a more significant effect of the treatment [252]. As there was no definitive threshold of significance, one was set based on the biological variation observed during the experiments. For the purposes of this study if  $D < 0.4$ , any difference observed between the aggregation profiles for two given treatments was attributed to biological variation. Where  $D \geq 0.4$  the distributions were deemed to be significantly different and the treatments identified as having an effect on bacterial aggregation.

## **2.10 Approvals**

Rumen Fluid was donated to this study following collection by the Rumen Microbiology team (AgResearch Ltd) at Grasslands Research Centre, Palmerston North under the Grasslands

animal ethics permit number AE 12174. Rumen fluid was also collected by the same team at Ruakura Research Centre, Hamilton under the Ruakura animal ethics permit number AE 11483.

Work using genetically modified bacteria was completed with compliance to New Zealand's Environmental Protection Authority (EPA) approval GMD004759-81.

Studies using *Vibrio* spp. were completed with compliance to New Zealand EPA approval GMC001332.

All *Galleria mellonella* work was completed with compliance to New Zealand's EPA approval GMD10112.



### **3 Effect of Quorum Sensing on Motility and the Influence of HosA**

#### **3.1 Introduction**

Bacteria use flagella and pili on the cell surface to move. Motion can be direct or more of a tumbling movement, and can be divided into two distinct forms; swimming and swarming motility. Studies have shown that AHL-dependent quorum sensing can affect the motility of pathogens such as *Yersinia* [242, 245]. In contrast, although *E. coli* is known to be motile in the absence of AHL, little is known of the effect of AHL-dependent quorum sensing in this species [68].

Swimming motility can be assessed in two ways:

- 1) Individual cell motility. This can be monitored using microscopy to observe the tumbling and swimming motions of each bacterium within the field of view.
- 2) Population Expansion. Observed motility on agar plates is a combination of both cell growth and division, and with the ability to move. For the purposes of this study we have defined this phenomenon as population expansion. The parameters population expansion covers are density of the motility zone and spread. Positive motility is characterised by an area of visible bacterial 'diffusion', or a motility zone around the inoculation site. The extent of swimming can be monitored by measuring the distance between the outer boundaries of the motility zone. Motility is linked to population growth: a high level of replication within a motile population results in a dense zone of motility, but if a low level of replication occurs within a motile population the motility zone becomes less dense. Negative motility is characterised by an area of high cell density around the point of inoculation.

In a study by Ferrándiz *et al* motility was linked to the presence of a functional HosA protein [68]. HosA, a SlyA homologue, is a transcriptional regulator associated with adaptation to environmental stress (Section 1.1.4.2). HosA is present in pathogenic strains of *E. coli* only, and has been associated with the regulation of a response to changes in temperature. Ferrándiz *et al*

determined that at 37°C the mutant E2348/69 *hosA*<sup>-</sup> strain was motile, however when the temperature was reduced to below 30°C population expansion decreased [68]. This observed change in expansion was not as a result of the inability of individual bacteria to swim, but instead was linked with the propensity of the population to form aggregates.

High levels of aggregation reduce population expansion and the absence of a functional HosA protein increases the propensity of the bacteria to aggregate. The aim of this chapter was to assess the effect of AHL-dependent quorum sensing on the population expansion of wild type E2348/69 and E2348/69 *hosA*<sup>-</sup>, and to determine whether HosA regulation and aggregation are influencing factors.

## **3.2 Results**

### **3.2.1 Role of AHL and Temperature on the Population Expansion of E2348/69**

Ferrándiz *et al* had shown population expansion of E2348/69 changed in response to different temperatures [68]. The same observation was made during this study, but at different temperatures to the Ferrándiz study [68].

Positive population expansion was observed for wild type E2348/69 at both 25°C and 37°C, producing distinct circular areas of 'diffusion' on motility agar plates (Figure 13). In all cases 2 biological replicates each consisting of 5 technical replicates were analysed. Representative images of these plates are shown in Figure 13. These images were chosen to illustrate the differences in the density of the motility zone therefore the diameter of the area of motility on the image may not be illustrative of the overall effect of the supplement. At 25°C the area of motility was clearly defined, with distinguishable rings (Figure 13). In comparison at 37°C, the motility zone appeared uniform and more dense throughout. At 25°C the bacteria were able to produce an area of motility with an average diameter of  $20.8 \pm 1.03\text{mm}$  (diameter  $\pm 1$

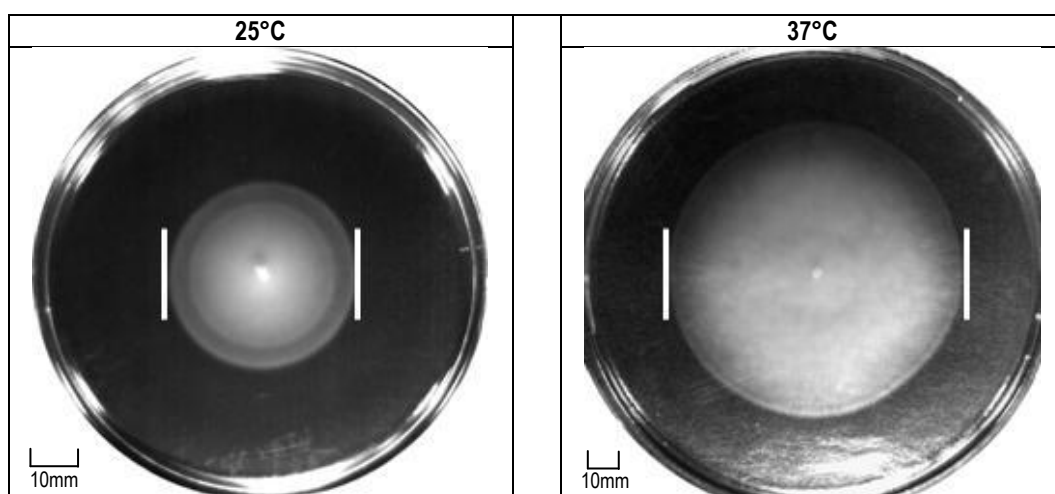


**Figure 13 - Effect of temperature on E2348/69 population expansion**

Images are representative of the motility zones produced after 18 hours incubation. Each image is representative of 2 independent biological cultures, each with 5 technical replicates.

White bars mark the boundaries of population expansion on each plate. Scale bars are indicated in the left hand corner and are set at 10mm.

N.B. Images are representative, therefore the size of motility ring on the image may not be illustrative of the overall effect of the supplement.

standard deviation). When the incubation temperature was increased to 37°C the area of motility increased to an average of  $80.9 \pm 3.6$ mm in diameter. Analysis of all the replicates at both temperatures by ANOVA showed this increase to be statistically significant ( $F = 1966.996$ ;  $p = <0.00001$ ).

The role of AHL-dependent quorum sensing and the link to temperature was investigated using a range of both short and long chain modified and non-modified AHLs to assess the impact on population-based motility of E2348/69. To ensure any effect observed was as a direct result of addition of the AHL, inactive *D*-isomers were used as a negative control in all experiments. As stated in the introduction (Section 1.3.2), there are two possible stereoisomers of AHLs; the *L*-isomer is able to activate the ligand-binding domain of the LuxR protein while the *D*-isomers are inactive [93]. In this study, *L*-isomers are defined as active AHLs, with *D*-isomers categorised as inactive. AHLs were added to both the motility media prior to pouring, and to the overnight culture in order to stimulate the quorum sensing regulon. AHLs were added twice to the overnight culture, once at time zero and again 1 hour prior to use in the motility experiments. Previous experimentation with bioreporters such as *C. violaceum* and exogenous AHL during this study had shown that 5nM of signal added to a culture of *E. coli* strain E2348/69 was sufficient to affect phenotypic behaviour for a limited period of time. As *E. coli* is unable to produce AHL this was hypothesised to be as a direct result of signal being internalised and used, thereby dropping the external concentration below the required quorum sensing threshold. To counteract this reduction in AHL and thereby the response, the signals were added multiple times to prime the bacteria and maintain a sufficient concentration of AHL to exert an observable effect during the course of experiment. Representative images of E2348/69 population expansion in the presence of different AHLs at 25°C are shown in Figure 14, and the average diameters of the area of motility are summarised in Table 10. In the absence of AHL, E2348/69 had an area of motility of average diameter  $20.8 \pm 1.03$ mm with clearly definable rings (Table 10; Figure 15).

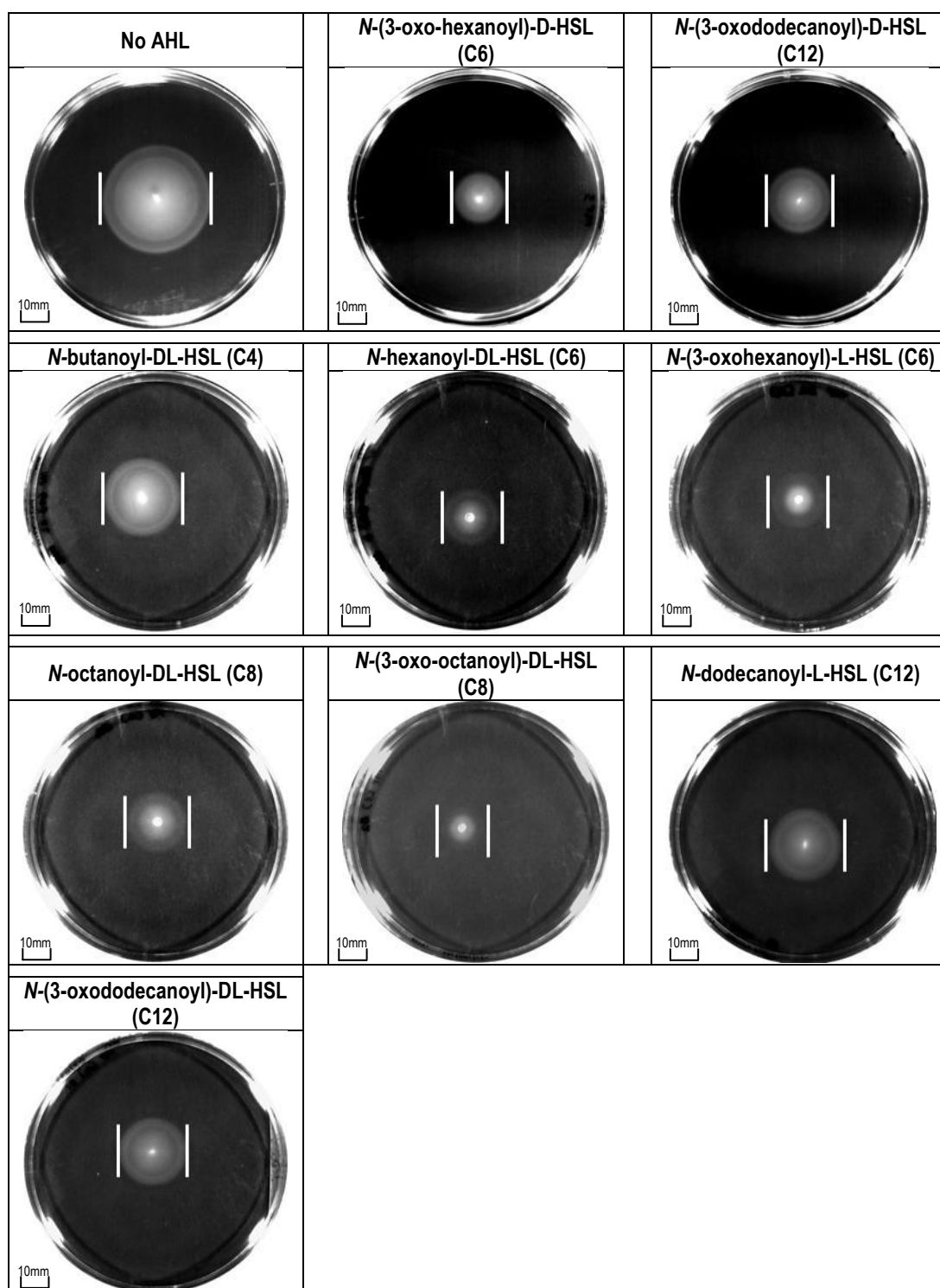


**Figure 14 - Effect of AHLs on E2348/69 population expansion at 25°C**

Images are representative of the motility zones produced after 18 hours incubation. Each image is representative of 2 independent biological cultures, each with 5 technical replicates. Supplementation with AHL was performed to a final concentration of 5nM.

White bars mark the boundaries of population expansion on each plate. Scale bars are indicated in the left hand corner and are set at 10mm.

N.B. Images are representative, therefore the size of motility ring on the image may not be illustrative of the overall effect of the supplement.

**Table 10 - Statistical analysis of the effect of AHL on E2348/69 population expansion at 25°C**

Side chain lengths of the AHLs are in brackets. Significant increases in population expansion are highlighted in blue, those that decrease population expansion are highlighted in pink.

	Average diameter of motility ring $\pm$ 1 standard deviation (mm)	ANOVA	
		*F-value	p-value
No AHL	20.8 $\pm$ 1.03		
<i>N</i> -(3-oxo-hexanoyl)-D-HSL (C6)	20.0 $\pm$ 1.41	2.09	0.166
<i>N</i> -(3-oxododecanoyl)-D-HSL (C12)	21.2 $\pm$ 1.39	0.53	0.476
<i>N</i> -butanoyl-DL-HSL (C4)	24.4 $\pm$ 1.35	44.86	2.80 $\times$ 10 <sup>-6</sup>
<i>N</i> -hexanoyl-DL-HSL (C6)	18.3 $\pm$ 0.95	31.78	2.40 $\times$ 10 <sup>-5</sup>
<i>N</i> -(3-oxohexanoyl)-L-HSL (C6)	13.8 $\pm$ 1.87	107.04	5.30 $\times$ 10 <sup>-9</sup>
<i>N</i> -octanoyl-DL-HSL (C8)	18.8 $\pm$ 0.63	27.27	5.80 $\times$ 10 <sup>-5</sup>
<i>N</i> -(3-oxo-octanoyl)-DL-HSL (C8)	14.9 $\pm$ 1.52	102.72	7.30 $\times$ 10 <sup>-9</sup>
<i>N</i> -dodecanoyl-L-HSL (C12)	25.2 $\pm$ 1.39	64.06	2.40 $\times$ 10 <sup>-7</sup>
<i>N</i> -(3-oxododecanoyl)-DL-HSL (C12)	23.9 $\pm$ 1.19	38.44	7.50 $\times$ 10 <sup>-6</sup>

\*F- critical value = 4.414

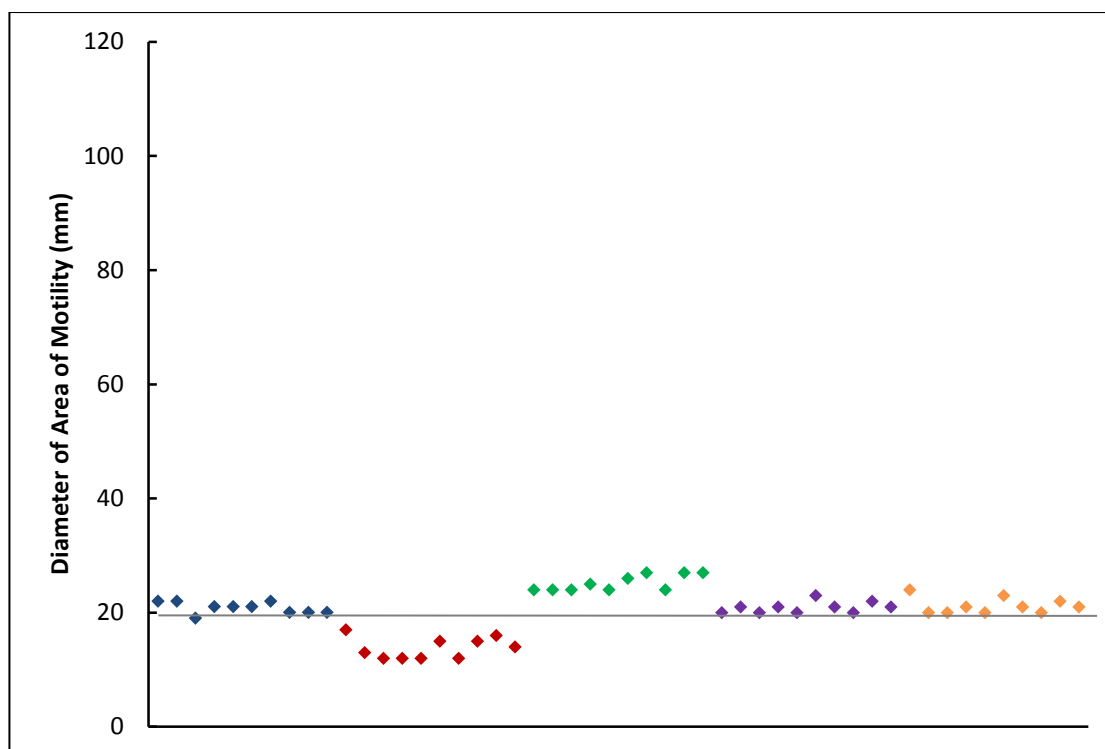


**Figure 15 - Variation in the diameter of the motility zones produced by E2348/69 in the presence and absence of different AHLs at 25°C**

For each of the 2 independent biological replicates, 5 technical replicates were analysed. Each point on the graph represents one technical replicate. Petri dishes measured 95 mm in diameter.

(Blue) No AHL

(Red) *N*-(3-oxo-hexanoyl)-L-HSL

(Green) *N*-dodecanoyl-L-HSL

(Purple) *N*-(3-oxo-hexanoyl)-D-HSL

(Orange) *N*-(3-oxo-dodecanoyl)-D-HSL

The grey line represents the average diameter of the motility zones measured for the unsupplemented isolates.

Biological variation between the two E2348/69 cultures was not significant ( $F = 0.348$ ;  $p = 0.572$ ) (Figure 15).

To determine which AHLs had the greatest effect on E2348/69 population expansion, each AHL was added individually. Three non-modified short chain AHLs namely *N*-butanoyl-DL-HSL, *N*-hexanoyl-DL-HSL and *N*-octanoyl-DL-HSL were tested. Addition of *N*-butanoyl-DL-HSL increased the average diameter of the motility zone from 20.8mm diameter to  $24.4 \pm 1.35$ mm, a statistically significant increase in bacterial population expansion ( $F = 44.86$ ;  $p = <0.0001$ ) (Table 10). In the presence of *N*-hexanoyl-DL-HSL the average diameter of the motility zone was  $18.3 \pm 0.95$ mm, a significant decrease in E2348/69 population expansion ( $F = 31.78$ ;  $p = <0.0001$ ) (Table 10). Addition of *N*-octanoyl-DL-HSL resulted in a significant decrease in the average diameter of the motility zone produced by E2348/69, measuring  $18.8 \pm 0.63$ mm ( $F = 27.27$ ;  $p = <0.0001$ ) (Table 10). A more significant decrease in population expansion was observed in the presence of the modified form of *N*-hexanoyl-DL-HSL, *N*-(3-oxohexanoyl)-L-HSL, which had an average diameter of  $13.8 \pm 1.87$ mm ( $F = 107.04$ ;  $p = <0.0001$ ) (Table 10; Figure 15). The modified form of *N*-octanoyl-DL-HSL, *N*-(3-oxo-octanoyl)-DL-HSL, caused a significant decrease in E2348/69 population expansion with the average diameter of the area of motility measuring  $14.9 \pm 1.52$ mm ( $F = 102.72$ ;  $p = <0.0001$ ) (Table 10; Figure 15). Furthermore, the areas of motility produced in the presence of the AHLs with an R-group of between 6 and 8 carbons in length were less dense with increasing distance from the point of inoculation compared to motility zones produced in the absence of AHL, suggesting fewer bacteria were able to swim. By comparison, in the presence of *N*-butanoyl-DL-HSL a dense motility zone was produced, which was more similar in density to the motility zone observed in the absence of AHL (Figure 14).

One modified and one non-modified long chain AHL were tested. Addition of *N*-dodecanoyl-L-HSL and *N*-(3-oxododecanoyl)-DL-HSL to E2348/69 resulted in a significant increase in the diameter of the motility zone to an average of  $25.2 \pm 1.39$ mm ( $F = 64.06$ ;

$p = <0.0001$ ) and  $23.9 \pm 1.19\text{mm}$  ( $F = 38.33$ ;  $p = <0.0001$ ) respectively (Table 10; Figure 15). The motility zones produced in the presence of *N*-dodecanoyl-L-HSL and *N*-(3-oxododecanoyl)-DL-HSL had clear boundaries (Figure 14).

It was observed that at 25°C addition of *N*-(3-oxohexanoyl)-L-HSL resulted in the largest decrease and *N*-dodecanoyl-L-HSL the largest increase in the population expansion of E2348/69 (Table 10; Figure 15).

The two *D*-isomers *N*-(3-oxo-hexanoyl)-D-HSL and *N*-(3-oxododecanoyl)-D-HSL were selected as negative controls for AHL-dependent activity. The average areas of motility produced by E2348/69 measured  $20 \pm 1.41\text{mm}$  in diameter ( $F = 2.09$ ;  $p = 0.166$ ) in the presence of *N*-(3-oxo-hexanoyl)-D-HSL, and  $21.2 \pm 1.39\text{mm}$  ( $F = 0.53$ ;  $p = 0.476$ ) after addition of *N*-(3-oxododecanoyl)-D-HSL (Table 10). Therefore, neither of these AHLs had a significant effect on the population expansion of E2348/69 when incubated at 25°C (Table 10; Figure 15).

Based on the observations of the AHL effect on E2348/69 population expansion, *N*-(3-oxohexanoyl)-L-HSL and *N*-dodecanoyl-L-HSL, in addition to the two *D*-isomers were used in the following experiments to investigate the role of quorum sensing on E2348/69 motility at 37°C. In the absence of AHL E2348/69 produced an area of motility measuring  $80.9 \pm 3.6\text{mm}$  on average (Table 11). The variation in the diameter of the motility zones produced at this higher temperature was much greater than that observed at 25°C, indicated by higher standard deviations and the spread of diameter measurements (Figure 16). Addition of both *N*-(3-oxohexanoyl)-L-HSL and *N*-dodecanoyl-L-HSL had no significant effect the size of the motility zone produced by E2348/69 at 37°C (Table 11; Figure 16). Furthermore, neither of the *D*-isomer controls had any significant effect on E2348/69 population expansion (Table 11; Figure 16).



**Table 11 - Statistical analysis of the effect of AHL on E2348/69 population expansion at 37°C**

Side chain lengths of the AHLs are in brackets.

	Average diameter of motility ring $\pm$ 1 standard deviation (mm)	ANOVA	
		*F-value	p-value
No AHL	80.9 $\pm$ 3.60		
<i>N</i> -(3-oxo-hexanoyl)-D-HSL (C6)	78.3 $\pm$ 1.89	4.083	0.0584
<i>N</i> -(3-oxododecanoyl)-D-HSL (C12)	81.0 $\pm$ 3.97	0.0035	0.953
<i>N</i> -(3-oxohexanoyl)-L-HSL (C6)	83.5 $\pm$ 4.72	1.916	0.183
<i>N</i> -dodecanoyl-L-HSL (C12)	81.5 $\pm$ 2.95	0.166	0.688

\*F- critical value = 4.414

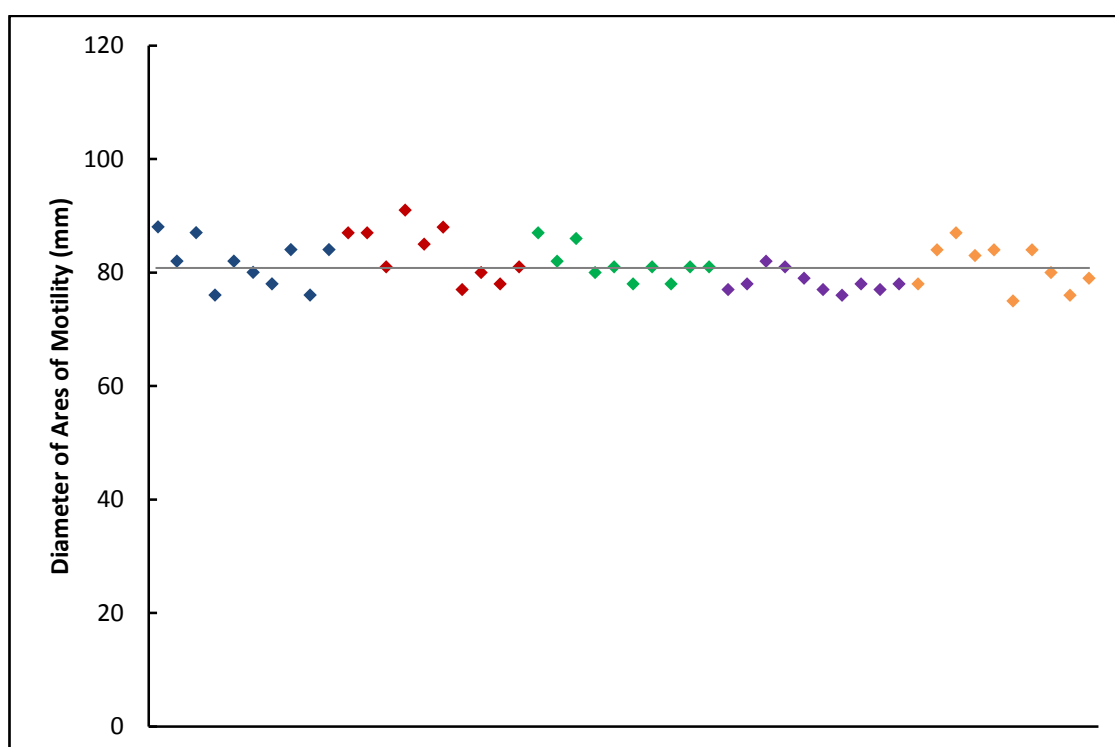


**Figure 16 - Variation in the diameter of the motility zones produced by E2348/69 in the presence and absence of different AHLs at 37°C**

For each of the 2 independent biological replicates, 5 technical replicates were analysed. Each point on the graph represents one technical replicate. Petri dishes measured 95 mm in diameter.

(Blue) No AHL

(Red) *N*-(3-oxo-hexanoyl)-L-HSL

(Green) *N*-dodecanoyl-L-HSL

(Purple) *N*-(3-oxo-hexanoyl)-D-HSL

(Orange) *N*-(3-oxo-dodecanoyl)-D-HSL

The grey line represents the average diameter of the motility zones measured for the unsupplemented isolates.

### **3.2.2 Role of HosA on the Population Expansion of E2348/69**

A previous study had shown that at lower temperatures the absence of HosA in E2348/69 resulted in a non-motile population, suggesting a role for HosA in the regulation of this phenotype [79]. At higher temperatures population expansion was restored and areas of motility were visible on swimming motility agar plates [68]. E2348/69 *hosA*<sup>-</sup> motility was investigated at both 25°C and 37°C.

E2348/69 *hosA*<sup>-</sup> was non-motile at 25°C (Figure 17). Incubation at 37°C restored population expansion and produced an area of motility with an average diameter of  $87.6 \pm 5.72$ mm (Figure 17). The population expansion of E2348/69 *hosA*<sup>-</sup> exhibited the same significant shift in response to temperature as that observed in E2348/69 ( $F = 2345.92$ ;  $p = <0.00001$ ).

To determine whether AHL-dependent quorum sensing affected the population expansion in the HosA mutant in a manner similar to the wild type E2348/69, all available AHLs were added to both broth and agar as in previous experiments. Plates were incubated at both 25°C and 37°C to establish whether any quorum sensing modulation was temperature-dependent.

A range of both short and long chain AHLs were assessed for their impact on the E2348/69 *hosA*<sup>-</sup> population expansion. A set of representative images of the areas of motility produced at 25°C is shown in Figure 18. The average diameter of the areas of motility are summarised in Table 12, with variation and range of the replicate values shown in Figure 19.

In the absence of AHL there was no area of motility with only the site of inoculation visible (Figure 18). The addition of inactive *D*-isomers, *N*-(3-oxo-hexanoyl)-D-HSL and *N*-(3-oxododecanoyl)-D-HSL, had no effect on the population expansion of E2348/69 *hosA*<sup>-</sup> (Table 12; Figure 19).

All of the active AHLs tested significantly increased the population expansion of E2348/69 *hosA*<sup>-</sup> when incubated at 25°C. Addition of short chain *N*-butanoyl-DL-HSL, *N*-

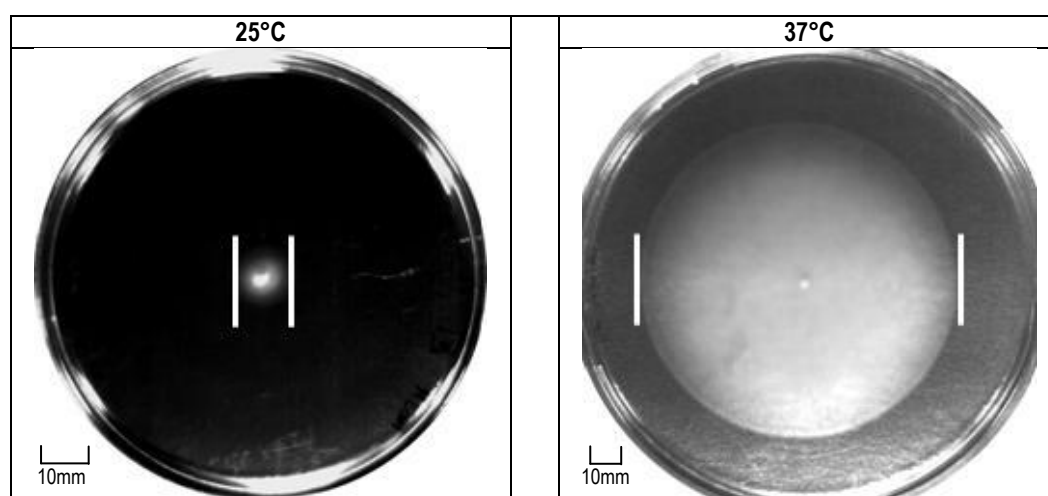


**Figure 17 - Effect of temperature on E2348/69 *hosA*<sup>-</sup> population expansion**

Images are representative of the motility zones produced after 18 hours incubation. Each image is representative of 2 independent biological cultures, each with 5 technical replicates.

White bars mark the boundaries of population expansion on each plate. Scale bars are indicated in the left hand corner and are set at 10mm.

N.B. Images are representative, therefore the size of motility ring on the image may not be illustrative of the overall effect of the supplement.

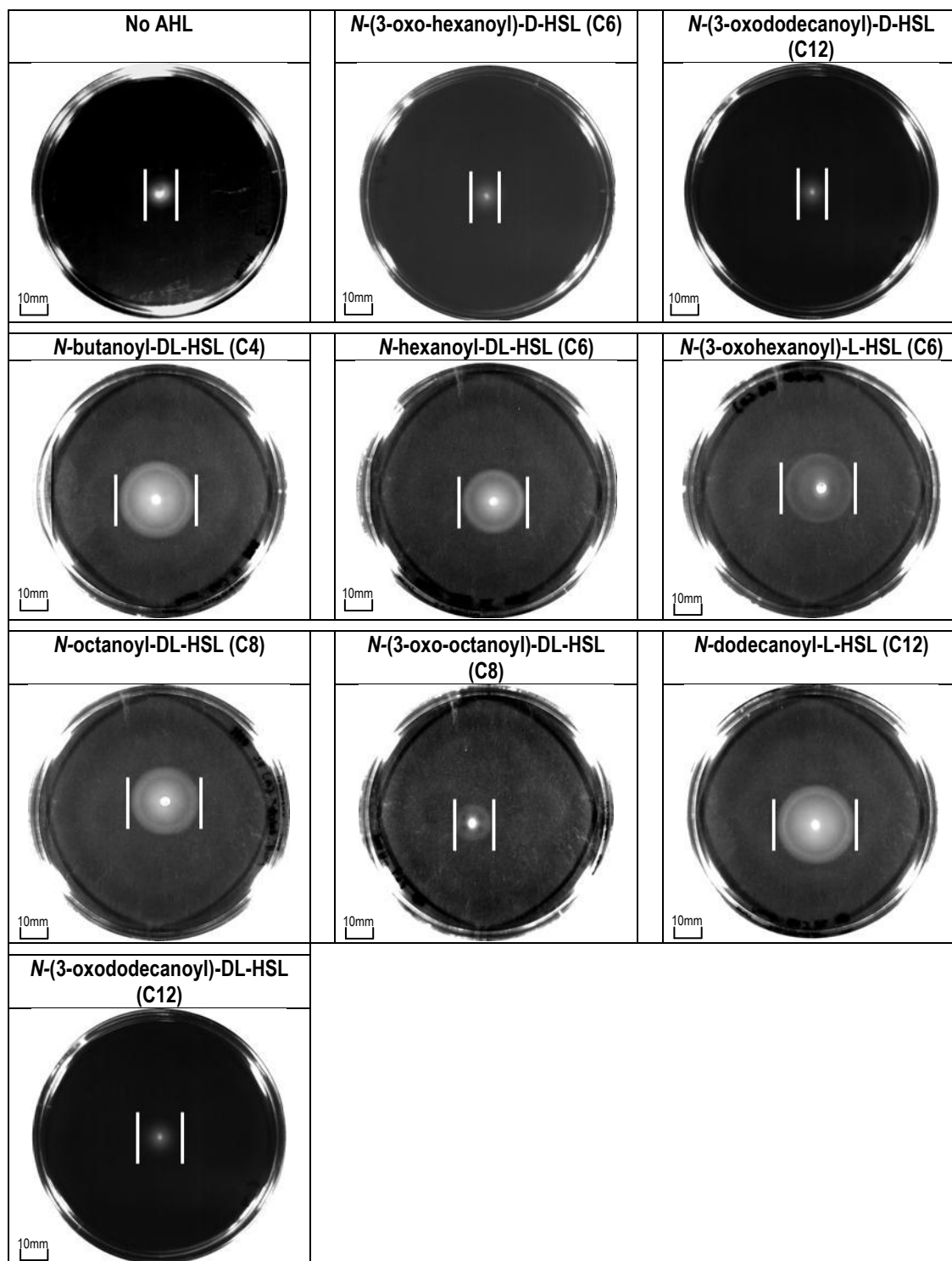


**Figure 18 - Effect of AHLs on E2348/69 *hosA*<sup>-</sup> population expansion at 25°C**

Images are representative of the motility zones produced after 18 hours incubation. Each image is representative of 2 independent biological cultures, each with 5 technical replicates. Supplementation with AHL was performed to a final concentration of 5nM.

White bars mark the boundaries of population expansion on each plate. Scale bars are indicated in the left hand corner and are set at 10mm.

N.B. Images are representative, therefore the size of motility ring on the image may not be illustrative of the overall effect of the supplement.

**Table 12 – Statistical analysis of the effect of AHL on E2348/69 *hosA*<sup>-</sup> population expansion at 25°C**

Side chain lengths of the AHLs are in brackets. Significant increases in population expansion are highlighted in blue.

	Average diameter of motility ring $\pm$ 1 standard deviation (mm)	ANOVA	
		*F-value	p-value
No AHL	0 $\pm$ 0		
<i>N</i> -(3-oxo-hexanoyl)-D-HSL (C6)	0 $\pm$ 0	N/A	N/A
<i>N</i> -(3-oxododecanoyl)-D-HSL (C12)	0 $\pm$ 0	N/A	N/A
<i>N</i> -butanoyl-DL-HSL (C4)	26.1 $\pm$ 1.52	2933.44	2.20 $\times$ 10 <sup>-21</sup>
<i>N</i> -hexanoyl-DL-HSL (C6)	20 $\pm$ 1.05	3600.00	3.50 $\times$ 10 <sup>-22</sup>
<i>N</i> -(3-oxohexanoyl)-L-HSL (C6)	20.7 $\pm$ 2.21	874.47	1.00 $\times$ 10 <sup>-16</sup>
<i>N</i> -octanoyl-DL-HSL (C8)	22.4 $\pm$ 1.64	1850.75	1.30 $\times$ 10 <sup>-19</sup>
<i>N</i> -(3-oxo-octanoyl)-DL-HSL (C8)	13.2 $\pm$ 0.79	2800.29	3.30 $\times$ 10 <sup>-21</sup>
<i>N</i> -dodecanoyl-L-HSL (C12)	26.1 $\pm$ 1.29	4114.69	1.00 $\times$ 10 <sup>-22</sup>
<i>N</i> -(3-oxododecanoyl)-DL-HSL (C12)	23.5 $\pm$ 1.27	3427.76	5.40 $\times$ 10 <sup>-22</sup>

\*F- critical value = 4.414

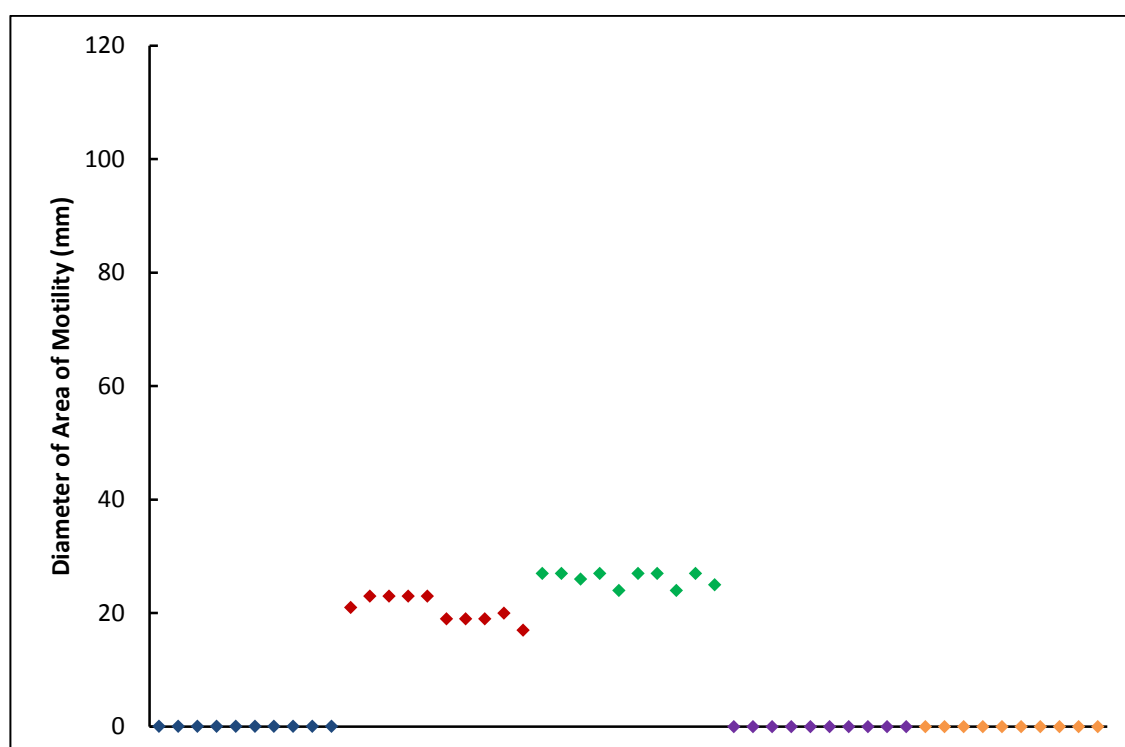


**Figure 19 - Variation in the diameter of the motility zones produced by E2348/69 *hosA*<sup>-</sup> in the presence and absence of different AHLs at 25°C**

For each of the 2 independent biological replicates, 5 technical replicates were analysed. Each point on the graph represents one technical replicate. Petri dishes measured 95 mm in diameter.

(Blue) No AHL

(Red) *N*-(3-oxo-hexanoyl)-L-HSL

(Green) *N*-dodecanoyl-L-HSL

(Purple) *N*-(3-oxo-hexanoyl)-D-HSL

(Orange) *N*-(3-oxo-dodecanoyl)-D-HSL

hexanoyl-DL-HSL and *N*-(3-oxohexanoyl)-L-HSL increased the diameter of the motility zone to  $26.1 \pm 1.52\text{mm}$  ( $F = 2933.44$ ;  $p = <0.0001$ ),  $20 \pm 1.05\text{mm}$  ( $F = 3600$ ;  $p = <0.0001$ ) and  $20.7 \pm 2.21\text{mm}$  ( $F = 874.47$ ;  $p = <0.0001$ ) respectively (Table 12; Figure 19). Addition of *N*-octanoyl-DL-HSL increased the diameter of the motility zone to  $22.4 \pm 1.64\text{mm}$  ( $F = 1850.75$ ;  $p = <0.0001$ ), with the addition of the modified form, *N*-(3-oxo-octanoyl)-DL-HSL, resulting in an increase of E2348/69 *hosA*<sup>-</sup> population expansion to  $13.2 \pm 0.79\text{mm}$  ( $F = 2800.29$ ;  $p = <0.0001$ ) (Table 12). In the presence of *N*-dodecanoyl-L-HSL the average diameter of the motility zone produced by E2348/69 *hosA*<sup>-</sup> was increased to  $26.1 \pm 1.29\text{mm}$  ( $F = 4114.69$ ;  $p = <0.0001$ ), while the modified form, *N*-(3-oxododecanoyl)-DL-HSL, increased the average diameter to  $23.5 \pm 1.27\text{mm}$  ( $F = 3427.79$ ;  $p = <0.0001$ ) (Table 12; Figure 19).

The AHLs which caused the most significant effect on the population expansion of wild type E2348/69 at 25°C were *N*-(3-oxohexanoyl)-L-HSL and *N*-dodecanoyl-L-HSL (Table 10; Figure 15). Addition of *N*-dodecanoyl-L-HSL increased the diameter of the motility zones produced by E2348/69 *hosA*<sup>-</sup> from zero to a level similar to that observed in the wild type strain (Table 13, Figure 20). In the presence of *N*-(3-oxohexanoyl)-L-HSL the population expansion of E2348/69 *hosA*<sup>-</sup> was increased from zero to a level exceeding that observed in wild type E2348/69 in the presence of the same AHL (Table 13; Figure 20).

The effects of *N*-(3-oxohexanoyl)-L-HSL, *N*-dodecanoyl-L-HSL and the 2 *D*-isomers on the population expansion of E2348/69 *hosA*<sup>-</sup> were analysed at 37°C. Compared to 25°C, the variation between the replicates of a culture was much greater at 37°C (Figure 21). Population expansion was restored in the absence of AHL, producing an area of motility with an average diameter of  $87.6 \pm 5.72\text{mm}$  (Table 14). Addition of *N*-(3-oxo-hexanoyl)-D-HSL, *N*-(3-oxododecanoyl)-D-HSL or *N*-dodecanoyl-L-HSL had no significant effect on the diameter of the area of motility (Table 14; Figure 21). However, in the presence of *N*-(3-oxohexanoyl)-L-HSL the motility zone significantly increased in size to an average of  $93.2 \pm 6.14\text{mm}$  ( $F = 5.491$ ;

**Table 13 – Comparison of E2348/69 and E2348/69 *hosA*<sup>-</sup> population expansion at 25°C**

Side chain lengths are in brackets.

Values show the average diameter measurements with one standard deviation for both strains at 25°C in the presence and absence of *N*-(3-oxohexanoyl)-L-HSL and *N*-dodecanoyl-L-HSL. Supplementation with AHL was performed to a final concentration of 5nM. Table is compiled of results from tables 10 and 12.

	E2348/69	E2348/69 <i>hosA</i> <sup>-</sup>
No AHL	20.8 ± 1.03	0
<i>N</i> -(3-oxohexanoyl)-L-HSL (C6)	13.8 ± 1.87	20.7 ± 2.21
<i>N</i> -dodecanoyl-L-HSL (C12)	25.2 ± 1.39	26.1 ± 1.29

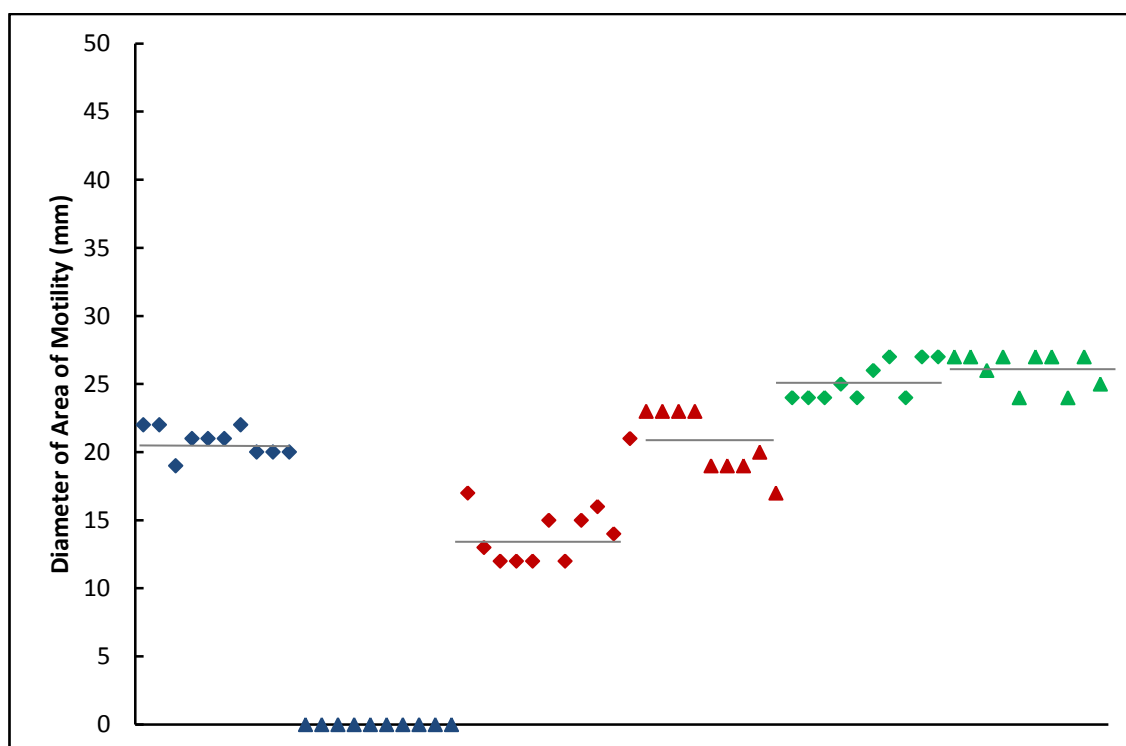


**Figure 20 – Comparison of variation of E2348/69 and E2348/69 *hosA*<sup>-</sup> population expansion at 25°C in the presence and absence of *N*-(3-oxohexanoyl)-L-HSL and *N*-dodecanoyl-L-HSL**

For each of the 2 independent biological replicates per strain, 5 technical replicates were analysed. Each point on the graph represents one technical replicate. Petri dishes measured 95 mm in diameter.

The motility of two different isolates are presented:

(Diamonds) E2348/69

(Triangles) E2348/69 *hosA*<sup>-</sup>

The colours represent the treatment applied:

(Blue) No AHL

(Red) *N*-(3-oxohexanoyl)-L-HSL

(Green) *N*-dodecanoyl-L-HSL

The grey lines represent the average diameter of the motility zones measured for each treatment

**Table 14 - Statistical analysis of the effect of AHL on E2348/69 *hosA*<sup>-</sup> population expansion at 37°C**

Side chain lengths of the AHLs are in brackets. Significant increases in population expansion are highlighted in blue.

	Average diameter of motility ring $\pm$ 1 standard deviation (mm)	ANOVA	
		*F-value	p-value
No AHL	87.6 $\pm$ 5.72		
<i>N</i> -(3-oxo-hexanoyl)-D-HSL (C6)	87.8 $\pm$ 5.22	0.00067	0.936
<i>N</i> -(3-oxododecanoyl)-D-HSL (C12)	84.6 $\pm$ 2.87	2.196	0.156
<i>N</i> -(3-oxohexanoyl)-L-HSL (C6)	93.2 $\pm$ 6.14	5.491	0.031
<i>N</i> -dodecanoyl-L-HSL (C12)	89.7 $\pm$ 4.94	0.625	0.439

\*F- critical value = 4.414

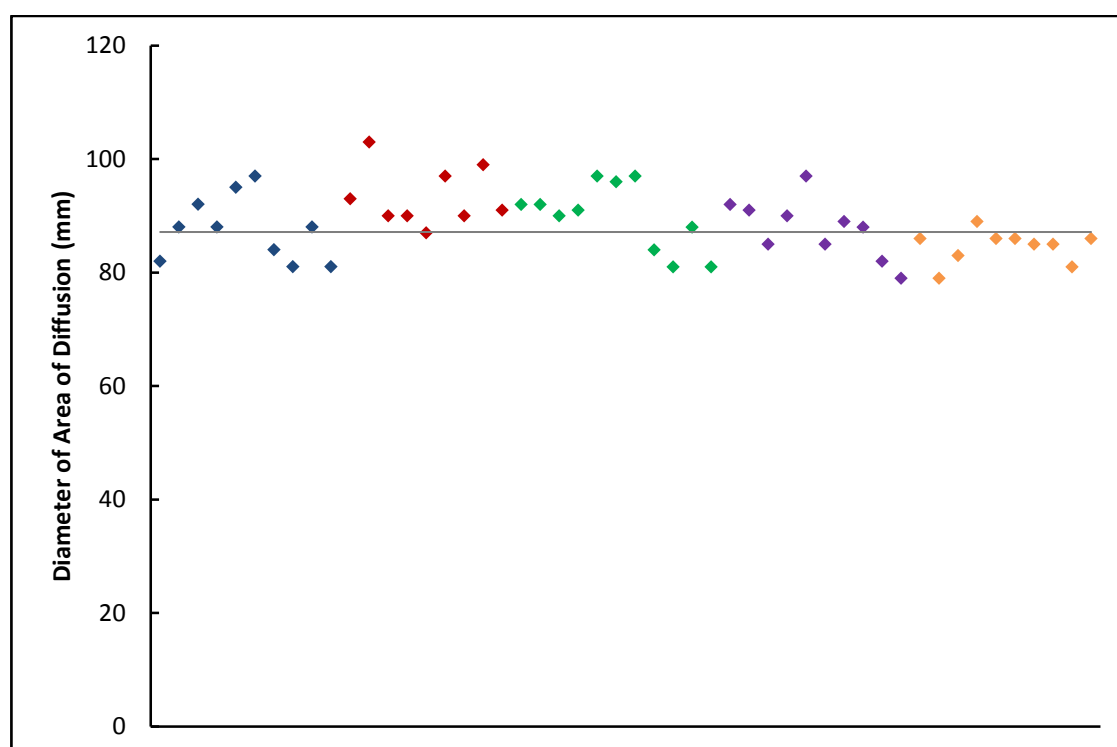


**Figure 21 - Variation in the diameter of the motility zones produced by E2348/69 *hosA*<sup>-</sup> in the presence and absence of different AHLs at 37°C**

For each of the 2 independent biological replicates, 5 technical replicates were analysed. Each point on the graph represents one technical replicate. Petri dishes measured 145 mm in diameter.

(Blue) No AHL

(Red) *N*-(3-oxo-hexanoyl)-L-HSL

(Green) *N*-dodecanoyl-L-HSL

(Purple) *N*-(3-oxo-hexanoyl)-D-HSL

(Orange) *N*-(3-oxo-dodecanoyl)-D-HSL

The grey line represents the average diameter of the motility zones measured for the unsupplemented isolates.



$p=0.031$ ) (Table 14; Figure 21).

### **3.2.3 Effect of HosA and AHL on Aggregation by E2348/69**

Ferrándiz *et al* observed that in the absence of HosA the population of E2348/69 became less motile [68]. No changes in expression of flagella between the wild type strain and the mutant were found in that study, but clumping was observed in the HosA mutant broth cultures which formed non-motile aggregates that were absent in the wild type culture. To determine whether the changes observed in population expansion were in response to changes in cell aggregation, this section described the application of the method by Rowe *et al* to calculate the aggregation indices for both the wild type and mutant in the absence of AHL [79].

The aggregation index (AI) is a comparative measure of the proportion of bacteria within a culture that have aggregated. Growth was monitored during the course of the experiment to illustrate the equivalence of the optical density of both E2348/69 and E2348/69 *hosA*<sup>-</sup> cultures (Figure 22A). The AI values represent the proportion of the population within aggregates, for example an AI of 0.5 is equivalent to 50% of the population. At 25°C E2348/69 had a low proportion of aggregated cells after 3 hours incubation. The AI increased exponentially after 4 hours until 8 hours (Figure 22B). Maximum aggregation was achieved at 8 hours with 77% (AI = 0.77) of the bacteria located in aggregates. Between 8 and 12 hours the aggregates began to disperse and the AI decreased to 0.43 (Figure 22B).

E2348/69 *hosA*<sup>-</sup> had a higher AI than the wild type strain of 0.79 after 3 hours incubation. Maximum aggregation was achieved at 6 hours incubation (AI = 0.98), but a decrease was observed by 8 hours (AI = 0.93). The aggregates began to disperse with 82% (AI = 0.82) remaining aggregated by 12 hours incubation (Figure 22B). No formal statistical confirmation of these observations was performed.

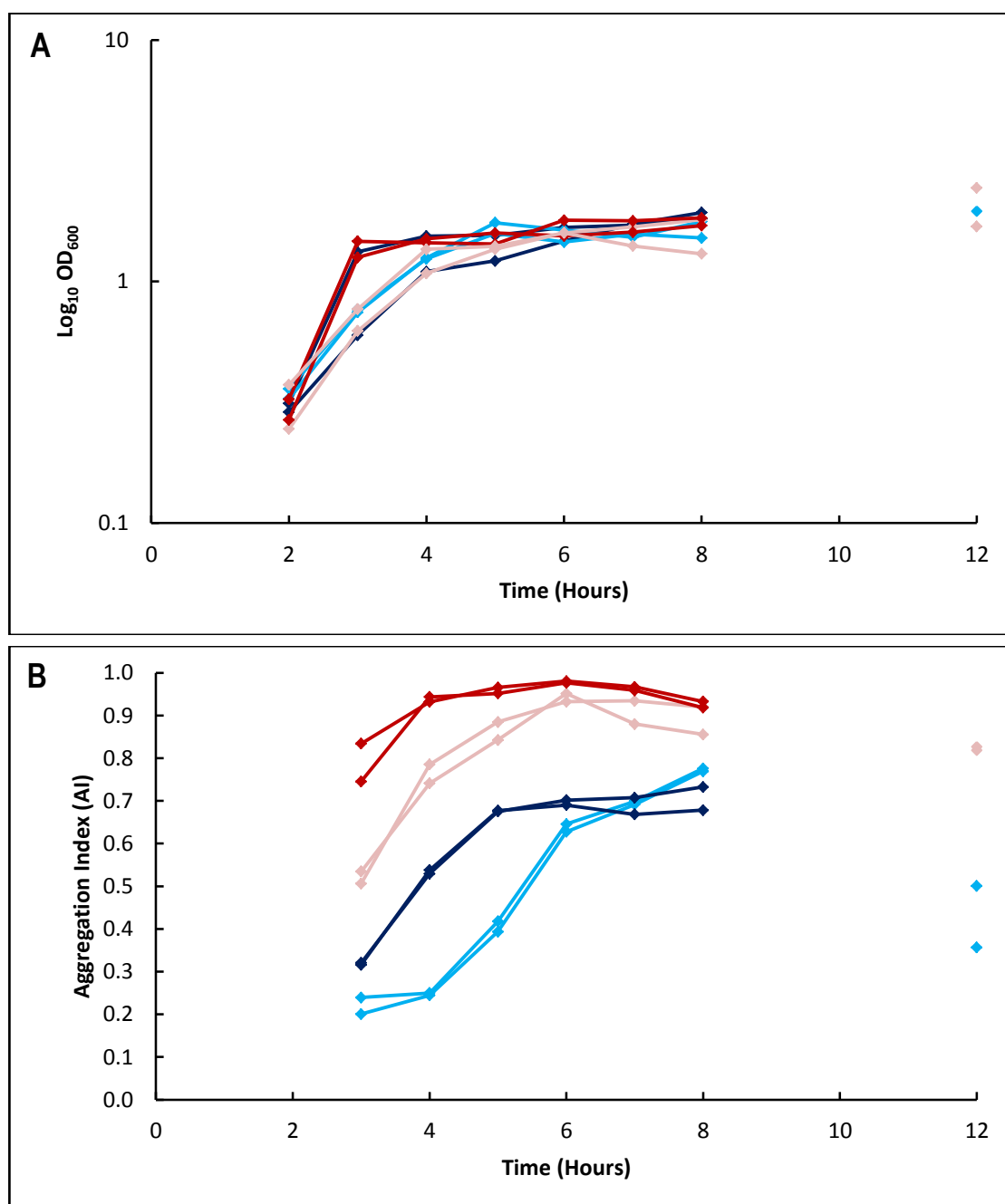


**Figure 22 – Comparison of cell aggregation by E2348/69 and E2348/69 *hosA*<sup>-</sup> using aggregation indices and incubation at 25°C**

The aggregation indices method uses differential centrifugation to determine the proportion of the bacterial population bound together to form aggregates. An AI of 1.0 indicates 100% of the population are aggregated. Four independent experiments are shown. Two different shades of colour are used for each strain to allow differentiation between the experiments.

(Dark/Light Blue) Wild type E2348/69

(Dark/Light Red) E2348/69 *hosA*<sup>-</sup>

Two different conditions are described:

(A) Growth curve of the aggregating cultures determined using log<sub>10</sub> optical density (Log<sub>10</sub>OD<sub>600</sub>)

(B) Aggregation indices of the cultures

*N*-(3-oxohexanoyl)-L-HSL had significantly increased the population expansion of E2348/69 *hosA*<sup>-</sup> (Section 3.2.2). To determine whether this was as a result of *N*-(3-oxohexanoyl)-L-HSL affecting cell aggregation, the AI was calculated in the presence and absence of 5 nM *N*-(3-oxohexanoyl)-L-HSL supplemented into the culture after 4 hours incubation.

In the absence of AHL, the proportion of aggregating cells within the culture was high correlating with previous experiments. Peak aggregation was achieved at 6 hours (AI = 0.82) (Figure 23A). Addition of *N*-(3-oxohexanoyl)-L-HSL decreased the level of cell aggregation of E2348/69 *hosA*<sup>-</sup> to a maximum of 79% (AI = 0.79) at 7 hours incubation. Between 7 and 9 hours the aggregates began to disperse in both cultures regardless of supplementation, indicated by a decrease in AI indices (Figure 23A).

The maximum difference in the AI in the presence and absence of AHL was calculated at 0.048 after 6 hours incubation, suggesting *N*-(3-oxohexanoyl)-L-HSL had little effect on the aggregation of E2348/69 *hosA*<sup>-</sup> (Figure 23A).

After 5 hours incubation, samples were centrifuged. 10µl samples were taken from the bottom 4ml of both the unsupplemented and *N*-(3-oxohexanoyl)-L-HSL -treated E2348/69 *hosA*<sup>-</sup> cultures and analysed using phase contrast microscopy at 1000x magnification (Figures 23B<sub>(1)</sub> and B<sub>(2)</sub>). In the absence of AHL, E2348/69 *hosA*<sup>-</sup> formed large complex aggregates which spanned the fields of view (Figure 23B<sub>(1)</sub>). *N*-(3-oxohexanoyl)-L-HSL was added to technical replicates of the same initial biological culture which had equivalent optical density to that of the unsupplemented culture. Addition of this AHL resulted in much smaller aggregates being formed, with a higher proportion of non-aggregated planktonic cells (Figure 23B<sub>(2)</sub>). The difference in visual aggregation analysis appeared to be greater than the AI analysis indicated (Figure 23). Therefore, a new method was required to investigate the effect of AHL-dependent quorum sensing on the aggregation of E2348/69 and the *HosA* mutant and this is described in the following section.

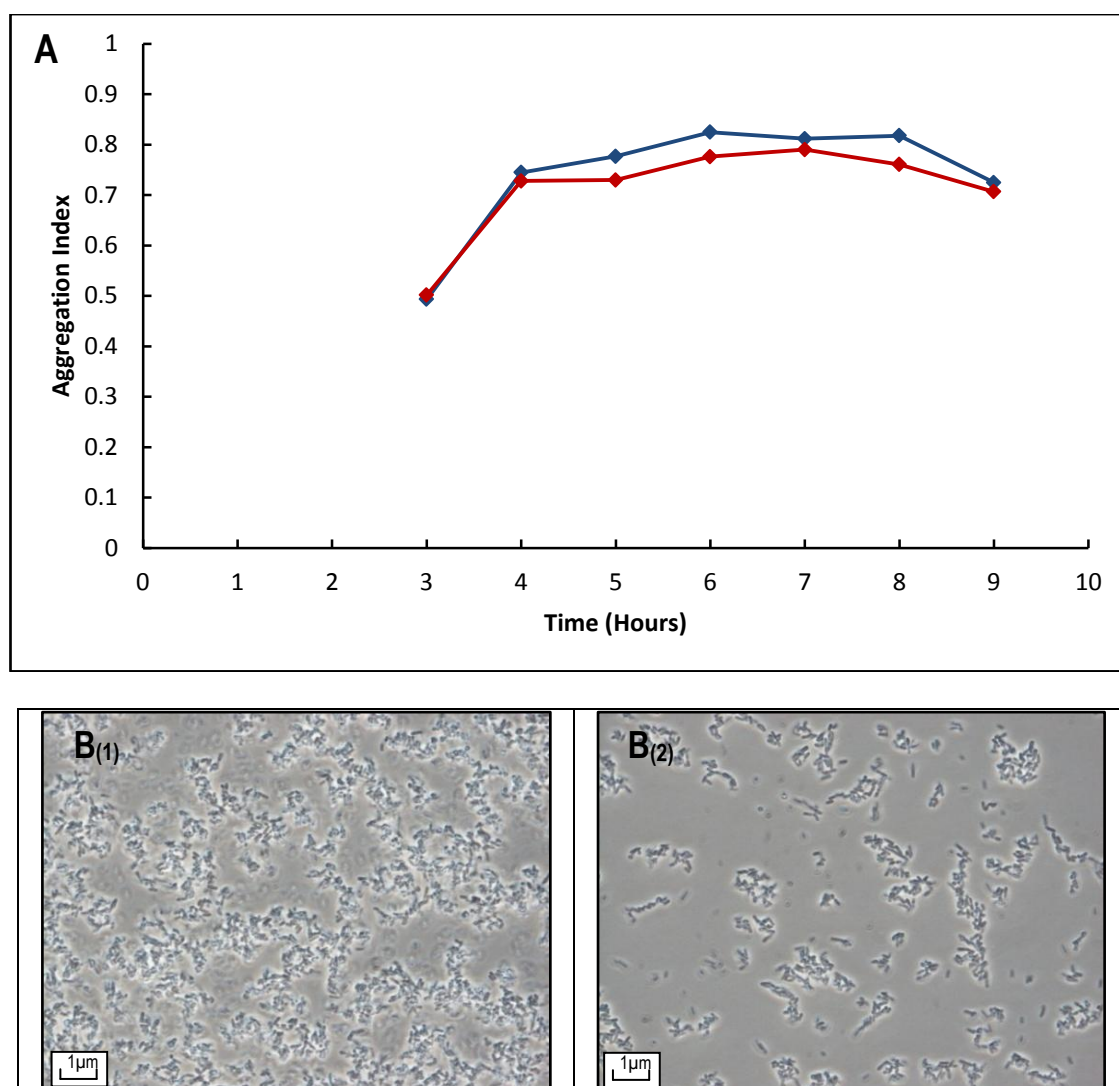


**Figure 23 – Effect of *N*-(3-oxohexanoyl)-L-HSL on cell aggregation by E2348/69 *hosA*<sup>-</sup> at 25°C**

Comparison of aggregation by E2348/69 *hosA*<sup>-</sup> in the presence and absence of *N*-(3-oxohexanoyl)-L-HSL. Supplementation with *N*-(3-oxohexanoyl)-DL-HSL was performed at 4 hours incubation to a final concentration of 5nM. Effect of AHL was assessed using two different methods:

(A) Aggregation Indices. This method uses differential centrifugation to determine the proportion of the bacterial population bound together to form aggregates. An AI of 1.0 indicates 100% of the population are aggregated.

(Blue) E2348/69 *hosA*<sup>-</sup> with no AHL supplement

(Red) E2348/69 *hosA*<sup>-</sup> in the presence of *N*-(3-oxohexanoyl)-L-HSL

(B) Phase contrast microscopy. Images are representative of the aggregates formed by E2348/69 *hosA*<sup>-</sup> in the presence and absence of *N*-(3-oxohexanoyl)-L-HSL after 5 hours incubation. Images were taken at 1000x magnification. Cell densities of the cultures were recorded using optical densities at OD<sub>600</sub> = 0.6.

[B<sub>(1)</sub>] E2348/69 *hosA*<sup>-</sup> with no AHL supplement

[B<sub>(2)</sub>] E2348/69 *hosA*<sup>-</sup> in the presence of *N*-(3-oxohexanoyl)-L-HSL

### **3.2.4 Development of a Phase Contrast Microscopy Method for Aggregation Analysis**

Due to the weak nature of the aggregates formed by E2348/69 *hosA*<sup>-</sup>, it was necessary to develop an AI method combining microscopy with imaging and statistical analysis. Microscopic analysis of E2348/69 *hosA*<sup>-</sup> at 10000x magnification had already shown the cell aggregation in liquid culture (Figure 23B). Using 100x magnification the biological variation in size and shape of the aggregates formed by a single culture of the HosA mutant were observed (Figure 24). By comparison the wild type E2348/69 consistently produced very small aggregates with a high proportion of non-aggregating planktonic cells (Figure 24).

For each experiment 2 biological replicates, each comprising of 6 technical replicates, were analysed using CellProfiler™. The software produced an output for each image, which was divided into 4 separate sections. First, the original image was converted to greyscale (Figures 25A<sup>1</sup> and 25B<sup>1</sup>), and each object within the image was automatically identified and differentiated using arbitrary colours (Figures 25A<sup>2</sup> and 25B<sup>2</sup>). Using the parameters input into the software each object was outlined in red or green depending on whether they were within the required dimensions (Figures 25A<sup>3</sup> and 25B<sup>3</sup>). Any objects falling outside these parameters were outlined in red. The final section of the output was a summary table indicating the number of identified objects, the interquartile range of the diameter of the objects, and the total area within the image covered by the objects (Figures 25A<sup>4</sup> and 25B<sup>4</sup>).

Microscopic analysis clearly revealed that the size of aggregates produced by E2348/69 and E2348/69 *hosA*<sup>-</sup> were different (Figures 25A and B respectively). For a single image, E2348/69 produced 1940 aggregates with 80% of those between 2.3 and 7.3 pixels in diameter (Figure 25A). A single technical replicate of E2348/69 *hosA*<sup>-</sup> contained only 169 aggregates, with 80% of those identified of between 2.0 and 85.1 pixels in diameter (Figure 25B).

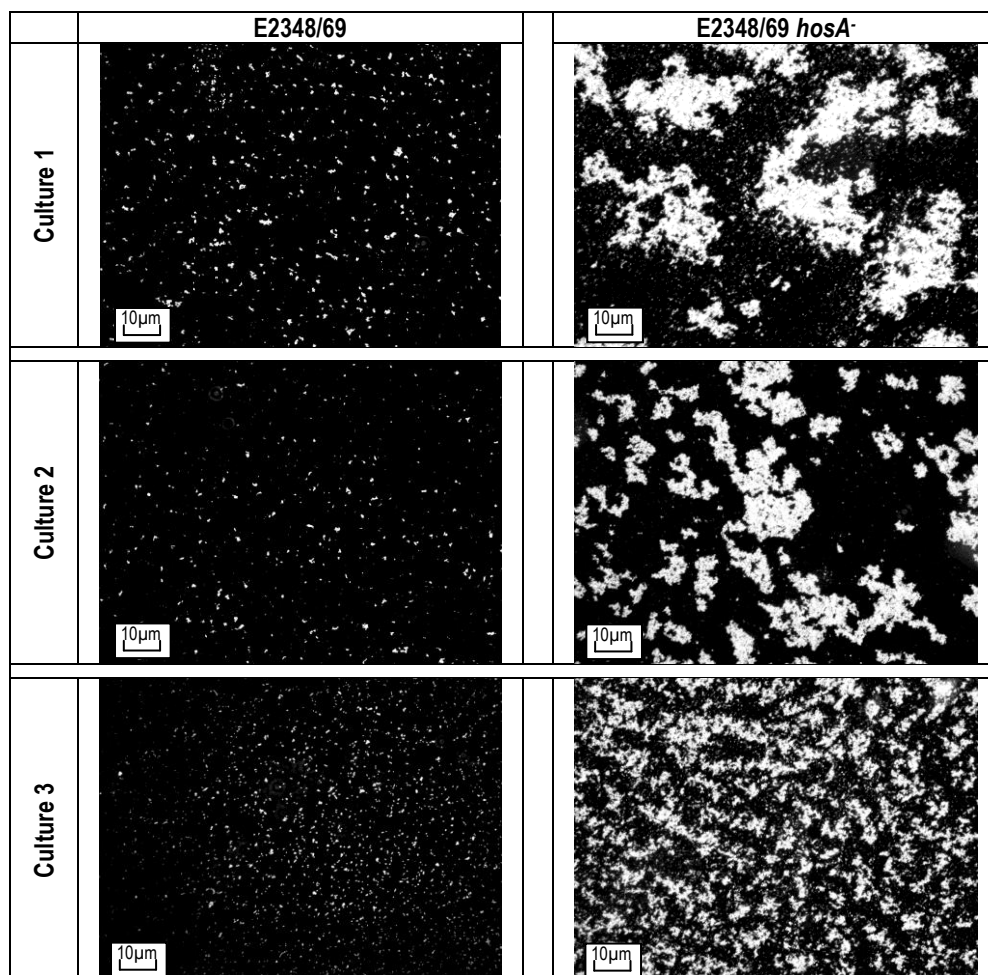


**Figure 24 - Aggregates formed by E2348/69 and E2348/69 *hosA*<sup>-</sup> in three independent biological replicates**

Images were taken using phase contrast microscopy at 100x magnification. Each image is representative of an independent biological replicate comprising 6 technical replicates.

Scale bars are indicated in the left hand corner of the image, and set to 10µm.

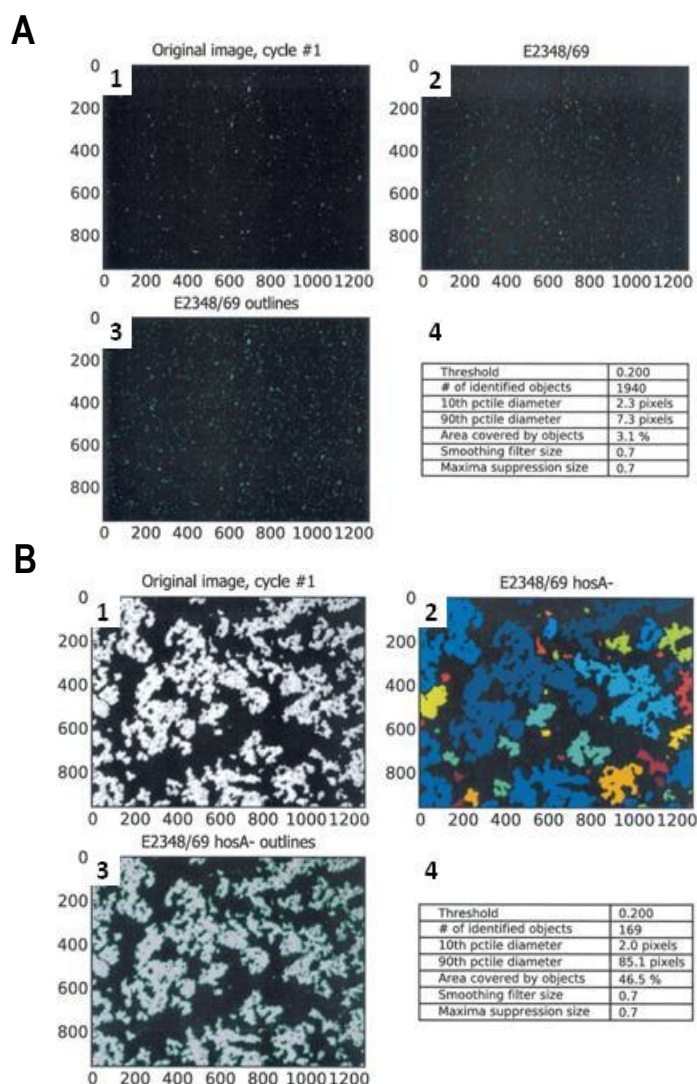


**Figure 25 – CellProfiler™ outputs produced during analysis of microscopy images illustrating the aggregation of E2348/69 and E2348/69 *hosA*<sup>-</sup>**

One output was produced for each image analysed using CellProfiler™. All axes show the position on the image for identification of each object by x and y co-ordinates (pixels). Similar outputs were produced for the images represented in figure 24.

There are four components to each output:

- (1) Original phase contrast microscopy image taken at 100x magnification converted to greyscale
- (2) Aggregates identified by the software and assigned an arbitrary colour for clearer differentiation
- (3) Aggregates within the size parameters were outlined in green, those outside the range would be highlighted in red
- (4) Summary table

The outputs for 2 images are provided for comparison:

- (A) A non-aggregating sample from E2348/69
- (B) An aggregating sample from E2348/69 *hosA*<sup>-</sup>

Once identified, several aggregate characteristics such as perimeter, area, position within the image and Zernike polynomials were calculated by the software for each object. For the purposes of aggregation analysis, only the area values were used to describe differences in the size and distribution of aggregates between both individual images and cultures.

Using Microsoft Excel™, the aggregates were divided by area into ranges of size such as 0-50 pixels<sup>2</sup> and 1000-1500 pixels<sup>2</sup>. The total number of aggregates within each group was counted. By multiplying the number of aggregates by the average area of each group, an aggregation profile was created for a population which represented the distribution of bacteria within the aggregates and the 3-dimensional quality of the aggregates.

The images in Figure 24 were analysed using CellProfiler™ and the profiles plotted as separate dot plots for the analysis of biological variation (Figure 26). Each colour within the graph represents one technical replicate, i.e. one image. The majority of aggregates produced by parental E2348/69 fell between the range of 0 – 400 pixels<sup>2</sup>, with the largest aggregates measuring approximately 8000 pixels<sup>2</sup>. The replicates showed some variation in frequency of each aggregate size, but the overall aggregation profile remained the same (Figure 26A). The aggregation profile produced for the *HosA* mutant had the opposite distribution to the wild type strain. The majority of aggregates were between 8000 and 20,000+ pixels<sup>2</sup>, with a lower number of smaller aggregates between 0 – 8000 pixels<sup>2</sup> (Figure 26B). The variation between replicates of E2348/69 *hosA*<sup>-</sup> was small in the lower size ranges, but increased with area (Figure 26B).

Comparison of the replicates for each of E2348/69 and E2348/69 *hosA*<sup>-</sup> was performed using the Kolmogorov-Smirnov (K-S) test. This test utilises a non-parametric pair-wise comparison of the continuous one-dimensional aggregation profile to test for the equality of the 2 treatments. The resultant D-value represents the distance between the empirical distribution



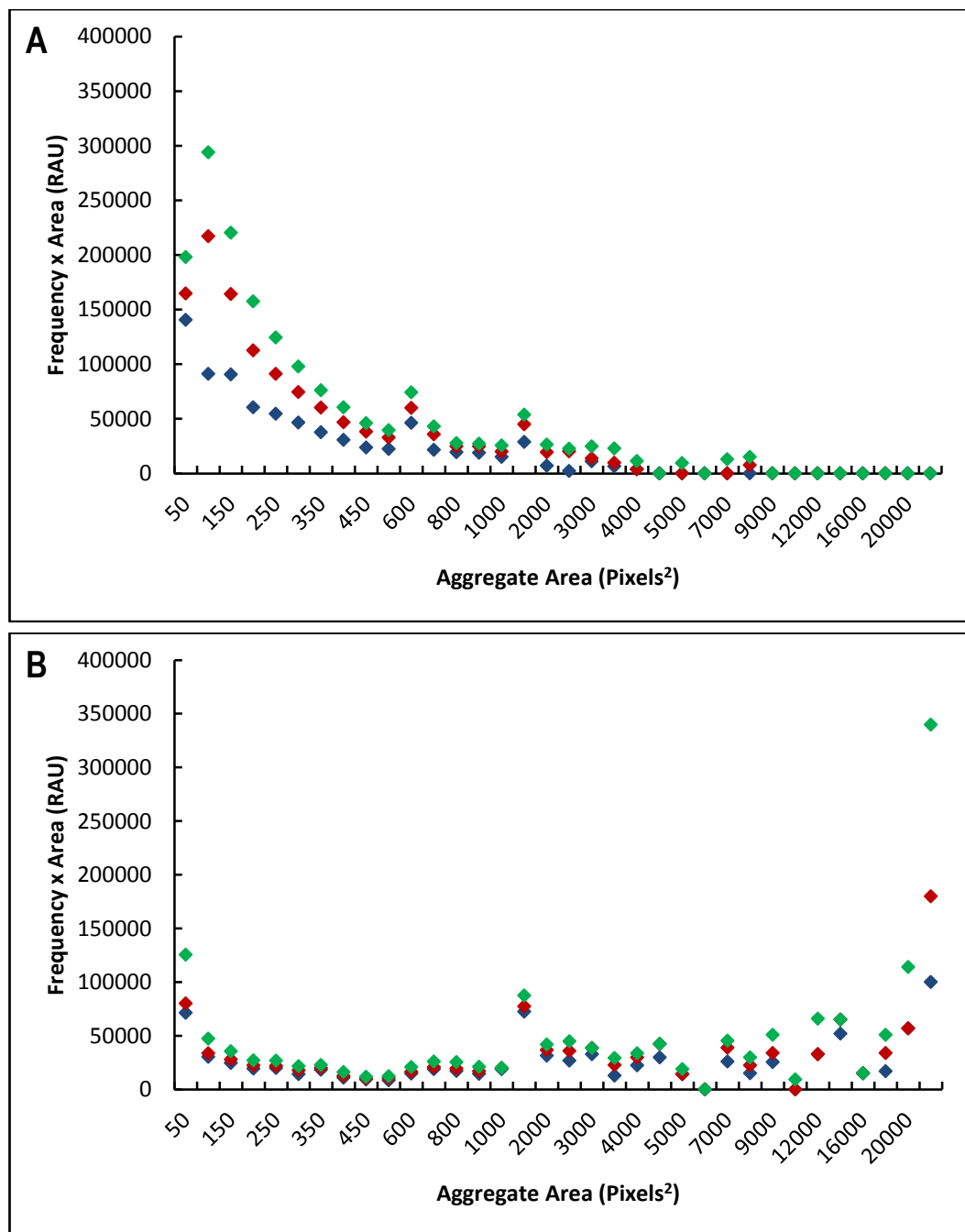


**Figure 26 – Aggregation profiles of independent biological replicates of E2348/69 and E2348/69 *hosA*<sup>-</sup> at 25°C**

Aggregation profile is defined as the distribution of aggregates differentiated by size formed by a given population. Images provided in Figure 24 were analysed using CellProfiler™ with the parameters provided in Table 7. Each colour is representative of the aggregation profile of an independent biological replicate.

(A) Wild type E2348/69

(B) E2348/69 *hosA*<sup>-</sup>

**Table 15 – Statistical comparison of the aggregation profiles produced by independent biological replicates of E2348/69 and E2348/69 *hosA*<sup>-</sup>**

Comparisons were completed between the profiles of two of the independent cultures of either E2348/69 or E2348/69 *hosA*<sup>-</sup> provided in Figure 24. Where  $D < 0.4$  any differences in the aggregation profiles was attributed to biological variation. If  $D \geq 0.4$ , the effect of a given treatment was identified as significant.

	E2348/69	E2348/69 <i>hosA</i> <sup>-</sup>
D-Value	0.13	0.13

functions of the two profiles, i.e. the higher the value the greater the difference between the population distributions. The variation between the replicates of E2348/69 shown in Figure 26A was calculated as  $D = 0.13$  (Table 15). A similar comparison for E2348/69 *hosA*<sup>-</sup> showed biological variation also to be  $D = 0.13$  (Table 15). Validation experiments and analyses were performed using multiple repeated experiments with both wild type and mutant. As part of the validation process, a dilution series of E2348/69 *hosA*<sup>-</sup> aggregates was analysed using the new AI method. Dilutions of 1:2, 1:5 and 1:10 were analysed and compared to similar dilutions in the wild type. A higher level of aggregation was maintained in E2348/69 *hosA*<sup>-</sup> at all dilutions tested when compared to the wild type (data not shown).

During the validation process biological variation was observed to range between 0.01 and 0.3 depending on the size and distribution of the aggregation profile. Due to this wide variation between biological and technical replicates during the validation process, it was determined that  $D < 0.4$  would be a useful cut-off point for biological variation. Thereby, if  $D \geq 0.4$  the two distributions were deemed as being significantly different. As the values calculated for the profiles in Figure 26 were  $D = 0.13$  the differences between independent cultures was deemed to be as a result of biological variation.

In addition to calculating statistical significance,  $R^{\text{TM}}$  was utilised to provide graphical representations of the data (Figure 27). Two different graphical methods were used; a kernel density plot and a box and whisker plot. The kernel density plot displays the actual data on an axis to demonstrate the difference in distribution (Figure 27A). The two E2348/69 replicates shown exhibited very little difference in the aggregation profile (Figure 27A). The box and whisker plot can be used for more descriptive statistics displaying differences in the data without making any assumptions on distribution (Figure 27B). In this case the box and whisker plot was used to show the spread of the data. Using the same two replicates used in Figure 27A, it was observed that replicate 1 had fewer outliers and the maximum aggregate size was lower when

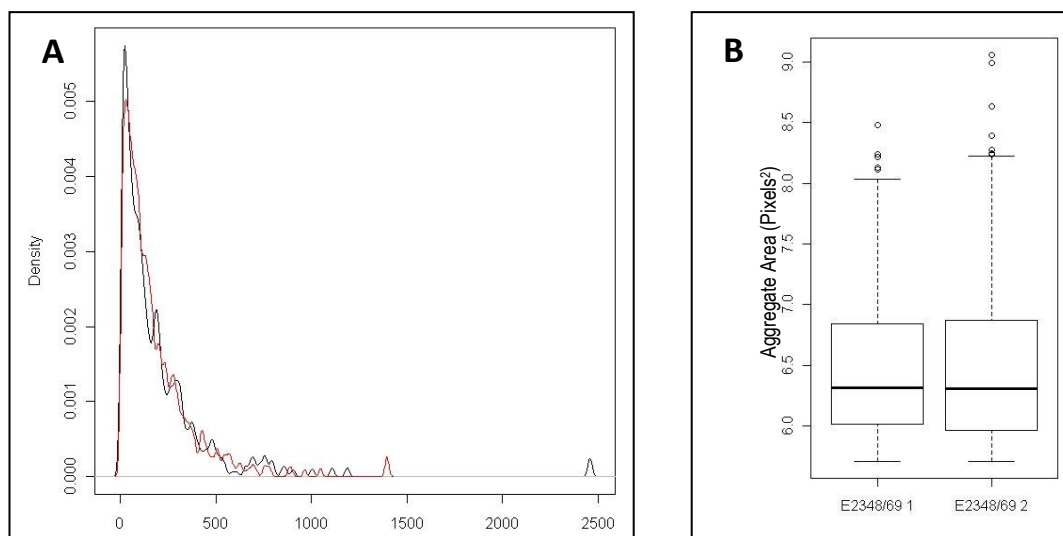


**Figure 27 – Graphical representations of variation between the aggregation profiles of two independent replicates of E2348/69**

(A) Kernel Density Plot of the two biological replicates plotting the actual values on the axis rather than the ranges specified in Figure 26

(Black) E2348/69 Culture 1

(Red) E2348/69 Culture 2

(B) Box and whisker plot showing more descriptive statistics for the two independent cultures represented in Figure 25A

compared to replicate 2 (Figure 27B). The interquartile range and overall spread of the data between the two replicates was similar (Figure 27B).

### **3.2.5 Effect of HosA on Cell Aggregation of E2348/69**

After 5 hours incubation a total of 12 independent biological replicates were analysed per strain and the resultant aggregation profile compared for E2348/69 and E2348/69 *hosA*<sup>-</sup> after 5 hours incubation. The profiles provided in Figure 28 are representative of the aggregation observed in all technical replicates from 2 independent cultures of each strain. E2348/69 produced a high number of planktonic cells with an area below 50 pixels<sup>2</sup>, with some small aggregates also identified (Figure 28). There were no E2348/69 aggregates produced that exceeded 7000 pixels<sup>2</sup> (Figure 28). By comparison, the aggregation profile produced by E2348/69 *hosA*<sup>-</sup> increased exponentially relative to area (Figure 28). Comparison using the K-S test calculated the difference between the aggregation of E2348/69 and E2348/69 *hosA*<sup>-</sup> at D = 0.96 indicating these distributions are significantly different. Biological variation between replicates was calculated as 0.045 for E2348/69 and 0.27 for E2348/69 *hosA*<sup>-</sup>, meaning the overall comparison of observed differences in aggregation was not due to biological variation.

### **3.2.6 Role of AHL in Cell Aggregation of E2348/69 and E2348/69 *hosA*<sup>-</sup>**

Having determined the motile E2348/69 produced only small sized aggregates in the absence of AHL, specific signals were added to the aggregating cells to investigate the link between aggregation, motility and quorum sensing. It was hypothesised that where addition of AHL to E2348/69 decreased population expansion, a concurrent increase in bacterial aggregation would be observed. Conversely where addition of AHL had increased the population expansion of E2348/69 *hosA*<sup>-</sup> it was hypothesised a decrease in aggregation would be observed.

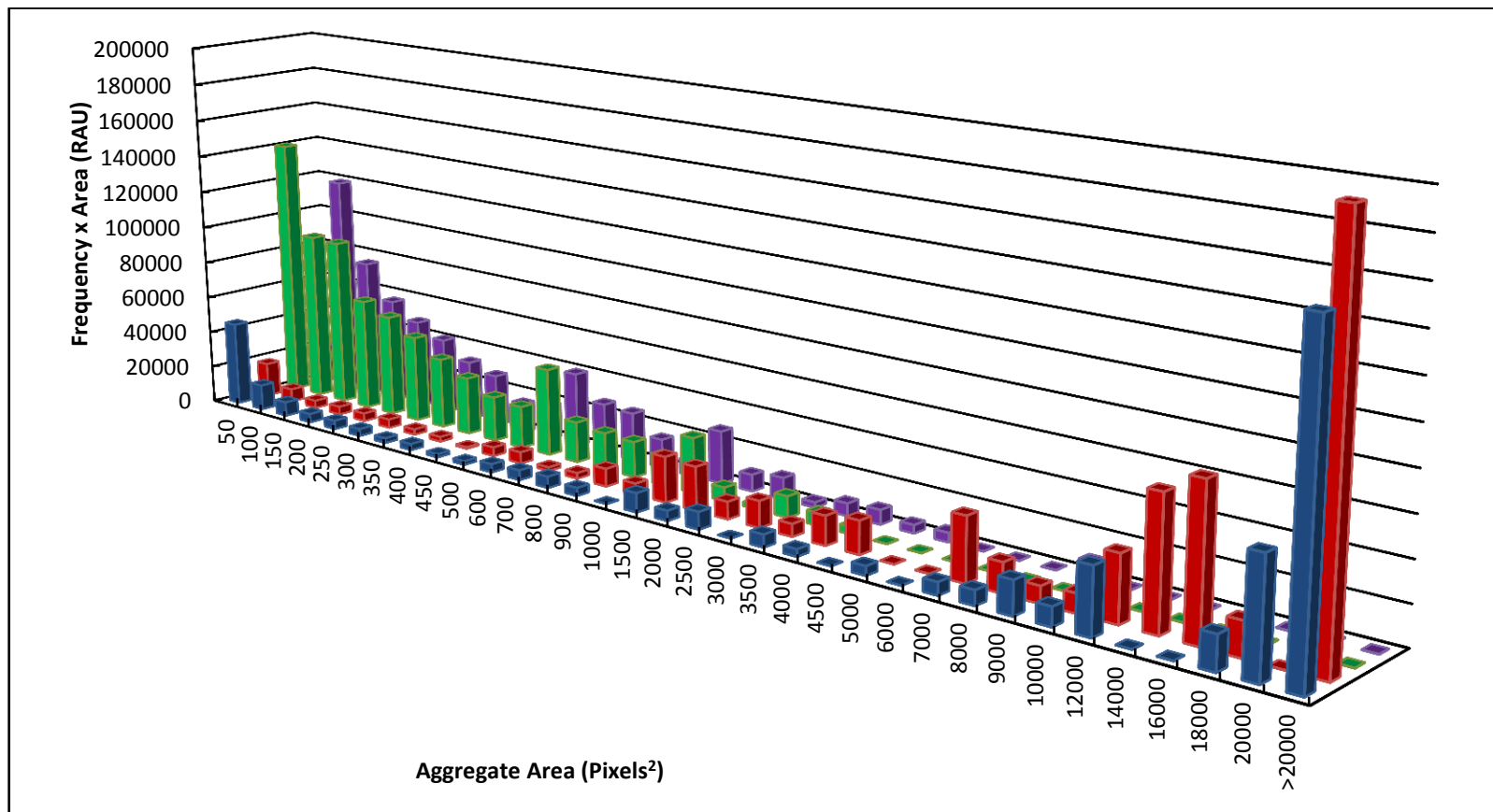


**Figure 28 – Comparison of the aggregation profiles produced by E2348/69 and E2348/69 *hosA*<sup>-</sup> at 25°C**

Aggregation profiles showing the distribution of aggregate sizes formed by 2 independent cultures of both E2348/69 and E2348/69 *hosA*<sup>-</sup> after 5 hours incubation. The images analysed were represented in Figure 24.

(Blue) E2348/69 *hosA*<sup>-</sup> Culture 1

(Red) E2348/69 *hosA*<sup>-</sup> Culture 2

(Green) E2348/69 Culture 1

(Purple) E2348/69 Culture 2

Cultures were grown for a total of 5 hours at 25°C, with 5 nM final concentration AHL added at 4 hours. A representative sample of the microscopy images are shown in Figure 29 illustrating the visual properties of the aggregates produced by E2348/69 in the presence and absence of both active and inactive AHLs. In the absence of AHL, E2348/69 produced small aggregates with a high proportion of planktonic cells. Visually, addition of both active AHLs, *N*-(3-oxohexanoyl)-L-HSL and *N*-dodecanoyl-L-HSL, appeared to increase the size of the aggregates (Figure 29). In the presence of the inactive *N*-(3-oxo-hexanoyl)-D-HSL and *N*-(3-oxododecanoyl)-D-HSL aggregates were small in size and high in number (Figure 29).

Two biological replicates were analysed per treatment. Evaluation of the aggregation profile of both independent E2348/69 cultures in the absence of AHL showed a high proportion of planktonic cells with some small aggregates (Figure 30). Technical variation between images from the same culture was calculated as  $D = 0.12$  (Table 16). Biological variation between culture A and B was calculated at  $D = 0.045$  (Table 16). The addition of *N*-(3-oxohexanoyl)-L-HSL significantly increased the size of the aggregates formed in comparison to those formed in the absence of AHL in both cultures A and B ( $D = 0.49$  and  $D = 0.56$  respectively) (Table 16). The aggregation profile in both cultures A and B shifted to the right, with a peak between 1501 – 2000 pixels<sup>2</sup> (Figures 30A and B). Biological variation was calculated as  $D = 0.11$ , meaning the overall increase in aggregation was not due to biological variance ( $D = 0.53$ ) (Table 16).

In the presence of *N*-dodecanoyl-L-HSL the aggregation profile shifted to the right in both cultures with peak aggregation falling between 1501 – 2000 pixels<sup>2</sup> for both culture A and B (Figures 30A and B). Aggregate size significantly increased in both culture A and B in the presence of *N*-dodecanoyl-L-HSL ( $D = 0.71$  and  $D = 0.71$  respectively) (Table 16). Biological variation was calculated as  $D = 0.04$ , thereby the overall increase in aggregation was not due to biological variation ( $D = 0.70$ ) (Table 16).

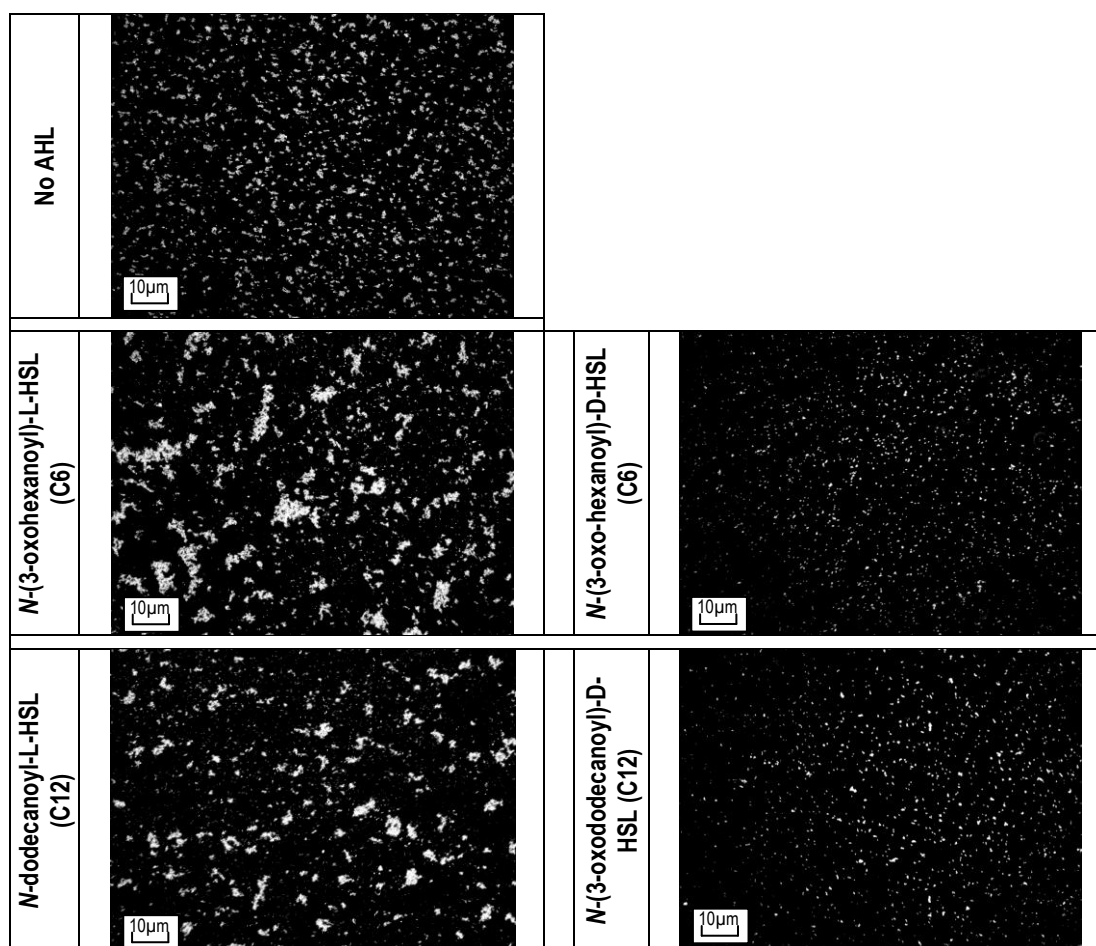


**Figure 29 –Aggregates formed by E2348/69 in the presence and absence of AHL at 25°C**

Microscopy images were taken at 100x magnification phase contrast microscopy after 5 hours incubation. Images are representative of 2 independent biological replicates, each with 6 technical replicates. Supplementation with AHL was performed at 4 hours incubation to a final concentration of 5nM.

Scale bars are indicated in the left hand corner of each image, and set to 10µm.

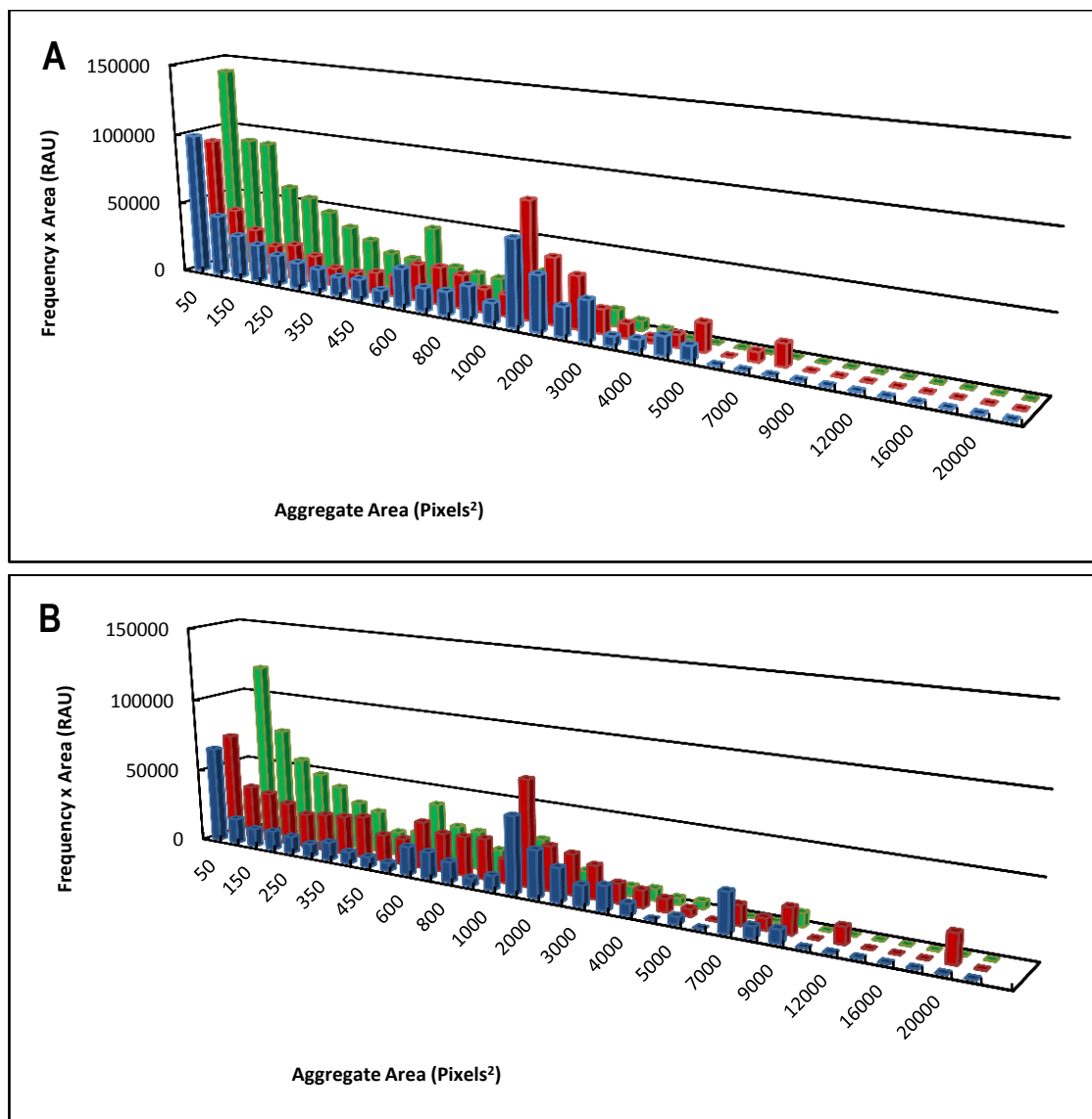


**Figure 30 – Aggregation profile of E2348/69 in the presence and absence of *N*-(3-oxohexanoyl)-L-HSL and *N*-dodecanoyl-L-HSL at 25°C**

Each profile is representative of the distribution of aggregate sizes produced by E2348/69 in the presence and absence of *N*-(3-oxohexanoyl)-L-HSL and *N*-dodecanoyl-L-HSL. AHLs were supplemented at 4 hours growth to a final concentration of 5nM. The images analysed were represented in Figure 29.

(A) Culture A; and (B) Culture B

(Blue) E2348/69 in the presence of *N*-(3-oxohexanoyl)-L-HSL

(Red) E2348/69 in the presence of *N*-dodecanoyl-L-HSL

(Green) E2348/69 with no AHL supplement

**Table 16 – Statistical comparison of the effect of active AHL on E2348/69 aggregation**

Biological variation compares profiles between cultures independent A and B; technical variation compares the profiles within a culture. Where  $D < 0.4$  there is no significant difference between the profiles of the given treatments, but where  $D \geq 0.4$  the difference is deemed to be significant.

	Biological Variation (A vs B)		Technical Variation	
E2348/69	0.045		0.12	
	A	B	Biological Variation (A vs B)	Unsupplemented vs Supplemented
<i>N</i> -(3-oxohexanoyl)-L-HSL (C6)	0.49	0.56	0.11	0.53
<i>N</i> -dodecanoyl-L-HSL (C12)	0.71	0.71	0.04	0.70



Both of the *D*-isomers, *N*-(3-oxo-hexanoyl)-*D*-HSL and *N*-(3-oxododecanoyl)-*D*-HSL had no significant effect on the aggregation of E2348/69 at 25°C ( $D = 0.22$  and  $D = 0.21$  respectively) (Table 17; Figure 31). Aggregation profiles of both cultures A and B had the same distribution as that observed in the absence of AHL (Figures 31A and B). Biological variation was calculated as  $D = 0.11$  for *N*-(3-oxohexanoyl)-*D*-HSL and  $D = 0.14$  for *N*-(3-oxododecanoyl)-*D*-HSL (Table 17). These results show E2348/69 cell aggregation is affected by the presence of *L*-isomer AHL only.

E2348/69 *hosA*<sup>-</sup> produced large complex aggregates in the absence of AHL (Figure 32). Addition of *N*-(3-oxohexanoyl)-*L*-HSL and *N*-dodecanoyl-*L*-HSL resulted in a visual decrease in the size of the aggregates formed by E2348/69 *hosA*<sup>-</sup> (Figure 32). In the presence of both *N*-(3-oxo-hexanoyl)-*D*-HSL and *N*-(3-oxododecanoyl)-*D*-HSL large and complex aggregates were observed, which were visually similar to that observed in the absence of AHL (Figure 32).

Technical variation in the absence of AHL between images from the same culture was calculated as  $D = 0.13$  (Table 18). Biological variation between the independent cultures in the absence of AHL was estimated to be  $D = 0.27$  (Table 18).

Addition of *N*-(3-oxohexanoyl)-*L*-HSL and *N*-dodecanoyl-*L*-HSL resulted in a shift from the distribution observed in the absence of AHL, to a bell shaped curve in both cultures (Figures 33A and B). In the presence of *N*-(3-oxohexanoyl)-*L*-HSL the size of the aggregates decreased significantly in comparison to the supplemented for both A and B cultures ( $D = 0.77$  and  $D = 0.50$  respectively) (Table 18). Peak aggregation shifted to the left from 20,000+ pixels<sup>2</sup> in the absence of AHL, to between 1501 – 2000 pixels<sup>2</sup> after addition of *N*-(3-oxohexanoyl)-*L*-HSL (Figures 33A and B). Biological variation was calculated at  $D = 0.17$  meaning the overall decrease in aggregation was not attributable to biological variation ( $D = 0.65$ ) (Table 18).

Addition of *N*-dodecanoyl-*L*-HSL significantly decreased the size of aggregates formed in both cultures A and B ( $D = 0.77$  and  $D = 0.51$  respectively) (Table 18). Peak aggregation decreased from 20,000+ in the absence of AHL to between 1501 – 2000 pixels<sup>2</sup> upon addition of

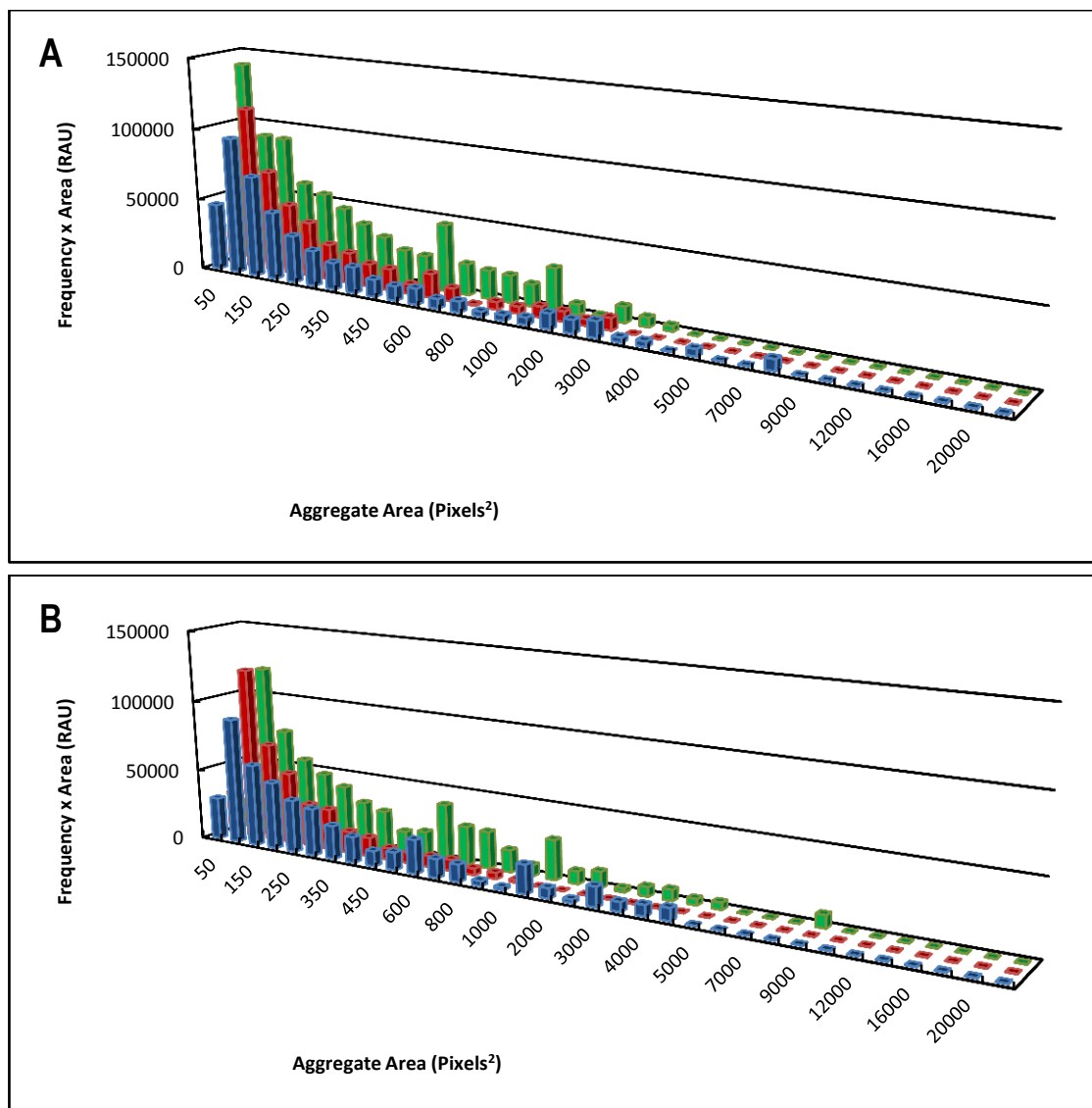


**Figure 31 – Aggregation profile of E2348/69 in the presence and absence of *N*-(3-oxo-hexanoyl)-D-HSL and *N*-(3-oxododecanoyl)-D-HSL at 25°C**

Each profile is representative of the distribution of aggregate sizes produced by E2348/69 in the presence and absence of *N*-(3-oxo-hexanoyl)-D-HSL and *N*-(3-oxododecanoyl)-D-HSL. AHLs were supplemented at 4 hours growth to a final concentration of 5nM. The images analysed were represented in Figure 29.

(A) Culture A; and (B) Culture B

(Blue) E2348/69 in the presence of *N*-(3-oxo-hexanoyl)-D-HSL

(Red) E2348/69 in the presence of *N*-(3-oxododecanoyl)-D-HSL

(Green) E2348/69 with no AHL supplement

**Table 17 – Statistical comparison of the effect of *D*-isomers on E2348/69 aggregation**

Biological variation compares profiles between cultures independent A and B; technical variation compares the profiles within a culture. Where  $D < 0.4$  there is no significant difference between the profiles of the given treatments, but where  $D \geq 0.4$  the difference is deemed to be significant.

	Biological Variation (A vs B)		Technical Variation	
E2348/69	0.045		0.12	
	A	B	Biological Variation (A vs B)	Unsupplemented vs Supplemented
<i>N</i> -(3-oxo-hexanoyl)-D-HSL (C6)	0.26	0.16	0.11	0.22
<i>N</i> -(3-oxododecanoyl)-D-HSL (C12)	0.29	0.14	0.14	0.21

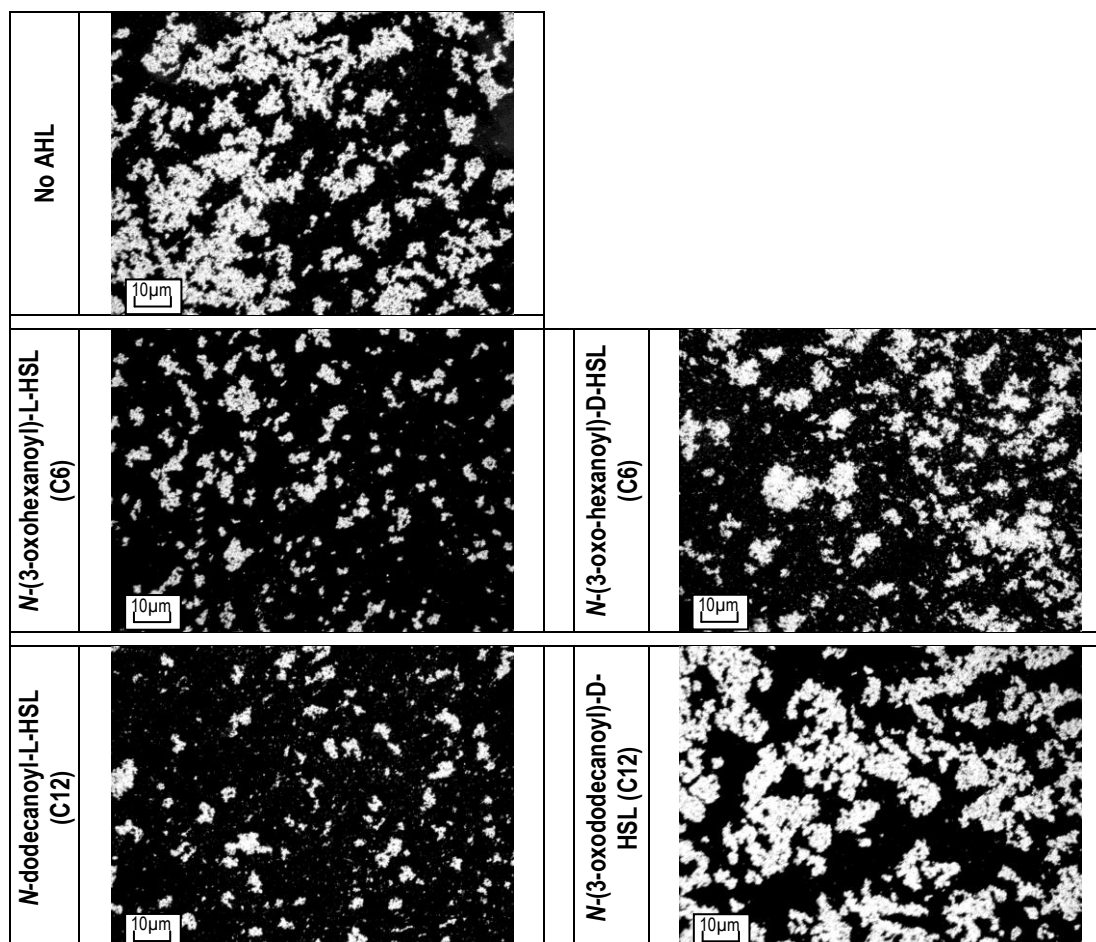


**Figure 32 - Aggregates formed by E2348/69 *hosA*<sup>-</sup> in the presence and absence of AHL at 25°C**

Microscopy images were taken at 100x magnification phase contrast microscopy after 5 hours incubation. Images are representative of 2 independent biological replicates, each with 6 technical replicates. Supplementation with AHL was performed at 4 hours incubation to a final concentration of 5nM.

Scale bars are indicated in the left hand corner of each image, and set to 10µm.

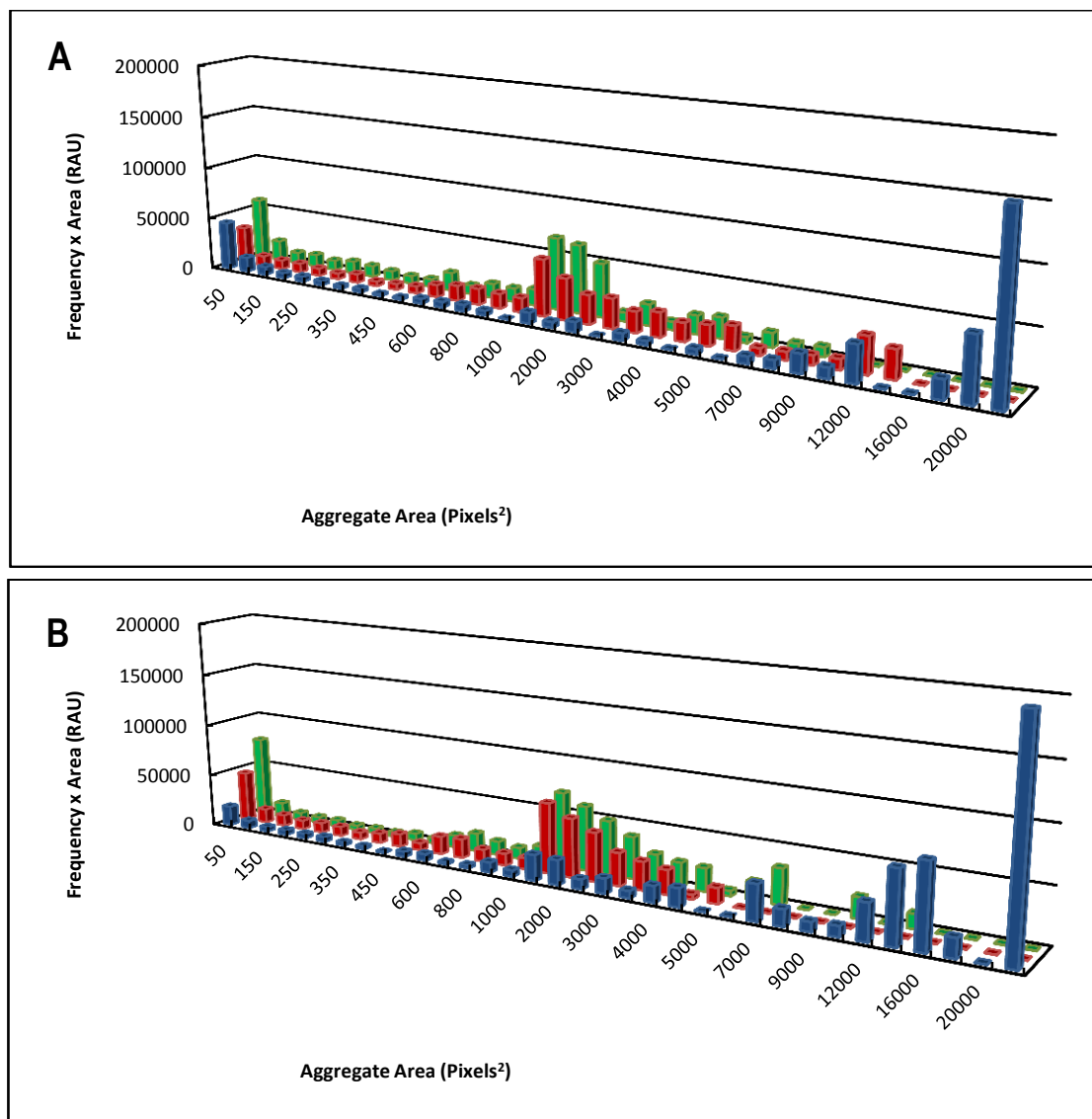


**Figure 33 – Aggregation profile of E2348/69 *hosA*<sup>-</sup> in the presence and absence of *N*-(3-oxohexanoyl)-L-HSL and *N*-dodecanoyl-L-HSL at 25°C**

Each profile is representative of the distribution of aggregate sizes produced by E2348/69 *hosA*<sup>-</sup> in the presence and absence of *N*-(3-oxohexanoyl)-L-HSL and *N*-dodecanoyl-L-HSL. AHLs were supplemented at 4 hours growth to a final concentration of 5nM. The images analysed were represented in Figure 32.

(A) Culture A; and (B) Culture B

(Blue) E2348/69 *hosA*<sup>-</sup> with no AHL supplement

(Red) E2348/69 *hosA*<sup>-</sup> in the presence of *N*-(3-oxohexanoyl)-L-HSL

(Green) E2348/69 *hosA*<sup>-</sup> in the presence of *N*-dodecanoyl-L-HSL

**Table 18 – Statistical comparison of the effect of active AHL on E2348/69 *hosA*<sup>-</sup> aggregation**

Biological variation compares profiles between cultures independent A and B; technical variation compares the profiles within a culture. Where  $D < 0.4$  there is no significant difference between the profiles of the given treatments, but where  $D \geq 0.4$  the difference is deemed to be significant.

	Biological Variation (A vs B)			Technical Variation	
E2348/69 <i>hosA</i> <sup>-</sup>	0.27			0.13	
	A		B	Biological Variation (A vs B)	Unsupplemented vs Supplemented
<i>N</i> -(3-oxohexanoyl)-L-HSL (C6)	0.77		0.50	0.17	0.65
<i>N</i> -dodecanoyl-L-HSL (C12)	0.77		0.51	0.13	0.64

*N*-dodecanoyl-L-HSL (Figures 33A and B). Biological variation was calculated at  $D = 0.13$ , thereby the overall decrease in aggregation was not as a result of biological variation ( $D = 0.64$ ) (Table 18). These results confirm that addition of both short chain *N*-(3-oxohexanoyl)-L-HSL and *N*-dodecanoyl-L-HSL affected cell aggregation in E2348/69 *hosA*<sup>-</sup>.

Neither *N*-(3-oxo-hexanoyl)-D-HSL nor *N*-(3-oxododecanoyl)-D-HSL had any significant effect on the aggregation profile of E2348/69 *hosA*<sup>-</sup> at 25°C ( $D = 0.23$  and  $D = 0.33$  respectively) (Table 19; Figure 34). The aggregation profiles of both culture A and B in the presence of either AHL had the same distribution as the unsupplemented culture (Figures 34A and B). Although  $D = 0.33$  is close to the cut-off for biological variation, it is still below the significance threshold of  $D \geq 0.4$ . This shows the effect observed in the presence of *N*-(3-oxohexanoyl)-L-HSL and *N*-dodecanoyl-L-HSL was stereoisomerically specific.

Similarities were observed between the size of aggregates formed by wild type E2348/69 and E2348/69 *hosA*<sup>-</sup> in the presence of active AHLs (Figure 35A). Addition of *N*-(3-oxohexanoyl)-L-HSL and *N*-dodecanoyl-L-HSL to E2348/69 cultures significantly increased aggregation peaking at 1501 – 2000 pixels<sup>2</sup> (Figure 35B). Comparatively, aggregation of E2348/69 *hosA*<sup>-</sup> decreased in the presence of both active AHLs, again peaking between 1501 – 2000 pixels<sup>2</sup> (Figure 35B). Comparison between the wild type and mutant strains showed the distributions produced in the presence of the same AHL were not significantly different ( $D = 0.17$  in the presence of *N*-(3-oxohexanoyl)-L-HSL and  $D = 0.29$  with *N*-dodecanoyl-L-HSL) (Table 20).

### **3.2.7 *hosA* Promoter Expression as a Response to Temperature and AHL**

To determine whether expression of the *HosA* protein was under quorum sensing regulation the activity of the *hosA* promoter in both wild type E2348/69 and E2348/69 *hosA*<sup>-</sup> was investigated. The pMJFA18 plasmid contained a *luxCDABE* operon downstream of the PCR-amplified *hosA* promoter. As the promoter activity increased bioluminescence was produced. Transformation of

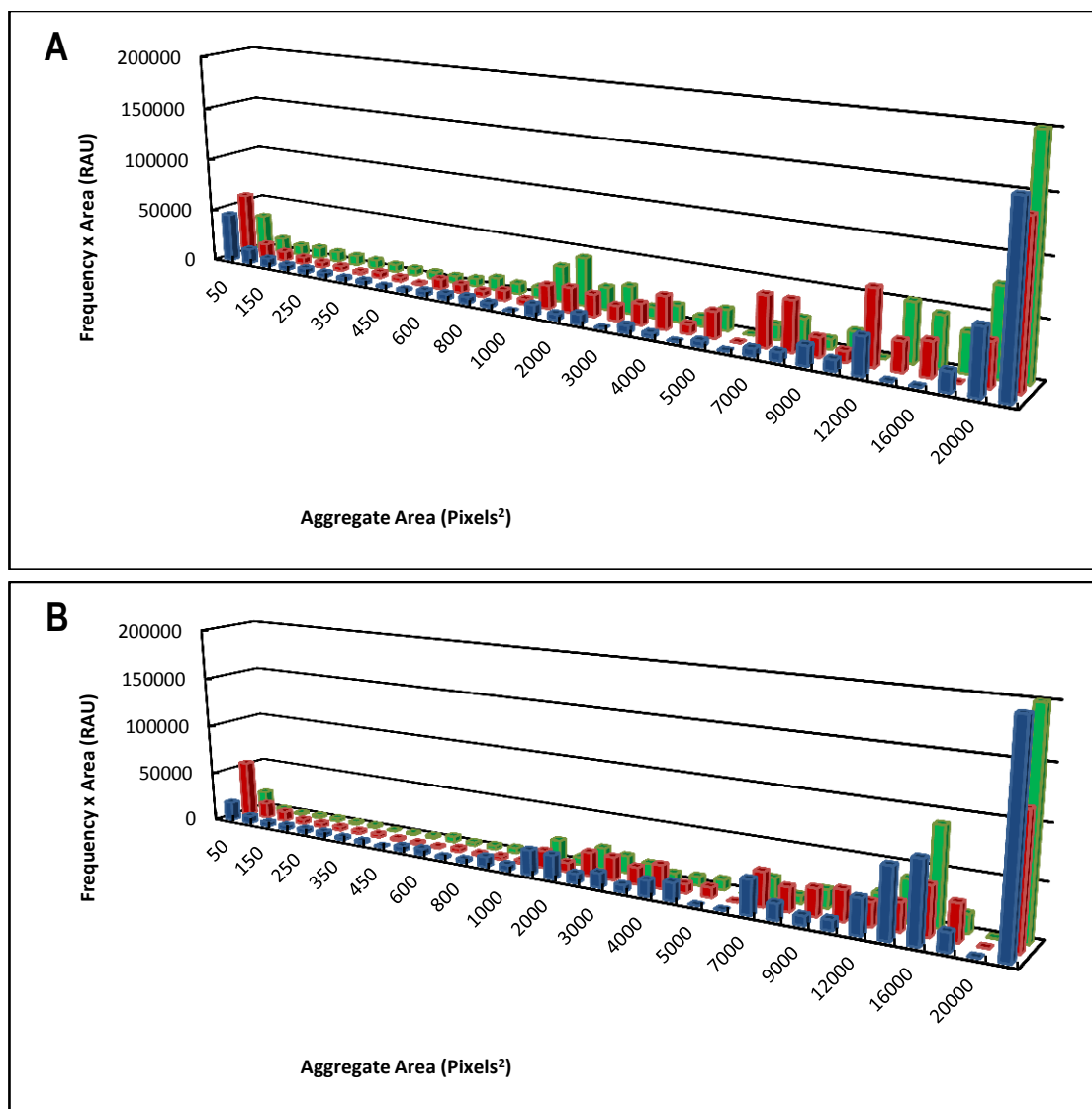


**Figure 34 - Aggregation profile of E2348/69 *hosA*<sup>-</sup> in the presence and absence of *N*-(3-oxo-hexanoyl)-D-HSL and *N*-(3-oxododecanoyl)-D-HSL at 25°C**

Each profile is representative of the distribution of aggregate sizes produced by E2348/69 *hosA*<sup>-</sup> in the presence and absence of *N*-(3-oxo-hexanoyl)-D-HSL and *N*-(3-oxododecanoyl)-D-HSL. AHLs were supplemented at 4 hours growth to a final concentration of 5nM. The images analysed were represented in Figure 32.

(A) Culture A; and (B) Culture B

(Blue) E2348/69 *hosA*<sup>-</sup> with no AHL supplement

(Red) E2348/69 *hosA*<sup>-</sup> in the presence of *N*-(3-oxo-hexanoyl)-D-HSL

(Green) E2348/69 *hosA*<sup>-</sup> in the presence of *N*-(3-oxododecanoyl)-D-HSL

**Table 19 - Statistical comparison of the effect of *D*-isomers on E2348/69 *hosA*<sup>-</sup> aggregation**

Biological variation compares profiles between cultures independent A and B; technical variation compares the profiles within a culture. Where  $D < 0.4$  there is no significant difference between the profiles of the given treatments, but where  $D \geq 0.4$  the difference is deemed to be significant.

	Biological Variation (A vs B)		Technical Variation	
E2348/69 <i>hosA</i> <sup>-</sup>	0.27		0.13	
	A	B	Biological Variation (A vs B)	Unsupplemented vs Supplemented
<i>N</i> -(3-oxo-hexanoyl)-D-HSL (C6)	0.47	0.23	0.21	0.23
<i>N</i> -(3-oxododecanoyl)-D-HSL (C12)	0.47	0.19	0.14	0.33

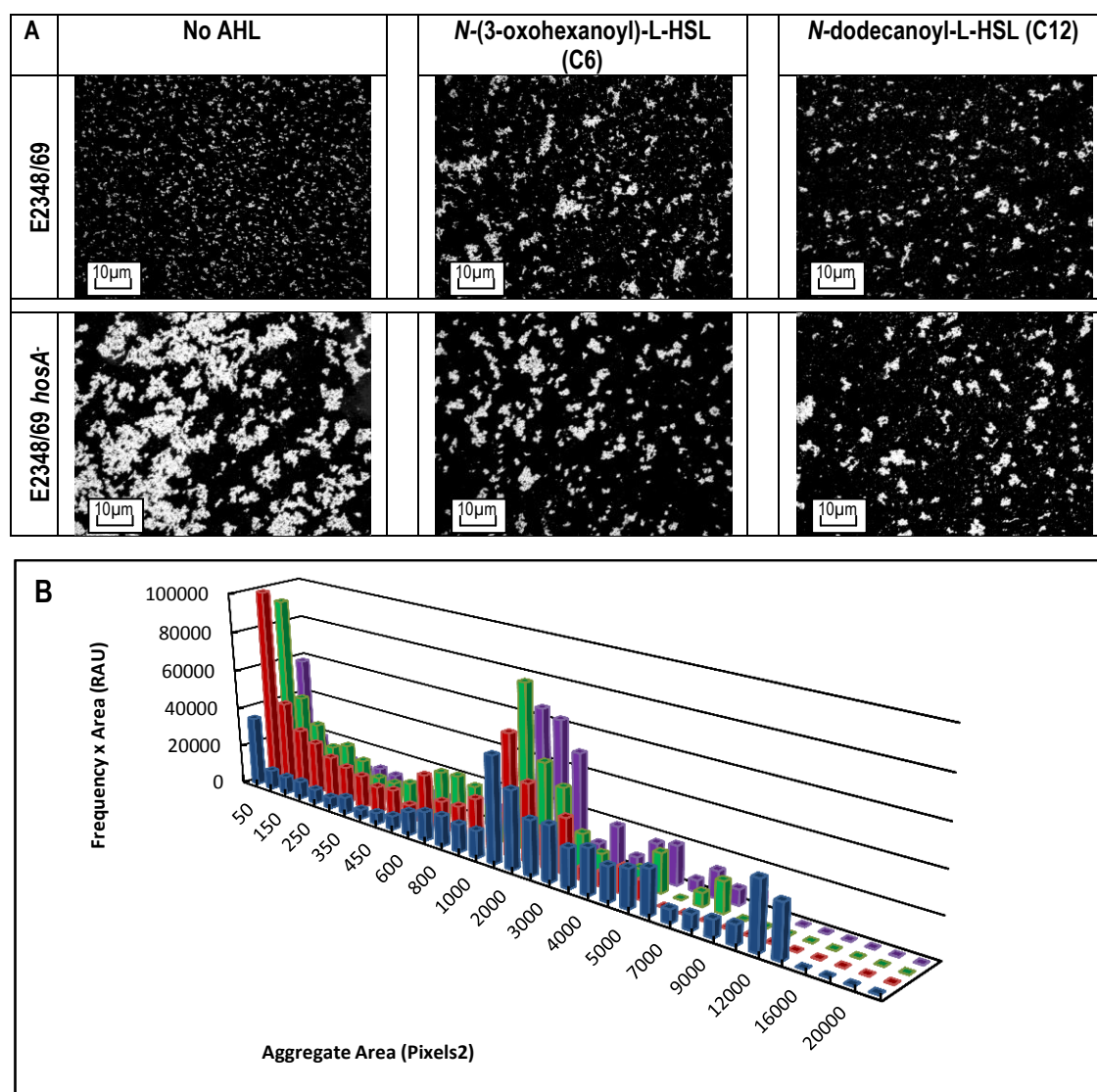


**Figure 35 – Comparison of the aggregates formed by E2348/69 and E2348/69 *hosA*<sup>-</sup> in the presence and absence of *N*-(3-oxohexanoyl)-L-HSL and *N*-dodecanoyl-L-HSL at 25°C**

Supplementation with AHL was performed at 4 hours to a final concentration of 5nM. Samples were taken at 5 hours incubation.

(A) Phase contrast microscopy images were taken at 100x magnification phase contrast microscopy after 5 hours incubation. Images are representative of 2 independent biological replicates, each with 6 technical replicates. Scale bars are indicated in the left hand corner of each image, and set to 10µm.

(B) Aggregation profiles showing the distribution of aggregate sizes formed by E2348/69 and E2348/69 *hosA*<sup>-</sup>. The images analysed were represented in Figure 35A.

(Blue) E2348/69 *hosA*<sup>-</sup> in the presence of *N*-(3-oxohexanoyl)-L-HSL

(Red) E2348/69 in the presence of *N*-(3-oxohexanoyl)-L-HSL

(Green) E2348/69 *hosA*<sup>-</sup> in the presence of *N*-dodecanoyl-L-HSL

(Purple) E2348/69 in the presence of *N*-dodecanoyl-L-HSL

**Table 20 – Statistical comparison of the effect of active AHL on the aggregation of E2348/69 and E2348/69 *hosA*<sup>-</sup>**

Where  $D < 0.4$  there is no significant difference between the profiles of the given treatments, but where  $D \geq 0.4$  the difference is deemed to be significant.

	No AHL	<i>N</i> -(3-oxohexanoyl)-L-HSL	<i>N</i> -dodecanoyl-L-HSL
D-value	0.96	0.17	0.29

this plasmid into both parental E2348/69 and E2348/69 *hosA*<sup>-</sup> allowed the activity of the *hosA* promoter to be monitored in the presence and absence of AHL, and as a response to changes in temperature.

When the wild type strain was incubated at 37°C in the absence of AHL, bioluminescence expression increased exponentially until 4.5 hours when it reached maximum expression, before bioluminescence decreased between 4.5 and 8 hours incubation (24207 RLU at maximum expression to 8660 RLU) (Figure 36A). Addition of both *N*-(3-oxohexanoyl)-L-HSL and *N*-dodecanoyl-L-HSL after 4 hours incubation resulted in an increase in bioluminescence production, indicating increased *hosA* promoter activity. In the presence of *N*-(3-oxohexanoyl)-L-HSL, bioluminescence rapidly increased with maximum expression at 5 hours incubation (Figure 36A). Addition of *N*-dodecanoyl-L-HSL resulted in a slower increase in bioluminescence, peaking at 6.25 hours incubation (Figure 36A). Bioluminescence remained high in the supplemented cultures in comparison to E2348/69 pMJFA18 in the absence of AHL (Figure 36A).

At 25°C a similar pattern was observed in E2348/69, but the increase in bioluminescence in response to addition of either AHL were lower (Figure 36C). In the absence of AHL bioluminescence peaked at 13905 RLU after 7.75 hours incubation, while the addition of *N*-(3-oxohexanoyl)-L-HSL and *N*-dodecanoyl-L-HSL at 7 hours resulted in peak bioluminescence at 7.75 and 8 hours respectively (Figure 36C).

Ferrándiz *et al* showed that the presence of a functional HosA protein is not an essential requirement for *hosA* expression due to autoregulation [68]. By inserting pMJFA18 into E2348/69 *hosA*<sup>-</sup> it was shown that the *hosA* promoter is still active [68]. At 37°C in the absence of AHL the *HosA* mutant had a similar bioluminescence expression profile to the wild type strain (Figure 36B). Bioluminescence peaked after 4.25 hours incubation. When added after 4 hours incubation both *N*-(3-oxohexanoyl)-L-HSL and *N*-dodecanoyl-L-HSL resulted in an increase in bioluminescence expression (Figure 36B). In the presence of both AHLs, bioluminescence peaked 1 hour after



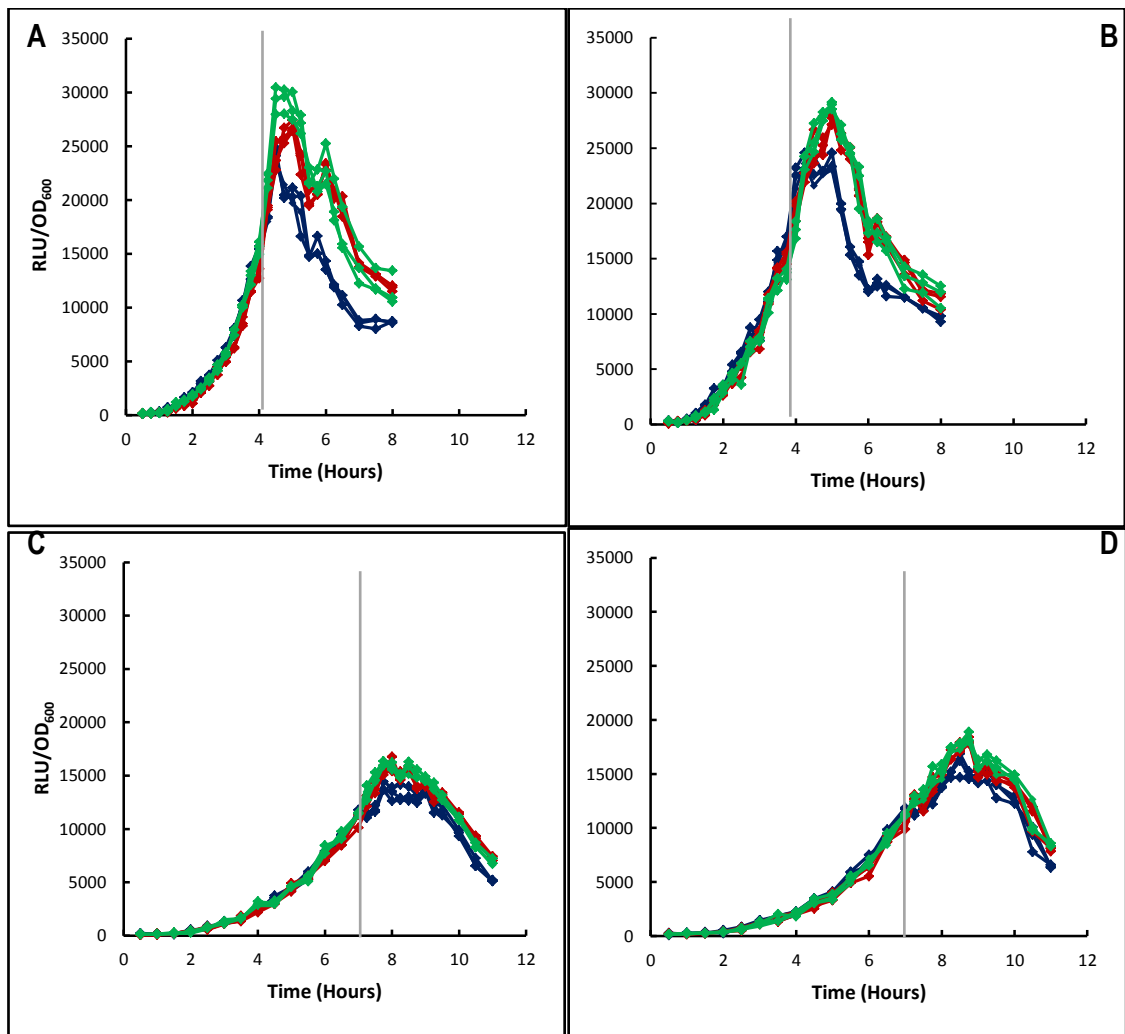


**Figure 36 - Effect of temperature and active AHL on *hosA* promoter activity in E2348/69 and E2348/69 *hosA*<sup>-</sup>**

The *hosA* promoter region was amplified using PCR and cloned into pSB377 upstream of the *luxCDABE* operon. The resulting plasmid was transformed into E2348/69 and E2348/69 *hosA*<sup>-</sup>. By measuring bioluminescence the activity of the *hosA* promoter was observed in response to temperature and AHL. Each line is representative of an independent biological replicate used for each treatment.

The graphs represent *hosA* promoter activity in:

- (A) E2348/69 with incubation at 37°C
- (B) E2348/69 *hosA*<sup>-</sup> with incubation at 37°C
- (C) E2348/69 with incubation at 25°C
- (D) E2348/69 *hosA*<sup>-</sup> with incubation at 25°C

The coloured lines represent *hosA* promoter activity with:

- (Blue) no AHL supplement
- (Red) addition of *N*-(3-oxohexanoyl)-L-HSL to a final concentration of 5nM
- (Green) addition of *N*-dodecanoyl-L-HSL to a final concentration of 5nM

The grey line represents the point of supplementation with AHL

supplementation with expression levels higher than that observed in the wild type (Figure 36B).

At 25°C in the absence of AHL peak bioluminescence was achieved after 8.5 hours incubation, reaching 15899 RLU (Figure 36D). Supplementation with *N*-(3-oxohexanoyl)-L-HSL and *N*-dodecanoyl-L-HSL stimulated an increase in bioluminescence expression to 18302 RLU and 18073 RLU respectively after 0.75 hours further incubation (Figure 36D).

At 37°C *N*-(3-oxohexanoyl)-L-HSL induced the largest increase in bioluminescence production in E2348/69 pMJFA18, while *N*-dodecanoyl-L-HSL had the greatest effect in the *HosA* mutant (Figures 36A and B). The bioluminescence produced by E2348/69 *hosA*- pMJFA18 at 25°C in the presence of *N*-(3-oxohexanoyl)-L-HSL and *N*-dodecanoyl-L-HSL were similar to that produced by E2348/69 pMJFA18 in the presence of equivalent AHLs (Figures 36C and D).

### **3.3 Discussion**

*E. coli* have a dual lifestyle, existing both inside and outside a host. The optimal and most favourable place for the bacteria is to be within the host where the conditions are warm and nutrient rich. Conversely, they must be able to survive outside the host in nutrient poor environments where temperatures are lower and fluctuate. By comparing phenotypic changes at different temperatures, it is possible to replicate this change in environmental conditions *in vitro*.

Diarrheagenic strains of *E. coli* are predominantly gut organisms, which optimally colonise the intestinal tract [4, 6]. Enteropathogenic *E. coli* optimally colonise the small intestine, whereas enterohaemorrhagic *E. coli* are found predominantly in the lower bowel [4, 6]. The alimentary tract in mammals contains a diverse microflora along the length [3]. *E. coli* must be able to survive the gastro-intestinal tract in order to colonise the optimal niche. Pathogenic *E. coli* must utilise an infection strategy to survive within a host, consisting of three major stages; colonisation of the mucosal site, evasion of host defences and replication and growth [4, 6]. Infection by diarrheagenic *E. coli* causes host damage to varying levels depending on the

pathotype and virulence of the strain [4, 6]. An important factor in *E. coli* survival is the ability to attach within the host and replicate, but also detach from the mucosa and translocate to a new area of the intestinal tract, or to a new host [4, 6].

Bacterial dissemination and motility have been associated with social networking, which is reliant on cell density for the regulation of 'public goods', such as enzymes. As production of these external factors is regulated by quorum sensing, the concentration of these molecules is indicative of cell density [124]. If the cell density is too high, competition for nutrients and colonisation sites increase. Each bacterium engages in self-preservation by detaching from the host mucosa and translocating to a new colonisation site, leaving the relative 'safety' of the larger colonies. There is selective advantage in doing this early as by leaving a site of high colonisation and moving into a host or new colonisation site with potentially lower numbers of competing bacteria, the *E. coli* are able to reduce competition and increase the availability of nutrients. Through this mechanism, *E. coli* has become the most abundant facultative anaerobe of the intestinal microflora, within both the bovine and human hosts [4].

Diarrheagenic *E. coli* are ingested on contaminated foodstuffs, and so must survive from the mouth through the gastric fluids to the optimal niche, either in the small or large intestine. During passage through the host, bacteria are carried in material being actively digested by chemical and enzymatic breakdown. In a healthy gut the material is moved by peristalsis in a continual flow. As a result of infection with some pathogens, the material moves through the gut much faster as diarrhoea due to increased flow rate. The *E. coli* must be able to move from within the digestive material to the epithelia of the intestines and successfully adhere to the mucosal wall [4, 6, 64].

The ability of the bacterium to swim is an important mechanism in dissemination and colonisation of the optimal sites and *E. coli* utilises the peritrichous flagella to swim [4, 6, 253]. In *Yersinia* spp. environmental conditions such as pH and temperature have been shown to affect

the ability of the bacteria to swim [68, 69, 79, 94, 182, 242, 245]. This observation was also true in enteropathogenic *E. coli* [68, 79]. There are two methods of assessing bacterial swimming; as individual bacteria and as a population. Individual *E. coli* are able to move, and are observable using a microscope. The expression 'population expansion' was used in this study as a collective term to describe the motility of a population of cells on swimming motility agar plates. The density of the area of motility produced on a plate was indicative of the ability of the population to replicate, while the diameter of the motility zone described the movement of the population.

The evidence presented in this chapter confirmed that population expansion of wild type *E. coli* E2348/69 was decreased at lower temperatures (Tables 10 and 11). An interesting point to note was the formation of clear and evenly distributed rings within the area of motility produced by this strain at the lower temperature of 25°C (Figure 13). These rings were of different cell densities, with the least dense at the outer edge of the overall motility zone. These rings are likely to be caused by increased levels of bacterial growth and/or changes in cell motility within the population. Similar rings are observed during swarming by *Proteus* species, which indicate multiple periods of growth and motility [254].

Previous studies have shown changes in the motility of *Yersinia* to be linked with the propensity of the population to clump and form aggregates [69, 245]. A study by Ferrándiz *et al* showed a link between aggregation and motility in E2348/69 [68]. Where this bacterium existed as individual cells they retained the ability to swim, however as the population started to clump together population expansion was reduced [68]. A bacterium does not swim in a straight line, but rather tumbles and produces an erratic but directional pattern of movement [68, 253]. By clumping together, the bacteria effectively inhibit individual movement, thereby the ability to swim is reduced relative to the proportion of the population within an aggregate [68, 245]. The evidence provided in this chapter shows *E. coli* E2348/69 was unable to form aggregates at either temperature tested, which correlated with the ability to swim.

Although an individual bacterium is able to successfully translocate, this lifestyle is more risky than when part of a population as the individual bacterium is more susceptible to host immune responses, and less likely to successfully adhere to the mucosa. As an aggregate, the bacteria are better able to overwhelm the host immune responses and successfully colonise a host [68, 245]. The ability to form aggregates is not limited to being within a host, as several bacterial species successfully form complex aggregates, or biofilms, in the external environment. For example, *Pseudomonas aeruginosa* is able to produce biofilms on medical equipment such as catheters, feeding tubes and intra venous access devices such as needles and cannulas [70, 72, 74, 182]. *Ps. aeruginosa* also forms biofilms within the lungs of patients with cystic fibrosis [70, 72, 74, 182]. In dentistry *Porphyromonas gingivalis* forms biofilms on tooth enamel and prosthetics, such as dentures and bridges [255]. Biofilms produced by both of these opportunistic pathogens are difficult to remove and the formation of these complex communities provides protection from interventions such as antibiotics [70, 72, 74, 104, 110, 152, 182].

Quorum sensing has been linked to the ability of a population to form aggregates. For example, in *Yersinia* spp. the deletion of *ypsRI* increased population expansion in a temperature dependent manner [69, 182, 242, 245]. *E. coli* as a species cannot produce AHLs, relying on those released by other bacteria. The individual *E. coli*, in response to an increased concentration of signal initiate a phenotypic response through the activity of SdiA, an orphan LuxR homologue, which binds the exogenous AHLs (Section 1.3.1.1) [119, 121, 122, 134, 138, 140, 155, 156, 160, 162, 169, 170].

Concomitantly with this study, work was being completed within the Food Assurance team at AgResearch Ltd to produce an *sdiA* deletion mutant in E2348/69, E2348/69 *hosA*<sup>-</sup> and in *E. coli* O157:H7. Generation of a deletion mutant in these strains would allow the elucidation of the role of SdiA in the detection and regulation of quorum sensing cues in pathogenic *E. coli*. Over the course of 18 months various strategies were attempted. P1 transduction of EHEC and

EPEC using MG1655 *sdhA* as a donor was initially attempted as this method has low impact on the stability of the naturally-occurring plasmids in the recipient strain. This strategy was unsuccessful as all the EHEC and EPEC lab strains used were P1 resistant. The second method was based on the lambda RED system of transfer [256]. Briefly, this method is based on the introduction of lambda plasmid-encoded recombinases into the strain to be mutagenized. Donor DNA with homology to the site for mutagenesis and the mutation is provided on a second plasmid. Mutagenesis occurs as a result of two homologous recombination events, which result in the elimination of the plasmid vector and retention of the mutated gene. With this method the first recombination event was successful placing the plasmid in the chromosome, however the second event either did not occur or the insertion was not in *sdhA*. PCR analysis of genomic DNA isolated from possible clones showed retention of a wildtype *sdhA* fragment. Both short arm and long arm homologous regions located on either circularised or linearised plasmids were used, in addition to both high and low concentrations of DNA. Addition of arabinose to the growth medium, which has been shown to improve recombination efficiency, had no effect. Further investigation showed that for some potential clones, the plasmid was retained and this suggested the enzyme encoded on the plasmid which was required for plasmid linearization was not effective (Personal Communication, H. Withers and T. Gupta, 2010 - 2012). Due to time constraints and the lack of other possible modifications to the mutagenesis strategy, the production of an *sdhA* mutant was abandoned, rather concentrating on observing effects of the signals on the bacteria at a phenotypic level, which provided data in line with the global aim of the IMPACT programme (Section 1.7).

The *E. coli* population within the same niche initiate the same response at a similar time point, causing the population to exhibit multicellular behaviour [93-95]. It was confirmed during this study that addition of exogenous AHL affected the propensity of an E2348/69 population to form aggregates. By supplementing actively growing and metabolising cells with specific AHLs

during the exponential phase of growth, it was possible to increase cell aggregation by E2348/69 (Table 16, Figures 29 and 30). This effect was stereoisomer specific, observed for the *L*-isomer of *N*-(3-oxohexanoyl)-L-HSL and *N*-dodecanoyl-L-HSL only, with the *D*-isomers having no effect (Table 17). These observed changes in E2348/69 aggregation from non-aggregating in the absence of AHL to aggregating in the presence of active AHL were not as a result of cell density, but rather changes in regulation demonstrated by equivalent cell densities between cultures determined by optical density (OD<sub>600</sub>).

The two AHLs used during the aggregation studies had different chain lengths, *N*-(3-oxohexanoyl)-L-HSL classified as a short chain AHL and *N*-dodecanoyl-L-HSL a long chain signal [91, 93, 94, 109, 127, 143, 155, 175]. The specificity of a LuxR protein for a cognate AHL is related to the size of the hydrophobic binding pocket and the length of the fatty acid side chain, or R-group [130, 140]. During the population expansion assays performed in this study, it was observed that both short and long chain AHLs had a significant effect on the population expansion of E2348/69 (Table 10). The literature shows that SdiA in *Salmonella* spp. has been shown to bind *N*-(3-oxohexanoyl)-L-HSL and *N*-(3-oxo-octanoyl)-DL-HSL when expressed from the genome [136, 155, 158]. As there is a 69% homology at the amino acid level between SdiA in *Salmonella* and *E. coli*, it would be likely that they bind similar AHLs [136, 162]. As the AHLs shown to have an effect on E2348/69 are so different and diverse in the length of R-group, it could be hypothesised that a second AHL-binding protein may be present within *E. coli* which would function in a hierarchy similar to that observed in *Ps. aeruginosa* [77, 97, 109-111, 135, 157, 177, 178, 180, 181, 186, 191, 201, 257]. Alternatively, it is possible that the phenotypic effects observed in the presence of different AHLs may be as a result of activation or inhibitory competition by SdiA. Further study of SdiA protein structure and functional assays in the presence and absence of AHL would be required to investigate this. Although there has been no evidence in the literature to suggest the presence of a second LuxR-type protein in *E. coli*, it does

not rule out the possibility. Screening for common LuxR-type motifs would identify standard proteins, but the potential remains for a second unknown protein to be present. Further investigation using an *sdiA* deletion mutant of *E. coli* would allow the possibility of a second AHL-binding protein to be identified.

The changes in aggregation observed in this study correlated with changes in population expansion, further emphasising the link between motility and aggregation. Of the AHLs tested, the short chain AHL decreased population expansion, while the long chain AHL resulted in an increase in the size of the motility zone. AHLs act as cofactors and are bound by the LuxR proteins resulting in a conformational change in the DNA binding domain of the regulator [73, 111, 136, 140, 145, 148]. The short and long chain AHLs would not bind the same hydrophobic pocket at the N-terminus of the regulator. The difference in phenotypic responses to the short and long chain AHLs thereby suggest a secondary AHL-binding protein may exist. Confirmation of this hypothesis would require analysis of the structure of SdiA and the changes that occurred upon binding different AHLs.

The MarR family of transcriptional regulators, such as SlyA, are found in several species of pathogenic bacteria and have been shown to affect adaptation to environmental stress [68]. Ferrándiz *et al* showed HosA, a SlyA homologue, was important in the cell aggregation of E2348/69 [68]. *E. coli* must survive a dual lifestyle, translocating from internal environments to external from the host [4, 6, 9, 10, 15, 20, 21, 26, 27, 31, 49, 60, 86, 120, 134, 258]. Within the host the temperature is constant and at the optimal 37°C required for *E. coli* proliferation. Conversely, outside a host the temperatures fluctuate and are much lower than those within a host. HosA expression has been shown to be affected by external factors such as pH and temperature (Figure 36) [68]. Evidence presented in this chapter showed that *hosA* promoter activity was increased in the presence of active AHL (Figure 36). These results suggest a link between HosA and AHL-dependent quorum sensing in E2348/69.



By deleting *hosA*, the effect of this regulator on the aggregation and population expansion of E2348/69 at different temperatures can be evaluated. Results presented in this study correlate with observations made by Ferrándiz *et al* confirming that the population of E2348/69 was non-motile at temperatures lower than 30°C in the absence of HosA [68]. Deletion of *hosA* had no effect on the population expansion of E2348/69 at temperatures more representative being within the host environment (Table 14). Although no motility zones were observed at 25°C, bacterial growth was visible around the point of inoculation, suggesting that deletion of HosA significantly affected the population expansion in a temperature-dependent manner.

Where wild type E2348/69 was non-aggregating in the absence of AHL, deletion of *hosA* significantly increased bacterial aggregation at the lower temperature, which corresponded with the decrease in population expansion. Compared to that observed at 25°C the activity of the *hosA* promoter was higher at 37°C, correlating with a lower level of cell aggregation at the higher temperature. A higher level of aggregation was observed at 25°C when compared to 37°C. This further demonstrated population expansion is affected by the cell aggregation of E2348/69 which changes in response to environmental stimuli. The evidence presented in this study also suggests aggregation by E2348/69 may be part of the HosA regulon.

Furthermore, it had been observed in the wild type that addition of exogenous AHL significantly changed the aggregation profile, and thereby overall population expansion. By comparison, supplementation with *L*-isomers significantly increased the population expansion of the HosA mutant, to levels similar to that observed in the wild type. The change in motility suggested this phenotypic behaviour may be a result of cell aggregation. Further investigation would be required to confirm this. Although changes in aggregation were observed during this study, the propensity for the population to clump together is not the only possible target for AHL-dependent regulation. Ferrándiz *et al* showed that while structurally the flagella were unaffected, the function may have been impaired in the absence of HosA. Further investigations into the

effect of exogenous AHL on this function would determine if *fliC* was the target of AHL intervention. Other effectors of motility exist, such as pili which may be affected by the presence of AHL and thereby have a role in the changes of this phenotypic behaviour. Not all of the E2348/69 cells formed aggregates, with a large proportion remaining as planktonic cells. The aggregates formed by the wild type in the presence of AHL were small in size, which correlated with a marked decrease in population expansion but not a total inhibition of movement. By comparison the HosA mutant produced large aggregates in the absence of AHL, which required the addition of sodium chloride and significant vortexing to disperse [79]. In the presence of AHL the aggregates formed were significantly smaller at 25°C, becoming more similar in size to those produced by the wild type in the presence of equivalent AHLs (Table 13; Figure 35). When analysed at 37°C, *N*-dodecyl-L-HSL had no effect on the population expansion of the HosA mutant (Table 14). This evidence further highlighted the link between AHL-dependent quorum sensing and HosA in E2348/69.

HosA is an important regulatory protein in the adaptation of pathogenic *E. coli* to environmental stress. The results in this chapter show that a non-functional HosA protein decreased the ability of the bacterial population to disseminate, but suggested an increased potential for infection through the formation of aggregates. There is evidence that a bacterial population with a propensity to aggregate has a higher potential for colonisation of a host, through adherence to the mucosal wall and evasion of host immune responses [13, 14, 70, 79]. Furthermore, addition of AHL to the E2348/69 controlled these traits, suggesting *E. coli* may utilise these AHLs produced by the microflora within a host to encourage attachment and colonisation.

Growth media affects the expression of cell surface components in addition to the behaviour of bacteria. Availability of macro- and micro-nutrients and ions, such as iron have been shown to affect specific phenotypic behaviours in pathogenic *E. coli* [79]. Studies have shown

the use of DMEM as a growth medium to be important in the formation of bacterial clumps and the formation of A/E lesions by both EPEC and EHEC due to priming of pathogenic mechanisms and expression of cell surface factors such as bundle forming pili [14]. Previous work carried out by members of the Food Assurance team at AgResearch Ltd that showed changes in gene expression and AI-2 levels at different temperatures were performed in Luria Broth (LB). As this study followed on from this work the decision was made to continue to use LB. In addition, LB is nutrient rich with a good source of iron, allowing study of phenotypic behaviours in a healthy growth environment [259].

The evidence presented in this chapter supports the hypothesis of hierarchical regulation of the HosA-driven effects by AHL-dependent quorum sensing.

## **4 Identification of Cell Surface Macromolecules affected by AHLs in**

### **E2348/69**

#### **4.1 Introduction**

We have shown that the propensity of a bacterial population to form aggregates affects the population expansion in enteropathogenic *E. coli* E2348/69. The evidence presented in this study has also shown aggregation to be controlled by hierarchical regulation involving HosA and AHL-dependent quorum sensing within this strain. In this chapter the aim was to identify the QS regulon controlling the aggregation by targeting expression of specific cell surface components. We hypothesise that quorum sensing changes the expression of these cell surface components, and through these changes QS controls population expansion.

A number of different cell surface components have been associated with the ability of bacteria to form aggregates:

- 1) Flagella [245]
- 2) Cellulose [79]
- 3) Antigen 43 [260] and,
- 4) The type IV pilus, or bundle forming pilus, of enteropathogenic *E. coli* [13, 14, 57, 261]

The expression of some of these components has been found to be under quorum sensing regulation in other pathogens [245]. *E. coli* encodes two quorum sensing systems; AHL/SdiA and AI-2/LuxS (Sections 1.3 and 1.4 respectively). Although AI-2 production is part of core cellular metabolism, it has been shown that AI-2 can act as a quorum sensing signal and affect population-wide behaviours [183, 184, 198]. DeLisa *et al* suggested that *E. coli* utilised AI-2 to communicate the stress or burden imposed as a function of the overall accumulation rate of foreign protein, although the exact mechanism remains unknown [262]. De Keersmaecker *et al* showed that transcription of *luxS* is induced by acid, with synthesis of AI-2 subject to catabolite

repression through the cAMP-cAMP receptor protein [195]. Interestingly, Sperandio *et al* suggested AI-2 was part of a global regulatory system in *E. coli* due to observed changes in transcriptional regulation in the absence of *luxS* compared to the wildtype [263]. However, this study does not account for the vital role of LuxS in the AMC. The role of AI-2 as a quorum sensing signal in *E. coli* remains a topic of scientific debate; Is it true quorum sensing or just a metabolism by-product with diverse functions? As part of this study the effect of AI-2 on the aggregation of E2348/69 will be assessed to determine whether the effects observed in chapter 3 were truly as a result of AHL-dependent quorum sensing and not AI-2 signalling.

## **4.2 Results**

### **4.2.1 Effect of AHL on Aggregation and Population Expansion in a LuxS/AI-2 Negative**

#### **Background**

AE2348/69 *luxS*<sup>-</sup> had a non-functional LuxS protein, and was unable to produce AI-2, relying instead upon a different pathway for the detoxification of SAH (Section 1.4.1). By removing the ability of the bacterium to produce AI-2, a background was produced which allowed evaluation of the effect of AHL. In order to determine whether the changes observed in motility and aggregation of wildtype E2348/69 described in chapter 3 were due to AHL-dependent quorum sensing, the population expansion of AE2348/69 *luxS*<sup>-</sup> was investigated.

With the exception of one biological replicate, AE2348/69 *luxS*<sup>-</sup> exhibited positive population expansion at 25°C in the absence of AHL producing an area of motility with an average diameter of 6mm (Table 21; Figures 37 and 38). When compared to the area of motility in wild type E2348/69 ( $20.8 \pm 1.03\text{mm}$ ), the motility zone produced by AE2348/69 *luxS*<sup>-</sup> was much smaller in diameter.

Addition of the short chain *N*-(3-oxohexanoyl)-L-HSL had no significant effect on the size of the motility zone produced by AE2348/69 *luxS*<sup>-</sup> (diameter = 5.7mm;  $F = 0.012$ ;  $p = 0.915$ )

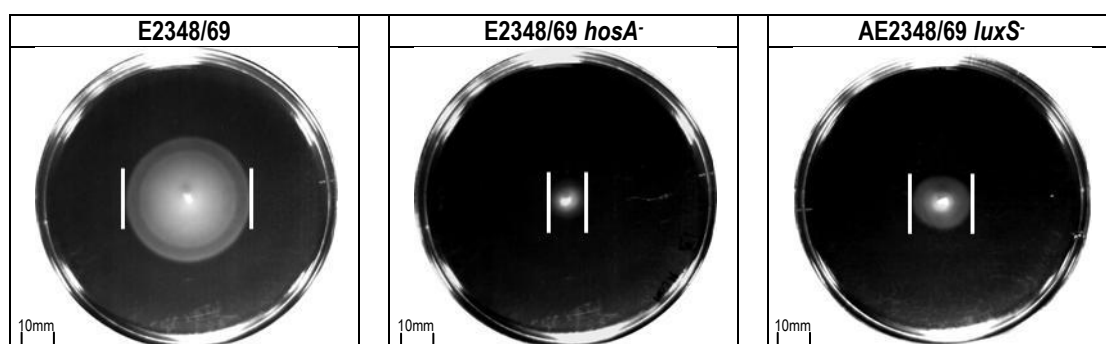


**Figure 37 – Comparison of E2348/69 population expansion with that of the *HosA* and *LuxS* mutants at 25°C**

Images are representative of the motility zones produced by each strain after 18 hours incubation. Each strain was used to inoculate 2 independent biological cultures, each with 5 technical replicates.

White bars mark the boundaries of population expansion on each plate. Scale bars are indicated in the left hand corner and are set at 10mm.

N.B. Images are representative, therefore the size of motility ring on the image may not be illustrative of the overall effect of the supplement.

**Table 21 – Statistical analysis of the effect of AHL on AE2348/69 *luxS*<sup>-</sup> population expansion at 25°C**

Side chain length for each the AHL are in brackets.

	Average diameter of motility zone $\pm$ 1 standard deviation (mm)	ANOVA	
		*F-value	p-value
No AHL	6 $\pm$ 6.38		
<i>N</i> -(3-oxo-hexanoyl)-D-HSL (C6)	6.1 $\pm$ 6.44	0.00122	0.973
<i>N</i> -(3-oxododecanoyl)-D-HSL (C12)	6 $\pm$ 6.34	0	1.00
<i>N</i> -(3-oxohexanoyl)-L-HSL (C6)	5.7 $\pm$ 6.04	0.01167	0.915
<i>N</i> -dodecanoyl-L-HSL (C12)	6.2 $\pm$ 6.54	0.00479	0.946

\*F- critical value = 4.414

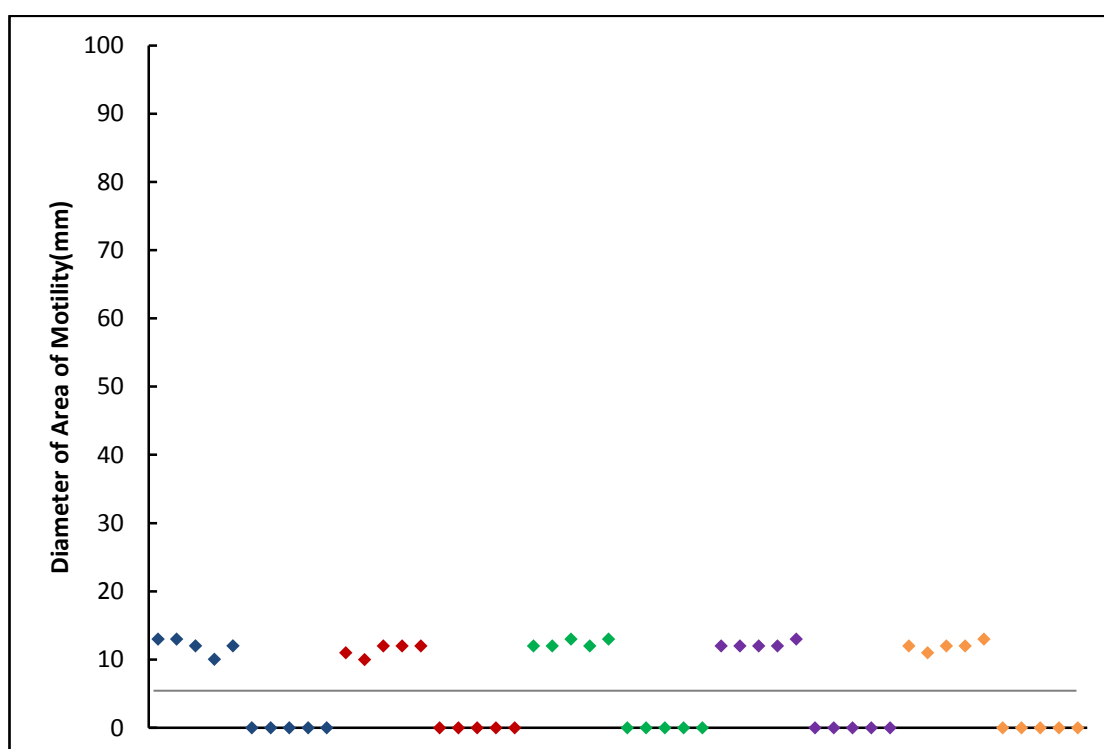


**Figure 38 – Variation in the diameter of the motility zones produced by AE2348/69 *luxS*<sup>-</sup> in the presence and absence of different AHLs at 25°C**

For each of the 2 independent biological replicates, 5 technical replicates were analysed. Each point on the graph represents one technical replicate. Petri dishes measured 95 mm in diameter.

(Blue) No AHL

(Red) *N*-(3-oxo-hexanoyl)-L-HSL

(Green) *N*-dodecanoyl-L-HSL

(Purple) *N*-(3-oxo-hexanoyl)-D-HSL

(Orange) *N*-(3-oxo-dodecanoyl)-D-HSL

The grey line represents the average diameter of the motility zones measured for the unsupplemented isolates.

(Table 21). Likewise, the addition of long chain *N*-dodecanoyl-L-HSL had no significant effect on the diameter of the area of motility produced by AE2348/69 *luxS*<sup>-</sup> (diameter = 6.2mm;  $F = 0.0048$ ;  $p = 0.946$ ) (Table 21). Therefore, these experiments provide no evidence that either AHL had any effect on the population expansion of AE2348/69 *luxS*<sup>-</sup> (Table 21; Figure 38). Similarly, no significant change in population expansion was observed with the addition of *D*-isomers (Table 21).

In chapter 3, population expansion was linked to the propensity of a population to form aggregates. To determine whether the difference in population expansion between wild type E2348/69 and AE2348/69 *luxS*<sup>-</sup> were as a result of aggregation, the size and distribution of the aggregates formed by these two strains was investigated using phase contrast microscopy.

E2348/69 formed very small aggregates with a high proportion of non-aggregating planktonic cells (Figure 39A). When incubated at 25°C for 5 hours in the absence of AI-2, AE2348/69 *luxS*<sup>-</sup> formed larger aggregates in comparison to the wild type with a lower proportion of planktonic cells (Figure 39A). The difference in the aggregation profiles of wildtype E2348/69 and AE2348/69 *luxS*<sup>-</sup> was determined using the K-S test (Section 2.9). With this test the distance between the equality of the two profiles is provided as a *D*-value, with higher values indicating a more significant difference. For the purposes of this study a significance threshold was used to differentiate between biological variation ( $D < 0.4$ ) and true variation between treatment groups ( $D \geq 0.4$ ) (Sections 2.9 and 3.2.4). The difference in the aggregation profiles between wildtype E2348/69 and AE2348/69 *luxS*<sup>-</sup> was calculated as significant ( $D = 0.80$ ). Analysis of the microscope images confirmed AE2348/69 *luxS*<sup>-</sup> formed large aggregates in the absence of AI-2. A representative aggregation profile is shown in Figure 40. In the absence of AI-2 the majority of the aggregates were between 2000 and 20,000+ pixels<sup>2</sup> in size (Figure 40). Technical variation between images from the same culture was calculated as  $D = 0.31$ , with biological variation between cultures A and B calculated as  $D = 0.32$  (Table 22).



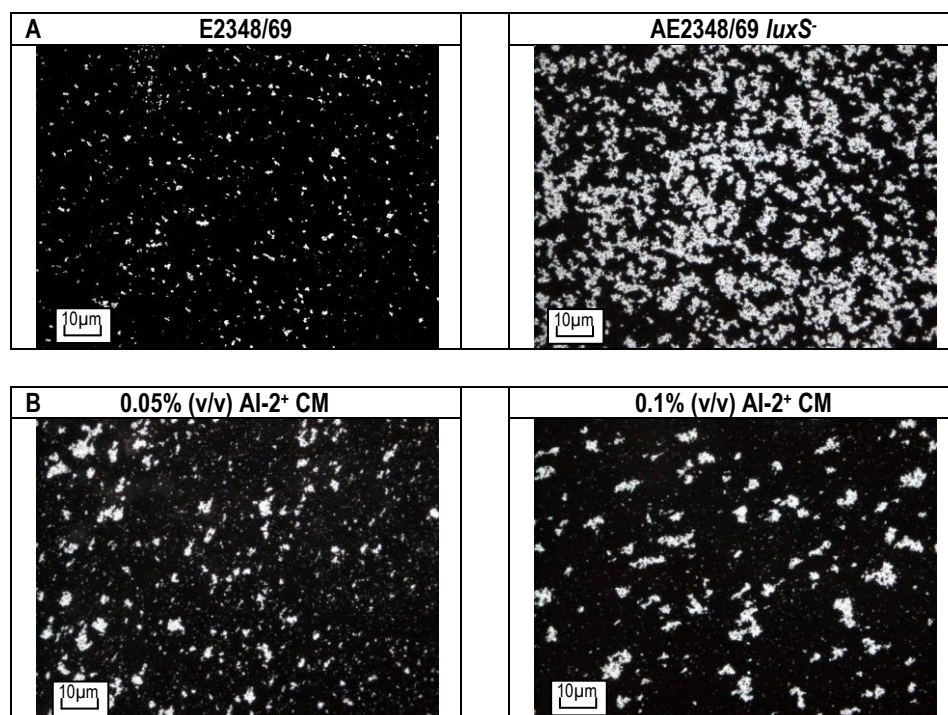


**Figure 39 – Aggregates formed by AE2348/69 *luxS*<sup>-</sup> in the presence and absence of exogenous Al-2 at 25°C**

Microscopy images were taken at 100x magnification phase contrast microscopy after 5 hours incubation.

(A) Comparison of the aggregates produced by wild type E2348/69 with AE2348/69 *luxS*<sup>-</sup> in the absence of supplements. Images are representative of 2 independent biological replicates, each with 6 technical replicates

(B) Effect of exogenous Al-2 on the size of the aggregates formed by AE2348/69 *luxS*<sup>-</sup>. Supplementation was completed at 4 hours incubation. Images are representative of 1 biological replicate comprising 6 technical replicates.

Scale bars are indicated in the left hand corner of each image, and set to 10µm.

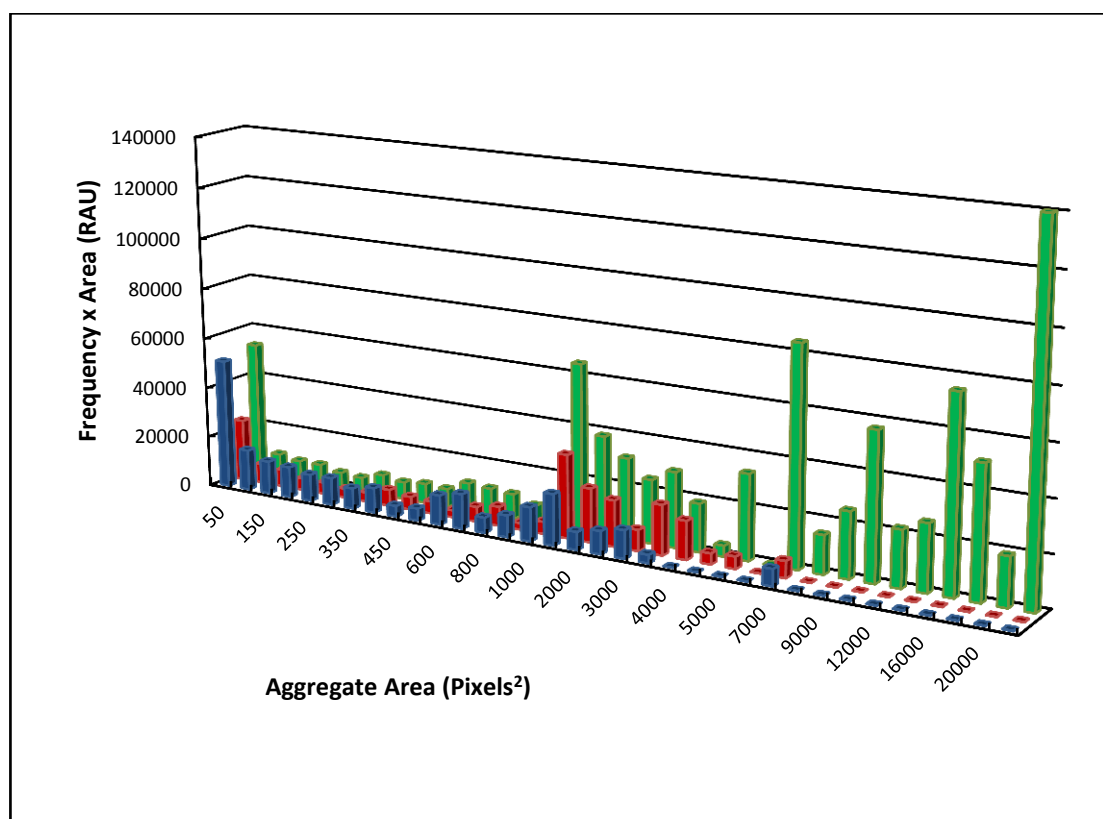


**Figure 40 – Aggregation profile of AE2348/69 *luxS*<sup>-</sup> and the effect of exogenous AI-2 at 25°C**

Each profile is representative of the distribution of different aggregate sizes produced by AE2348/69 *luxS*<sup>-</sup> in the presence and absence of exogenous AI-2. The images analysed were represented in Figure 39. Supplementation with AI-2 positive CM from an 8 hour culture of NCTC12900 was completed at 4 hours incubation. The AI-2 positive profiles are representative of 1 biological replicate comprising 6 technical replicates, and the AI-2 negative culture is representative of 2 biological replicates, each with 6 technical replicates.

(Blue) AE2348/69 *luxS*<sup>-</sup> in the presence of 0.05% (v/v) AI-2 positive CM

(Red) AE2348/69 *luxS*<sup>-</sup> in the presence of 0.1% (v/v) AI-2 positive CM

(Green) AE2348/69 *luxS*<sup>-</sup> with no AI-2

**Table 22 – Statistical analysis of the effect of exogenous AI-2 on AE2348/69 *luxS*<sup>-</sup> aggregation**

Biological variation compares profiles between independent cultures A and B; technical variation compares the profiles within a culture. The concentration effect compares the profiles produced in the presence of AI-2 to determine whether addition of a higher concentration of CM had a significant effect compared to the lower concentration. Where  $D < 0.4$  there is no significant difference between the profiles of the given treatments, but where  $D \geq 0.4$  the difference is deemed to be significant.

	Biological Variation (A vs B)	Technical Variation
AE2348/69 <i>luxS</i> <sup>-</sup>	0.32	0.31
	Concentration Effect (0.05% vs 0.1%)	Unsupplemented vs Supplemented
0.05% (v/v) AI-2	0.06	0.55
0.1% (v/v) AI-2		0.50

To determine the effect of exogenous AI-2 on aggregation, AI-2 positive conditioned media harvested from an 8-hour culture of *E. coli* strain NCTC12900 was added to AE2348/69 *luxS*<sup>-</sup> after 4 hours incubation to a final concentration of either 0.05% (v/v) or 0.1% (v/v) (Figure 39B).

Conditioned media (CM) was produced by filtering liquid culture grown in LB to remove bacterial cells. The resulting culture supernatant contained a complex mixture of molecules including nutrients, toxins and waste products of metabolism, in addition to any signalling molecules present in the external milieu at the time of filtration. Bacteria grown in LB do not deplete the available nutrients during growth to stationary phase and therefore CM harvested from these cultures is not substrate limited. An added benefit of using CM was that it could be harvested at particular cell densities or during specific phases of growth, providing some control over the nutrient and signal molecule concentrations. This results in a balanced, natural concentration of the molecules within the CM. Storage of bulk supplies at refrigeration temperatures reduced the potential for changes in the chemical composition between experiments.

The actual concentration of AI-2 within the CM was unknown however, the *Vibrio harveyi* MM32 bioassay produced a high level of bioluminescence in the presence of the NCTC12900 8 hour CM, indicating the presence of AI-2. AI-2 is difficult to purify and synthesise. A number of different structures of this molecule exist depending on the availability of stabilising cations (Introduction Section 1.4.1). Any AI-2 produced would therefore be a mixture of compounds in equilibrium making determination of concentration even more difficult. Although AI-2 was available in a purified form commercially, it was unclear whether or not the manufactured signal differed from that required to interact with *E. coli* proteins. The possibility that the commercially derived molecule could interfere with, inhibit or fail to activate effects in *E. coli* made CM the optimal choice for these experiments.

Addition of both 0.05% and 0.1% AI-2-positive CM to AE2348/69 *luxS*<sup>-</sup> reduced the size and frequency of the aggregates formed (Figure 39B). In the presence of exogenous AI-2, regardless of concentration, the aggregation profile shifted to the left, with more aggregates of between 0 and 8000 pixels<sup>2</sup> in area (Figure 40). To determine whether one concentration of exogenous AI-2 had a greater effect on the aggregation of AE2348/69 *luxS*<sup>-</sup>, the profiles were compared using the K-S test. The concentration effect was found to be insignificant ( $D = 0.06$ ) (Table 22). The observed decrease in aggregation of  $D = 0.55$  and  $D = 0.50$  in the presence of 0.05% (v/v) and 0.1% (v/v) AI-2 positive CM respectively was thereby greater than would be expected if this was as a result of biological variation (Table 22).

The addition of AHL had no effect on the population expansion of the QS negative AE2348/69 *luxS*<sup>-</sup>. Having established that AHL significantly affected the aggregation of wildtype E2348/69 (Figures 29 and 30) and that addition of exogenous AI-2 changed the aggregation profile of the *LuxS* mutant (Figure 40), it was necessary to evaluate the effect of AHL on aggregation of AE2348/69 *luxS*<sup>-</sup> to determine whether the effects observed in chapter 3 were truly a result of AHL-dependent quorum sensing.

Upon supplementation with *N*-(3-oxohexanoyl)-L-HSL and *N*-dodecanoyl-L-HSL the size of the aggregates produced by AE2348/69 *luxS*<sup>-</sup> visually decreased and a higher proportion of planktonic cells were observed (Figure 41). Furthermore, the aggregates produced by AE2348/69 *luxS*<sup>-</sup> in the presence of *N*-(3-oxohexanoyl)-L-HSL were of similar size to those produced by the parental E2348/69 in the presence of the same AHL (Figure 41). The same observation was made in the presence of *N*-dodecanoyl-L-HSL (Figure 41). The *D*-isomers had no significant effect on the aggregation of the *LuxS* mutant (Figure 41).

Addition of *N*-(3-oxohexanoyl)-L-HSL and *N*-dodecanoyl-L-HSL resulted in the aggregation profile shifting to the left in comparison to the baseline produced in the absence of

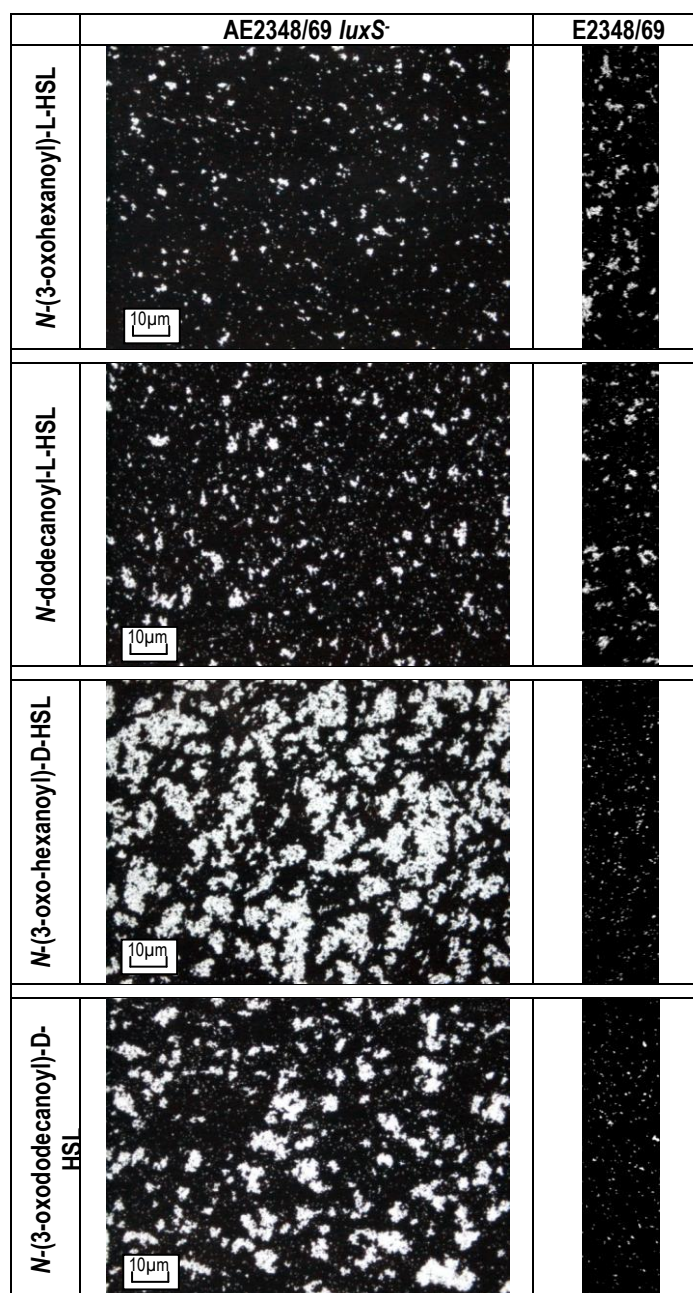


**Figure 41 –Aggregates formed by AE2348/69 *luxS*<sup>-</sup> in the presence of AHL at 25°C**

Microscopy images were taken at 100x phase contrast microscopy after 5 hours incubation. Supplementation with AHL was performed at 4 hours incubation. Images are representative of 2 independent biological replicates, each with 6 technical replicates

A representative cross-section from an image showing the aggregates formed by wild type E2348/69 is provided for each treatment.

Scale bars are indicated in the left hand corner of each image, and set to 10µm.

AHL (Figures 42A and B). In the presence of *N*-(3-oxohexanoyl)-L-HSL the size of the aggregates was significantly decreased in both cultures A and B when compared to the unsupplemented baseline ( $D = 0.74$  and  $D = 0.68$  respectively) (Table 23). Peak aggregation shifted from 20,000 pixels<sup>2</sup> in the absence of AHL, to 2000 pixels<sup>2</sup> in the presence of *N*-(3-oxohexanoyl)-L-HSL (Figures 42A and B). Biological variation was calculated at  $D = 0.21$ , therefore the overall decrease in aggregation was not due to biological variation ( $D = 0.73$ ) (Table 23).

Similarly the addition of *N*-dodecanoyl-L-HSL significantly decreased the size of the aggregates formed by AE2348/69 *luxS*<sup>-</sup> in both cultures A and B when compared to those observed in the equivalent unsupplemented culture ( $D = 0.71$  and  $D = 0.50$  respectively) (Table 23). As biological variation was calculated as  $D = 0.03$  the significant decrease in aggregation of  $D = 0.66$  was not as a result of biological variation (Table 23).

Addition of the *D*-isomers was used as a negative control for the activity of AHL. Addition of either *D*-isomer had no significant effect on the aggregation of AE2348/69 *luxS*<sup>-</sup> at 25°C ( $D = 0.12$  for *N*-(3-oxo-hexanoyl)-D-HSL and  $D = 0.30$  for *N*-(3-oxododecanoyl)-D-HSL) (Table 24). In the presence of either *N*-(3-oxo-hexanoyl)-D-HSL or *N*-(3-oxododecanoyl)-D-HSL both cultures A and B had similar aggregation profiles to the unsupplemented baseline control (Figures 43A and B). Biological variation was calculated as  $D = 0.11$  in the presence of *N*-(3-oxo-hexanoyl)-D-HSL and  $D = 0.24$  with addition of *N*-(3-oxododecanoyl)-D-HSL (Table 24).

The evidence presented shows that AHLs have a significant effect on aggregation in the absence of AI-2. Cell aggregation occurs as a result of interactions between cell surface components holding the bacteria together. The effect of AHL on the expression of a number of cell surface components was investigated to identify the quorum sensing regulon controlling aggregation of E2348/69.

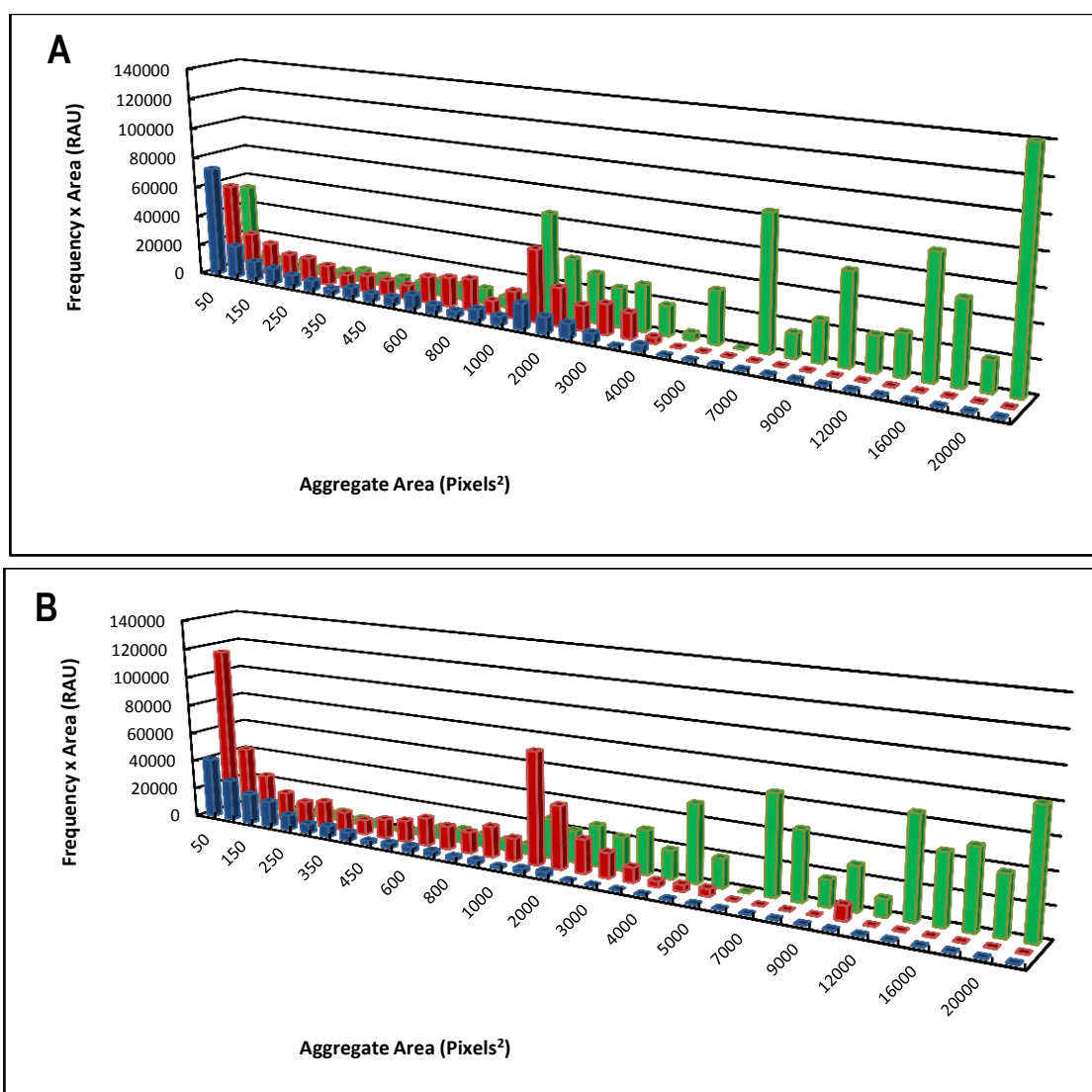


**Figure 42 – Aggregation profile of AE2348/69 *luxS*<sup>-</sup> in the presence and absence of *N*-(3-oxohexanoyl)-L-HSL and *N*-dodecanoyl-L-HSL at 25°C**

Each profile is representative of the distribution of aggregate sizes produced by AE2348/69 *luxS*<sup>-</sup> in the presence and absence of *N*-(3-oxohexanoyl)-L-HSL and *N*-dodecanoyl-L-HSL. AHLs were supplemented at 4 hours growth to a final concentration of 5nM. The images analysed were represented in Figure 41.

(A) Culture A; and (B) Culture B

(Blue) AE2348/69 *luxS*<sup>-</sup> in the presence of *N*-(3-oxohexanoyl)-L-HSL

(Red) AE2348/69 *luxS*<sup>-</sup> in the presence of *N*-dodecanoyl-L-HSL

(Green) AE2348/69 *luxS*<sup>-</sup> with no AHL

**Table 23 – Statistical analysis of the effect of active AHL on AE2348/69 *luxS*<sup>-</sup> aggregation**

Biological variation compares profiles between cultures independent A and B; technical variation compares the profiles within a culture. Where  $D < 0.4$  there is no significant difference between the profiles of the given treatments, but where  $D \geq 0.4$  the difference is deemed to be significant.

	Biological Variation (A vs B)		Technical Variation	
AE2348/69 <i>luxS</i> <sup>-</sup>	0.32		0.31	
	A	B	Biological Variation (A vs B)	Unsupplemented vs Supplemented
<i>N</i> -(3-oxohexanoyl)-L-HSL (C6)	0.74	0.68	0.21	0.73
<i>N</i> -dodecanoyl-L-HSL (C12)	0.71	0.50	0.03	0.66



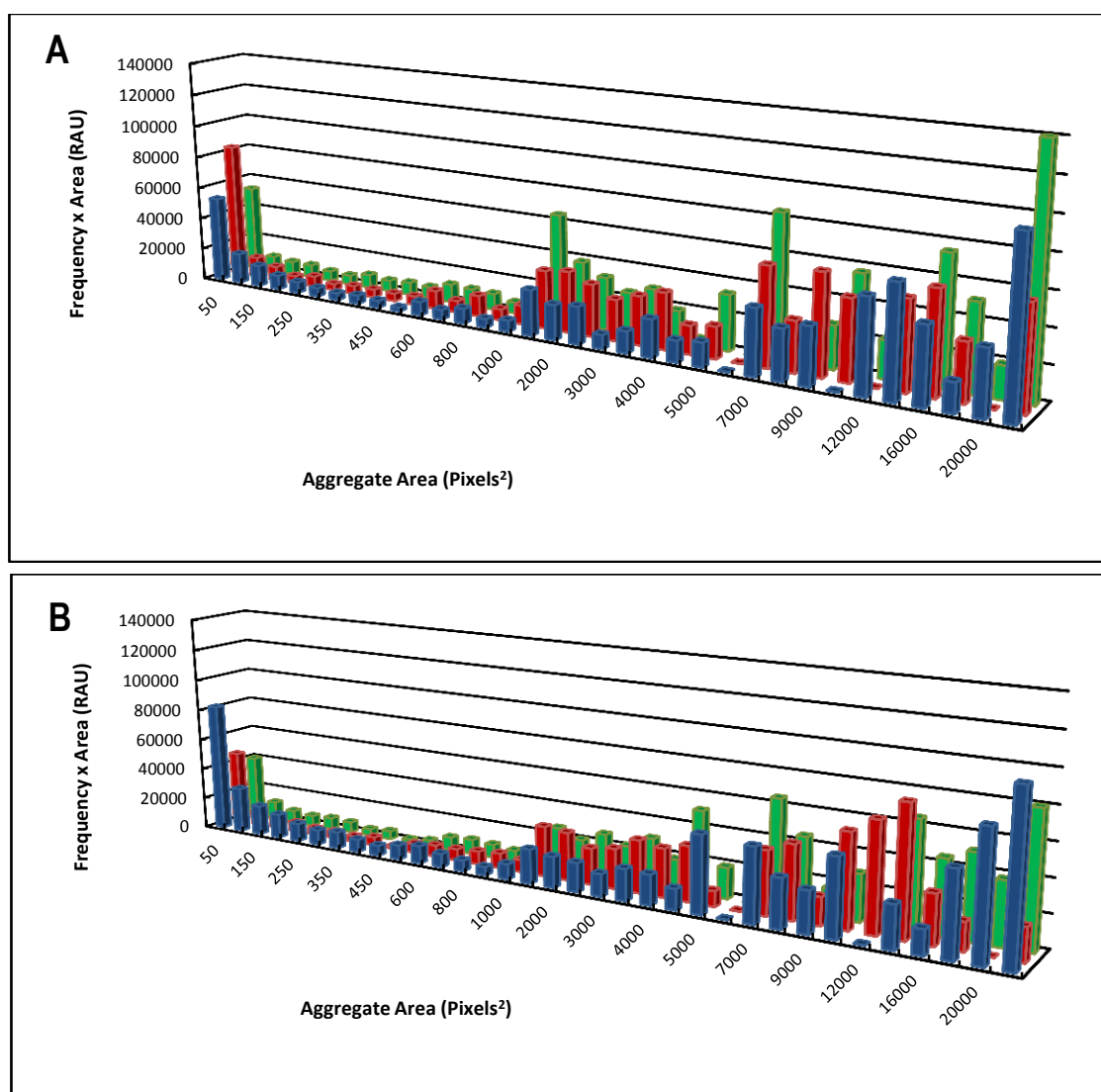


**Figure 43 – Aggregation profile of AE2348/69 *luxS*<sup>-</sup> in the presence and absence of *N*-(3-oxo-hexanoyl)-D-HSL and *N*-(3-oxododecanoyl)-D-HSL at 25°C**

Each profile is representative of the distribution of aggregate sizes produced by AE2348/69 *luxS*<sup>-</sup> in the presence and absence of *N*-(3-oxo-hexanoyl)-D-HSL and *N*-(3-oxododecanoyl)-D-HSL. AHLs were supplemented at 4 hours growth to a final concentration of 5nM. The images analysed were represented in Figure 41.

(A) Culture A; and (B) Culture B

(Blue) AE2348/69 *luxS*<sup>-</sup> in the presence of *N*-(3-oxo-hexanoyl)-D-HSL

(Red) AE2348/69 *luxS*<sup>-</sup> in the presence of *N*-(3-oxododecanoyl)-D-HSL

(Green) AE2348/69 *luxS*<sup>-</sup> with no AHL

**Table 24 – Statistical analysis of the effect of *D*-isomers on AE2348/69 *luxS*<sup>-</sup> aggregation**

Biological variation compares profiles between independent cultures A and B; technical variation compares the profiles within a culture. Where  $D < 0.4$  there is no significant difference between the profiles of the given treatments, but where  $D \geq 0.4$  the difference is deemed to be significant.

	Biological Variation (A vs B)		Technical Variation	
AE2348/69 <i>luxS</i> <sup>-</sup>	0.32		0.31	
	A	B	Biological Variation (A vs B)	Unsupplemented vs Supplemented
<i>N</i> -(3-oxo-hexanoyl)-D-HSL (C6)	0.25	0.29	0.11	0.12
<i>N</i> -(3-oxododecanoyl)-D-HSL (C12)	0.12	0.46	0.24	0.30



#### **4.2.2 Effect of AHL on Polysaccharide Expression in E2348/69 and the HosA mutant**

There are multiple forms of polysaccharide synthesised by bacteria, such as exopolysaccharide, lipopolysaccharide and polysaccharide. The synthesis and secretion of exopolysaccharide and/or cellulose has been associated with the formation of bacterial aggregates in species such as uropathogenic and enteropathogenic *E. coli* [79, 232]. In this section the effect of AHL-dependent quorum sensing on the expression of both of these cell surface components will be assessed.

Many gram negative bacteria produce an extracellular capsule, or slime layer which provides added protection from macrophages within a host [264, 265]. Several *E. coli* strains, such as E2348/69 express a colanic acid capsule composed of exopolysaccharide under particular environmental conditions. A component of the capsule in *E. coli* is the uronic acid [266]

Exopolysaccharide expression was monitored using two different methods. The first used changes in the morphology of bacterial colonies in the presence of 0.4% (final concentration) glucose on standard LA plates, and the second calculated the concentration of uronic acid within a sample. The results from the uronic acid concentration study lacked statistical power and were thereby inconclusive due to high levels of biological variation. The uronic acid data has not been presented. Addition of glucose to standard LA plates stimulated production of exopolysaccharide, resulting in the formation of mucoid colonies when left at room temperature for up to 7 days. Both E2348/69 and E2348/69 *hosA*<sup>-</sup> were streaked onto standard and glucose-containing LA plates to determine the effect of AHLs on the expression of exopolysaccharide (Figure 44). In the absence of AHL both strains produced glossy colonies on the glucose-containing plates in comparison to the standard LA, but no effect on the colony morphology was observed (Figure 44). Addition of 5nM (final concentration) of either *N*-(3-oxohexanoyl)-L-HSL or *N*-dodecanoyl-L-HSL had no significant effect on the morphology of the colonies in both strains (Figure 44).

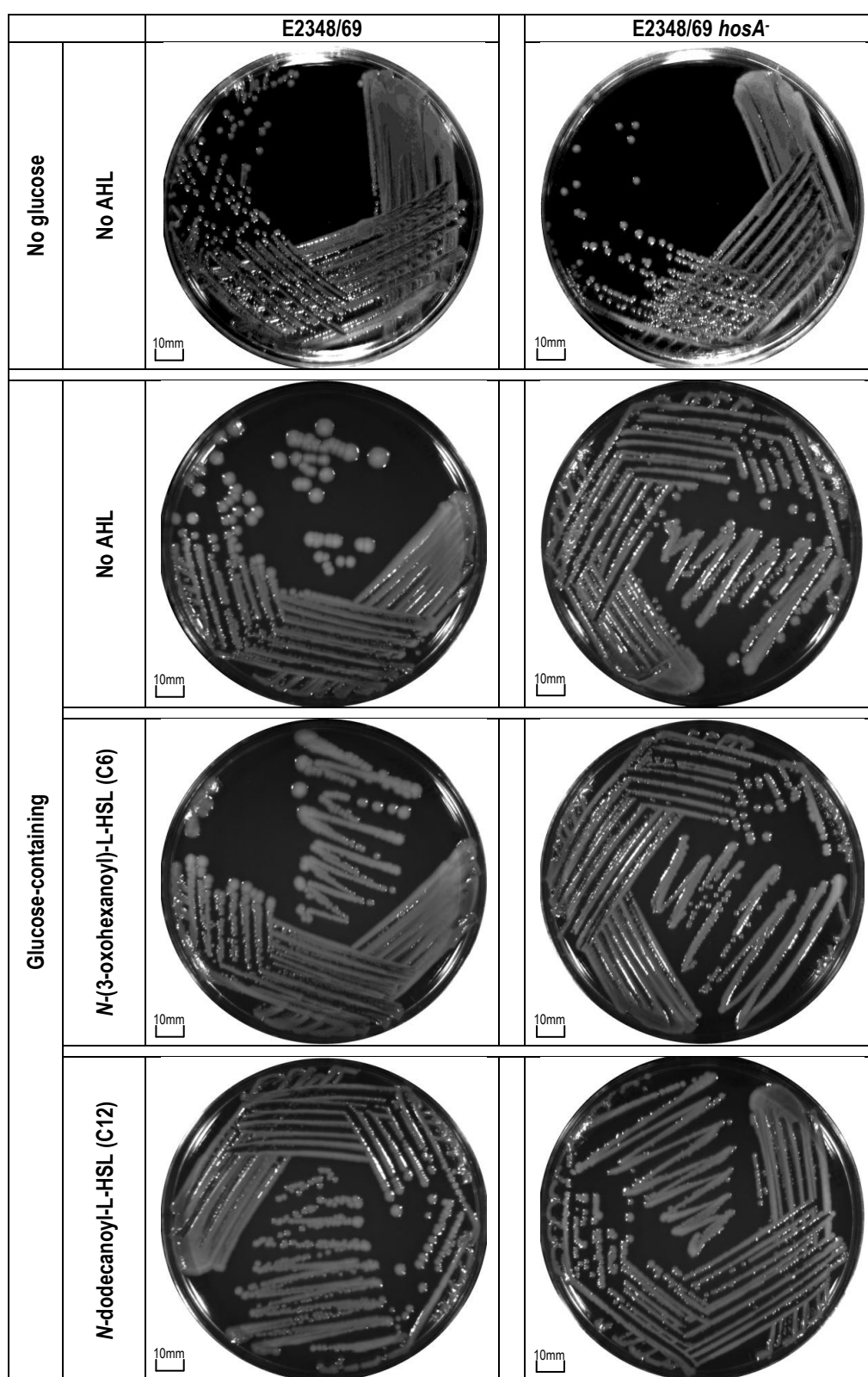


**Figure 44 – Comparison of exopolysaccharide production by E2348/69 and E2348/69 *hosA*<sup>-</sup>**  
 All glucose-containing agar were supplemented with 0.4% (v/v) glucose final concentration. All plates were incubated at room temperature for 7 days. AHL was added directly to the agar after sterilisation to a final concentration of 5nM. Images are representative of 3 replicates.  
 Scale bars are indicated in the left hand corner of each image, and set to 10mm.

The expression of cellulose, a polysaccharide, was monitored using Calcofluor White™ stain which produces a bright blue fluorescence when bound to cellulose.

A low level of fluorescence was observed from the aggregated cells of a 48 hour settle culture of E2348/69 when grown at 25°C (Figure 45). Similar staining of cells was observed when 9-day growth of E2348/69 on glucose-containing LA plates was resuspended in the stain (Figure 45). Where aggregating cells of E2348/69 *hosA*<sup>-</sup> were stained using Calcofluor White™, similar levels of fluorescence to the parent were observed (Figure 45).

#### **4.2.3 Effect of Protease on the Aggregation of E2348/69 *hosA*<sup>-</sup>**

To determine whether the aggregates were held together by proteins, 2 different proteases were added to an aggregated culture of E2348/69 *hosA*<sup>-</sup>. Both TrypLE™ (Gibco®) and Proteinase K are serine proteases which hydrolyse proteins into peptides. Trypsins, such as TrypLE™, target amino acids such as lysine or arginine, whereas Proteinase K targets mainly the aromatic amino acids such as phenylalanine and histidine. Both enzymes were added to aggregating cultures at a final concentration of 0.1% (v/v) after 4 hours incubation at 25°C. Samples were taken after 1 hour further incubation and analysed for changes in the aggregation profile.

Addition of both proteases to aggregated E2348/69 *hosA*<sup>-</sup> resulted in a decrease in the size and frequency of aggregates, and increased the number of planktonic cells (Figure 46). Analysis confirmed the shape of the aggregation profiles in both cultures A and B shifted to the left in the presence of protease when compared to the non- treated cultures (Figures 47A and B). In the non-treated culture the majority of the aggregates were between 2000 and 20,000+ pixels<sup>2</sup> in size. Upon addition of protease a higher proportion of the aggregates were of 2000 – 9000 pixels<sup>2</sup> in size (Figures 47A and B). Figure 46 shows that although the aggregates reduced in size, the cells were not fully dispersed in the presence of protease.

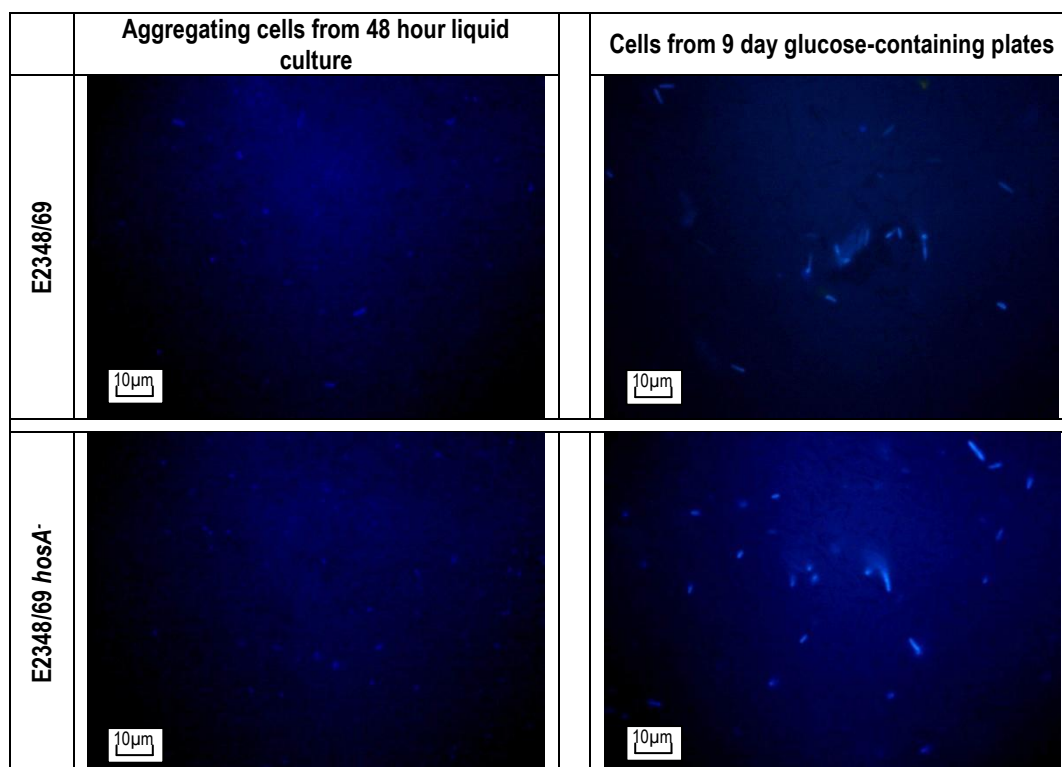


**Figure 45 – Cellulose expression by E2348/69 and E2348/69 *hosA*<sup>-</sup>**

Images were taken 1 minute after resuspension in Calcofluor White™ stain using a UV-filter on a fluorescence microscope and are representative of 3 technical replicates per treatment.

Aggregating cells were taken from 48-hour settle cultures and diluted 1:1 with Calcofluor White solution. Colonies from glucose-containing plates left at room temperature for 9 days were resuspended in 10µl of the stain solution.

Scale bars are indicated in the left hand corner of each image, and set to 10µm.

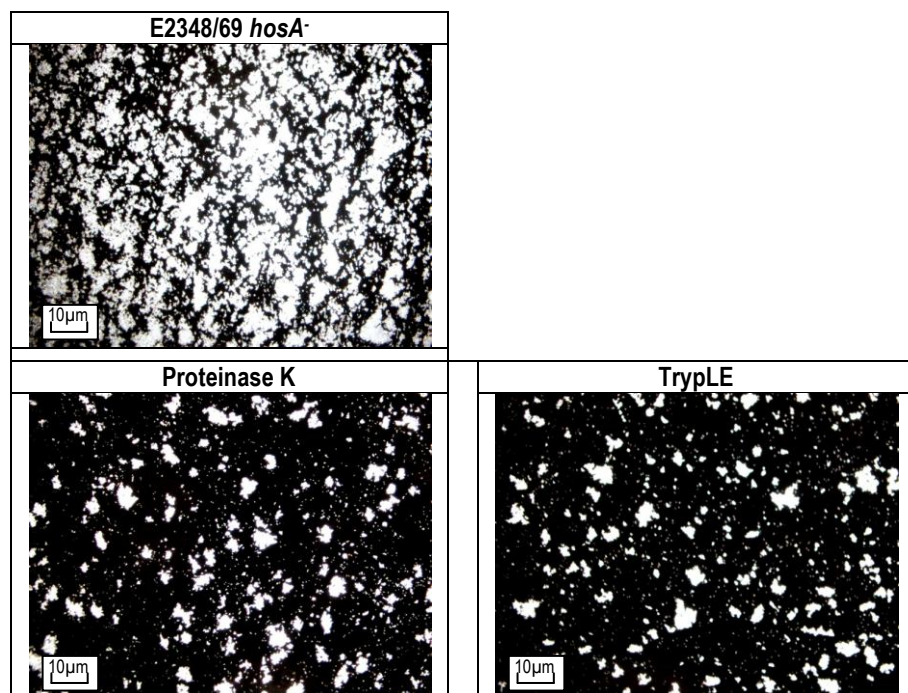


**Figure 46 – Aggregates formed by E2348/69 *hosA*<sup>-</sup> in the presence and absence of protease at 25°C**

Microscopy images were taken at 100x magnification phase contrast microscopy after 5 hours incubation. Images are representative of 2 independent biological replicates, each with 6 technical replicates. Supplementation with TrypLE™ and Proteinase K was performed at 4 hours incubation to a final concentration of 0.1% (v/v). Scale bars are indicated in the left hand corner of each image, and set to 10µm.

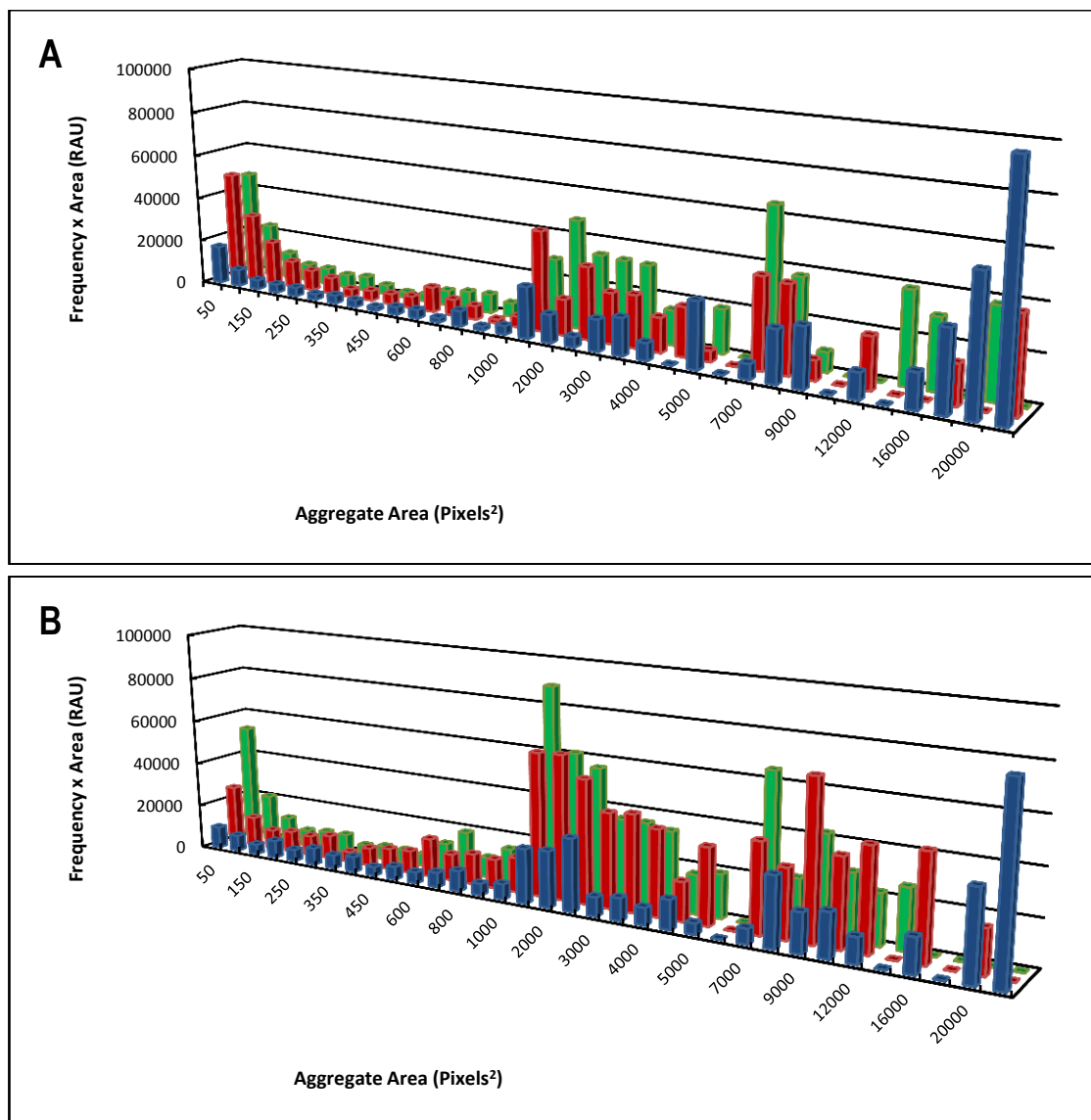


**Figure 47 – Aggregation profile of E2348/69 *hosA*<sup>-</sup> in the presence and absence of protease at 25°C**

Each profile is representative of the distribution of aggregate sizes produced by E2348/69 *hosA*<sup>-</sup> in the presence and absence of TrypLE and Proteinase K. Proteases were supplemented at 4 hours growth to a final concentration of 0.1% (v/v). The images analysed were represented in Figure 47.

(A) Culture A; and (B) Culture B

(Blue) Aggregation profile of E2348/69 *hosA*<sup>-</sup> with no protease

(Red) Aggregation profile of E2348/69 *hosA*<sup>-</sup> in the presence of TrypLE™

(Green) Aggregation profile of E2348/69 *hosA*<sup>-</sup> in the presence of Proteinase K

**Table 25 - Statistical analysis of the effect of protease on E2348/69 *hosA*<sup>-</sup> aggregation**

Biological variation compares profiles between independent cultures A and B; technical variation compares the profiles within a culture. The aggregation profiles between TrypLE™- and Proteinase K-supplemented cultures were compared to determine if one protease was more effective than the other. Where  $D < 0.4$  there is no significant difference between the profiles of the given treatments, but where  $D \geq 0.4$  the difference is deemed to be significant.

	Biological Variation (A vs B)		Technical Variation	
E2348/69 <i>hosA</i> <sup>-</sup>	0.21		0.31	
	A	B	Biological Variation (A vs B)	Unsupplemented vs Supplemented
TrypLE™	0.69	0.78	0.19	0.71
Proteinase K	0.74	0.77	0.17	0.73
TrypLE™ vs Proteinase K			0.11	

Technical variation between images from the same culture of E2348/69 *hosA*<sup>-</sup> was calculated at D = 0.31 (Table 25). Biological variation between cultures A and B was calculated at D = 0.21 (Table 25). Addition of TrypLE™ significantly decreased the size of the aggregates formed in comparison to the non-treated in both cultures A and B (D = 0.69 and D = 0.78 respectively) (Table 25; Figures 47A and B). As biological variation was calculated at D = 0.19, the overall decrease in aggregation was not attributed to biological variation (D = 0.71) (Table 25).

In the presence of Proteinase K, the size of aggregates formed by E2348/69 *hosA*<sup>-</sup> significantly decreased in both cultures A and B when compared to the non-treated cultures (D = 0.74 and D = 0.77 respectively) (Table 25; Figures 47A and B). Biological variation was calculated at D = 0.17. The overall decrease in aggregation of D = 0.73 in the presence of Proteinase K was therefore not as a result of biological variation (Table 25; Figures 47A and B).

The difference in aggregation profiles between TrypLE™ and Proteinase K treated cultures was calculated at D = 0.11, showing neither of the proteases was more effective than the other in dispersing the aggregates formed by E2348/69 *hosA*<sup>-</sup> (Table 25).

#### **4.2.4 Effect of AHL on Cell Surface Factors in E2348/69 and E2348/69-derived strains**

The decrease in aggregation of E2348/69 *hosA*<sup>-</sup> in the presence of protease showed the aggregates were held together by protein-protein interactions. Other studies had shown several cell surface factors to be important in the production and viability of bacterial aggregates. For example flagella were shown to be important for *Yersinia pseudotuberculosis* and cellulose was observed to affect adhesion by uropathogenic *E. coli*. Further, Antigen 43 was shown to be an effector in *E. coli*, as was the type IV pilus, or bundle forming pilus of EPEC [13, 14, 57, 79, 245, 260, 261]. Ferrándiz *et al* showed that flagella formation was unaffected in the *HosA* mutant, but the rotation of the flagella may have been affected [68]. As the presence of flagella had been

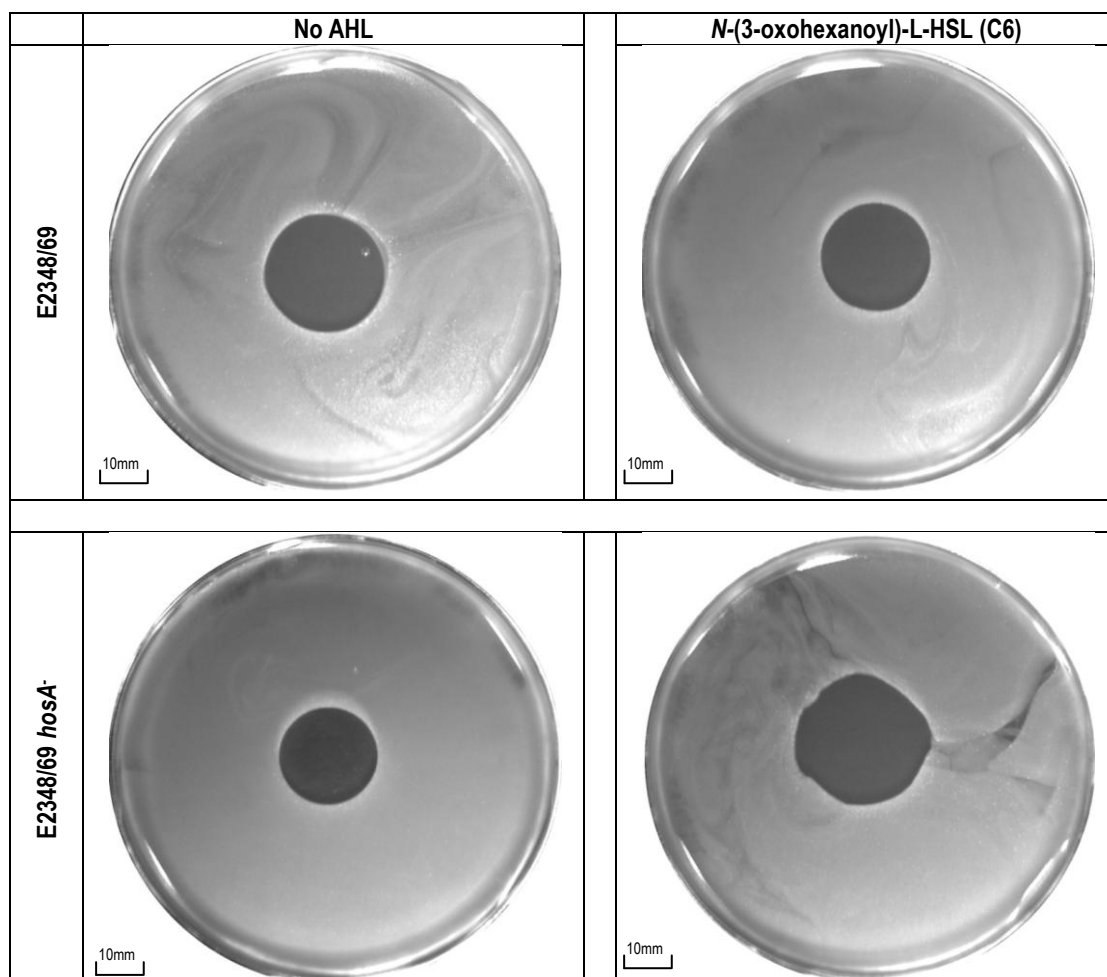
confirmed during the Ferrándiz *et al* study, an initial investigation into other cell surface factors was performed to determine if a clear and observable effect occurred between strains and in the presence of exogenous AHL. The first class of protein investigated were the pili, of which 2 different types were targeted. Antigen 43 is a self-recognising surface adhesin and autotransporter found in most *E. coli* strains which promotes cell-to-cell aggregation, clumping and fluffing of a bacterial population [260]. In addition, expression of Antigen 43 confers resistance to hydrogen peroxide. Curli are short pili on the surface of bacteria that may have a role in bacteria-bacteria interactions and aggregation.

To investigate the role of quorum sensing on antigen 43 expression, molten agar was seeded with an overnight culture of either E2348/69 or E2348/69 *hosA*<sup>-</sup> and poured into plates. *N*-(3-oxohexanoyl)-L-HSL was added at a final concentration of 5nM at three different points during the experiment: at the time of inoculation of the overnight culture, 1 hour prior to the seeding of the agar, and directly into the agar. Once the agar had set, a drop of hydrogen peroxide was placed on the surface of the agar to produce a zone of clear growth inhibition in the centre of the plate. The production of colonies within this zone indicated resistance to hydrogen peroxide and therefore expression of antigen 43.

Both E2348/69 and E2348/69 *hosA*<sup>-</sup> had a clear zone of inhibition in the absence of AHL with no visible colonies (Figure 48). An air bubble was observed in the E2348/69 plate. Addition of *N*-(3-oxohexanoyl)-L-HSL to either strain had no detectable effect on the resistance to hydrogen peroxide (Figure 48).

The expression of both curli and flagella can be monitored using congo red, a secondary diazo dye which is water soluble and readily binds these amyloid fibres to produce red colonies.





\* The small spot in the zone of inhibition on the E2348/69 in the absence of AHL is an agar defect and not a colony

**Figure 48 – Effect of *N*-(3-oxohexanoyl)-L-HSL on antigen 43 expression in E2348/69 and E2348/69 *hosA*<sup>-</sup>**

A positive response, and thereby Antigen 43 expression, is indicated by the presence of colonies within the zone of inhibition.

Images are representative of 3 technical replicates per treatment. Plates were incubated at 37°C overnight.

Supplementation with *N*-(3-oxohexanoyl)-L-HSL was performed to a final concentration of 5nM.

Scale bars are indicated in the left hand corner of each image, and set to 10mm.

In the absence of AHL on 3.7% (v/v) congo red plates, E2348/69 produced a clearly defined red halo, approximately 2mm wide, with strong pigmentation within the colony (Figure 49). E2348/69 *hosA*<sup>-</sup> and AE2348/69 *luxS*<sup>-</sup> had similar morphology in the absence of AHL (Figure 49). Cultures of other E2348/69-derived strains E2348/69 *bfpA*<sup>-</sup>, E2348/69 *espA*<sup>-</sup> and E2348/69 MAR001 did not produce halos, and the colonies remained more neutral in colour (Figure 49).

Addition of *N*-(3-oxohexanoyl)-L-HSL to the growth medium resulted in a decrease in the diameter of the congo red halo of parental strain E2348/69 (Figure 50). In the presence of *N*-dodecanoyl-L-HSL, the centre of the colony appeared pinker in colour when compared to the unsupplemented (Figure 50). No change was observed in the diameter of the halos of E2348/69 *hosA*<sup>-</sup> and AE2348/69 *luxS*<sup>-</sup> in the presence of any AHL added, although the strength of the red pigment appeared to decrease when compared to that produced in the absence of AHL (Figure 50).

#### **4.2.5 Role of the EAF plasmid in the Aggregation and Population Expansion of E2348/69**

The EAF plasmid, found only in enteropathogenic *E. coli*, contains the genes encoding bundle forming pili (Bfp) in addition to various regulators and transporter proteins (Section 1.1.4.4). The Bfp are long peritrichous filaments composed of BfpA protein, and are important for forming rafts and micro-colonies during attachment to mammalian cells and infection of a host.

E2348/69 *bfpA*<sup>-</sup> contains a single point mutation inhibiting production of bundle forming pili, but still retains the rest of the plasmid. At 25°C E2348/69 *bfpA*<sup>-</sup> was motile, producing an area of motility with an average diameter of  $54.6 \pm 3.06$ mm, which was double the size of the motility zone produced by parental E2348/69 ( $20.8 \pm 1.03$ mm) (Table 26). Addition of the active AHLs *N*-(3-oxohexanoyl)-L-HSL and *N*-dodecanoyl-L-HSL had no significant effect on the population expansion of E2348/69 *bfpA*<sup>-</sup> (Table 26; Figure 51). The average diameter of the



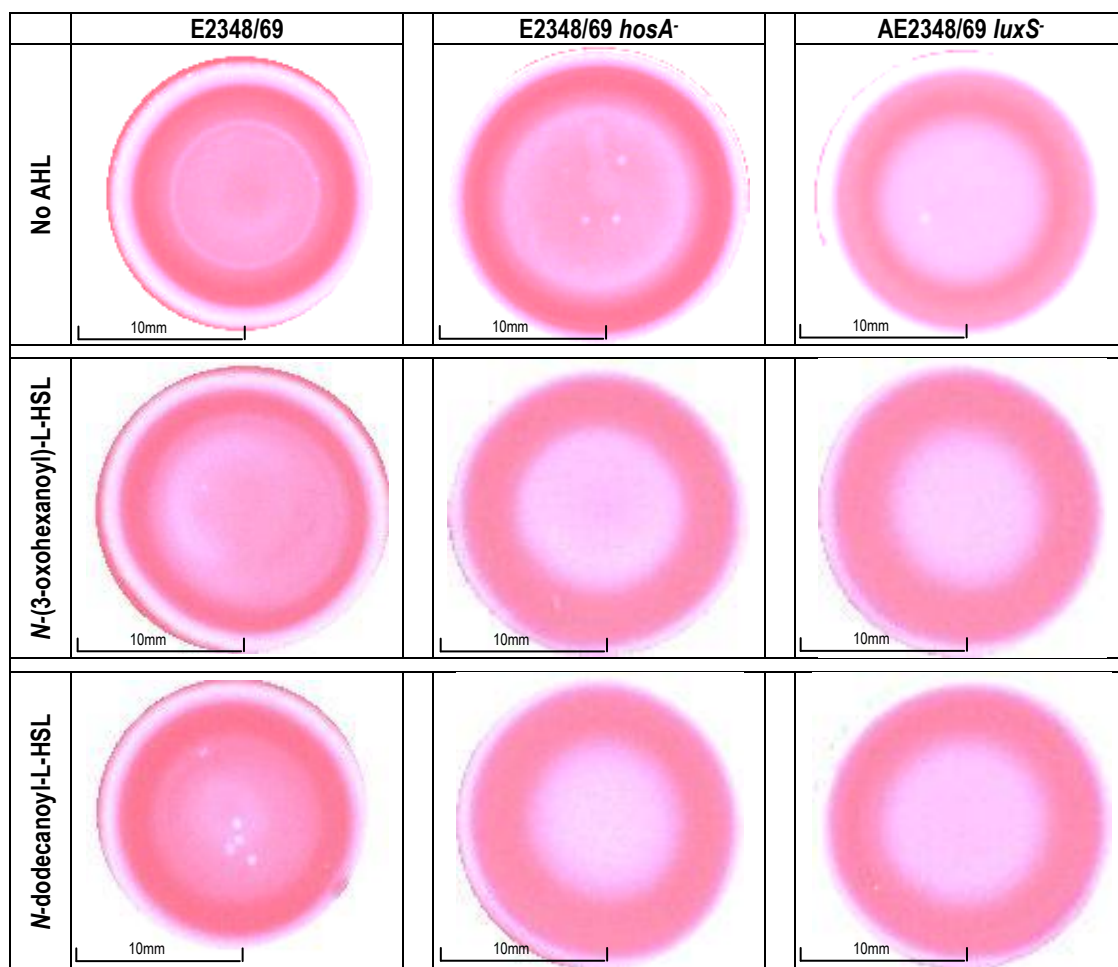


**Figure 50 – Effect of AHL on curli expression in E2348/69, E2348/69 *hosA*<sup>-</sup> and AE2348/69 *luxS*<sup>-</sup>**

Plates contained 3.7% (w/v) congo red (final concentration) and were incubated overnight at 37°C. Images are representative of duplicate samples.

Scale bars are indicated in the left hand corner of each image, and set to 10mm

**Table 26 – Statistical analysis of the effect of AHL on E2348/69 *bfpA*<sup>-</sup> population expansion at 25°C**

Side chain lengths of the AHLs are in brackets.

	Average diameter of motility zone $\pm$ 1 standard deviation (mm)	ANOVA	
		*F-value	p-value
No AHL	54.6 $\pm$ 3.06		
<i>N</i> -(3-oxo-hexanoyl)-D-HSL (C6)	53.1 $\pm$ 2.38	1.496	0.237
<i>N</i> -(3-oxododecanoyl)-D-HSL (C12)	52.5 $\pm$ 1.78	3.515	0.077
<i>N</i> -(3-oxohexanoyl)-L-HSL (C6)	54.7 $\pm$ 3.37	0.0048	0.945
<i>N</i> -dodecanoyl-L-HSL (C12)	52.9 $\pm$ 1.37	2.567	0.126

\*F- critical value = 4.414

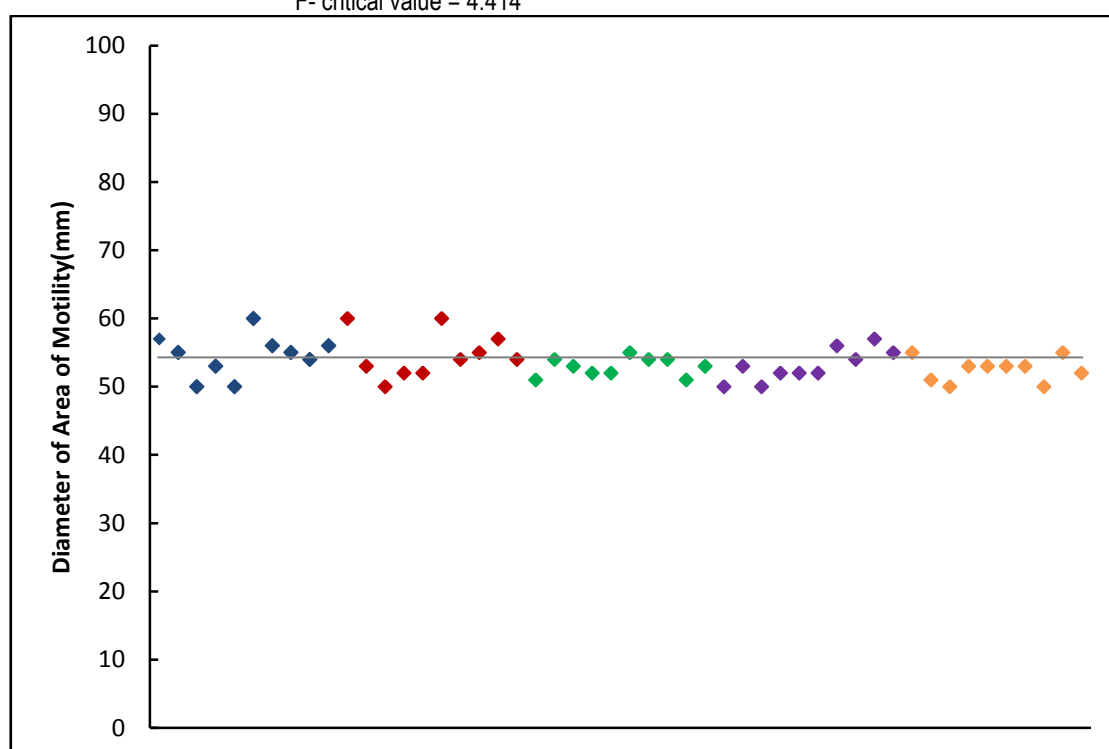


**Figure 51 –Variation in the diameter of the motility zones produced by E2348/69 *bfpA*<sup>-</sup> in the presence and absence of different AHLs at 25°C**

For each of the 2 independent biological replicates, 5 technical replicates were analysed. Each point on the graph represents one technical replicate. Petri dishes measured 95 mm in diameter.

(Blue) No AHL

(Red) *N*-(3-oxo-hexanoyl)-L-HSL

(Green) *N*-dodecanoyl-L-HSL

(Purple) *N*-(3-oxo-hexanoyl)-D-HSL

(Orange) *N*-(3-oxo-dodecanoyl)-D-HSL

The grey line represents the average diameter of the motility zones measured for the unsupplemented isolates.

motility zone in the presence of *N*-(3-oxohexanoyl)-L-HSL was measured at  $54.7 \pm 3.37\text{mm}$  ( $F = 0.0048$ ;  $p = 0.945$ ), while addition of *N*-dodecanoyl-L-HSL produced an area of motility measuring  $52.9 \pm 1.37\text{mm}$  on average ( $F = 2.56$ ;  $p = 0.126$ ) (Table 26; Figure 51). In the presence of *N*-(3-oxo-hexanoyl)-D-HSL and *N*-(3-oxododecanoyl)-D-HSL, no significant effect on population expansion was observed ( $[F = 1.49$ ;  $p = 0.237]$  and  $[F = 3.51$ ;  $p = 0.077]$  respectively) (Table 26; Figure 51).

Having determined that inactivation of BfpA increased population expansion, the effect of quorum sensing on the aggregation of E2348/69 *bfpA*<sup>-</sup> was assessed. E2348/69 *bfpA*<sup>-</sup> produced no visible aggregates, with all fields of view examined containing only planktonic cells (Figure 52A). Addition of *N*-(3-oxohexanoyl)-L-HSL and *N*-dodecanoyl-L-HSL had no effect on the aggregation of the BfpA mutant (Figure 52B).

Analysis of the aggregation profile of E2348/69 *bfpA*<sup>-</sup> in the absence of AHL showed this strain was unable to produce aggregates exceeding 100 pixels<sup>2</sup> in size in either culture A or B (Figures 53A and B). Technical variation between images of the same culture was calculated at  $D = 0.16$  (Table 27). Biological variation between cultures of E2348/69 *bfpA*<sup>-</sup> in the absence of AHL was calculated at  $D = 0.36$  (Table 27). Addition of either *N*-(3-oxohexanoyl)-L-HSL or *N*-dodecanoyl-L-HSL had no significant effect on the aggregation of E2348/69 *bfpA*<sup>-</sup> ( $D = 0.21$  and  $D = 0.16$  respectively) (Table 27; Figures 53A and B). Biological variation was calculated as  $D = 0.16$  in the presence of *N*-(3-oxohexanoyl)-L-HSL and  $D = 0.15$  with *N*-dodecanoyl-L-HSL (Table 27; Figures 53A and B).

Having identified that addition of AHL had no significant effect on aggregation or population expansion in the BfpA mutant, the same phenotypic traits were analysed in an EAF negative mutant. E2348/69 MAR001 lacked the EAF plasmid, making it possible to investigate whether this plasmid was important in population expansion and aggregation in E2348/69.

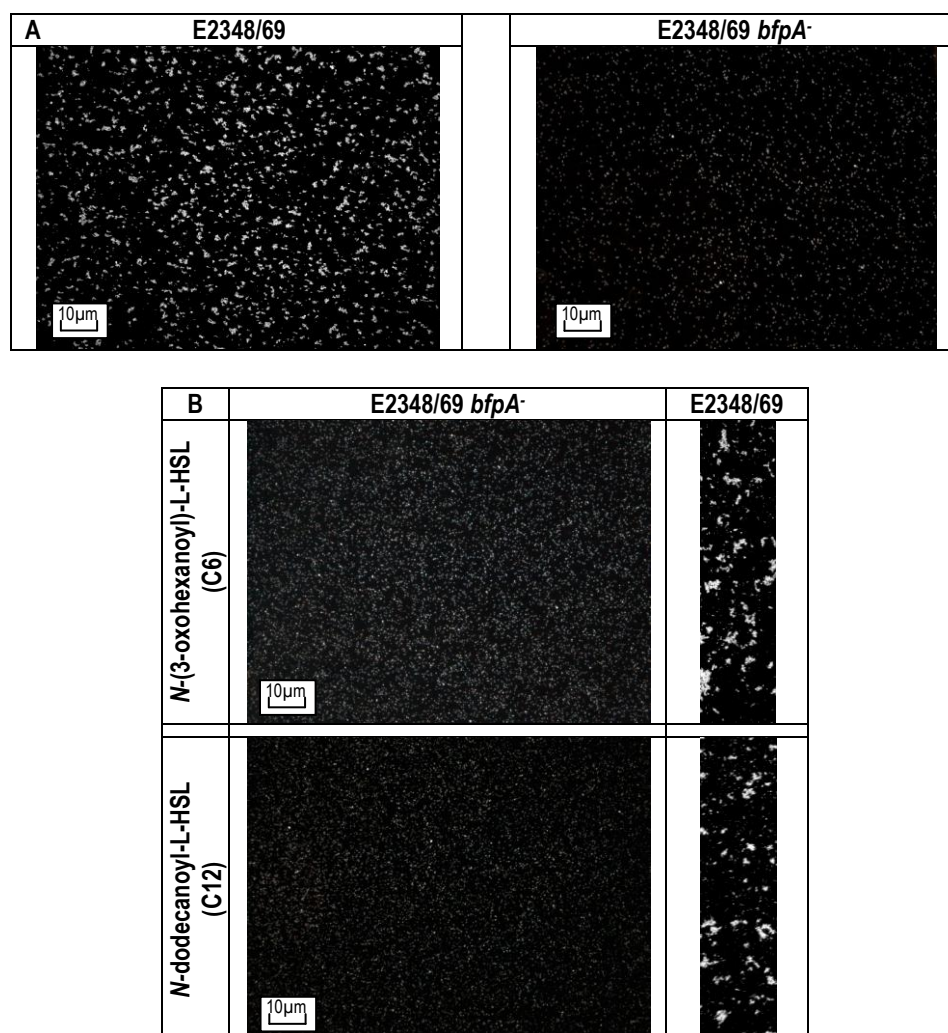


**Figure 52 – Aggregates formed by E2348/69 *bfpA*<sup>-</sup> in the presence and absence of AHL at 25°C**

Microscopy images were taken at 100x magnification phase contrast microscopy after 5 hours incubation. Images are representative of 2 independent biological replicates, each with 6 technical replicates.

(A) Comparison of the aggregates produced by wild type E2348/69 with E2348/69 *bfpA*<sup>-</sup> in the absence of supplements.

(B) Effect of *N*-(3-oxohexanoyl)-L-HSL and *N*-dodecanoyl-L-HSL on the size of the aggregates formed by E2348/69 *bfpA*<sup>-</sup>. Supplementation with AHL was completed at 4 hours incubation to a final concentration of 5nM. A representative cross-section of the aggregates formed by wild type E2348/69 in the presence of the same AHL is provided.

Scale bars are indicated in the left hand corner of each image, and set to 10µm.

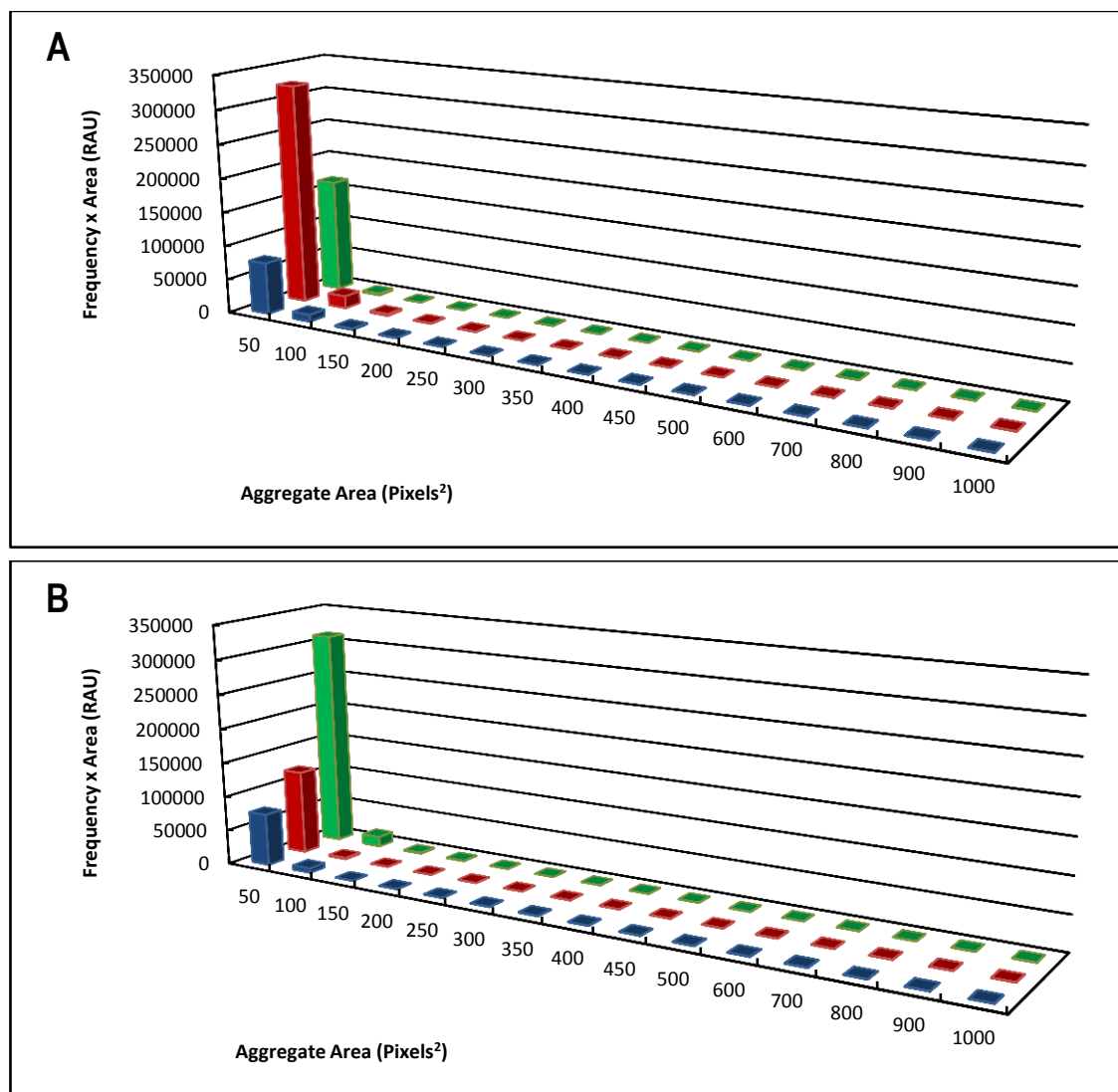


**Figure 53 – Aggregation profile of E2348/69 *bfpA*<sup>-</sup> in the presence and absence of *N*-(3-oxohexanoyl)-L-HSL and *N*-dodecanoyl-L-HSL at 25°C**

Each profile is representative of the distribution of aggregate sizes produced by E2348/69 *bfpA*<sup>-</sup> in the presence and absence of *N*-(3-oxohexanoyl)-L-HSL and *N*-dodecanoyl-L-HSL. AHLs were supplemented at 4 hours growth to a final concentration of 5nM. The images analysed were represented in Figure 53.

(A) Culture A; and (B) Culture B

(Blue) E2348/69 *bfpA*<sup>-</sup> with no AHL

(Red) E2348/69 *bfpA*<sup>-</sup> in the presence of *N*-(3-oxohexanoyl)-L-HSL

(Green) E2348/69 *bfpA*<sup>-</sup> in the presence of *N*-dodecanoyl-L-HSL

**Table 27 – Statistical analysis of the effect of active AHL on E2348/69 *bfpA*<sup>-</sup> aggregation**

Biological variation compares profiles between cultures independent A and B; technical variation compares the profiles within a culture. Where  $D < 0.4$  there is no significant difference between the profiles of the given treatments, but where  $D \geq 0.4$  the difference is deemed to be significant.

	Biological Variation (A vs B)		Technical Variation	
E2348/69 <i>bfpA</i> <sup>-</sup>	0.16		0.36	
	A	B	Biological Variation (A vs B)	Unsupplemented vs Supplemented
<i>N</i> -(3-oxohexanoyl)-L-HSL (C6)	0.23	0.04	0.16	0.21
<i>N</i> -dodecanoyl-L-HSL (C12)	0.42	0.11	0.15	0.16



E2348/69 MAR001 produced an area of motility of  $50.2 \pm 1.68\text{mm}$  on average in the absence of AHL at  $25^{\circ}\text{C}$ , similar in size to that observed for the BfpA mutant (Table 28; Figure 54). Addition of *N*-(3-oxohexanoyl)-L-HSL or *N*-dodecanoyl-L-HSL had no significant effect on population expansion with motility zones measuring on average  $50.4 \pm 1.64\text{mm}$  ( $F = 0.072$ ;  $p = 0.791$ ) and  $49.4 \pm 1.77\text{mm}$  ( $F = 1.07$ ;  $p = 0.315$ ) respectively (Table 28; Figure 54). In the presence of *N*-(3-oxo-hexanoyl)-D-HSL and *N*-(3-oxododecanoyl)-D-HSL, no significant effect on population expansion was observed ( $[F = 3.15$ ;  $p = 0.092]$  and  $[F = 4.07$ ;  $p = 0.058]$  respectively) (Table 28; Figure 54).

Phase contrast microscopy confirmed E2348/69 MAR001 did not produce large aggregates, but rather formed small aggregates with a high proportion of planktonic cells, similar to the parental E2348/69 (Figure 55A). No significant effect was observed with the addition of the inactive *D*-isomers (Figure 55B). Addition of *N*-(3-oxohexanoyl)-L-HSL and *N*-dodecanoyl-L-HSL visually increased the size of the aggregates to a level similar in size to that observed in the parent (Figure 55B).

In the absence of AHL aggregates of maximum  $150\text{ pixels}^2$  were produced by E2348/69 MAR001 (Figure 56). Technical variation between images was calculated at  $D = 0.03$  (Table 29). Biological variation between cultures A and B in the absence of AHL was calculated as  $D = 0.12$  (Table 29).

Addition of *N*-(3-oxohexanoyl)-L-HSL significantly increased the size of the aggregates formed by E2348/69 MAR001 when compared to the unsupplemented for both cultures A and B ( $D = 0.49$  and  $D = 0.45$  respectively) (Table 29; Figures 56A and B). The profile shifted to the right in comparison to that observed in the absence of AHL with the maximum aggregate size measured at  $1500\text{ pixel}^2$  (Figure 56A and B). Biological variation was calculated at  $D = 0.05$ ,

**Table 28 – Statistical analysis of the effect of AHL on E2348/69 MAR001 population expansion at 25°C**

Side chain lengths of the AHLs are in brackets.

	Average diameter of motility ring $\pm$ 1 standard deviation (mm)	ANOVA	
		*F-value	p-value
No AHL	50.2 $\pm$ 1.68		
<i>N</i> -(3-oxo-hexanoyl)-D-HSL (C6)	49.1 $\pm$ 0.99	3.156	0.0925
<i>N</i> -(3-oxododecanoyl)-D-HSL (C12)	48.7 $\pm$ 1.63	4.074	0.0587
<i>N</i> -(3-oxohexanoyl)-L-HSL (C6)	50.4 $\pm$ 1.64	0.072	0.791
<i>N</i> -dodecanoyl-L-HSL (C12)	49.4 $\pm$ 1.77	1.067	0.315

\*F- critical value = 4.414

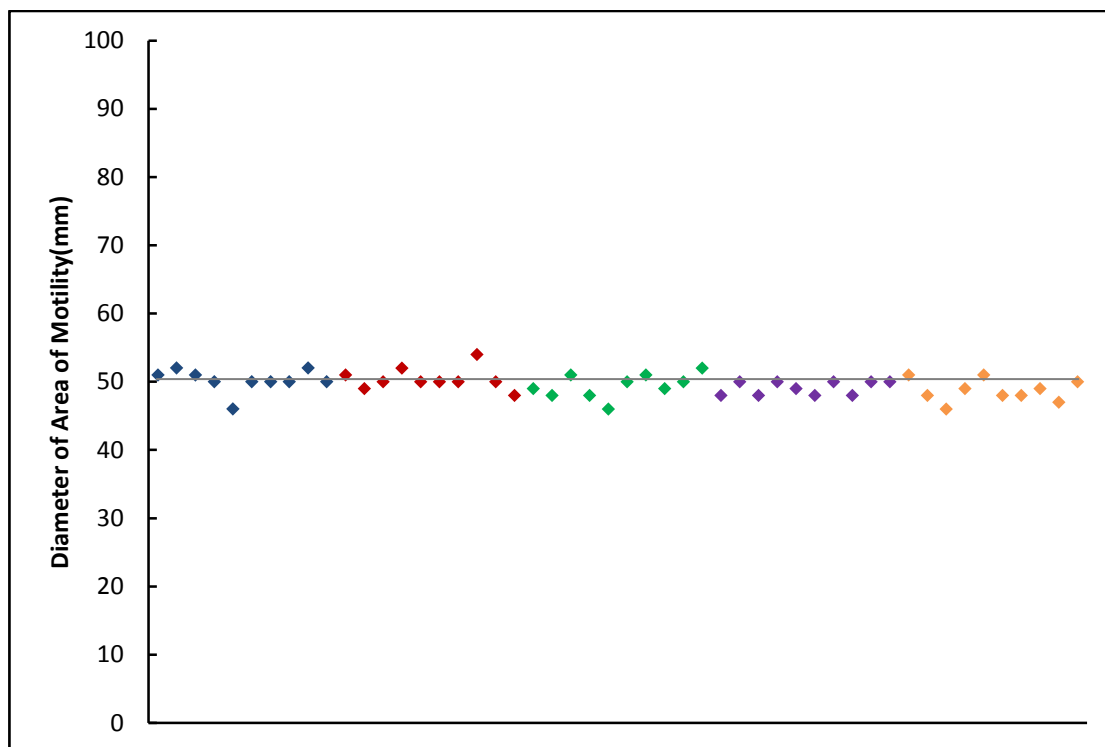


**Figure 54 - Variation in the diameter of the motility zones produced by E2348/69 MAR001 in the presence and absence of different AHLs at 25°C**

For each of the 2 independent biological replicates, 5 technical replicates were analysed. Each point on the graph represents one technical replicate. Petri dishes measured 95 mm in diameter.

(Blue) No AHL

(Red) *N*-(3-oxo-hexanoyl)-L-HSL

(Green) *N*-dodecanoyl-L-HSL

(Purple) *N*-(3-oxo-hexanoyl)-D-HSL

(Orange) *N*-(3-oxo-dodecanoyl)-D-HSL

The grey line represents the average diameter of the motility zones measured for the unsupplemented isolates.

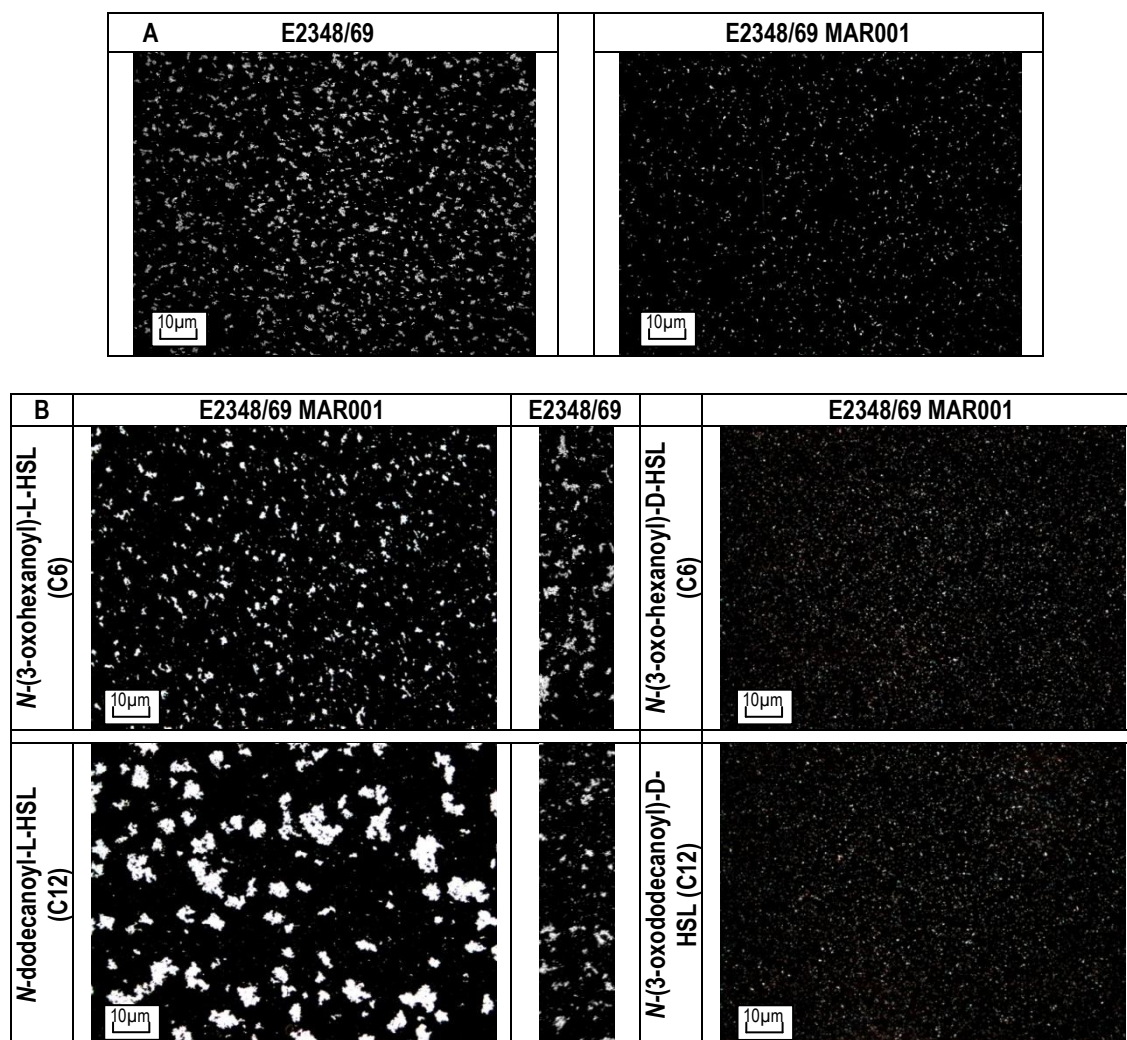


**Figure 55 – Aggregates formed by E2348/69 MAR001 in the presence and absence of AHL at 25°C**

Microscopy images were taken at 100x magnification phase contrast microscopy after 5 hours incubation. Images are representative of 2 independent biological replicates, each with 6 technical replicates.

(A) Comparison of the aggregates produced by wild type E2348/69 with E2348/69 MAR001 in the absence of supplements.

(B) Effect of *N*-(3-oxohexanoyl)-L-HSL and *N*-dodecanoyl-L-HSL on the size of the aggregates formed by E2348/69 MAR001. Supplementation was completed at 4 hours incubation to a final concentration of 5nM. A representative cross-section of the aggregates formed by wild type E2348/69 in the presence of the same AHL is provided.

Scale bars are indicated in the left hand corner of each image, and set to 10µm.

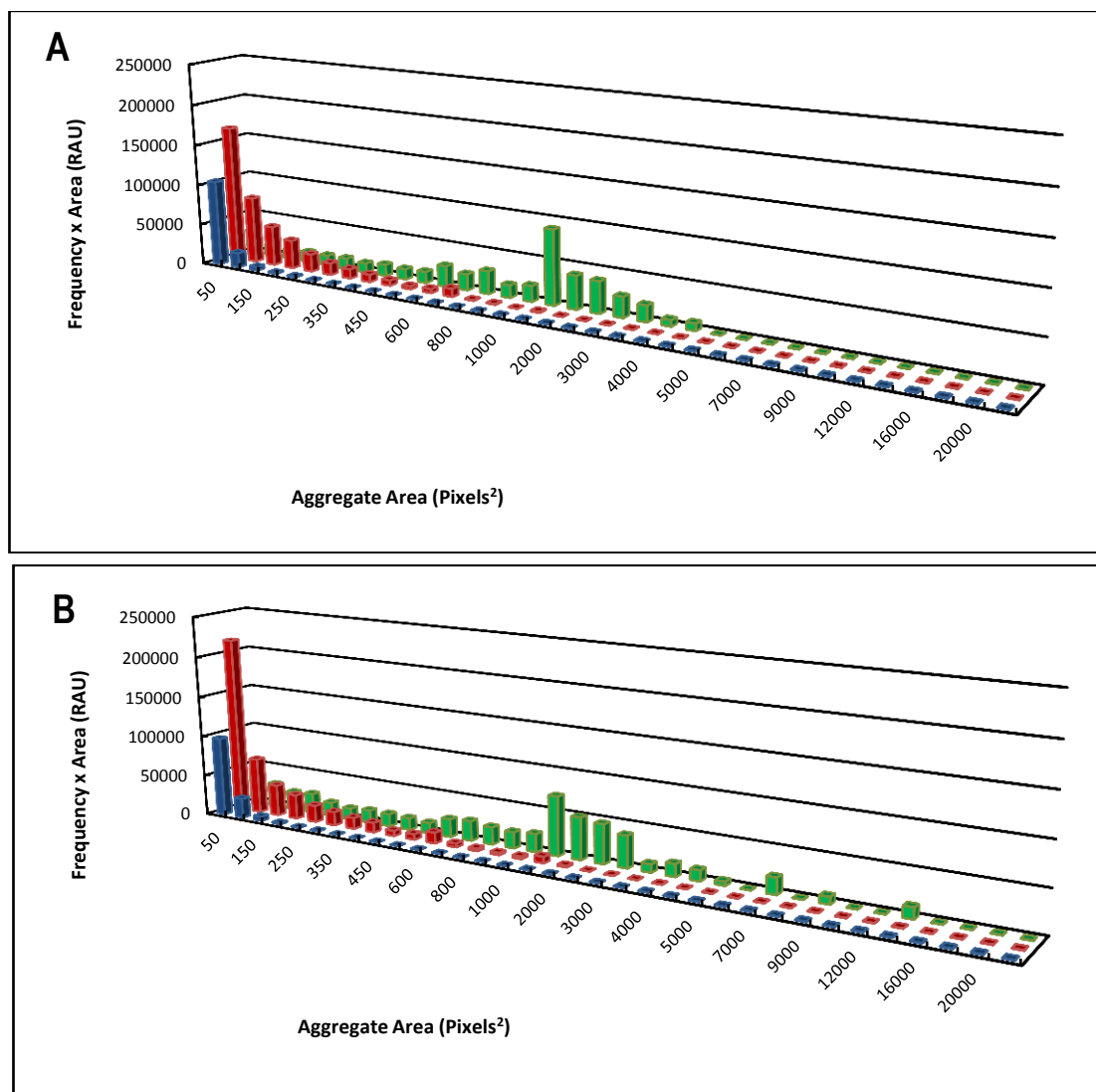


**Figure 56 – Aggregation profile of E2348/69 MAR001 in the presence and absence of *N*-(3-oxohexanoyl)-L-HSL and *N*-dodecanoyl-L-HSL at 25°C**

Each profile is representative of the distribution of aggregate sizes produced by E2348/69 MAR001 in the presence and absence of *N*-(3-oxohexanoyl)-L-HSL and *N*-dodecanoyl-L-HSL. AHLs were supplemented at 4 hours growth to a final concentration of 5nM. The images analysed were represented in Figure 56.

(A) Culture A; and (B) Culture B

(Blue) E2348/69 MAR001 with no AHL

(Red) E2348/69 MAR001 in the presence of *N*-(3-oxohexanoyl)-L-HSL

(Green) E2348/69 MAR001 in the presence of *N*-dodecanoyl-L-HSL

**Table 29 – Statistical analysis of the effect of active AHL on E2348/69 MAR001 aggregation**

Biological variation compares profiles between cultures independent A and B; technical variation compares the profiles within a culture. Where  $D < 0.4$  there is no significant difference between the profiles of the given treatments, but where  $D \geq 0.4$  the difference is deemed to be significant.

	Biological Variation (A vs B)		Technical Variation	
E2348/69 MAR001	0.12		0.03	
	A	B	Biological Variation (A vs B)	Unsupplemented vs Supplemented
<i>N</i> -(3-oxohexanoyl)-L-HSL (C6)	0.49	0.45	0.05	0.47
<i>N</i> -dodecanoyl-L-HSL (C12)	0.54	0.89	0.63	0.72

meaning the overall increase in aggregation was not as a result of biological variation ( $D = 0.47$ ) (Table 29).

In the presence of *N*-dodecanoyl-L-HSL, aggregation was increased in both cultures A and B when compared to the unsupplemented ( $D = 0.54$  and  $D = 0.89$  respectively) (Table 29; Figures 56A and B). The aggregation profile shifted to the right after addition of *N*-dodecanoyl-L-HSL with peak aggregation at 1500 pixels<sup>2</sup>, and a maximal aggregate area of 14,000pixels<sup>2</sup> measured (Figures 56A and B). Biological variation was significant ( $D = 0.63$ ) (Table 29). Although both cultures increased in aggregation in the presence of *N*-dodecanoyl-L-HSL ( $D = 0.72$ ), it cannot be determined whether this was as a result of biological variation or as an effect of treatment (Table 29). Addition of *N*-(3-oxo-hexanoyl)-D-HSL and *N*-(3-oxododecanoyl)-D-HSL had no significant effect on the aggregation of E2348/69 MAR001 ( $D = 0.13$  and  $D = 0.08$  respectively) (Table 30; Figures 57A and B).

As E2348/69 MAR001 had an aggregating profile that was similar to that of the parental strain, the presence of two specific genes on the EAF plasmid were targeted in the wild type to determine whether the EAF plasmid was present in E2348/69. Two PCRs were performed targeting two genes located on the plasmid (*bfpA* and *perA*) in order to determine whether the wild type strain had also lost the plasmid.

A number of different E2348/69 isolates were available in the culture collection derived from different research laboratories. SS, a different wild type isolate of E2348/69 containing the plasmid was used as a positive PCR control. The PCR product generated for *bfpA* (705bp) was present in both the positive control and the BfpA mutant (Figure 58A). E2348/69 *bfpA*<sup>-</sup> was constructed by Knutton *et al* as a substitution mutation replacing a serine residue with a cysteine, therefore the PCR product generated by E2348/69 *bfpA*<sup>-</sup> was expected [14]. E2348/69, E2348/69 *hosA*<sup>-</sup> and E2348/69 MAR001 did not contain *bfpA* (Figure 58A).

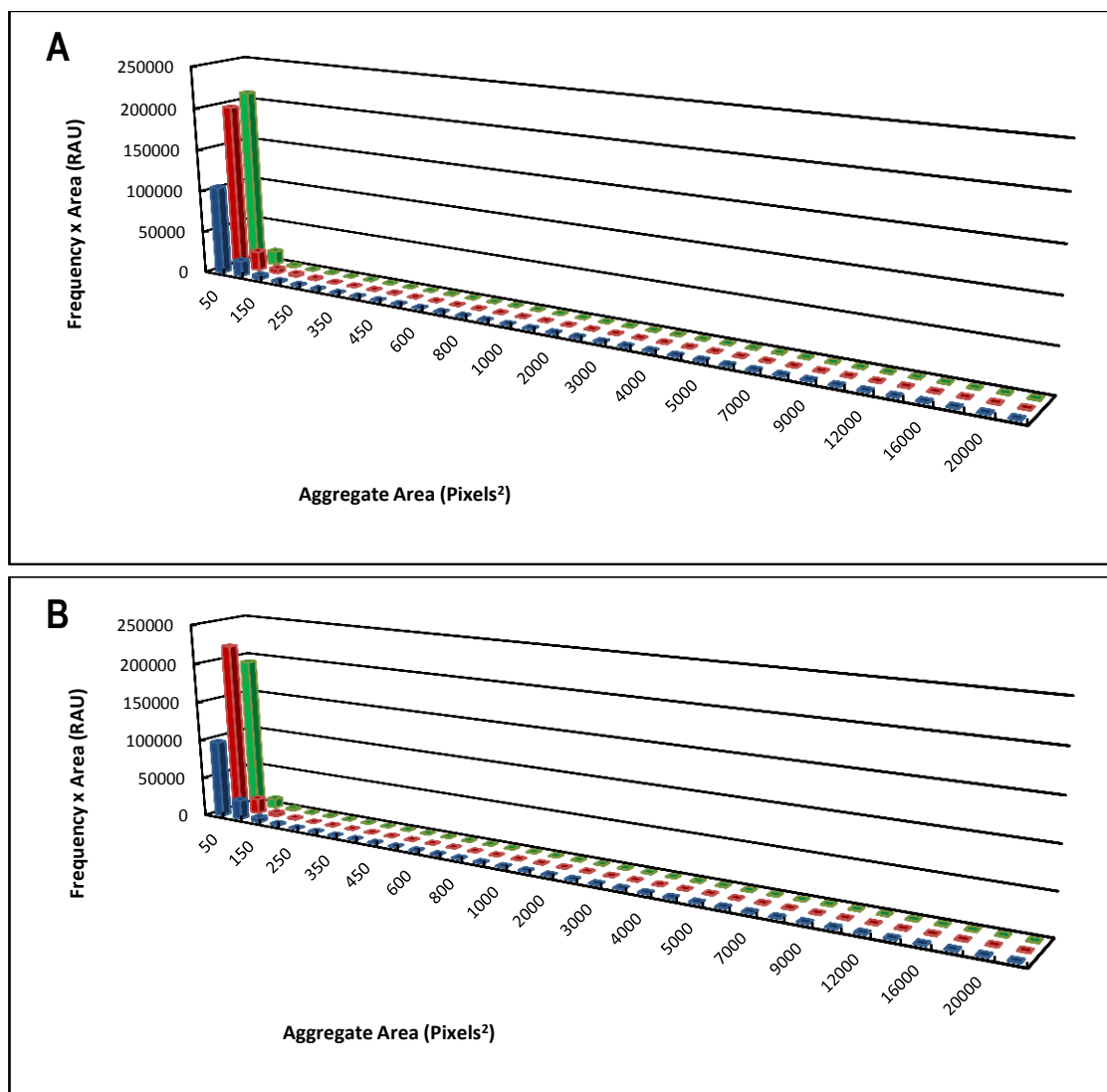


**Figure 57 – Aggregation profile of E2348/69 MAR001 in the presence and absence of *N*-(3-oxo-hexanoyl)-D-HSL and *N*-(3-oxododecanoyl)-D-HSL at 25°C**

Each profile is representative of the distribution of aggregate sizes produced by E2348/69 MAR001 in the presence and absence of *N*-(3-oxo-hexanoyl)-D-HSL and *N*-(3-oxododecanoyl)-D-HSL. AHLs were added at 4 hours growth to a final concentration of 5nM. The images analysed were represented in Figure 56.

(A) Culture A; and (B) Culture B

(Blue) E2348/69 MAR001 with no AHL

(Red) E2348/69 MAR001 in the presence of *N*-(3-oxo-hexanoyl)-D-HSL

(Green) E2348/69 MAR001 in the presence of *N*-(3-oxododecanoyl)-D-HSL

**Table 30 – Statistical analysis of the effect of *D*-isomers on E2348/69 MAR001 aggregation**

Biological variation compares profiles between cultures independent A and B; technical variation compares the profiles within a culture. Where  $D < 0.4$  there is no significant difference between the profiles of the given treatments, but where  $D \geq 0.4$  the difference is deemed to be significant.

	Biological Variation (A vs B)			Technical Variation	
E2348/69 MAR001	0.12			0.03	
	A		B	Biological Variation (A vs B)	Unsupplemented vs Supplemented
<i>N</i> -(3-oxo-hexanoyl)-D-HSL (C6)	0.13		0.17	0.02	0.13
<i>N</i> -(3-oxododecanoyl)-D-HSL (C12)	0.09		0.14	0.08	0.08

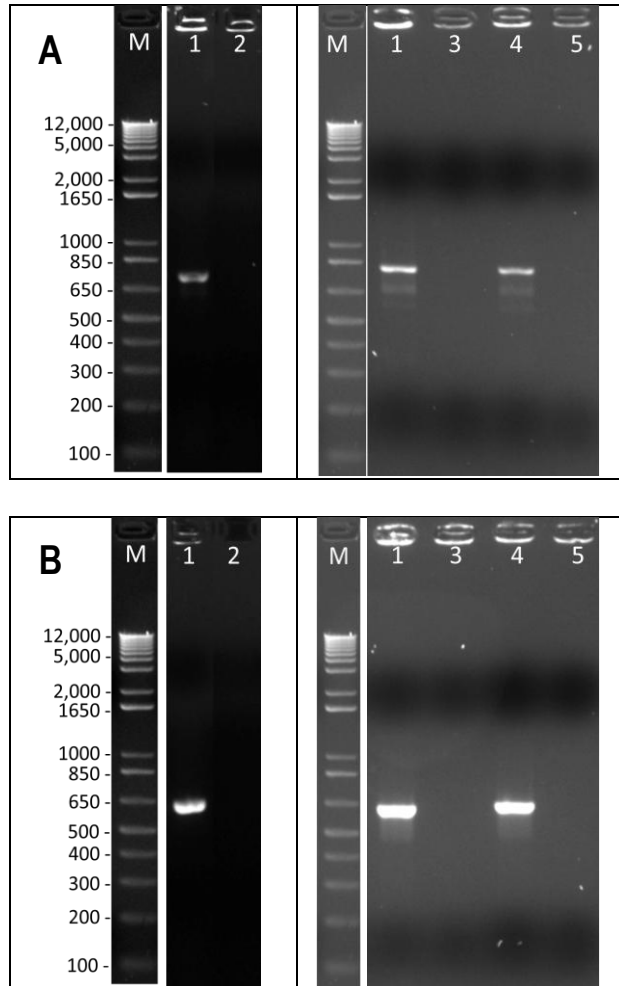


**Figure 58 – Detection of the EAF plasmid by PCR**

Lanes:

- (1) Positive control, wild type strain E2348/69 SS
- (2) Wild type E2348/69 used during this study
- (3) E2348/69 *hosA*<sup>-</sup>, *hosA* deletion mutant derived from E2348/69 in lane (2)
- (4) E2348/69 *bfpA*<sup>-</sup>, contains a single point mutation in *bfpA* but retains the gene
- (5) EAF negative control E2348/69 MAR001
- (M) 1kB+ DNA marker (Invitrogen™)

(A) PCR product for the detection of *bfpA* (705bp in length)

(B) PCR product for the detection of *perA* (652bp in length)

The PCR product generated for *perA* was 652bp in length and was present in both E2348/69 SS and the BfpA mutant (Figure 58B). E2348/69, E2348/69 *hosA*<sup>-</sup> and E2348/69 MAR001 did not contain *perA* (Figure 58B). Thereby, neither E2348/69 nor E2348/69 *hosA*<sup>-</sup> contained the EAF plasmid, confirming both of these strains used during this study had lost the EAF plasmid.

#### **4.2.6 Association Between the EspA Filament and Cell Aggregation in E2348/69**

EspA, encoding a pilin associated with the TTSS, has been linked with intracellular bonds, micro-colony formation and the invasion of host cells by enteropathogenic *E. coli* E2348/69. The effect of EspA on aggregation and the role of AHLs in this phenotype in E2348/69 were investigated. The strain used for this study, E2348/69 *espA*<sup>-</sup>, retained the EAF plasmid and *bfpA* and is therefore was still able to produce bundlin protein filaments.

In the absence of AHL, E2348/69 *espA*<sup>-</sup> produced a clearly defined area of motility measuring on average  $19.4 \pm 1.43$ mm in diameter at 25°C (Table 31; Figure 59). Addition of *N*-(3-oxohexanoyl)-L-HSL significantly decreased the diameter of the motility zone to an average of  $16.7 \pm 1.49$ mm ( $F = 17.04$ ;  $p = <0.001$ ) (Table 31; Figure 59). Addition of *N*-dodecanoyl-L-HSL, *N*-(3-oxo-hexanoyl)-D-HSL and *N*-(3-oxododecanoyl)-D-HSL had no significant effect on the population expansion of E2348/69 *espA*<sup>-</sup> (Table 31; Figure 59).

Phase contrast microscopy confirmed E2348/69 *espA*<sup>-</sup> produced small aggregates with a high proportion of planktonic cells in the absence of AHL. This phenotype was similar to that observed for the EAF-negative wild type E2348/69 (Figure 60A). In the presence of *N*-dodecanoyl-L-HSL, *N*-(3-oxo-hexanoyl)-D-HSL and *N*-(3-oxododecanoyl)-D-HSL no significant changes in the size of the aggregates were observed (Figure 60B). Addition of *N*-(3-oxohexanoyl)-L-HSL appeared to significantly increase aggregation in E2348/69 *espA*<sup>-</sup> to levels similar to that observed in wild type E2348/69 (Figure 60B).



**Table 31 – Statistical analysis of the effect of AHL on E2348/69 *espA*<sup>-</sup> population expansion at 25°C**

Side chain lengths of the AHLs are provided in brackets.

	Average diameter of motility ring $\pm$ 1 standard deviation (mm)	ANOVA	
		*F-value	p-value
No AHL	19.4 $\pm$ 1.43		
<i>N</i> -(3-oxo-hexanoyl)-D-HSL (C6)	18.2 $\pm$ 1.99	2.4	0.139
<i>N</i> -(3-oxododecanoyl)-D-HSL (C12)	18.6 $\pm$ 1.71	1.286	0.272
<i>N</i> -(3-oxohexanoyl)-L-HSL (C6)	16.7 $\pm$ 1.49	17.04	0.000631
<i>N</i> -dodecanoyl-L-HSL (C12)	18.1 $\pm$ 1.79	3.216	0.089

\*F- critical value = 4.414

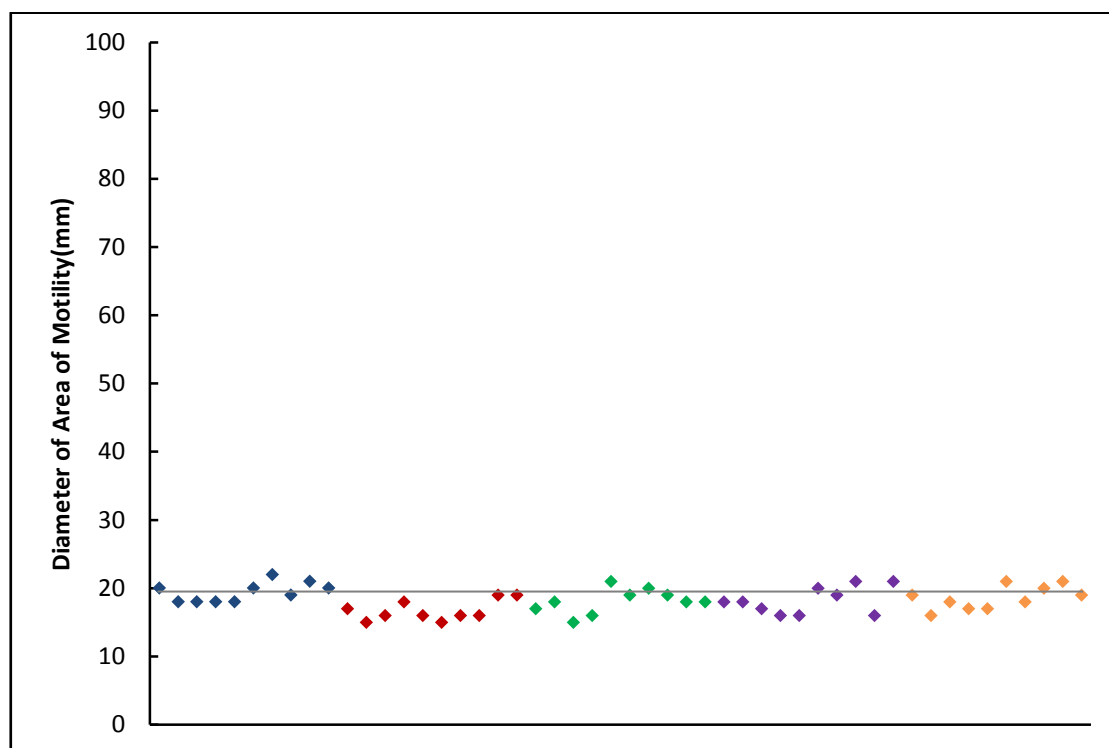


**Figure 59 –Variation in the diameter of the motility zones produced by E2348/69 *espA*<sup>-</sup> in the presence and absence of different AHLs at 25°C**

For each of the 2 independent biological replicates, 5 technical replicates were analysed. Each point on the graph represents one technical replicate. Petri dishes measured 95 mm in diameter.

(Blue) No AHL

(Red) *N*-(3-oxo-hexanoyl)-L-HSL

(Green) *N*-dodecanoyl-L-HSL

(Purple) *N*-(3-oxo-hexanoyl)-D-HSL

(Orange) *N*-(3-oxo-dodecanoyl)-D-HSL

The grey line represents the average diameter of the motility zones measured for the unsupplemented isolates.

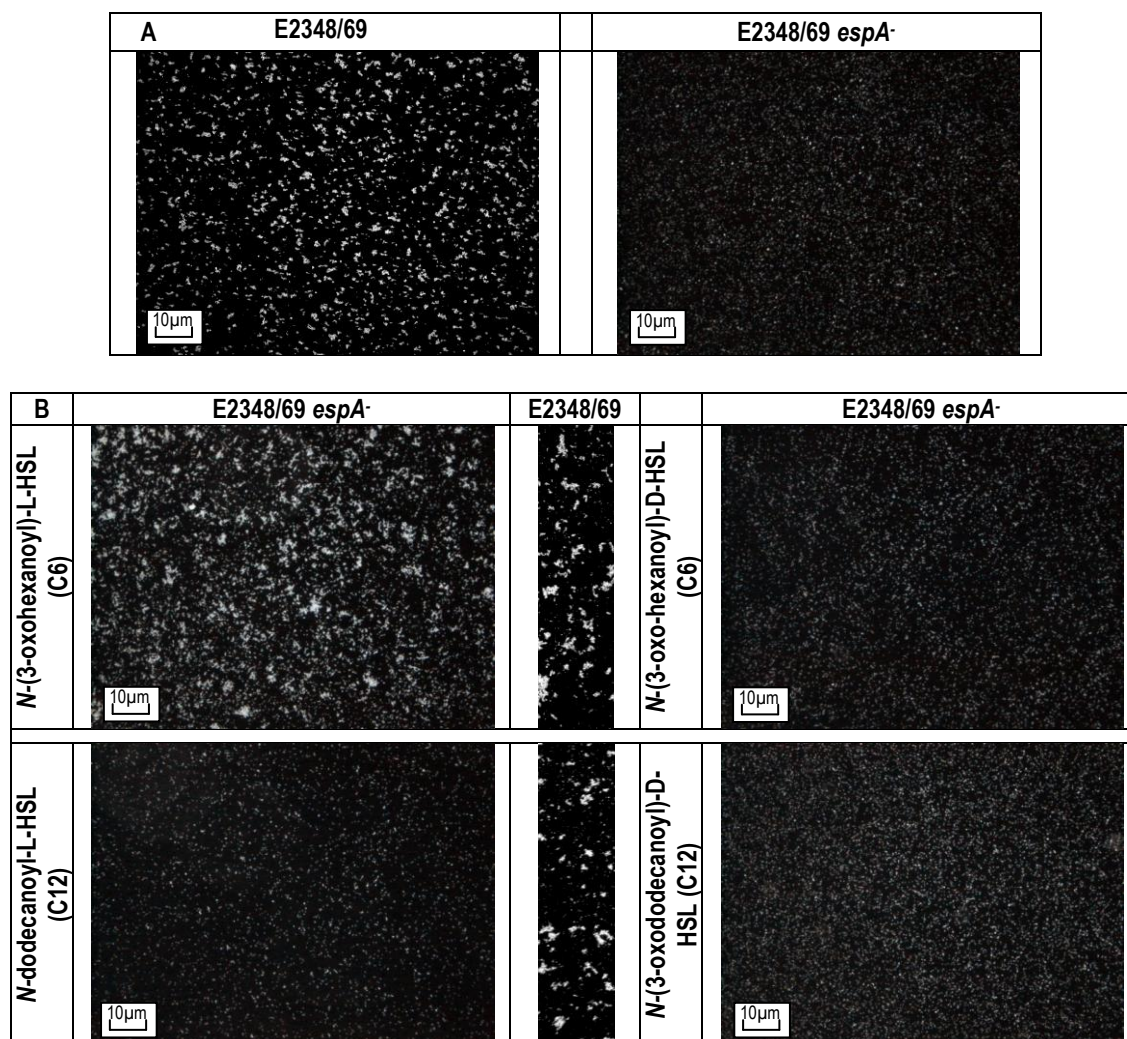


**Figure 60 – Aggregates formed by E2348/69 *espA*<sup>-</sup> in the presence and absence of AHL**

Microscopy images were taken at 100x magnification phase contrast microscopy after 5 hours incubation. Images are representative of 2 independent biological replicates, each with 6 technical replicates.

(A) Comparison of the aggregates produced by wild type E2348/69 with E2348/69 *espA*<sup>-</sup> in the absence of supplements.

(B) Effect of AHL on the size of the aggregates formed by E2348/69 *espA*<sup>-</sup>. Supplementation was completed at 4 hours incubation to a final concentration of 5nM. A representative cross-section of the aggregates formed by wild type E2348/69 in the presence of the same AHL is provided.

Scale bars are indicated in the left hand corner of each image, and set to 10µm.

Analysis of the aggregation profile confirmed that in the absence of AHL the EspA mutant formed small aggregates with a predominance of planktonic cells (Figures 61A and B). Technical variation between replicates of the same culture was calculated at  $D = 0.11$  (Table 32). Biological variation between cultures was calculated at  $D = 0.22$  (Table 32).

Addition of *N*-(3-oxohexanoyl)-L-HSL significantly increased the aggregation of E2348/69 *espA*<sup>-</sup> in both cultures A and B ( $D = 0.79$  and  $D = 0.69$  respectively) when compared to that produced in the absence of AHL (Table 32; Figures 61A and B). Biological variation was calculated at  $D = 0.06$ , meaning the increase in aggregation to  $D = 0.72$  was not as a result of biological variance (Table 32).

Addition of *N*-dodecanoyl-L-HSL had no significant effect on the aggregation profile of E2348/69 *espA*<sup>-</sup> ( $D = 0.02$ ) (Table 32; Figure 61A and B). Neither *N*-(3-oxo-hexanoyl)-D-HSL nor *N*-(3-oxododecanoyl)-D-HSL had a significant effect on the aggregation of E2348/69 *espA*<sup>-</sup> at 25°C ( $D = 0.04$  and  $D = 0.07$  respectively) (Table 33; Figures 62A and B).

#### **4.2.7 Effect of AHL on the Formation of Attaching-effacing Lesions by E2348/69 and E2348/69-derived strains**

Cell surface proteins of enteropathogenic *E. coli* are involved with the formation of attaching-effacing (A/E) lesions on mammalian cells. Using FITC-phalloidin it was possible to stain the actin of the mammalian cells to visualise these pedestals. An individual bacterium was located at the centre of each pedestal. To determine whether the ability of E2348/69 to form aggregates affected the propensity of the bacteria to form A/E lesions, the FAS test was performed in the presence and absence of AHL. For the purposes of this study human colonic cell-line HT-29 was used to produce the eukaryotic monolayer. We hypothesised that more aggregative cultures would produce a higher number of A/E lesions on the human cells.

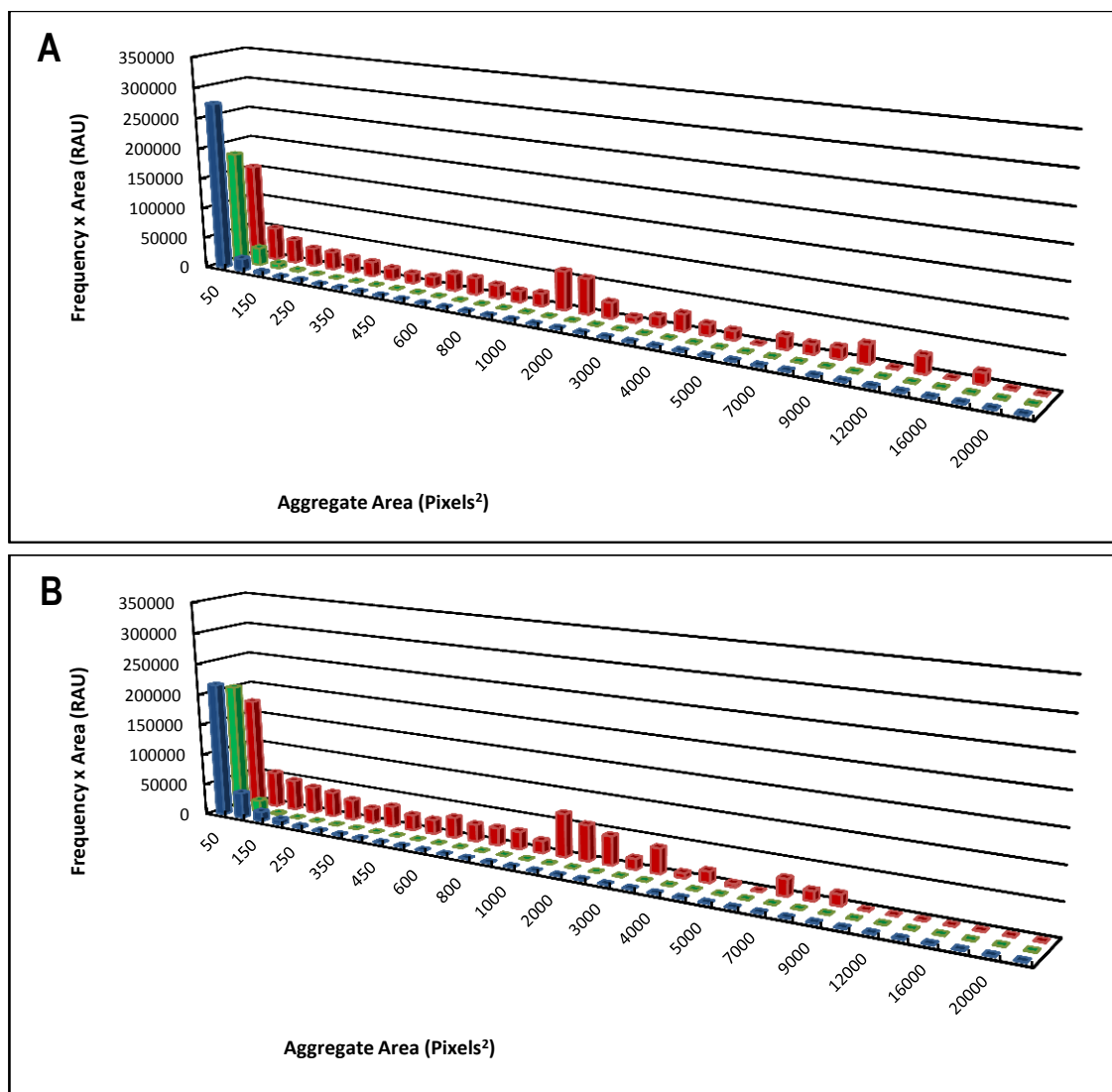


**Figure 61 – Aggregation profile of E2348/69 *espA*<sup>-</sup> in the presence and absence of *N*-(3-oxohexanoyl)-L-HSL and *N*-dodecanoyl-L-HSL at 25°C**

Each profile is representative of the distribution of aggregate sizes produced by E2348/69 *espA*<sup>-</sup> in the presence and absence of *N*-(3-oxohexanoyl)-L-HSL and *N*-dodecanoyl-L-HSL. AHLs were added at 4 hours growth to a final concentration of 5nM. The images analysed were represented in Figure 61.

(A) Culture A; and (B) Culture B

(Blue) E2348/69 *espA*<sup>-</sup> with no AHL

(Red) E2348/69 *espA*<sup>-</sup> in the presence of *N*-(3-oxohexanoyl)-L-HSL

(Green) E2348/69 *espA*<sup>-</sup> in the presence of *N*-dodecanoyl-L-HSL

**Table 32 – Statistical analysis of the effect of active AHL on E2348/69 *espA*<sup>-</sup> aggregation**

Biological variation compares profiles between cultures independent A and B; technical variation compares the profiles within a culture. Where  $D < 0.4$  there is no significant difference between the profiles of the given treatments, but where  $D \geq 0.4$  the difference is deemed to be significant.

	Biological Variation (A vs B)		Technical Variation	
E2348/69 <i>espA</i> <sup>-</sup>	0.22		0.11	
	A	B	Biological Variation (A vs B)	Unsupplemented vs Supplemented
<i>N</i> -(3-oxohexanoyl)-L-HSL (C6)	0.79	0.69	0.06	0.72
<i>N</i> -dodecanoyl-L-HSL (C12)	0.15	0.07	0.03	0.02

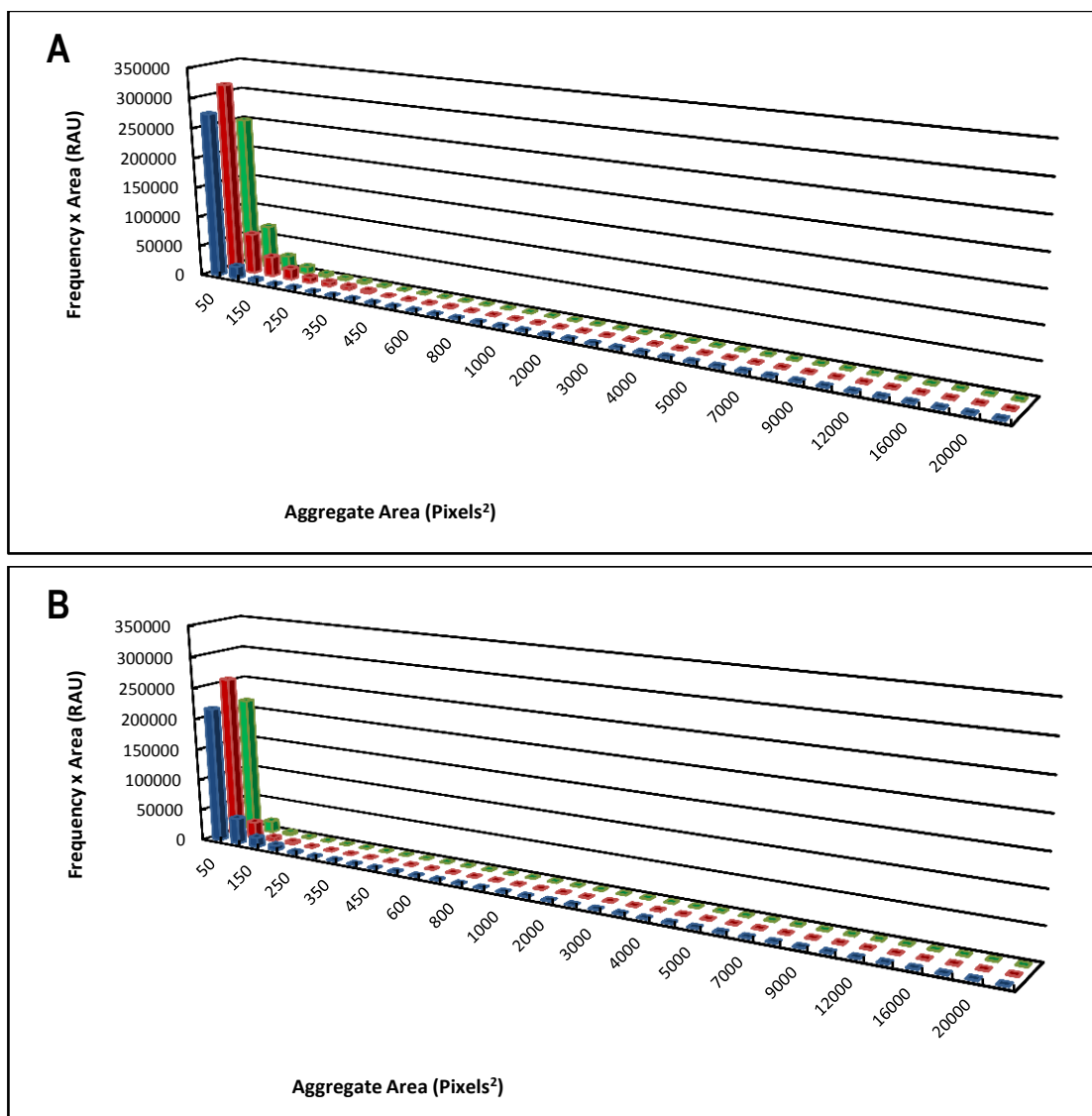


**Figure 62 – Aggregation profile of E2348/69 *espA*<sup>-</sup> in the presence and absence of *N*-(3-oxo-hexanoyl)-D-HSL and *N*-(3-oxododecanoyl)-D-HSL at 25°C**

Each profile is representative of the distribution of aggregate sizes produced by E2348/69 *espA*<sup>-</sup> in the presence and absence of *N*-(3-oxo-hexanoyl)-D-HSL and *N*-(3-oxododecanoyl)-D-HSL. AHLs were added at 4 hours growth to a final concentration of 5nM. The images analysed were represented in Figure 61.

(A) Culture A; and (B) Culture B

(Blue) E2348/69 *espA*<sup>-</sup> with no AHL

(Red) E2348/69 *espA*<sup>-</sup> in the presence of *N*-(3-oxo-hexanoyl)-D-HSL

(Green) E2348/69 *espA*<sup>-</sup> in the presence of *N*-(3-oxododecanoyl)-D-HSL

**Table 33 – Statistical analysis of the effect of *D*-isomers on E2348/69 *espA*<sup>-</sup> aggregation**

Biological variation compares profiles between cultures independent A and B; technical variation compares the profiles within a culture. Where  $D < 0.4$  there is no significant difference between the profiles of the given treatments, but where  $D \geq 0.4$  the difference is deemed to be significant.

	Biological Variation (A vs B)			Technical Variation	
E2348/69 <i>espA</i> <sup>-</sup>	0.22			0.11	
	A		B	Biological Variation (A vs B)	Unsupplemented vs Supplemented
<i>N</i> -(3-oxo-hexanoyl)-D-HSL (C6)	0.23		0.07	0.07	0.04
<i>N</i> -(3-oxododecanoyl)-D-HSL (C12)	0.15		0.07	0.13	0.07

Furthermore, we hypothesised that where addition of AHL changed the aggregative behaviour of the population, a corresponding change would be observed in the A/E lesion formation.

In the absence of bacterial culture, HT-29 cells were outlined faintly in green, with no intense areas of fluorescence (Figure 63). Addition of *N*-(3-oxohexanoyl)-L-HSL and *N*-dodecanoyl-L-HSL at a final concentration of 5nM, or ethyl acetate at 0.1% (v/v) had no effect on the fluorescence observed in the absence of bacteria (Figure 63).

E2348/69 produced a high number of A/E lesions on HT-29 cells in all biological replicates analysed (Figure 64). No obvious change in the quantity of A/E lesions formed was observed with the addition of *N*-(3-oxohexanoyl)-L-HSL and *N*-dodecanoyl-L-HSL (Figure 64).

Although important for localised adherence of EPEC to host epithelial cells, using the FAS test we showed that in the absence of BfpA, E2348/69 was able to form A/E lesions on HT-29 cells (Figure 65). The absence of Bfp resulted in a significant decrease in the observed number of A/E lesions formed by E2348/69, which was in the order of 100 fold less (Figure 65).

AE2348/69 *luxS*<sup>-</sup> showed areas of intense fluorescence, but the characteristic pedestal structure was not visible. Previous work by S. Snape had shown AE2348/69 *luxS*<sup>-</sup> did produce pedestals, but these were often masked by high density micro-colonies [232]. Intense green fluorescence indicated actin cytoskeleton rearrangements in the HT-29 cells, showing AE2348/69 *luxS*<sup>-</sup> successfully attached to the epithelial cells. When compared to the wildtype, a higher frequency of fluorescent colonies were observed (Figure 66A). AE2348/69 *luxS*<sup>-</sup> contained the EAF plasmid and therefore *bfpA*, so conclusive comparisons between the LuxS mutant and the wild type strain of E2348/69 used in this study cannot be drawn from this data. With addition of *N*-(3-oxohexanoyl)-L-HSL or *N*-dodecanoyl-L-HSL the number of intense fluorescent spots appeared to decrease (Figure 66B).

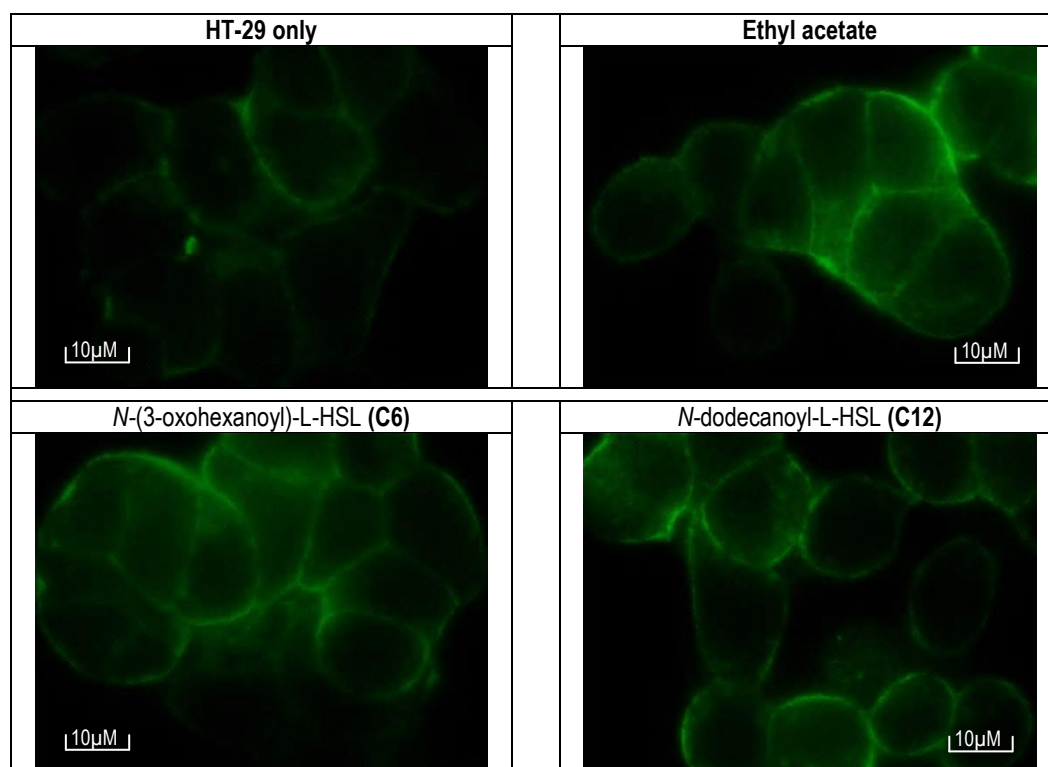


**Figure 63 – FITC-Phalloidin staining of HT-29 cells in the presence and absence of AHL and solvent**

Representative images of the negative controls used for all assays investigating attaching/effacing lesions formation (Figures 64-67).

AHLs were added to the growth medium to a final concentration of 5nM, with an equivalent volume of ethyl acetate added to a separate sample to provide a negative control for the effect of AHL and the solvent used to dilute the signals. HT-29 cells were treated with FITC-Phalloidin to show the background staining of epithelial cells that do not have bacteria attached.

Scale bars are indicated in the corner of each image, and set to 10µm.

Using Microsoft Word the brightness of each image has been increased by 30%.



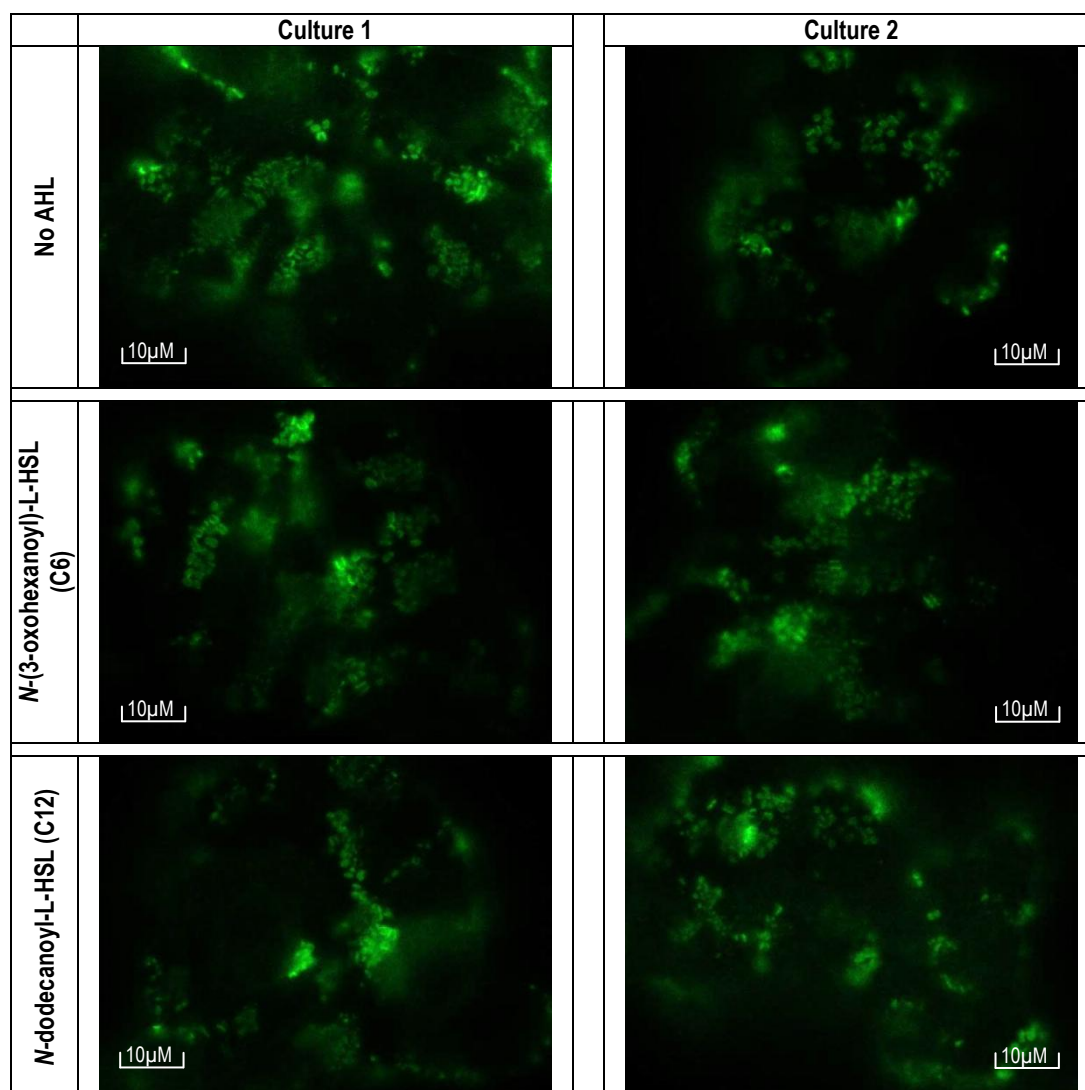


**Figure 64 – A/E lesion formation by E2348/69 in the presence and absence of AHLs**

FITC-Phalloidin attached to actin within the HT-29 cells creating green fluorescence where attaching/effacing lesions are located. Each image was taken at 1000x magnification using fluorescence microscopy.

Culture 1 and culture 2 represent independent bacterial cultures used to inoculate 1 well containing HT-29 cells. Within each well were 3 coverslips, and for each coverslip a representative 3 images were taken as technical replicates. Images are representative of the patterns of A/E lesion formation for all technical replicates.

Supplementation of the cultures with AHL was completed to a final concentration of 5nM prior to inoculation onto the HT-29 cells.

Scale bars are indicated in the corner of each image, and set to 10µm.

Using Microsoft Word the brightness of each image has been increased by 30%.



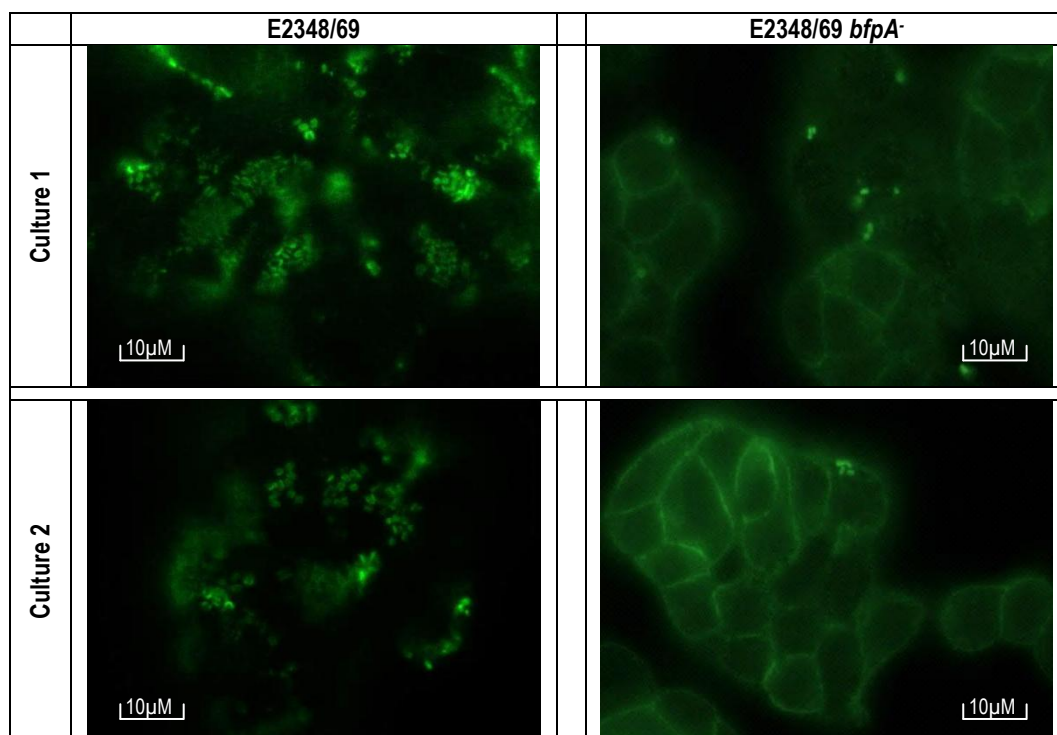


**Figure 65 – Comparison of A/E lesion formation by E2348/69 and E2348/69 *bfpA*<sup>-</sup>**

FITC-Phalloidin attached to actin within the HT-29 cells creating green fluorescence where attaching/effacing lesions are located. Each image was taken at 1000x magnification using fluorescence microscopy.

Culture 1 and culture 2 represent independent bacterial cultures used to inoculate 1 well containing HT-29 cells. Within each well were 3 coverslips, and for each coverslip a representative 3 images were taken as technical replicates. Images are representative of the patterns of A/E lesion formation for all technical replicates.

Scale bars are indicated in the corner of each image, and set to 10µm.

Using Microsoft Word the brightness of each image has been increased by 30%.

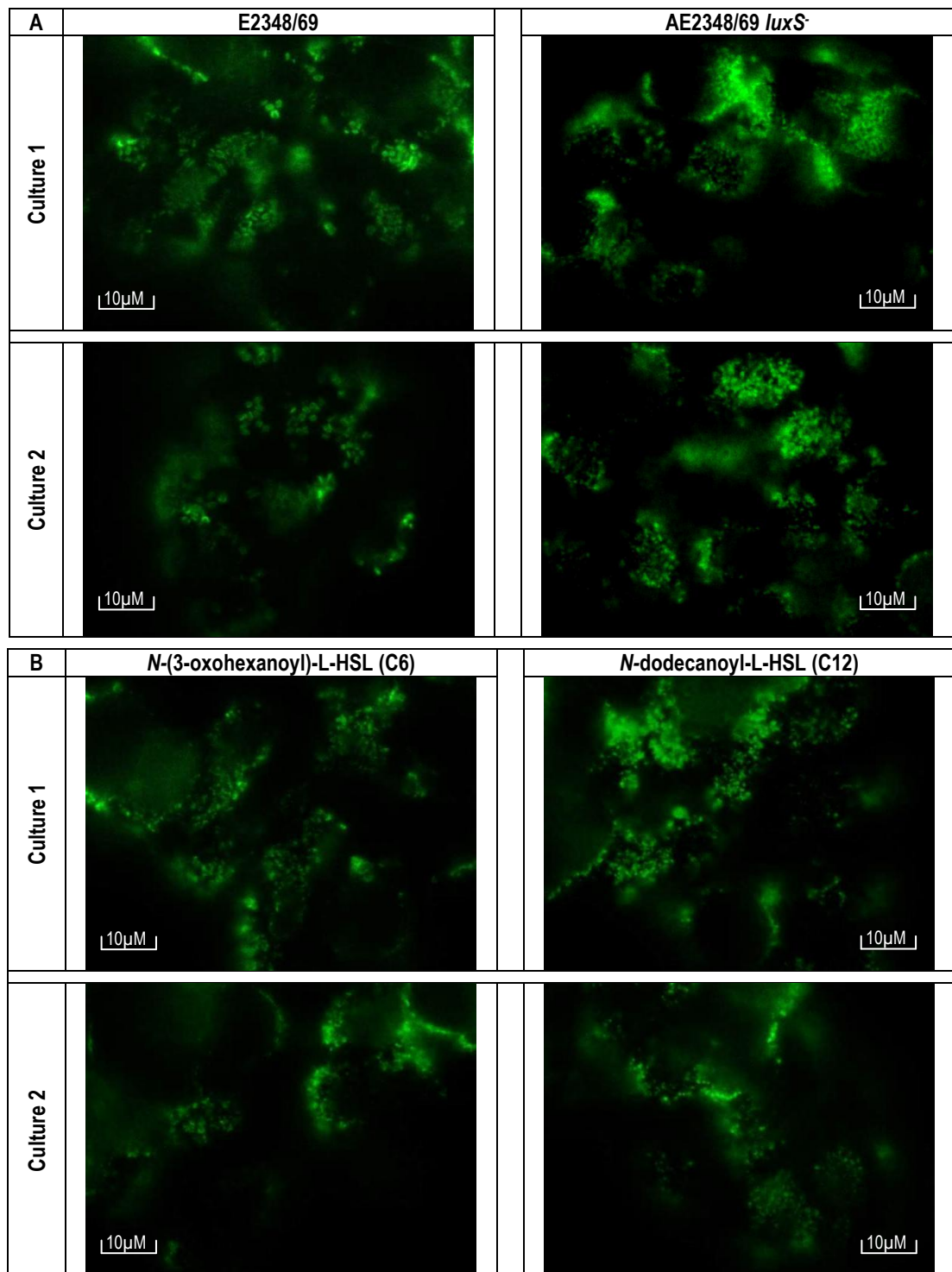


**Figure 66 – A/E lesion formation by AE2348/69 *luxS*<sup>-</sup> in the presence and absence of AHLs**  
 FITC-Phalloidin attached to actin within the HT-29 cells creating green fluorescence where attaching/effacing lesions are located. Each image was taken at 1000x magnification using fluorescence microscopy.  
 Culture 1 and culture 2 represent independent bacterial cultures used to inoculate 1 well containing HT-29 cells. Within each well were 3 coverslips, and for each coverslip a representative 3 images were taken as technical replicates. Images are representative of the patterns of A/E lesion formation for all technical replicates.  
 (A) Comparison of the A/E lesions formed by wild type E2348/69 and AE2348/69 *luxS*<sup>-</sup>  
 (B) Effect of active AHL on the formation of A/E lesions by AE2348/69 *luxS*<sup>-</sup>. Supplementation of the cultures with AHL was completed to a final concentration of 5nM prior to inoculation onto the HT-29 cells.  
 Scale bars are indicated in the corner of each image, and set to 10µm.  
 Using Microsoft Word the brightness of each image has been increased by 30%.

E2348/69 *hosA*<sup>-</sup> produced a high number of A/E lesions in the absence of AHL, which appeared similar to the parental E2348/69 (Figure 67A). Addition of *N*-(3-oxohexanoyl)-L-HSL or *N*-dodecanoyl-L-HSL had no significant effect on the number of pedestals formed by the *HosA* mutant (Figure 67B).

### **4.3 Discussion**

Bacterial aggregation has a negative effect on population expansion, and the evidence presented in this study confirmed that wild type E2348/69 formed aggregates in response to quorum sensing cues (Section 3.2.5) [68]. The formation of aggregates is important for bacterial pathogenesis as it increases the potential for colonisation and persistence within a host. If within an aggregate, the probability for successful colonisation increases and the potential for overwhelming the host immune system rises [2-4, 6].

Enteropathogenic *E. coli* colonise the mucosa of the small intestine of a human host. Successful colonisation and persistence in an environment of constant movement relies upon the production of attaching-effacing (A/E) lesions, which anchor the bacterial micro-colony to the epithelial cells. This process uses secreted proteins to form intimate attachments to and subvert the cytoskeleton of the host cell to form bacterial cradles [4, 6, 34, 55, 56]. A by-product of A/E lesions is damage to the microvilli and the loss of surface area, resulting in a loss of absorptive capacity and diarrhoea [4, 6, 24, 64]. Once attached, the bacteria can replicate, thereby increasing the population within a localised area [4, 6]. Furthermore, E2348/69 is known to form bacteria-bacteria interactions, producing aggregates over the A/E lesions, which are often described as rafts or micro-colonies [21, 22, 82, 83]. Micro-colonies of E2348/69 would increase the potential for further production of A/E lesions. Regulation of aggregation by exogenous AHL confirmed in this study suggested these cues may be important in the formation of A/E lesions.

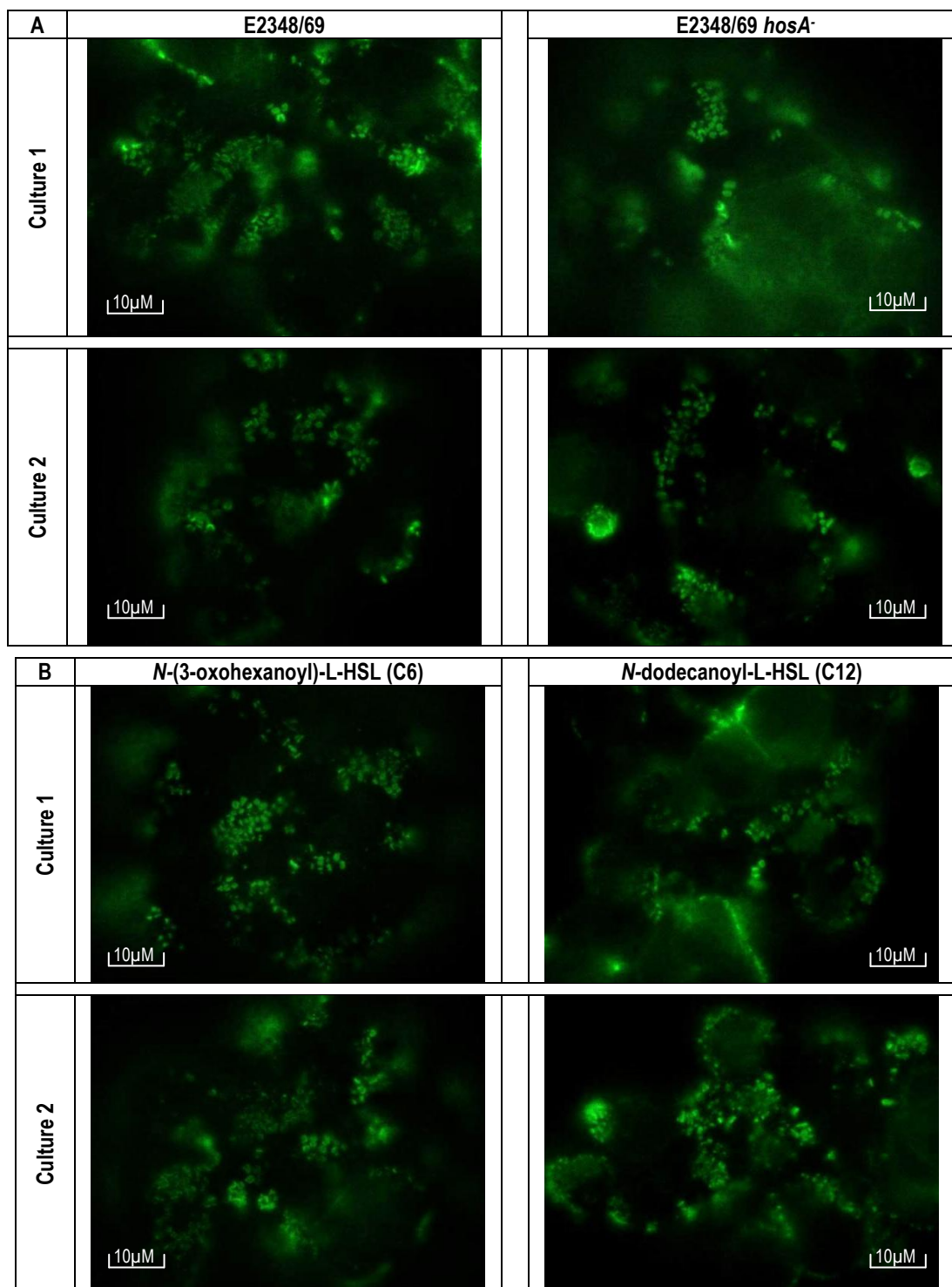


**Figure 67 – A/E lesion formation by E2348/69 *hosA*<sup>-</sup> in the presence and absence of AHLs**

FITC-Phalloidin attached to actin within the HT-29 cells creating green fluorescence where attaching/effacing lesions are located. Each image was taken at 1000x magnification using fluorescence microscopy.

Culture 1 and culture 2 represent independent bacterial cultures used to inoculate 1 well containing HT-29 cells. Within each well were 3 coverslips, and for each coverslip a representative 3 images were taken as technical replicates. Images are representative of the patterns of A/E lesion formation for all technical replicates.

(A) Comparison of the A/E lesions formed by wild type E2348/69 and E2348/69 *hosA*<sup>-</sup>

(B) Effect of active AHL on the formation of A/E lesions by E2348/69 *hosA*<sup>-</sup>. Supplementation of the cultures with AHL was completed to a final concentration of 5nM prior to inoculation onto the HT-29 cells.

Scale bars are indicated in the corner of each image, and set to 10µm.

Using Microsoft Word the brightness of each image has been increased by 30%.

By increasing the propensity of the population to form lesions, the bacterium would become more pathogenic to the host [4, 6, 13, 14, 52-54]. Using the FAS assay, the ability of the wild type to form A/E lesions was investigated. In the absence of quorum sensing cues the wild type E2348/69 formed a high number of clustered lesions, characterised by intense green fluorescence, and a molar tooth morphology (Figure 64). Within each of these individual bright spots of fluorescence a single bacterium was intimately attached to the human colonic HT-29 cell line. The lesions were located in clusters, and were rarely observed as separate entities.

The initial working hypothesis was that by increasing the rate of bacterial cell aggregation within a given population, the number of lesions produced would increase. Due to the 3-dimensional nature of the HT-29 monolayer, quantification of the number of lesions was not possible, and thereby only subjective observations were able to be made. Although other human colorectal cell lines such as Caco-2 were available, the decision to use HT-29 cells was made based on their use in previous studies with EPEC. The attachment experiments completed during this study were included to identify any obvious and significant changes in the production of A/E lesions. Further work using different staining methods, such as combining FITC-Phalloidin with DAPI, in addition to the use of multiple cell lines and confocal microscopy allowing production of 3-dimensional images may improve the definition of the images and allow more defined conclusions to be drawn.

The second hypothesis stated that where an AHL increased the aggregative behaviour of the population, a correlating increase in the production of A/E lesions would be observed. Unfortunately, addition of either *N*-(3-oxohexanoyl)-L-HSL or *N*-dodecanoyl-L-HSL to E2348/69 appeared to have no significant effect on the distribution or morphology of the A/E lesions (Figure 64). This does not necessarily mean there was no difference, but more quantitative techniques such as flow cytometry need to be used to conclusively determine a change in the levels of fluorescence.

The EspA filament is essential in the formation of A/E lesions forming the pilus used to translocate the secreted proteins from the bacterium into the host cells [6, 14, 53, 55-58]. Despite the presence of the EAF plasmid and *bfpA* allowing localised adherence of the bacteria to the epithelial cells, deletion of EspA resulted in the bacteria being unable to form the characteristic pedestals on the HT-29 cells [57, 231]. This evidence illustrates the importance of this protein in the pathogenicity and persistence of E2348/69. As was expected deletion of *espA* had no effect on the population expansion. The protein is known to be important in cell to cell interactions, but the evidence presented in this study confirmed this to be between host and bacteria. Interestingly, addition of the short chain signal *N*-(3-oxohexanoyl)-L-HSL significantly increased the aggregation of the EspA mutant to a level similar to that observed in the parent, but the long chained *N*-dodecanoyl-L-HSL had no effect. In chapter 3 it was hypothesised that the two AHLs, due to the differences in structure, may activate different transcriptional regulators which would control different genes within a larger interconnected quorum sensing regulon. The change in aggregation in E2348/69 *espA*<sup>-</sup> in the presence of *N*-(3-oxohexanoyl)-L-HSL, which is similar to that observed for the parental E2348/69, further highlights this difference and suggests that specific AHLs may potentially have an effect on EspA expression.

Several studies have highlighted the importance of pili in the formation of intimate attachments and A/E lesions by E2348/69 [13, 14, 52, 54, 57, 59, 64, 82, 83, 208, 231, 261, 267, 268]. There are several types of pili in EPEC, such as bundle forming pili (Bfp) and curli, both of which have been associated with aggregation and pathogenicity [13, 14, 52, 54, 57, 82, 83, 88, 89, 170, 260, 261, 268]. The effects of AHL on curli expression were inconclusive. While changes in colony pigmentation and the diameter of the pigmented halo were observed qualitatively, further investigation using quantifiable techniques such as qPCR would be required before any conclusions could be drawn on the role of AHL in these observed changes in

expression. High definition microscopy, such as electron microscopy coupled with specific staining of the curli fibrils would allow clearly defined observations to be made.

Bfp are specific to EPEC, encoded on the EAF plasmid [4, 6, 13, 14, 54, 57, 64, 83, 261, 268]. They are long peritrichous filaments which form a complex matrix between the bacteria, forming the micro-colonies characteristic of an E2348/69 infection [4, 6, 13, 14, 54, 57, 64, 83, 261, 268]. The absence of Bfp has been associated with a reduction in pathogenicity in some studies [14, 52, 54, 261]. The evidence provided in this study showed that where E2348/69 was unable to produce BfpA the population did not aggregate which had a positive effect on population expansion almost tripling the size of the motility zone. This correlated with a decrease in the ability to form A/E lesions (Figure 65). This relationship between aggregation and population expansion suggested that BfpA was an important factor in cell aggregation, and that by rendering it inactive the pathogenicity of the bacterium was decreased. However, this did not agree with the other observations made during this study. The E2348/69 wild type isolate used for all the assays performed in this study did not contain the EAF plasmid, and yet produced a high number of A/E lesions and was able to aggregate under quorum sensing regulation. These phenotypes were confirmed using E2348/69 MAR001, which also lacks the EAF plasmid and had been used as an EAF-negative control in other studies [232]. These results therefore suggest that where BfpA is non-functional but the rest of the EAF plasmid is intact, regulators such as Per, encoded on the plasmid, may regulate cell aggregation and thereby population motility independent of quorum sensing.

Bacteria adapt rapidly to laboratory conditions, losing pathogenicity phenotypes not required to grow under these conditions. Lab adaptation leads to the production of spontaneous mutations in bacterial cultures. The bacterial genome is constantly changing with prolonged growth and repeated subculturing allowing mutation to develop and persist within a population. During this project, in order to reduce the probability of persistent mutations within the bacterial

populations, repeated subculturing was not used, relying instead on fresh cultures recovered from the -80°C storage. Manipulation of bacterial chromosomal DNA is a common tool used in scientific research. The production of deletion, substitution or insertion mutations allows scientists to monitor the effect of specific genes on bacterial behaviour and survival. As with many techniques, there are problems associated with the production and maintenance of these genetically modified organisms. During production, as occurred with the strain of E2348/69, other genetic material, which is not associated with the region of DNA being manipulated, can be affected. In this case, during deletion of *hosA*, the EAF plasmid was lost resulting in a strain of typical EPEC becoming more characteristic of atypical EPEC strains. While this provided a unique opportunity to monitor phenotypic changes in a type of EPEC which is dominating infections in the developed world, it also increased the complexity of any conclusions drawn.

In chapter 3 a hierarchical system of regulation of cell aggregation in E2348/69 was suggested linking quorum sensing with the environmental stress regulator, HosA. In the absence of HosA cell aggregation increased in comparison to the parental, but the ability to clump was regulated by quorum sensing in both strains. Both wild type and the HosA mutant lacked the EAF plasmid. In comparison, in E2348/69 *bfpA*<sup>-</sup> and E2348/69 *espA*<sup>-</sup> where the EAF plasmid was present, no cell aggregation was observed and addition of quorum sensing signals had no significant effect on the phenotype. This suggests that where the EAF plasmid is present cell aggregation may be regulated by Per, which overwhelms any additional regulation by quorum sensing. It would be interesting to determine if a link existed between Per and HosA by restoring the EAF plasmid to E2348/69 *hosA*<sup>-</sup> and analysing changes in cell aggregation.

Having determined that the absence of the EAF plasmid increased the propensity of the bacteria to form aggregates, the identity of the quorum sensing regulon in the EAF negative isolates was investigated further. E2348/69 has the serotype O127:H6, and has been used as a



virulence model for enterohaemorrhagic *E. coli* O157:H7. This is possible as both serotypes were derived from the same progenitor strain and have a high level of genetic homology [15, 63, 269]. The related EHEC strain *E. coli* O157:H7 does not contain the EAF plasmid. It was therefore important to identify the quorum sensing regulon associated with aggregation in the EAF-negative E2348/69 isolate used during this study, as it may be conserved across the pathotypes.

A number of cell surface components have been associated with cell aggregation in other bacteria [13, 14, 69, 70, 79, 80, 157, 260]. Polysaccharides such as exopolysaccharides and cellulose are important in providing the bacterium with protection from enzymatic activity, whilst increasing the adhesive characteristics of the cell surface. Addition of glucose to standard agar resulted in increased production of exopolysaccharide, changing the colony morphology to be more mucoid. This is characterised by thicker more sticky colonies which have a glossy appearance. The colonies also tended to be larger and flatter in the presence of glucose. Addition of AHL had no effect on the morphology of these colonies. Uronic acid and colanic acid are components of the *E. coli* exopolysaccharide capsule. During this study differences were observed between the AHL-supplemented broth cultures of aggregating cells and those with no AHL. The concentrations of uronic acid calculated for the two biological replicates were highly variable, thereby increasing the uncertainty behind any conclusions drawn. Given the amount of variation these experiments lacked the statistical power required to test specific hypotheses and would need multiple repeat experiments with more technical and biological replicates before any conclusions could be drawn. Further investigations comparing the concentrations within planktonic with aggregating cells would also be required to monitor changes in uronic acid concentration. It would also be interesting to investigate the link between temperature and quorum sensing regulation regarding exopolysaccharide and uronic acid expression, in order to confirm these as part of the QS regulon.

Antigen 43 has been shown to play an important role in aggregation in *E. coli*. Both AHL-supplemented and unsupplemented cultures of E2348/69 and E2348/69 *hosA*<sup>-</sup> were susceptible to hydrogen peroxide, indicating antigen 43 was not being expressed under the experimental conditions used in this study. The technique used was simple and easy to replicate, but more quantifiable methods such as qPCR for antigen 43 motifs or an immunoblot with specific labelled antibodies would provide more conclusive data on the effect of exogenous AHL on the expression of this protein.

Rowe *et al* identified cellulose as an important factor in cell aggregation and pathogenicity of uropathogenic *E. coli*, strain 536 [79]. This strain of *E. coli* formed very large aggregates which were visible to the eye when grown in Roswell Park Memorial Institute (RPMI-1640) medium at 37°C, which were difficult to disperse requiring the addition of sodium chloride and intensive vortexing. By comparison the aggregates formed by enteropathogenic *E. coli* E2348/69 in LB at 25°C were weaker in nature. The effect of different media on aggregation was investigated during this study, using RPMI-1640, DMEM and Brain Heart Infusion (BHI) media. In this study, growth of E2348/69 in these media did not stimulate any aggregation, thus LB was used to monitor changes at 25°C. In order to completely disperse the aggregates during this study addition of sodium chloride was required, with at least 5 minutes high speed vortexing. However, it was observed that with the larger aggregates, slight agitation of the tube was sufficient to break them down into smaller constitutive parts. Low levels of cellulose were expressed by aggregating cells of both E2348/69 and E2348/69 *hosA*<sup>-</sup>, indicating it was unlikely that this component would be important in the cell aggregation (Figure 45).

However, interesting changes in the physical characteristics of the aggregates formed by E2348/69 were observed in AE2348/69 *luxS*<sup>-</sup>. *E. coli* encode two quorum sensing systems; the AHL/SdiA and AI-2/LuxS systems. By deleting LuxS and removing the ability to produce AI-2 a

quorum sensing -negative background can be produced. In the absence of any QS signal, the population expansion of E2348/69 was significantly reduced, which correlated with a significant increase in cell aggregation. The function of AI-2 in *E. coli* could be described as a controversial subject, with some scientists arguing a mainly metabolic function and others a major quorum sensing role. While it is true that AI-2 has been shown to be an important QS cue in species such as *Vibrio harveyi* and *Vibrio fischeri*, where it is responsible for regulating the production of bioluminescence, this is not the case for all bacteria (Section 1.4.4) [183, 184, 198, 202]. In *E. coli*, AI-2 is produced as a metabolic by-product of the activated methyl cycle (AMC) (Section 1.4.1) [94, 98, 194]. The concentration of AI-2 increases during the mid- to late-exponential phase of growth, where the cells are more metabolically active and growing. This links the signal more with growth and cell proliferation, rather than phenotypic switching [98].

The aggregates produced by the LuxS mutant were much stronger in comparison to E2348/69 and E2348/69 *hosA*<sup>-</sup>, and less likely to disperse upon gentle agitation. Addition of sodium chloride and intensive vortexing for extended periods of time was required to disperse the aggregates in the absence of any quorum sensing signal. Addition of AHL decreased the size of the aggregates, but did not affect the strength of the inter-bacterial connections. By comparison, in the presence of a low level of exogenous AI-2 the aggregates not only decreased in size, but the solidity of the clumps was also reduced. It would be interesting to determine whether addition of a higher concentration of AI-2 containing CM could disperse the aggregates completely. The evidence presented here suggests the AHL and AI-2 systems work concurrently to control the cell aggregation of E2348/69. One possible hypothesis is that the AHL system regulates the expression of the cell surface components responsible for the aggregation in E2348/69, whereas the AI-2 system influencing the strength of the bacterial interactions. Further work using techniques such as atomic force microscopy to monitor the strength of the inter-bacterial bonds would be required to confirm or refute this hypothesis.

LuxS has been shown to take part in the regulation of the LEE locus, which encodes the proteins required for intimate attachment and pedestal formation in E2348/69, suggesting AI-2 may be important in this phenotype [58, 208]. Analysis of the pattern of A/E lesion formation in the LuxS mutant that suggested this isolate was unable to form the fluorescence of actin filament network characteristic of successful attachment (Figure 66). However, a study completed by S. Snape showed the LuxS mutant did produce A/E lesions [232]. This observation combined with further analysis of the morphology of fluorescence in this study suggested that the A/E lesions were present, but were masked by high cell density and the formation of dense micro-colonies over the pedestals. Studies have shown that increasing the adhesive nature of the bacteria results in higher levels of cell aggregation and A/E lesion formation [4, 6, 13, 14, 52-54]. The evidence presented in this study suggests that by removing AI-2, the inter-bacterial bonds increase in strength. Using these results, it could be hypothesised that the increase in the density of the micro-colonies by the LuxS mutant would be due to the increase in the strength of the bonds within the aggregate.

A definitive identification of the quorum sensing regulon associated with cell aggregation in E2348/69 in the absence of the EAF plasmid was not possible using the evidence presented in this study. . Although full dispersion was not observed, addition of protease to aggregating cultures of E2348/69 *hosA*<sup>-</sup> reduced the size of the aggregates, suggesting the AHL/SdiA interaction may regulate the transcription of a specific protein. Further investigation using different concentrations of protease, and observing the effects of different incubation times and temperatures may identify whether full dispersal of the aggregates is possible following addition of the enzyme. Lysis of the cells and separation of the total protein content did not identify any significant changes in expression between the cultures grown in the presence of exogenous AHL and the unsupplemented cultures. Further work is required to identify the protein that was affected by the protease during the aggregation experiments. Extraction of secreted proteins

using trichloroacetic acid would identify whether or not the protein was secreted or intrinsic within the bacterium. In addition, further investigation using more complex separation methods such as 2D-PAGE would provide more information about the expression of proteins in both aggregating and planktonic cultures in the presence and absence of exogenous AHL. Mass Spectrometry could be used to identify differentially expressed proteins associated with the phenotypic behaviour.

Quorum sensing regulation of phenotypic traits is complex requiring multiple transcriptional regulators and combining the effects of multiple systems. *Ps. aeruginosa* has been shown to combine multiple AHL systems in a complex regulatory hierarchy [73, 75, 96, 98, 109, 185, 186]. The evidence presented in this study support the hypothesis that the AHL/SdiA and AI-2/LuxS systems function in a similar manner to the hierarchy in *Ps. aeruginosa*, combining the different systems with a collection of transcriptional regulator proteins. As Per was absent from the E2348/69 isolate used during this study, the results and hypotheses provided could be extrapolated to encompass *E. coli* O157:H7, which naturally does not contain EAF and Per.

## **5 Effect of AHL on the Motility and Aggregation of *E. coli* O157:H7**

### **5.1 Introduction**

Enterohaemorrhagic *E. coli* (EHEC) has evolved from a progenitor strain of enteropathogenic *E. coli* (EPEC) [63, 269]. *E. coli* O157:H7 has been identified as having evolved from EPEC strain O55:H7, acquiring *stx* through bacteriophage transduction [269]. Over time the somatic antigen changed from O55 to O157 as a result of acquisition of genes and other mutations [269].

EHEC and EPEC share some pathogenicity mechanisms as a result of a common ancestor, such as the ability to produce attaching-effacing lesions (Section 1.1.4.1). Both pathotypes encode the transcriptional regulator, HosA (Section 1.1.4.2). EPEC is the most studied diarrheagenic pathogen and shares similar mechanisms for adherence to host cells with EHEC, making it possible to use EPEC as a model for virulence of the attaching mechanism.

Cattle are the main animal reservoirs for toxigenic *E. coli* O157:H7 and colonisation is highest in the hindgut (Section 1.1.3). To pass through to the hindgut in cattle the bacteria must go through some complex biological matrices, such as saliva, rumen fluid and intestinal contents. The AHL composition of these matrices and the effect of the signals remain largely unknown. Recent research has shown links between the expression of SdiA, the LuxR homologue to the motility and adherence of *E. coli* O157:H7 *in vitro* [170]. Another study linked the expression of SdiA with the ability of *E. coli* O157:H7 to form intimate attachments with the epithelial cells in a 10-14 day old calf [171].

The aim of this chapter was to determine the effect of specific AHL signals on the phenotypic switching of *E. coli* O157:H7. Using the EPEC model described in chapters 3 and 4 as a basis, the phenotypes investigated were motility, aggregation and the attachment to human cells. The identity of the proteins controlling these phenotypes in *E. coli* O157:H7 was also investigated. The effect of quorum sensing on pathogenicity was performed using an infection model with *Galleria mellonella*. A secondary objective was to identify the AHLs present within

matrices associated with the bovine host that *E. coli* O157:H7 may be exposed to during the lifecycle.

## **5.2 Results**

### **5.2.1 Presence of AHL in Complex Biological Matrices**

AHLs are produced by many gram negative species. Using *Chromobacterium violaceum*, a bioreporter for short chain AHLs, the availability of signal was investigated. *C. violaceum* preferentially binds *N*-hexanoyl-L-HSL and the modified version, *N*-(3-oxohexanoyl-DL-HSL but also has affinity for *N*-octanoyl-L-HSL- and *N*-butanoyl-L-HSL [233, 237]. Violacein is a purple pigment produced by *C. violaceum* in the presence of these short chain AHLs [233, 237]. *C. violaceum* strain CV026 was genetically modified to no longer synthesise AHLs, thereby only produced violacein in response to exogenous AHL.

Psychrotolerant Enterobacteriaceae species such as *Hafnia alvei*, *Rahnella aquatilis* and *Serratia* are common commensals on fresh red meat products. To determine whether these species produced exogenous AHLs, T-streak assays were performed using *C. violaceum* CV026. Incubation at 25°C showed all 3 species produced short chain AHLs able to initiate production of violacein (Figure 68A-C). This was confirmed using the plate motility assay (Figure 68D). *Ps. aeruginosa* is known to produce short chain AHL, however no pigment was observed during the plate motility assay.

AHL expression in the rumen of the cow is affected by diet and season [35]. New Zealand cattle are on pasture for a significant part of the year, which is markedly different to cattle used in many of the published studies. As *E. coli* must pass through the rumen to get to the hindgut, assays were set up to identify the AHLs present within the rumen of a typical grazing New Zealand cow.

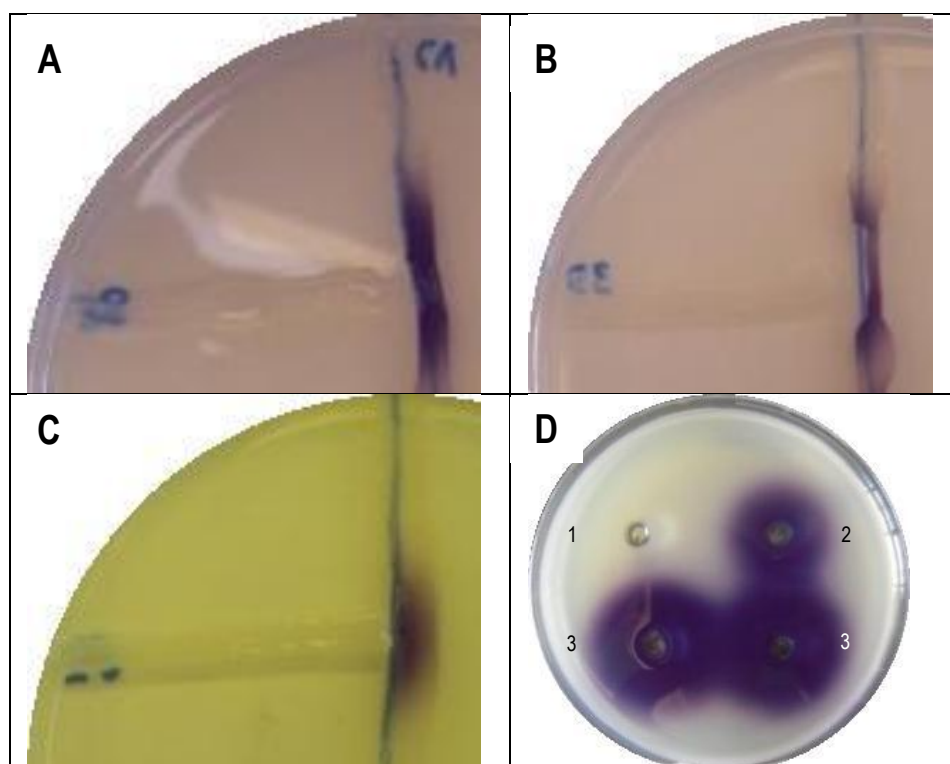


**Figure 68 – Short chain AHLs produced by psychrotolerant Enterobacteriaceae isolated from the surface of meat**

*Chromobacterium violaceum* CV026 was used as a bioreporter. CV026 is streaked vertically in A-C and was seeded into the agar of D.

(A) *Hafnia alvei* using a T-streak assay

(B) *Rahnella aquatilis* using a T-streak assay

(C) *Serratia* spp. using a T-streak

(D) Detection of short chain AHL using a well plate assay. The CM inoculated into the wells were produced from 8 hours cultures of:

[1] *Pseudomonas aeruginosa*

[2] *Rahnella aquatilis*

[3] Two independent isolates of *Hafnia alvei*



Signal molecules were extracted from unfiltered rumen fluid donated by the Rumen Microbiology team (AgResearch Ltd). Rumen fluid was obtained from two different source cows; one located at the Ruakura Research Centre in Hamilton, New Zealand and the second at Grasslands Research Centre in Palmerston North, New Zealand. The Hamilton animal was on a grass only diet, while the Palmerston North animal was fed on a mixture of grain and grass.

To obtain AHLs a total volume of 100ml rumen fluid was extracted using dichloromethane. Each extract was resuspended in 100µl acetonitrile, with 10µl used to spot on a thin layer chromatography which was utilised to separate the individual spots. No visible AHL spots were observed from the extracted rumen fluid from the Palmerston North cow. A single faint AHL spot was visualised from the rumen fluid collected from the Hamilton cow using *C. violaceum* CV026 (Figure 69). Modified AHLs produce a tear-drop shaped spot, whereas non-modified AHLs are characterised by circular spots.

For the AHL standards used, the R<sub>f</sub> values were calculated as 0.43, 0.11 and 0.09 for *N*-butanoyl-L-HSL, *N*-(3-oxohexanoyl)-L-HSL and *N*-hexanoyl-L-HSL respectively. By comparing this extracted rumen spot with the short chain AHL standards, it was observed that the spot moved a similar distance as *N*-hexanoyl-L-HSL. TLC is not exact, and due to the low concentration and poor visualisation it was unclear whether the spot produced by the extracted AHL was tear-drop or circular in shape. The R<sub>f</sub> value was calculated at 0.16 and the migration distance was closer to that of a C6-HSL standard than a C4-HSL, and falls between the values calculated for the two C6-HSL standards. While the extracted AHL can be classified as a short chain AHL, the identity remains unknown as the hydrocarbon chain length could be between five and six carbons in length, and could be modified or unmodified.

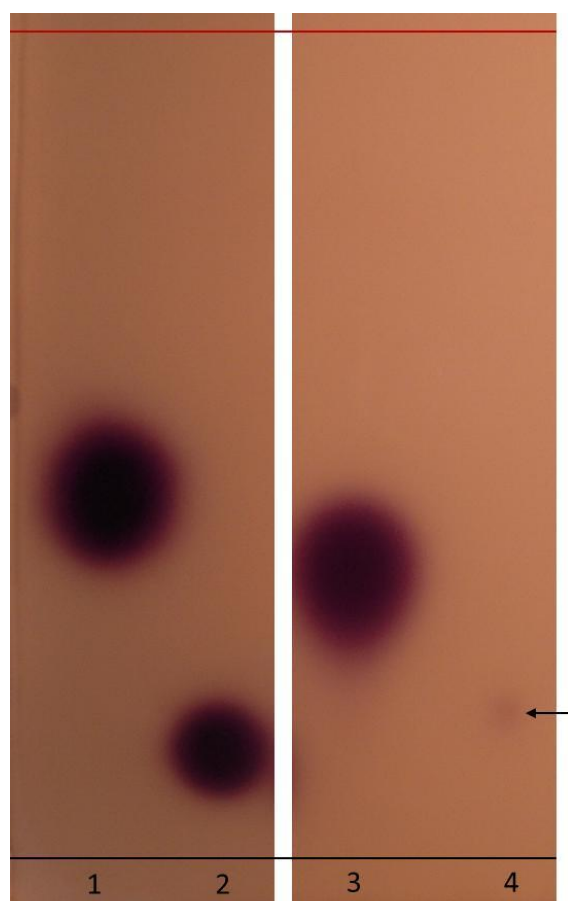


**Figure 69 - Separation of AHLs present in unfiltered rumen fluid by thin layer chromatography**

(1) 1mM *N*-butanoyl-DL-HSL (C4)

(2) 1mM *N*-(3-oxohexanoyl)-L-HSL (C6)

(3) 10μM *N*-hexanoyl-DL-HSL (C6)

(4) Dichloromethane extraction of unfiltered rumen fluid at neutral pH

Black arrows indicate the location of AHLs extracted from the rumen fluid.

Black line represents the origin and the red line represents the end of the solvent front.

### **5.2.2 Genetic Relatedness of a Selection of *E. coli* O157:H7 Isolates**

To identify the genetic diversity within the sample set of *E. coli* O157:H7 isolates used during this study, restriction digest and separation of the fragments was performed using pulsed field gel electrophoresis.

Five different isolates sourced from cattle were selected from the AgResearch culture collection for the investigation into quorum sensing regulation during this study. Of the 5 bovine isolates selected, 3 were collected from faeces (N427, N218 and N231) and 2 from the hide of very young calves (N635 and N236). A clinical isolate of *E. coli* O157:H7, sourced from ESR, NZRM3441 [E87] was also used. For the purposes of this study, populations from bovine faeces are termed 'faecal isolates', samples from the bovine hide are 'hide isolates' and those collected from human faeces are 'clinical isolates'.

Using restriction digest with *Xba*I and pulsed-field gel electrophoresis (PFGE) the genetic relatedness of these isolates was analysed. *Salmonella branderup* 4085 was used as a standard marker with a known digestion pattern (Figure 70A).

Although many studies have utilised PFGE to compare restriction digest patterns of *E. coli* O157:H7 isolates collected within New Zealand, it was unfortunately not possible to compare the samples used during this study with other profiles. The digest pattern of the standard *Salmonella branderup* 4085 appeared different in this PFGE gel to other profiles produced using the PulseNet protocol, therefore comparisons could only be made between the digests produced in this study. It is unknown whether this observed difference is as a result of differences in methodology used in this study or complete *Xba*I digestion.

The restriction digest pattern of N218 and N231 was the same, and these isolates were confirmed as being closely related genetically upon analysis of the banding patterns using BioNumerics 4.0 (Figure 70). The third faecal isolate appeared to have a different banding pattern to all other isolates, but was identified as being most closely related to N635, a hide

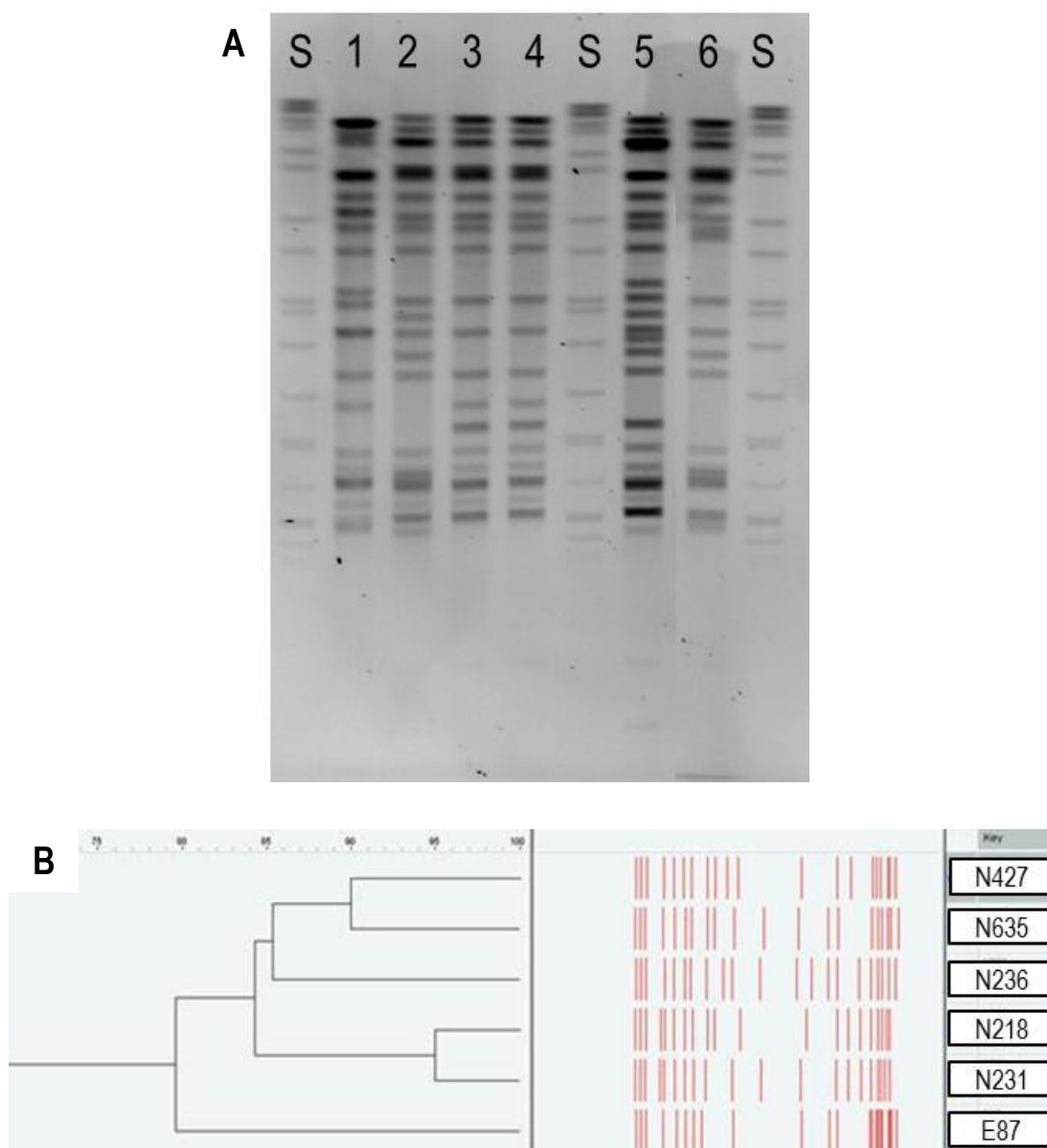


**Figure 70 – Pulsed Field Gel Electrophoresis separation of *E. coli* O157:H7 isolates**

PFGE used the enzyme *Xba*I for restriction digest of the *E. coli* O157:H7 genome.

(A) PFGE separation of fragments of the *E. coli* O157:H7 genome digested with enzyme BamH1.

(1) Faecal isolate N427 (Bovine) from PLANT A

(2) Hide isolate N635 (Bovine) from PLANT B

(3) Faecal isolate N218 (Bovine) from PLANT C

(4) Faecal isolate N231 (Bovine) from PLANT C

(5) Hide isolate N236 (Bovine) from PLANT C

(6) Faecal isolate NZRM3441 [E87] from human faeces (Clinical)

(S) *Salmonella branderup* 4085, used as a marker of known restriction digest pattern

(B) Similarity matrix of *E. coli* O157:H7 digestion patterns generated using the BioNumerics 4.0 software.

isolate collected from a different plant (Figure 70). The two hide isolates, N635 and N236 were observed to have the same restriction digest pattern on the gel, but analysis with the software showed them to be genetically diverse, while still closely related (Figure 70). The clinical isolate had a different banding pattern to the bovine isolates, although some similarities were observed on the gel (Figure 70).

These results showed that isolates collected from the same anatomical location shared some genetic homology, but similarities also existed between isolates sourced from different geographical locations.

### **5.2.3 Role of AHL and Temperature on the Population Expansion of *E. coli* O157:H7**

The effect of temperature on the population expansion of *E. coli* O157:H7 was investigated to determine whether this phenotype was temperature-dependent, using both 25°C and 37°C incubation. For each isolate 5 technical replicates were analysed. Images of N427, N635 and NZRM3441 [E87] were chosen to illustrate the difference in the size of the motility zones produced by faecal, hide and clinical isolates respectively (Figure 71).

All isolates produced clear dense areas of motility at both temperatures after 18 hours incubation (Figure 71). Interestingly, in comparison to the faecal isolates the motility zones produced by the hide isolates were smaller at both 25°C ( $F = 116.73$ ;  $p = <0.0001$ ), and 37°C ( $F = 214.63$ ;  $p = <0.0001$ ). At 25°C clinical isolate NZRM3441 [E87] produced large dense areas of motility (Figure 71). *E. coli* O157:H7 clinical isolate NCTC12900 has been used by laboratories for many years as a non-toxicogenic EHEC model. This isolate has become the reference *E. coli* O157:H7 strain for many applications, and it was included in this assay to identify differences between a laboratory strain and a toxigenic strain. In the absence of AHL, the motility ring was measured at  $46 \pm 5.62$ mm on average (Figure 71).

In chapter 3 it was shown that AHL-dependent quorum sensing affected the population

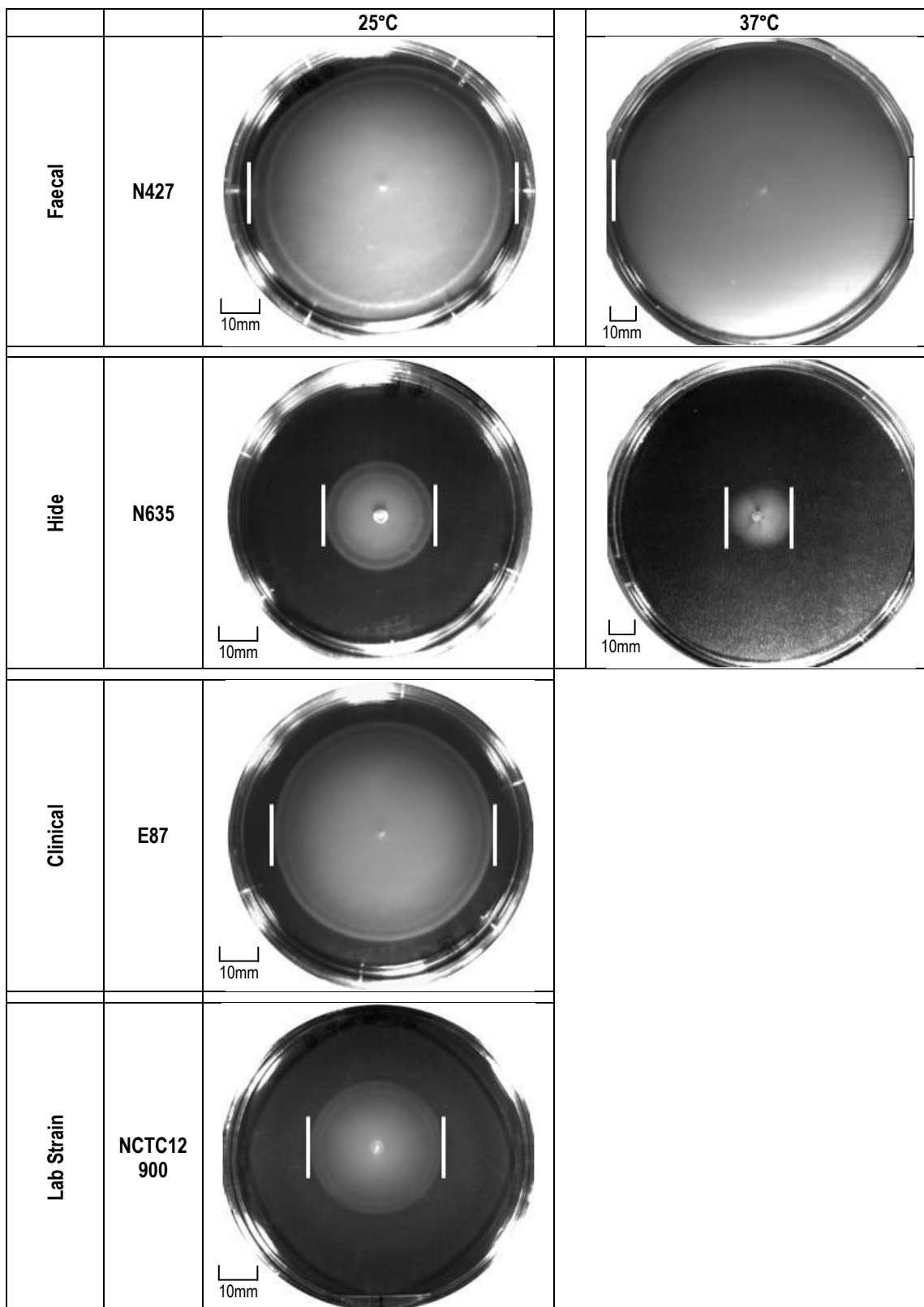


**Figure 71 –Effect of temperature on *E. coli* O157:H7 population expansion**

Images are representative of the motility zones produced after 18 hours incubation at 25°C and 37°C. Each image is representative of 1 biological culture consisting of 5 technical replicates.

White bars mark the boundaries of population expansion on each plate. Scale bars are indicated in the left hand corner and are set at 10mm.

N.B. Images are representative, therefore the size of motility ring on the image may not be illustrative of the overall effect.

expansion of model strain *E. coli* E2348/69. As the core genome of EPEC and EHEC are similar, it was hypothesised that a similar effect would be observed for the *E. coli* O157:H7 isolates. AHLs were added to the inoculation culture twice during growth and directly into the motility agar at a final concentration of 5nM.

The 3 faecal isolates produced large areas of motility at 25°C with an average diameter of  $70.35 \pm 4.52\text{mm}$ ,  $74.7 \pm 2.25\text{mm}$  and  $74.95 \pm 2.48\text{mm}$  (N427, N218 and N231 respectively) (Table 34). Addition of *N*-(3-oxo-hexanoyl)-D-HSL, *N*-(3-oxododecanoyl)-D-HSL and *N*-dodecanoyl-L-HSL had no significant effect on the population expansion of any of the faecal isolates at 25°C (Table 34, Figure 72). However, the addition of *N*-(3-oxohexanoyl)-L-HSL significantly decreased the size of the motility zone produced by all faecal isolates tested (Table 34, Figure 72). The population expansion of N427 decreased from  $70.35 \pm 4.52\text{mm}$  in the absence of AHL to  $52 \pm 1.0\text{mm}$  in the presence of *N*-(3-oxohexanoyl)-L-HSL ( $F = 392$ ;  $p = <0.0001$ ) and the motility zones of N218 decreased from  $74.7 \pm 2.25\text{mm}$  in diameter to  $69 \pm 2.91\text{mm}$  after addition of *N*-(3-oxohexanoyl)-L-HSL ( $F = 8.54$ ;  $p = 0.0192$ ) (Table 36). The diameter of the motility ring of N231 decreased from  $74.95 \pm 2.48\text{mm}$  in the absence of AHL to  $71.6 \pm 1.81\text{mm}$  in the presence of *N*-(3-oxohexanoyl)-L-HSL ( $F = 43.6$ ;  $p = 0.0002$ ) (Table 34).

In comparison, hide isolate N635 produced an area of motility of average diameter  $34.95 \pm 10.81\text{mm}$  and the N236 motility ring measured an average of  $48.35 \pm 12.11\text{mm}$  in diameter (Table 35). Addition of *N*-(3-oxo-hexanoyl)-D-HSL, *N*-(3-oxododecanoyl)-D-HSL and *N*-dodecanoyl-L-HSL to either of the hide isolates had no significant effect on the size of the area of motility produced (Table 35, Figure 73). Addition of *N*-(3-oxohexanoyl)-L-HSL significantly decreased the population expansion of N635 from  $34.95 \pm 10.81\text{mm}$  to a non-motile population ( $F = 8513$ ;  $p = <0.0001$ ) (Table 35, Figure 73). The diameter of the motility zone produced by N236 was significantly decreased from an average diameter of  $48.35 \pm 12.11\text{mm}$  in the absence

**Table 34 – Statistical analysis of the effect of AHLs on *E. coli* O157:H7 faecal isolate population expansion at 25°C**

Side chain lengths of the AHLs are in brackets. Significant decreases in population expansion are highlighted in pink.

		Average diameter of motility ring ± 1 standard deviation (mm)	ANOVA	
			*F-value	p-value
N427	No AHL	70.35 ± 4.52		
	<i>N</i> -(3-oxo-hexanoyl)-D-HSL (C6)	73.8 ± 0.44	1.28	0.291
	<i>N</i> -(3-oxododecanoyl)-D-HSL (C12)	72.8 ± 3.56	1.08	0.329
	<i>N</i> -(3-oxohexanoyl)-L-HSL (C6)	52 ± 1.0	392	4.0 × 10 <sup>-8</sup>
	<i>N</i> -dodecanoyl-L-HSL (C12)	66.2 ± 2.59	0*	0*
N218	No AHL	74.7 ± 2.25		
	<i>N</i> -(3-oxo-hexanoyl)-D-HSL (C6)	72 ± 1.58	4.38	0.0698
	<i>N</i> -(3-oxododecanoyl)-D-HSL (C12)	72.4 ± 2.19	1.63	0.237
	<i>N</i> -(3-oxohexanoyl)-L-HSL (C6)	69 ± 2.91	8.54	0.0192
	<i>N</i> -dodecanoyl-L-HSL (C12)	76.8 ± 1.58	0.01	0.916
N231	No AHL	74.95 ± 2.48		
	<i>N</i> -(3-oxo-hexanoyl)-D-HSL (C6)	71.2 ± 2.59	2.38	0.161
	<i>N</i> -(3-oxododecanoyl)-D-HSL (C12)	71.6 ± 1.14	4.27	0.0727
	<i>N</i> -(3-oxohexanoyl)-L-HSL (C6)	71.6 ± 1.81	43.6	0.0002
	<i>N</i> -dodecanoyl-L-HSL (C12)	74.4 ± 1.81	0.49	0.503

\*F- critical value = 5.317

\* The average values for unsupplemented and C12-HSL supplemented cultures were the same on the given day

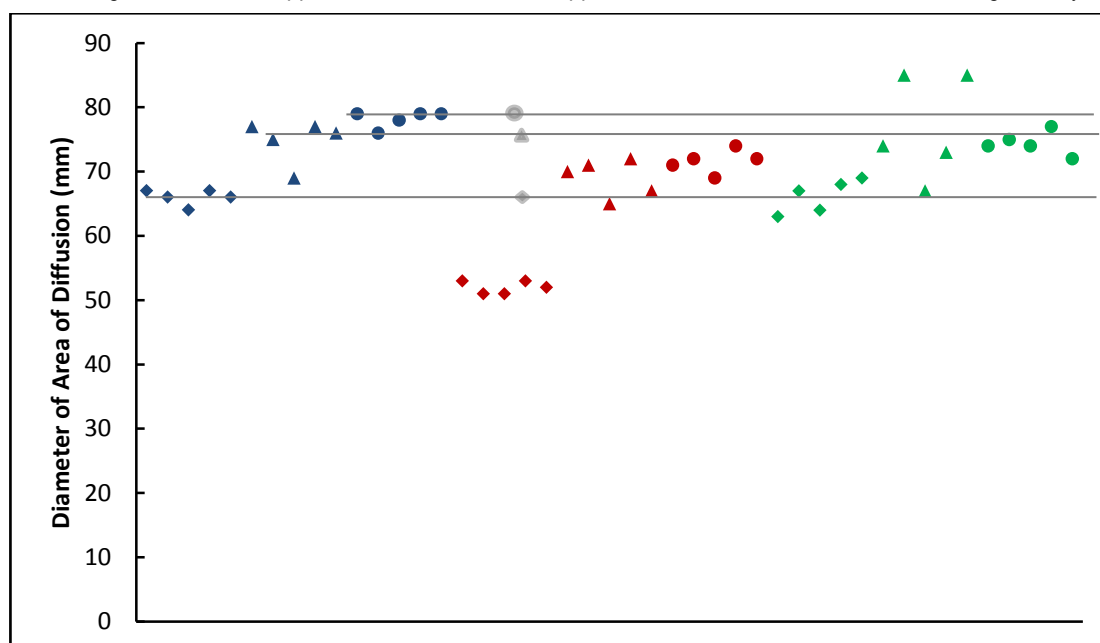


**Figure 72 – Variation in the diameter of the motility zones produced by faecal isolates of *E. coli* O157:H7 in the presence and absence of different AHLs at 25°C**

For each of the cultures 5 technical replicates were analysed. Each point on the graph represents one technical replicate. Petri dishes measured 95 mm in diameter.

(Blue) No AHL supplement

(Red) *N*-(3-oxohexanoyl)-L-HSL

(Green) *N*-dodecanoyl-L-HSL

Grey line represents the average diameter for the unsupplemented cultures.

Different strains are demarcated using shapes:

(Diamond) Faecal isolate N427

(Triangle) Faecal isolate N218

(Circle) Faecal isolate N231



**Table 35 – Statistical analysis of the effect of AHL on *E. coli* O157:H7 hide and clinical isolate population expansion at 25°C**

Side chain lengths of the AHLs are in brackets. Significant decreases in population expansion are highlighted in pink.

		Average diameter of motility ring $\pm$ 1 standard deviation (mm)	ANOVA	
			*F-value	p-value
N635	No AHL	34.95 $\pm$ 10.81		
	<i>N</i> -(3-oxo-hexanoyl)-D-HSL (C6)	32.3 $\pm$ 1.79	0.367	0.561
	<i>N</i> -(3-oxododecanoyl)-D-HSL (C12)	31.8 $\pm$ 2.16	0.781	0.403
	<i>N</i> -(3-oxohexanoyl)-L-HSL (C6)	0 $\pm$ 0	8513	2.0 $\times$ 10 <sup>-13</sup>
	<i>N</i> -dodecanoyl-L-HSL (C12)	48.6 $\pm$ 1.81	3.88	0.084
N236	No AHL	48.35 $\pm$ 12.11		
	<i>N</i> -(3-oxo-hexanoyl)-D-HSL (C6)	40 $\pm$ 0.71	0.0625	0.809
	<i>N</i> -(3-oxododecanoyl)-D-HSL (C12)	41 $\pm$ 0.71	2.25	0.172
	<i>N</i> -(3-oxohexanoyl)-L-HSL (C6)	34 $\pm$ 0.71	204	6.0 $\times$ 10 <sup>-7</sup>
	<i>N</i> -dodecanoyl-L-HSL (C12)	68.6 $\pm$ 1.51	0.13	0.725
E87	No AHL	62.4 $\pm$ 2.25		
	<i>N</i> -(3-oxo-hexanoyl)-D-HSL (C6)	58.8 $\pm$ 3.03	2.16	0.180
	<i>N</i> -(3-oxododecanoyl)-D-HSL (C12)	60.6 $\pm$ 2.88	0.077	0.788
	<i>N</i> -(3-oxohexanoyl)-L-HSL (C6)	42.2 $\pm$ 1.30	881	2.0 $\times$ 10 <sup>-9</sup>
	<i>N</i> -dodecanoyl-L-HSL (C12)	61 $\pm$ 2.83	1.1	0.325
NCTC12900	No AHL	46 $\pm$ 5.62		
	<i>N</i> -(3-oxohexanoyl)-L-HSL (C6)	36.8 $\pm$ 4.73	15.69	0.0009

\*F- critical value = 5.317

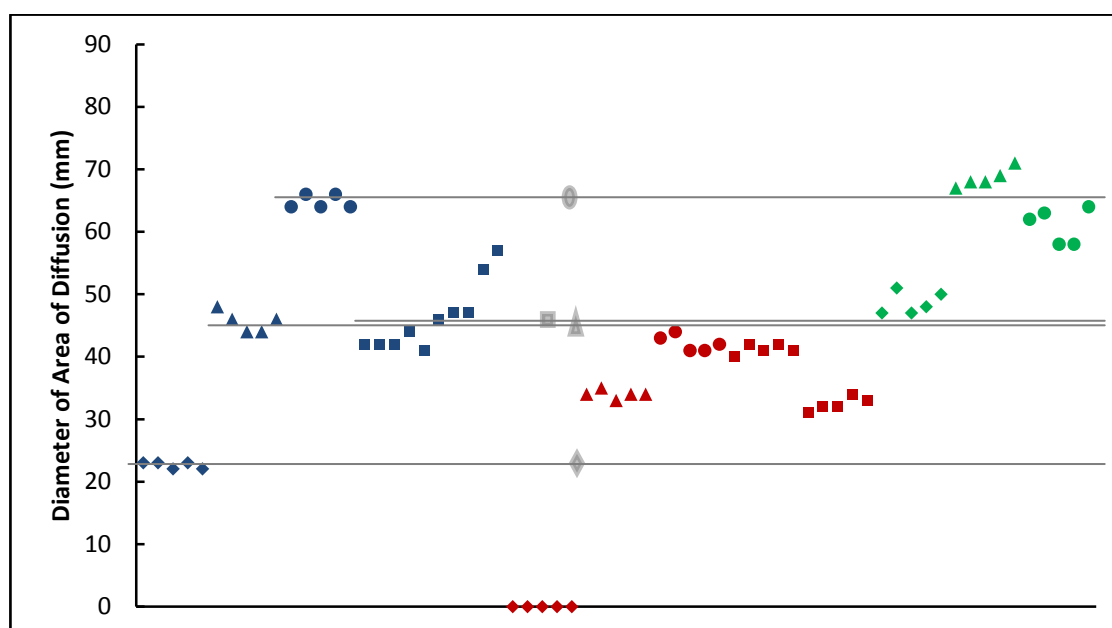


**Figure 73 – Variation in the diameter of the motility zones produced by hide and clinical isolates of *E. coli* O157:H7 in the presence and absence of different AHLs at 25°C**

For each of the cultures 5 technical replicates were analysed. Each point on the graph represents one technical replicate. Petri dishes measured 95 mm in diameter.

(Blue) No AHL supplement

(Red) *N*-(3-oxohexanoyl)-L-HSL

(Green) *N*-dodecanoyl-L-HSL

(Grey) Line represents the average diameter for the unsupplemented cultures.

Different strains are demarcated using shapes:

(Diamonds) Hide isolate N635

(Triangles) Hide isolate N236

(Circles) Clinical isolate NZRM3441 [E87]

(Squares) Reference strain NCTC12900

of AHL, to  $34 \pm 0.71\text{mm}$  in the presence of *N*-(3-oxohexanoyl)-L-HSL ( $F = 204$ ;  $p = <0.0001$ ) (Table 35, Figure 73).

The clinical isolate NZRM3441 [E87] produced areas of motility derived motility measuring  $62.4 \pm 2.25\text{mm}$  in the absence of AHL. Population expansion was not affected by the presence of *N*-(3-oxo-hexanoyl)-D-HSL, *N*-(3-oxododecanoyl)-D-HSL and *N*-dodecanoyl-L-HSL (Table 35, Figure 73). The diameter of the motility zone produced by the bacteria significantly decreased to  $42.2 \pm 1.30\text{mm}$  with the addition of  $5\text{nM}$  *N*-(3-oxohexanoyl)-L-HSL ( $F = 881$ ;  $p = <0.0001$ ) (Table 35, Figure 73). In the absence of AHL the motility zone produced by NCTC12900 was measured at  $46 \pm 5.62\text{mm}$ , which was significantly decreased to an average of  $36.8 \pm 4.73\text{mm}$  in the presence of *N*-(3-oxohexanoyl)-L-HSL ( $F = 15.69$ ;  $p = 0.0009$ ) (Table 35, Figure 73).

To identify if this quorum sensing effect was temperature-dependent the bovine isolates were incubated at  $37^\circ\text{C}$  in the presence and absence of AHL. The clinical isolate was not used in any further investigations.

Four out of the 5 isolates produced large areas of motility at  $37^\circ\text{C}$  (Table 36). The areas of motility were dense for all isolates, indicating a high level of bacterial growth with associated movement. Based on the EPEC model in chapter 3 it was hypothesised that no change would be observed upon addition of AHL. Addition of *N*-(3-oxo-hexanoyl)-D-HSL, *N*-(3-oxododecanoyl)-D-HSL and *N*-dodecanoyl-L-HSL had no significant effect on the size of the motility zone produced by any isolate, while *N*-(3-oxohexanoyl)-L-HSL significantly decreased the average diameter in all 5 isolates (Table 36).

#### **5.2.4 Cell Aggregation of *E. coli* O157:H7**

Having determined *N*-(3-oxohexanoyl)-L-HSL affected population expansion of the 5 *E. coli* O157:H7 isolates, the effect of this signal on cell aggregation was investigated. In chapter 3 it was observed that the formation of aggregates affected the population expansion in EPEC. If this

**Table 36 - Statistical analysis of the effect of AHL on *E. coli* O157:H7 population expansion at 37°C**

Average diameter values are representative of 1 biological replicate consisting of 5 technical replicates. Side chain lengths of the AHLs are in brackets. Significant decreases in population expansion are highlighted in pink. Petri dishes measured 145 mm in diameter.

			Average diameter of motility ring $\pm$ 1 standard deviation (mm)	ANOVA	
				*F-value	p-value
Faecal	N427	No AHL	131.5 $\pm$ 5.01		
		N-(3-oxo-hexanoyl)-D-HSL (C6)	131.7 $\pm$ 3.4	0.0108	0.918
		N-(3-oxododecanoyl)-D-HSL (C12)	133.1 $\pm$ 2.72	0.785	0.387
		N-(3-oxohexanoyl)-L-HSL (C6)	122.3 $\pm$ 5.98	13.88	0.0015
		N-dodecanoyl-L-HSL (C12)	130.1 $\pm$ 6.08	0.315	0.581
	N218	No AHL	134.2 $\pm$ 1.13		
		N-(3-oxo-hexanoyl)-D-HSL (C6)	134.1 $\pm$ 1.19	0.0367	0.850
		N-(3-oxododecanoyl)-D-HSL (C12)	134.5 $\pm$ 0.52	0.574	0.458
		N-(3-oxohexanoyl)-L-HSL (C6)	131.2 $\pm$ 2.20	14.67	0.00122
		N-dodecanoyl-L-HSL (C12)	133.5 $\pm$ 1.71	1.157	0.296
	N231	No AHL	134 $\pm$ 0.81		
		N-(3-oxo-hexanoyl)-D-HSL (C6)	134.4 $\pm$ 0.69	1.384	0.254
		N-(3-oxododecanoyl)-D-HSL (C12)	134 $\pm$ 0.67	0	1
		N-(3-oxohexanoyl)-L-HSL (C6)	127.7 $\pm$ 4.78	16.84	0.00067
		N-dodecanoyl-L-HSL (C12)	134.4 $\pm$ 0.69	1.384	0.254
Hide	N635	No AHL	24.1 $\pm$ 3.6		
		N-(3-oxo-hexanoyl)-D-HSL (C6)	28.6 $\pm$ 6.5	3.503	0.077
		N-(3-oxododecanoyl)-D-HSL (C12)	25 $\pm$ 3.49	0.321	0.577
		N-(3-oxohexanoyl)-L-HSL (C6)	0.7 $\pm$ 1.49	359.71	2.4 $\times 10^{-13}$
		N-dodecanoyl-L-HSL (C12)	24.7 $\pm$ 4.34	0.113	0.740
	N236	No AHL	81.5 $\pm$ 7.32		
		N-(3-oxo-hexanoyl)-D-HSL (C6)	81.3 $\pm$ 8.30	0.0032	0.955
		N-(3-oxododecanoyl)-DL-HSL (C12)	77.5 $\pm$ 4.95	2.05	0.169
		N-(3-oxohexanoyl)-L-HSL (C6)	69.6 $\pm$ 5.98	15.83	0.000088
		N-dodecanoyl-L-HSL (C12)	80.7 $\pm$ 7.7	0.056	0.815

\*F-critical value = 4.414

was true of *E. coli* O157:H7, the aggregation of the bacterial population would increase in the presence of *N*-(3-oxohexanoyl)-L-HSL when compared to that observed in the absence of signal.

None of the *E. coli* O157:H7 bovine isolates tested formed aggregates in the absence of AHL. In all cases a high proportion of planktonic cells with only some small aggregates observed that were less than 150 pixels<sup>2</sup> in size (Figure 74). Addition of *N*-(3-oxohexanoyl)-L-HSL or *N*-dodecanoyl-L-HSL had no significant effect on the aggregation profiles of these *E. coli* O157:H7 isolates (Table 37, Figure 74).

#### **5.2.5 Effect of AHL on the Expression of Exopolysaccharide in *E. coli* O157:H7**

AHL-dependent quorum sensing affected the population expansion of *E. coli* O157:H7 at both 25°C and 37°C, but not through changes in the degree of aggregation. Other targets for quorum sensing regulation were investigated. The first of these was exopolysaccharide production, which was shown to affect the adhesive properties in *Klebsiella pneumoniae* [102].

On standard LA plates, where metabolism is not carbohydrate based, all *E. coli* O157:H7 isolates produced small round colonies that were non-mucoid in nature, when incubated at 37°C or left at room temperature (RT) for up to 7 days (Figure 75). When inoculated onto LA plates containing 0.4% glucose and left at RT for up to 7 days, the colonies were larger than those produced on standard agar, retaining the circular morphology but had become more mucoid in consistency (Figure 75). Addition of *N*-(3-oxohexanoyl)-L-HSL and *N*-dodecanoyl-L-HSL had no observable effect on the size or morphology of the colonies produced by *E. coli* O157:H7 (Figure 75).

By stripping the exopolysaccharide from the cells the concentration of uronic acid, a component of the exopolysaccharide capsule of *E. coli* was monitored in the presence and absence of AHL to quantify the expression. The large amount of biological variation decreased the statistical power of this test and no conclusions could be drawn from the data.

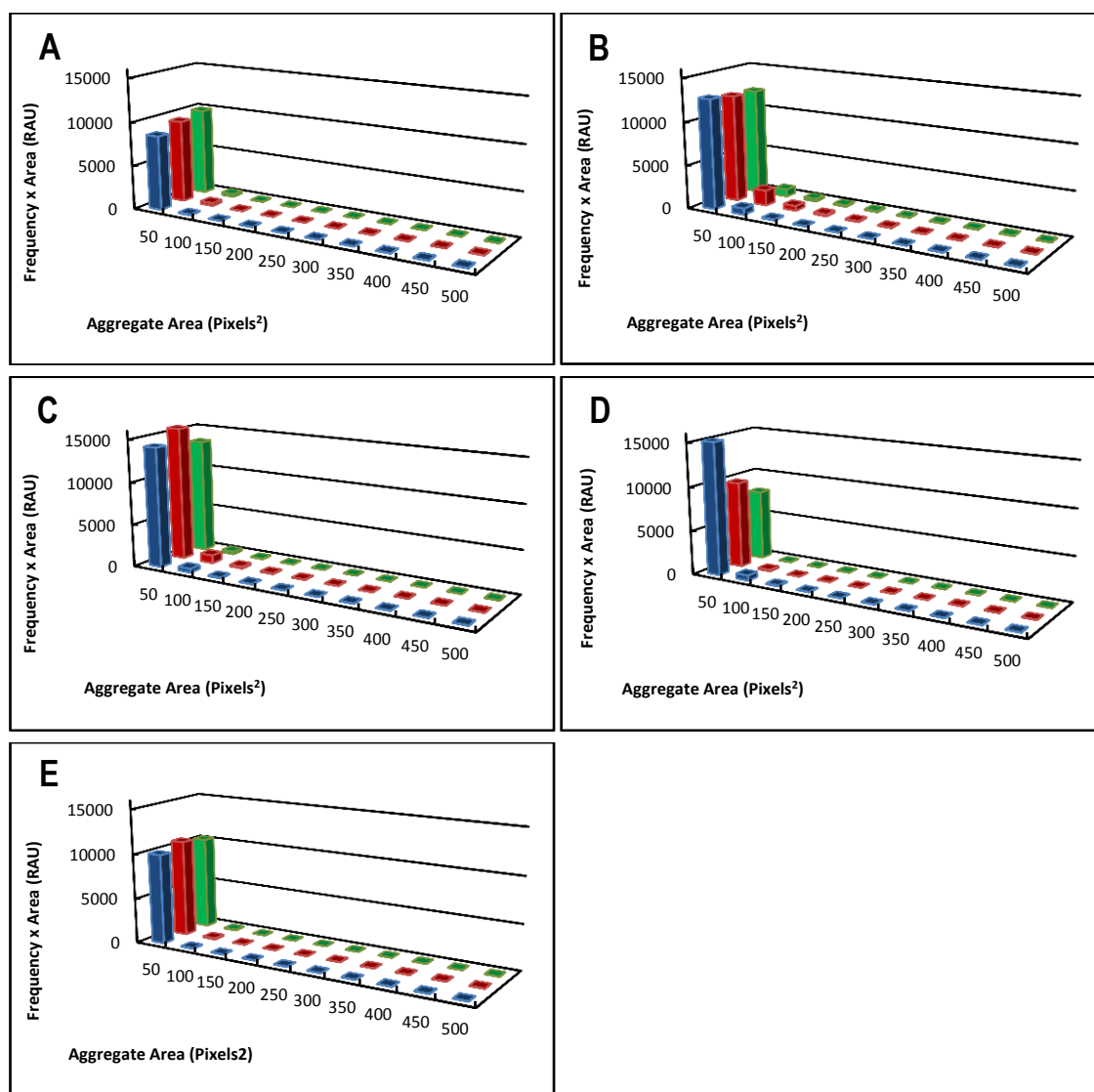


**Figure 74 – Aggregation profiles of *E. coli* O157:H7 isolates in the presence and absence of *N*-(3-oxohexanoyl)-L-HSL and *N*-dodecanoyl-L-HSL at 25°C**

Each profile is representative of the distribution of aggregate sizes formed by *E. coli* O157:H7 isolates in 2 independent biological replicates, each with 6 technical replicates. AHLs were supplemented at 4 hours of growth to a final concentration of 5nM.

Profiles are:

(Blue) *E. coli* O157:H7 with no AHL supplement

(Red) *E. coli* O157:H7 in the presence of *N*-(3-oxohexanoyl)-L-HSL

(Green) *E. coli* O157:H7 in the presence of *N*-dodecanoyl-L-HSL

*E. coli* O157:H7 isolates are:

(A) Faecal isolate N427

(B) Faecal isolate N218

(C) Faecal isolate N231

(D) Hide isolate N635

(E) Hide isolate N236

**Table 37 - Statistical analysis of the effect of AHLs on *E. coli* O157:H7 aggregation**

Statistical analysis of the aggregation profiles represented in figure 76. Biological variation compares profiles between cultures independent A and B; technical variation compares the profiles within a culture. Where  $D < 0.4$  there is no significant difference between the profiles of the given treatments, but where  $D \geq 0.4$  the difference is deemed to be significant.

N427		Biological Variation (A vs B)		Technical Variation	
	No AHL	0.035		0.059	
		A	B	Biological Variation (A vs B)	Unsupplemented vs Supplemented
	<i>N</i> -(3-oxohexanoyl)-L-HSL (C6)	0.044	0.18	0.22	0.12
	<i>N</i> -dodecanoyl-L-HSL (C12)	0.19	0.13	0.059	0.16
N218		Biological Variation (A vs B)		Technical Variation	
	No AHL	0.14		0.11	
		A	B	Biological Variation (A vs B)	Unsupplemented vs Supplemented
	<i>N</i> -(3-oxohexanoyl)-L-HSL	0.20	0.25	0.24	0.15
	<i>N</i> -dodecanoyl-L-HSL	0.097	0.33	0.25	0.21
N231		Biological Variation (A vs B)		Technical Variation	
	No AHL	0.022		0.061	
		A	B	Biological Variation (A vs B)	Unsupplemented vs Supplemented
	<i>N</i> -(3-oxohexanoyl)-L-HSL	0.29	0.10	0.18	0.23
	<i>N</i> -dodecanoyl-L-HSL	0.062	0.027	0.078	0.028
N635		Biological Variation (A vs B)		Technical Variation	
	No AHL	0.041		0.14	
		A	B	Biological Variation (A vs B)	Unsupplemented vs Supplemented
	<i>N</i> -(3-oxohexanoyl)-L-HSL	0.36	0.25	0.14	0.28
	<i>N</i> -dodecanoyl-L-HSL	0.17	0.47	0.32	0.23
N236		Biological Variation (A vs B)		Technical Variation	
	No AHL	0.28		0.18	
		A	B	Biological Variation (A vs B)	Unsupplemented vs Supplemented
	<i>N</i> -(3-oxohexanoyl)-L-HSL	0.15	0.021	0.14	0.14
	<i>N</i> -dodecanoyl-L-HSL	0.23	0.12	0.15	0.21

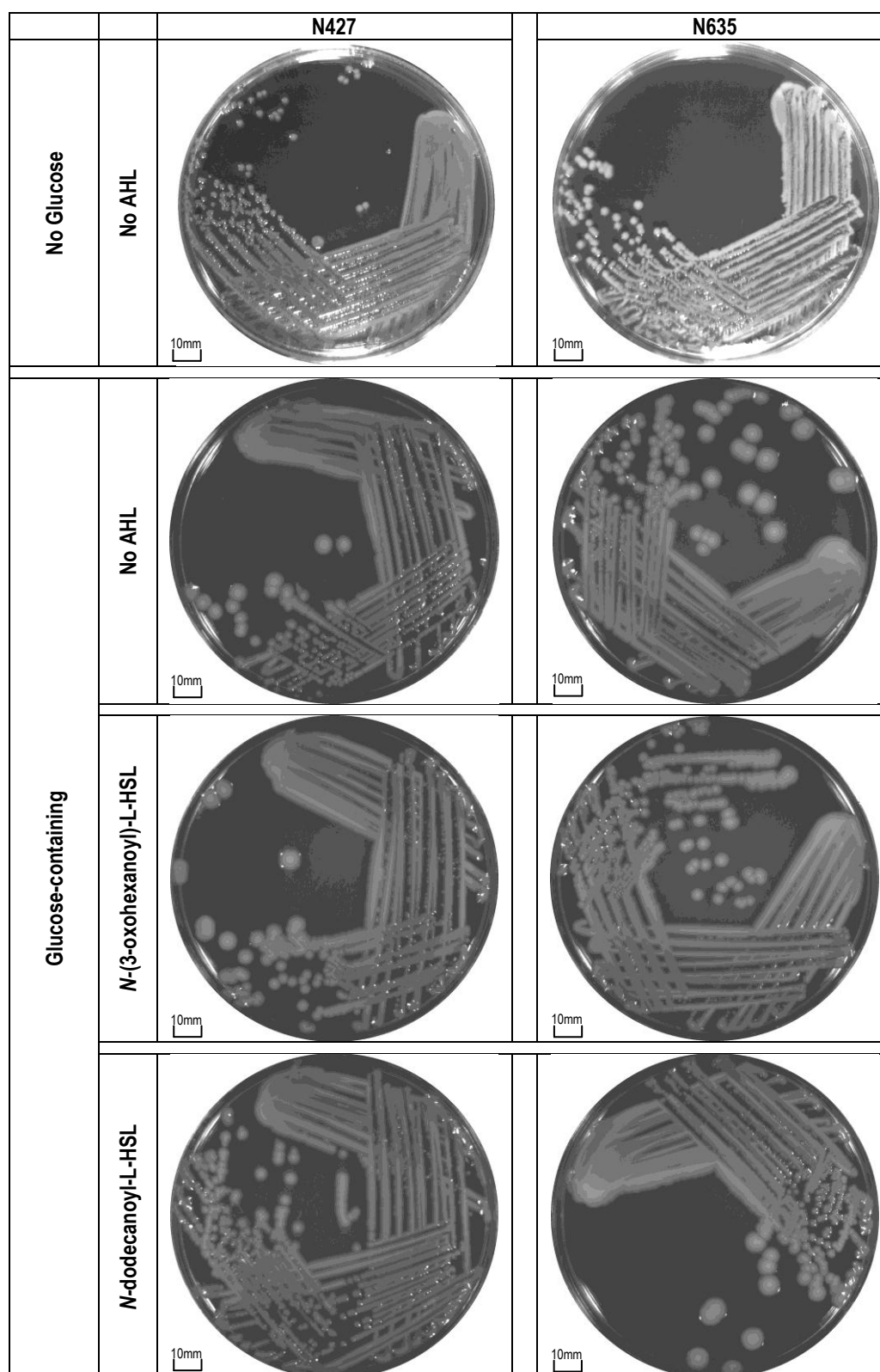


**Figure 75 - Comparison of exopolysaccharide production by *E. coli* O157:H7 in the presence and absence of AHL**

Glucose-containing agar was supplemented with 0.4% (v/v) glucose final concentration. All plates were incubated at room temperature for 7 days. AHL was added directly to the agar after sterilisation to a final concentration of 5nM. Images are representative of 3 replicates.

Scale bars are indicated in the left hand corner of each image, and set to 10mm.

Initial experiments observing changes in antigen 43 and curli expression were inconclusive. Due to the non-aggregative nature of the *E. coli* O157:H7 isolates used during this study, further investigations were not completed.

#### **5.2.6 Effect of AHL on the Attachment of *E. coli* O157:H7 to Mammalian Cells**

The ability of *E. coli* O157:H7 to form attaching-effacing (A/E) lesions on human cell line HT-29 was investigated in the presence and absence of AHL. The pathogenicity mechanisms required to form A/E lesions are similar in EHEC as they are in EPEC (Section 1.1.4.1). In the human host a high inoculum of EPEC is required to cause disease, resulting in the formation of rafts or micro-colonies and a high number of attaching-effacing lesions. In comparison, <100 EHEC bacteria are required to cause disease. EHEC does not form micro-colonies, and thereby a more sporadic pattern of individual A/E lesions was observed *in vitro*. The capacity for all 5 *E. coli* O157:H7 isolates to form A/E lesions was evaluated using the FAS test, and the effect of AHL was examined.

As in chapter 4 the addition of non-bacterial controls was used to provide a baseline fluorescence for the A/E lesion assays. In the absence of bacterial culture HT-29 cells were outlined faintly in green, with no intense areas of fluorescence. The addition of AHL at a final concentration of 5nM, or ethyl acetate at 0.1% (v/v) had no effect on uninfected host cell fluorescence (Figure 63).

Bacterial cultures were added at an OD<sub>600</sub> of 0.3 as with the experiments completed with EPEC in Chapter 4. In the absence of AHL, N427 produced a small number of visible pedestals, characterised by the localised intense green fluorescence of the FITC-phalloidin stain (Figure 76). Addition of *N*-(3-oxohexanoyl)-L-HSL and *N*-dodecanoyl-L-HSL appeared to decrease the number of A/E lesions formed. No characteristic A/E lesions were observed, but patches of bacteria appeared to adhere to the mammalian cell surface (Figure 76).



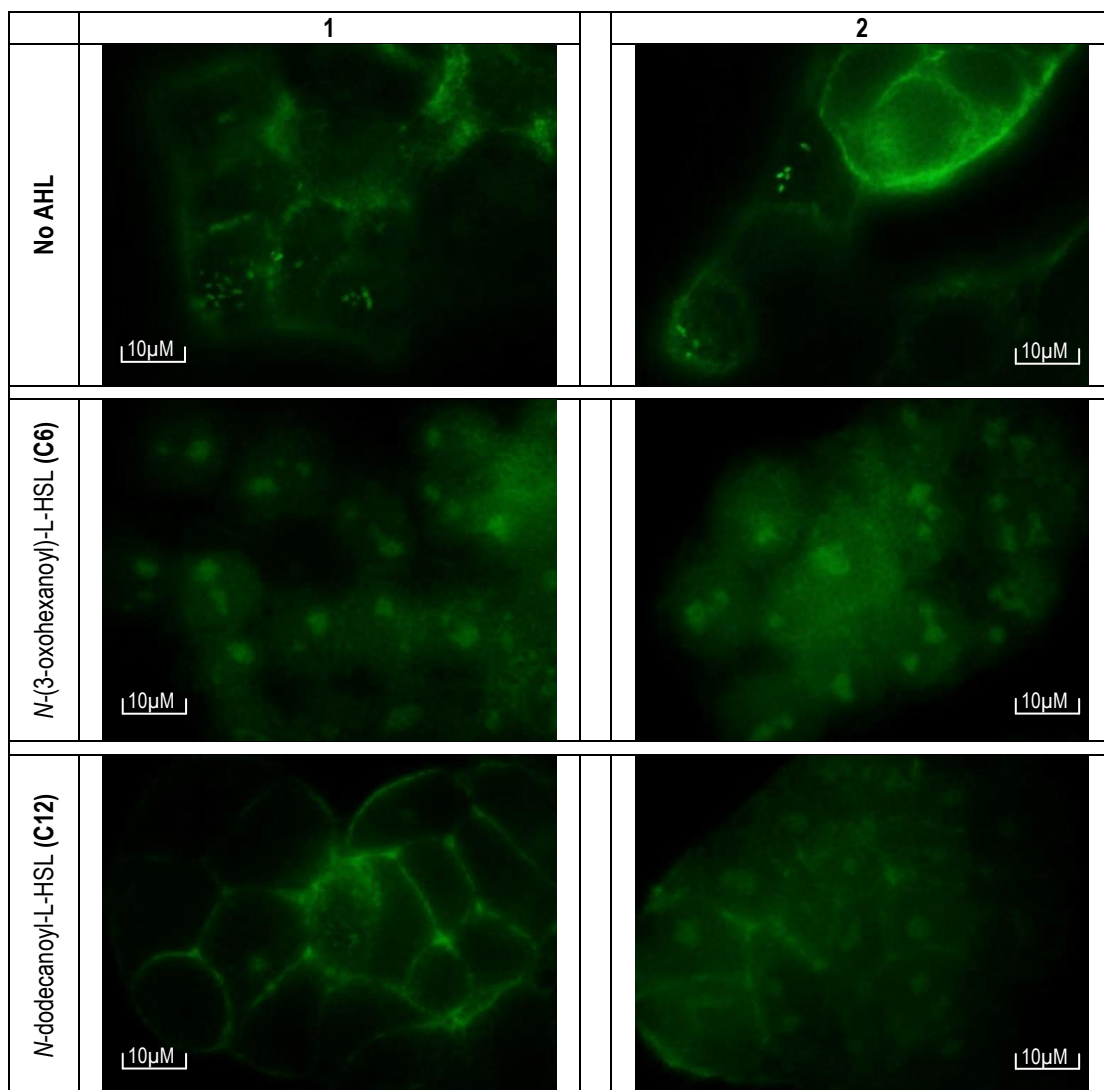


**Figure 76 – A/E lesion formation by *E. coli* O157:H7 isolate N427 in the presence and absence of AHLs**

FITC-Phalloidin attached to actin within the HT-29 cells (green fluorescence). Each image was taken at 1000x magnification using fluorescence microscopy.

Culture 1 and culture 2 represent independent bacterial cultures used to inoculate 1 well containing HT-29 cells. Within each well were 3 coverslips, and for each coverslip a representative 3 images were taken as technical replicates. Images are representative of the patterns of A/E lesion formation for all technical replicates.

Supplementation with AHL was completed to a final concentration of 5nM prior to inoculation onto the HT-29 cells.

Scale bars are indicated in the corner of each image, and set to 10µm.

Using Microsoft Word the brightness of each image has been increased by 30%.

N218 produced a small number of visible A/E lesions in the absence of AHL (Figure 77). In the presence of both *N*-(3-oxohexanoyl)-L-HSL and *N*-dodecanoyl-L-HSL, the number of visible lesions appeared to decrease, and were only present around the mammalian cell junctions, rather than distributed on the whole cell surface (Figure 77).

N231 produced a small number of A/E lesions in the absence of AHL (Figure 78). Addition of *N*-(3-oxohexanoyl)-L-HSL and *N*-dodecanoyl-L-HSL appeared to decrease the propensity of the bacteria to form A/E lesions (Figure 78).

N635 appeared to produce more A/E lesions in the absence of AHL when compared to N427 (Figure 79). Addition of *N*-(3-oxohexanoyl)-L-HSL and *N*-dodecanoyl-L-HSL appeared to have no visible effect on the number and extent of the A/E lesions formed by this isolate (Figure 79).

N236, also from the hide, appeared to produce A/E lesions in similar numbers to N427 (Figure 80). However, unlike N427, the addition of either *N*-(3-oxohexanoyl)-L-HSL or *N*-dodecanoyl-L-HSL appeared to have no effect on the number or extent of the A/E lesions formed by this *E. coli* O157:H7 isolate (Figure 80).

#### **5.2.7 Effect of Experimental Controls on *Galleria mellonella***

In contrast to the FAS assay, which was used to assess the changes in pathogenicity *in vitro*, the infection model was used to determine the effect *in vivo*. *Galleria mellonella* were injected with *E. coli* O157:H7 grown in the presence and absence of AHL to determine if these signals affected the toxicity and infectivity of the bacteria.

Using positive and negative controls the effect of several factors conserved between experiments was investigated. To determine whether the inoculation protocol was affecting the survival and health of the larvae, non-inoculated controls and PBS-inoculated controls were included in each assay. AHLs were resuspended in PBS to a final concentration of 5nM and

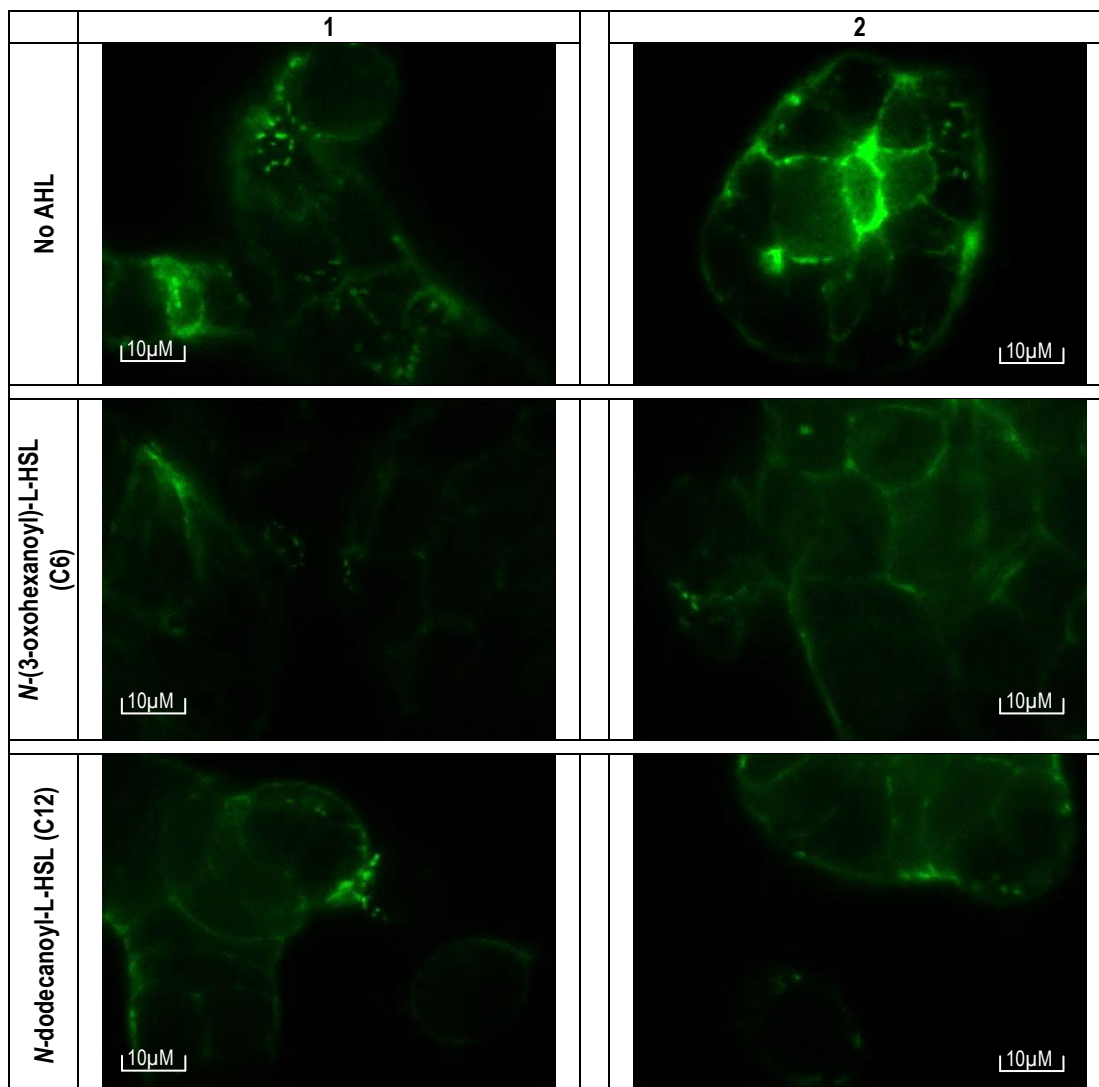


**Figure 77 - A/E lesion formation by *E. coli* O157:H7 isolate N218 in the presence and absence of AHLs**

FITC-Phalloidin attached to actin within the HT-29 cells (green fluorescence). Each image was taken at 1000x magnification using fluorescence microscopy.

Culture 1 and culture 2 represent independent bacterial cultures used to inoculate 1 well containing HT-29 cells. Within each well were 3 coverslips, and for each coverslip a representative 3 images were taken as technical replicates. Images are representative of the patterns of A/E lesion formation for all technical replicates.

Supplementation with AHL was completed to a final concentration of 5nM prior to inoculation onto the HT-29 cells. Scale bars are indicated in the corner of each image, and set to 10µm.

Using Microsoft Word the brightness of each image has been increased by 30%.

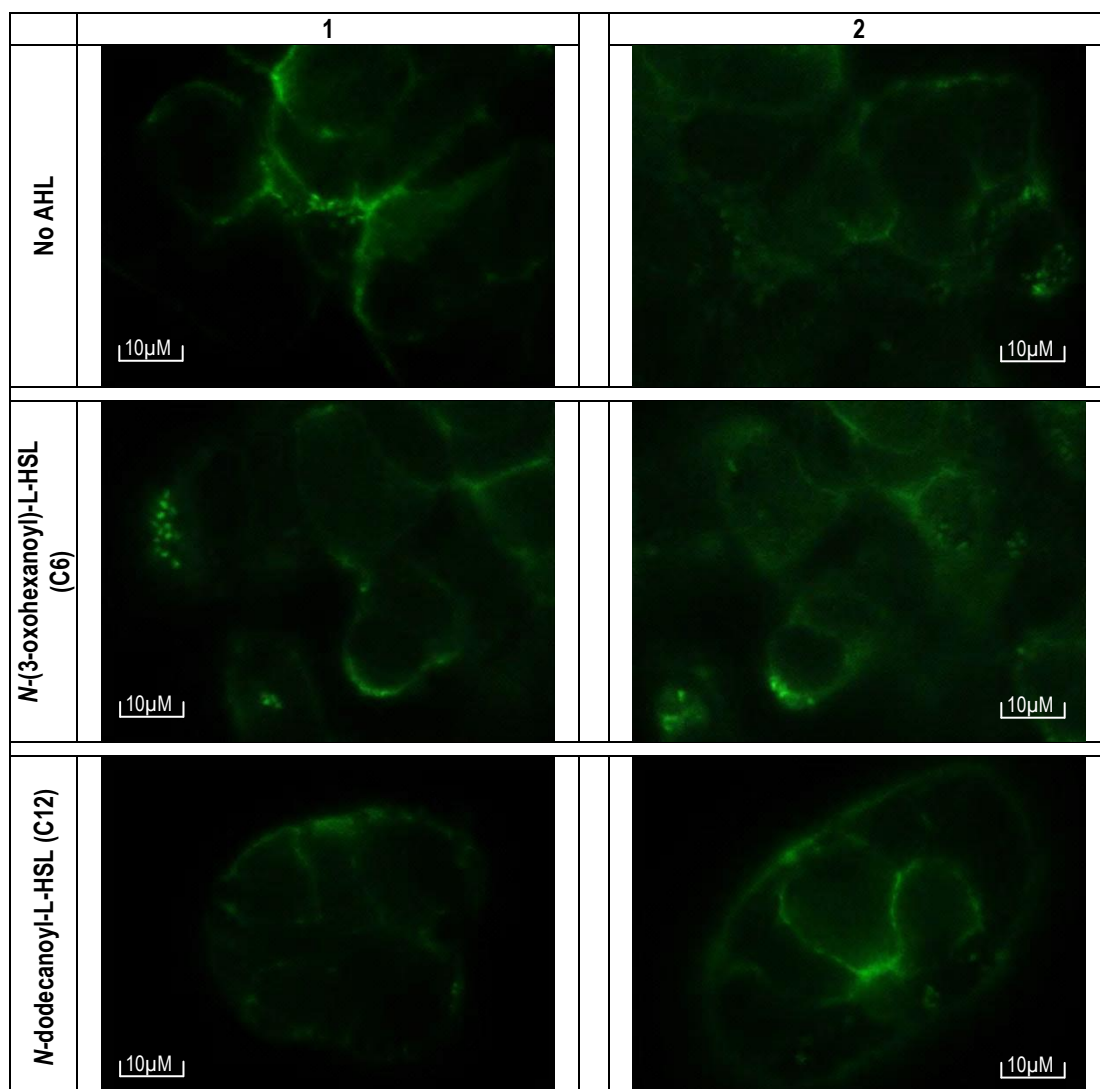


**Figure 78 - A/E lesion formation by *E. coli* O157:H7 isolate N231 in the presence and absence of AHLs**

FITC-Phalloidin attached to actin within the HT-29 cells (green fluorescence). Each image was taken at 1000x magnification using fluorescence microscopy.

Culture 1 and culture 2 represent independent bacterial cultures used to inoculate 1 well containing HT-29 cells. Within each well were 3 coverslips, and for each coverslip a representative 3 images were taken as technical replicates. Images are representative of the patterns of A/E lesion formation for all technical replicates.

Supplementation with AHL was completed to a final concentration of 5nM prior to inoculation onto the HT-29 cells.

Scale bars are indicated in the corner of each image, and set to 10µm.

Using Microsoft Word the brightness of each image has been increased by 30%.

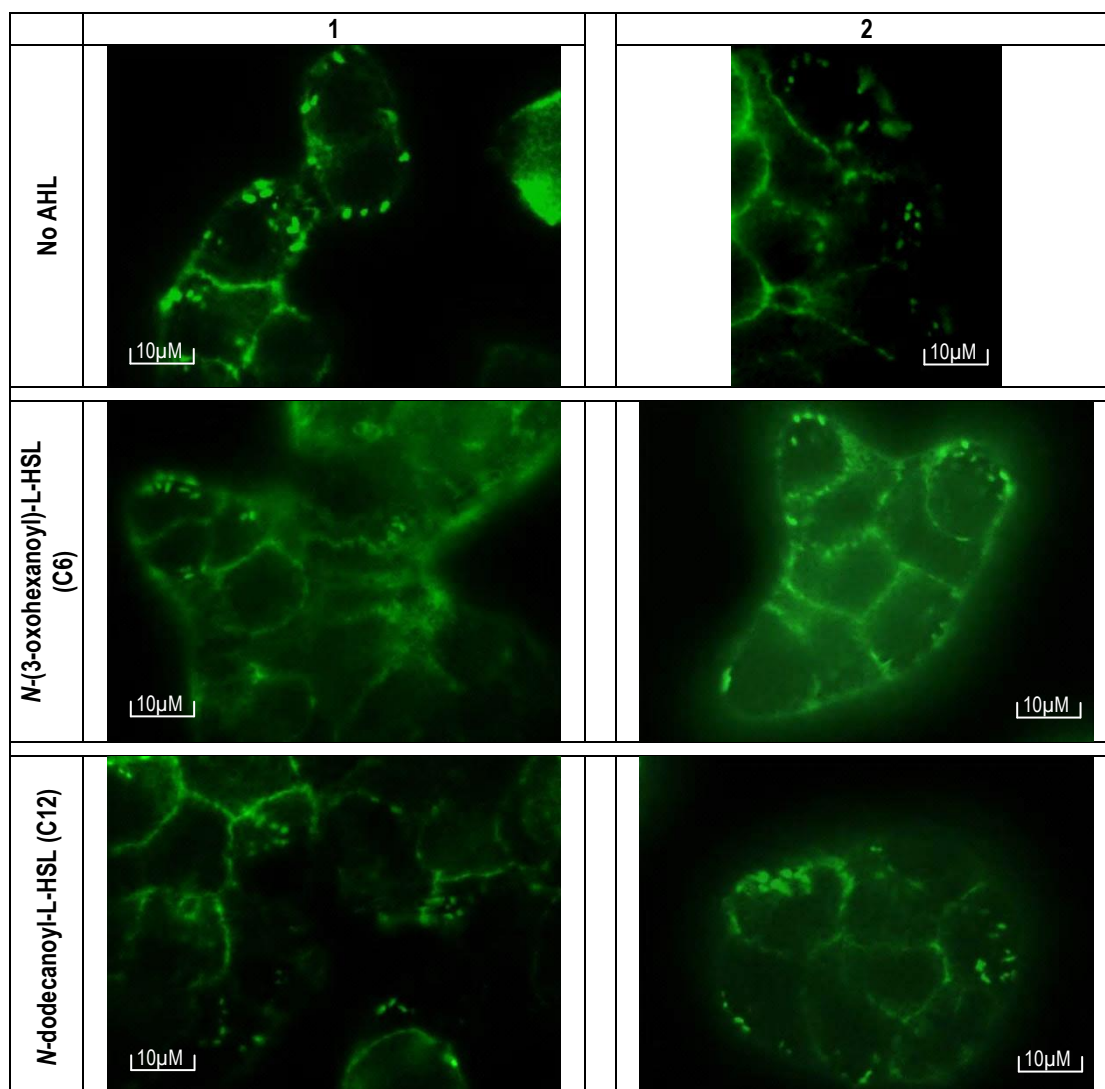


**Figure 79 - A/E lesion formation by *E. coli* O157:H7 isolate N635 in the presence and absence of AHLs**

FITC-Phalloidin attached to actin within the HT-29 cells (green fluorescence). Each image was taken at 1000x magnification using fluorescence microscopy.

Culture 1 and culture 2 represent independent bacterial cultures used to inoculate 1 well containing HT-29 cells. Within each well were 3 coverslips, and for each coverslip a representative 3 images were taken as technical replicates. Images are representative of the patterns of A/E lesion formation for all technical replicates.

Supplementation with AHL was completed to a final concentration of 5nM prior to inoculation onto the HT-29 cells.

Scale bars are indicated in the corner of each image, and set to 10µm.

Using Microsoft Word the brightness of each image has been increased by 30%.

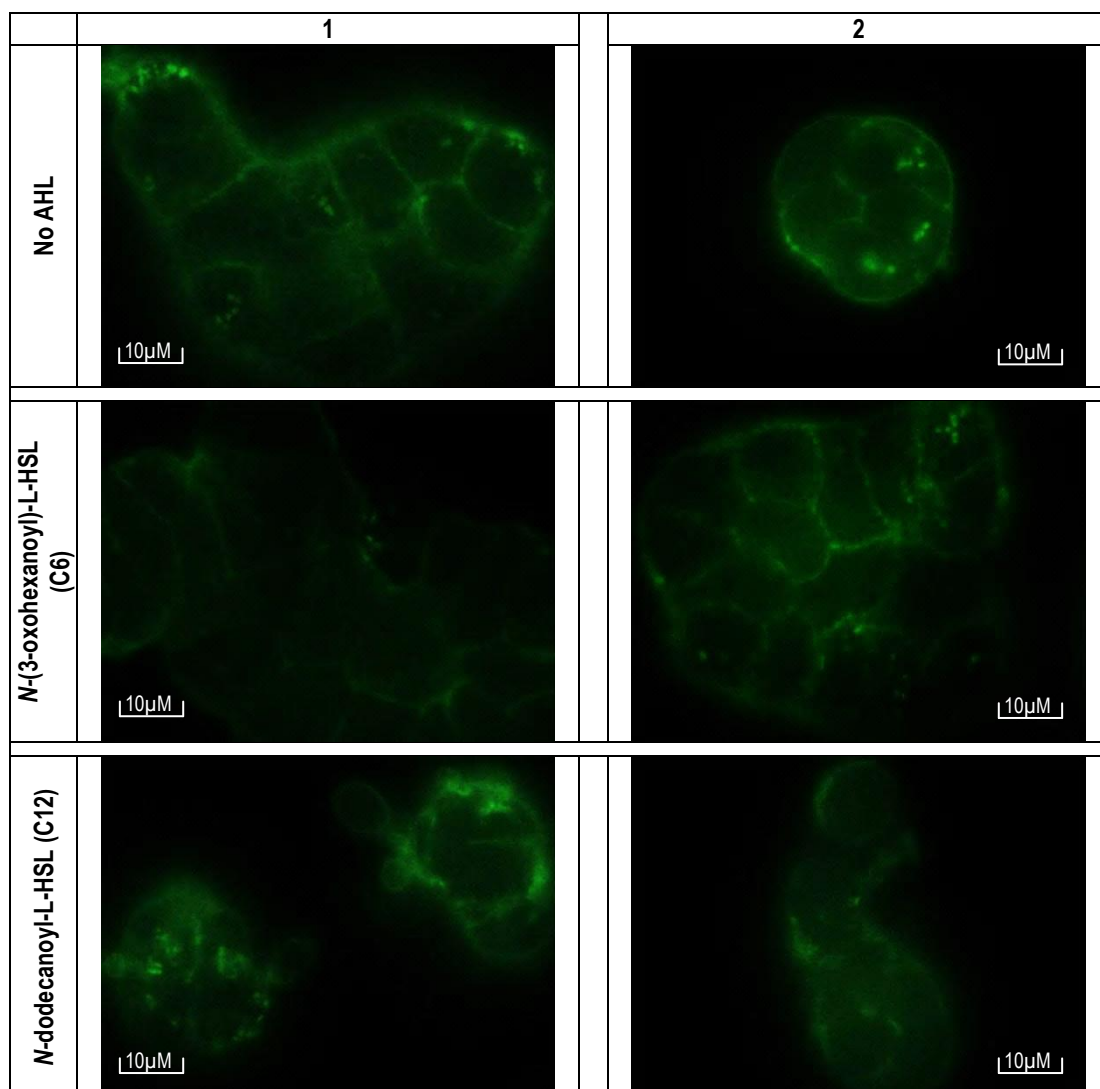


**Figure 80 - A/E lesion formation by *E. coli* O157:H7 isolate N236 in the presence and absence of AHLs**

FITC-Phalloidin attached to actin within the HT-29 cells (green fluorescence). Each image was taken at 1000x magnification using fluorescence microscopy.

Culture 1 and culture 2 represent independent bacterial cultures used to inoculate 1 well containing HT-29 cells. Within each well were 3 coverslips, and for each coverslip a representative 3 images were taken as technical replicates. Images are representative of the patterns of A/E lesion formation for all technical replicates.

Supplementation with AHL was completed to a final concentration of 5nM prior to inoculation onto the HT-29 cells.

Scale bars are indicated in the corner of each image, and set to 10µm.

Using Microsoft Word the brightness of each image has been increased by 30%.

inoculated into the larvae to identify any detrimental effects of the signals alone. None of the negative control larvae changed in pigmentation retaining their natural beige colouring, and all remained alive for the 72-hour experimental period (Table 38, Figure 81). *Ps. aeruginosa* PA01 is known to be highly pathogenic to *G. mellonella*, and was used as the positive control. All 15 larvae injected with this pathogen had died within 24 hours of inoculation (Table 38, Figure 81).

For the purposes of this study any larvae that turned black and stopped moving was determined as dying of infection. After death a representative sample of the larvae were dissected and the internal contents streaked onto agar. Presence of bacteria was confirmed and compared with the bacterial load of dead non-inoculated larvae.

#### **5.2.8 Effect of AHLs on *E. coli* O157:H7 Pathogenicity using the *Galleria mellonella* Model**

*Galleria mellonella* produce melanin in response to stress (Section 1.6). The inclusion of the negative controls in each experiment allowed the effect of a specific infectious agent to be assessed. By inoculating *G. mellonella* larvae with N427 and N635, the effect of toxigenic *E. coli* O157:H7 and the effect of AHL on the pathogenicity of the bacterium was observed using pigmentation changes and differences in the overall fatality rates. Bacterial cultures were primed in DMEM prior to dilution to increase expression of virulence proteins [14]. All cultures were diluted to a concentration of  $10^9$  cfu/ml in PBS prior to inoculation into *G. mellonella* meaning each larva was injected with 10 $\mu$ l containing  $10^7$  cfu.

During these preliminary experiments in the absence of AHL 11/15 larvae died as a result of infection with N427. All turned black and contained a high internal bacterial load (Table 39, Figure 82). Injection of N635 in the absence of AHL resulted in 13/15 larvae dying (Table 39, Figure 82). Addition of AHL occurred at 4 points during growth each to a final concentration of 5nM: to the overnight culture, at 4 hours incubation of the fresh culture, after dilution into DMEM and once resuspended in PBS prior to inoculation.



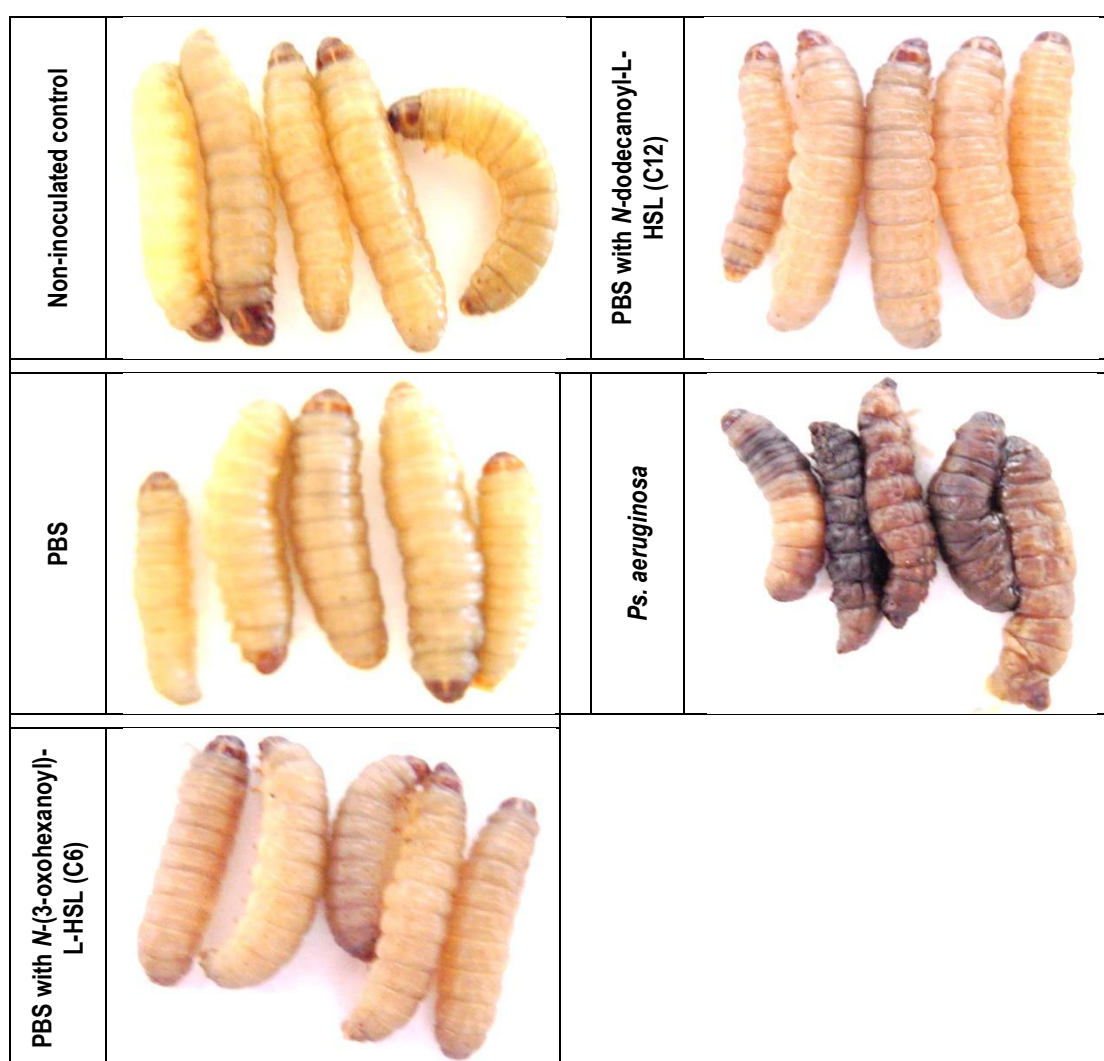


**Figure 81 – *Galleria mellonella* pigmentation after infection with inoculation medium and supplements. Positive control is *Ps. aeruginosa***

Representative images of the melanin production by *G. mellonella* upon injection with the negative and positive controls used for all infection model assays (Figures 88-90). All larvae were incubated at 37°C for up to 72 hours. Images are representative of observed pigmentation of the 15 larvae used for each treatment.

Non-inoculated control larvae were placed on the inoculation platform but were not injected with any solutions prior to incubation.

AHLs were added to PBS at a final concentration of 5nM and 10µL injected into each larvae.

*Ps. aeruginosa* inoculated larvae were injected with pathogen resuspended in PBS to a final density of 10<sup>7</sup> cfu/ml.

**Table 38 – Fatality rates of *Galleria mellonella* after inoculation with the control samples**

All infections involved 15 larvae, and the values in the table represent the total of dead larvae counted after each time point. The fatality rates are cumulative.

	24 Hours	48 Hours	72 Hours
Non-inoculated	0	0	0
PBS	0	0	0
PBS with <i>N</i> -(3-oxohexanoyl)-L-HSL (C6)	0	0	0
PBS with <i>N</i> -dodecanoyl-L-HSL (C12)	0	0	0
<i>Ps. aeruginosa</i>	15	15	15



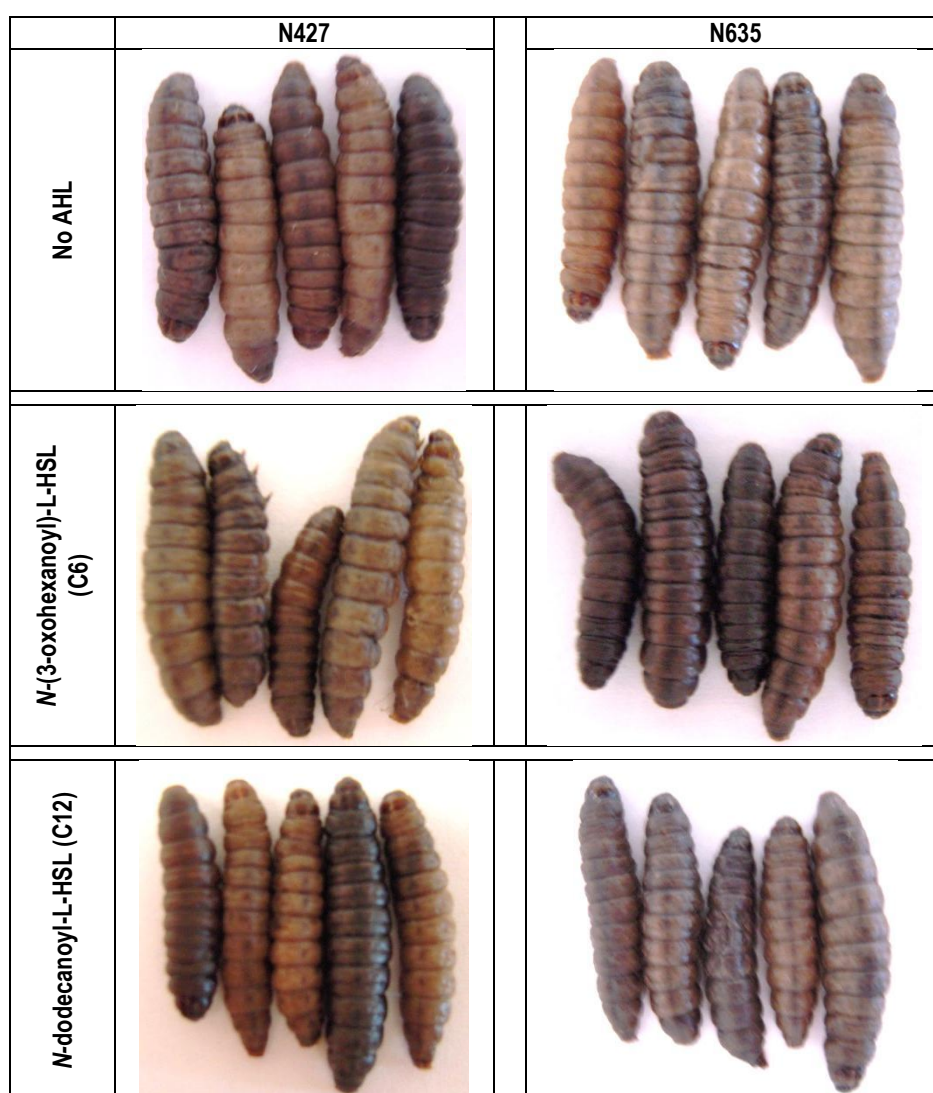


**Figure 82 – Effect of AHL on *E. coli* O157:H7 virulence and the impact on *Galleria mellonella* pigmentation**

Representative images of the melanin production by *G. mellonella* upon injection with the *E. coli* O157:H7 isolates N427 and N635 in the presence and absence of *N*-(3-oxohexanoyl)-L-HSL and *N*-dodecanoyl-L-HSL. All larvae were incubated at 37°C for up to 72 hours. Images are representative of the pigmentation of the 15 larvae used for each treatment.

Inoculums used:

N427 –  $4.7 \times 10^7$  cfu/ml grown in DMEM for 3 hours prior to resuspension in PBS for inoculation

N635 –  $3.9 \times 10^7$  cfu/ml grown in DMEM for 3 hours prior to resuspension in PBS for inoculation

**Table 39 – Fatality rates of *Galleria mellonella* after inoculation with *E. coli* O157:H7**

All infections involved 15 larvae, and the values in the table represent the total of dead larvae counted after each time point. The fatality rates are cumulative.

		24 Hours	48 Hours	72 Hours
<b>N427</b>	<b>No AHL</b>	6	11	11
	<b><i>N</i>-(3-oxohexanoyl)-L-HSL (C6)</b>	8	9	10
	<b><i>N</i>-dodecanoyl-L-HSL (C12)</b>	10	10	10
<b>N635</b>	<b>No AHL</b>	5	13	13
	<b><i>N</i>-(3-oxohexanoyl)-L-HSL (C6)</b>	11	15	15
	<b><i>N</i>-dodecanoyl-L-HSL (C12)</b>	7	11	11

In the presence of *N*-(3-oxohexanoyl)-L-HSL and *N*-dodecanoyl-L-HSL, inoculation with N427 resulted in 10/15 larvae dying from infection (Table 39, Figure 82). By comparison, addition of *N*-(3-oxohexanoyl)-L-HSL to N635 resulted in a fatal infection of all larvae tested within 48 hours (Table 39, Figure 82). In the presence of *N*-dodecanoyl-L-HSL, 11 / 15 of the larvae infected with N635 had died (Table 39, Figure 82). Statistical analysis was completed using the Fishers Exact 2-sided test for contingency tables. No difference was observed between the pathogenicity of N427 and N635 during these preliminary *G. mellonella* infection studies ( $p = 0.12$ ).

#### **5.2.9 Role of Signalling and Environment on E2348/69 Pathogenicity Using the *Galleria mellonella* Model**

Injection of larvae with *E. coli* O157:H7 had shown that addition of AHL may alter infectivity of the pathogen within an insect infection model. To determine whether this trait was conserved between related pathotypes, it was necessary to compare the pathogenicity of E2348/69 and E2348/69 *hosA*<sup>-</sup> within the *G. mellonella* model in the presence and absence of AHL.

In the absence of AHL, infection with E2348/69 caused 3 / 15 larvae to die and turn black (Table 40, Figure 83). Addition of *N*-(3-oxohexanoyl)-L-HSL resulted in all larvae surviving through to 72 hours. By comparison, in the presence of *N*-dodecanoyl-L-HSL infection by E2348/69 caused the death of 2 / 15 larvae under these conditions (Table 40, Figure 83).

Injection with E2348/69 *hosA*<sup>-</sup> in the absence of AHL resulted in a fatality rate of 5 / 15 larvae (Table 40; Figure 83). Addition of *N*-(3-oxohexanoyl)-L-HSL to the bacteria resulted in 3 / 15 larvae dying in response to infection. Infection with E2348/69 *hosA*<sup>-</sup>, in the presence of *N*-dodecanoyl-L-HSL, resulted in a fatality rate of zero after 72 hours (Table 40; Figure 83).

Although addition of AHL to both E2348/69 or E2348/69 *hosA*<sup>-</sup> appeared to change the fatality rates during these preliminary tests, the sample size was not large enough to detect a significant difference at the  $p < 0.05$  level.

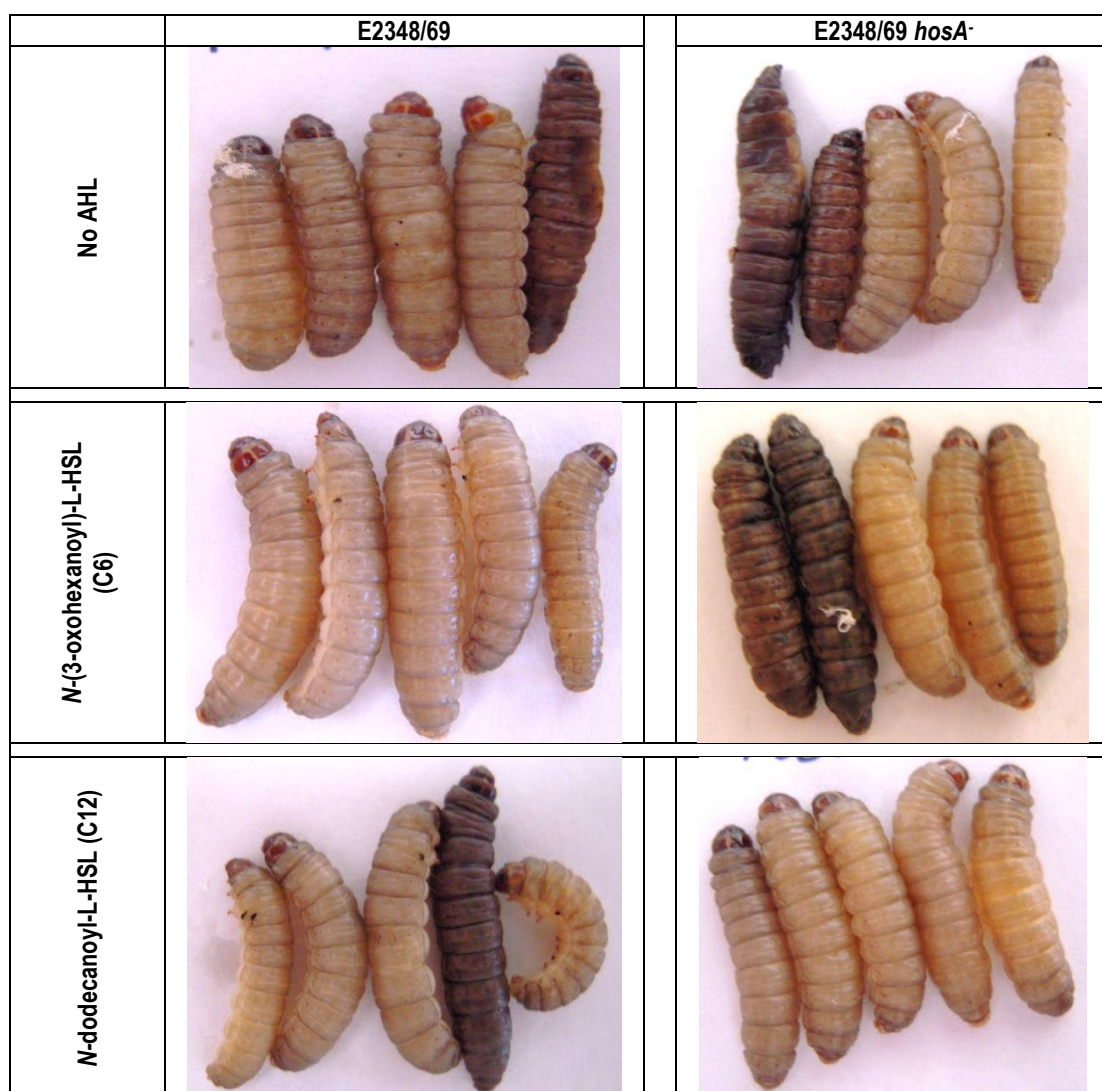


**Figure 83 - Effect of AHL on E2348/69 virulence and the impact on *Galleria mellonella* pigmentation**

Representative images of the melanin production by *G. mellonella* upon injection with E2348/69 and E2348/69 *hosA*<sup>-</sup> in the presence and absence of *N*-(3-oxohexanoyl)-L-HSL and *N*-dodecanoyl-L-HSL. All larvae were incubated at 37°C for up to 72 hours. Images are representative of the pigmentation of the 15 larvae used for each treatment.

Inoculums used:

E2348/69 – 3.8 x 10<sup>7</sup> cfu/ml grown in DMEM for 3 hours prior to resuspension in PBS for inoculation

E2348/69 *hosA*<sup>-</sup> – 3.0 x 10<sup>7</sup> cfu/ml grown in DMEM for 3 hours prior to resuspension in PBS for inoculation

**Table 40 – Fatality rates of *Galleria mellonella* after inoculation with E2348/69 or E2348/69 *hosA*<sup>-</sup>**

All infections involved 15 larvae, and the values in the table represent the total of dead larvae counted after each time point. The fatality rates are cumulative.

		24 Hours	48 Hours	72 Hours
E2348/69	No AHL	1	2	3
	<i>N</i> -(3-oxohexanoyl)-L-HSL (C6)	0	0	0
	<i>N</i> -dodecanoyl-L-HSL (C12)	0	1	2
E2348/69 <i>hosA</i> <sup>-</sup>	No AHL	1	3	5
	<i>N</i> -(3-oxohexanoyl)-L-HSL (C6)	2	2	3
	<i>N</i> -dodecanoyl-L-HSL (C12)	0	0	0

Using the Fisher Exact 2-sided test for contingency tables  $p = 0.11$ . Further experimentation and repeat experiments are required to determine if these statistical observations are correct.

Protein expression in E2348/69 has been shown to differ when grown in different media [14]. In order to determine the effect of these media on the pathogenicity of E2348/69 two groups of larvae were inoculated. In set A (Figure 84A) the bacteria were grown overnight in LB and diluted to a concentration of  $10^7$  cfu/ml in fresh media prior to inoculation. All larvae injected with inoculum A showed no signs of stress over the 72 hours of the experiment (Figure 84A). Set B was also grown in LB overnight (Figure 84B). The cells were pelleted and resuspended in DMEM before being incubated at  $37^\circ\text{C}$  in 5%  $\text{CO}_2$  for 3 hours. The cells were diluted to a concentration of  $10^6$  cfu/ml prior to inoculation. Infection with the DMEM primed E2348/69 cells proved fatal in all larvae within 72 hours, with all larvae turning dark brown in colour (Figure 84B).

E2348/69 *hosA*<sup>-</sup> had the potential to be more pathogenic than parental E2348/69 when grown in DMEM if inoculated into a larger sampling group. The difference between the strains during this study was not significant ( $p = 0.55$ ). Addition of *N*-(3-oxohexanoyl)-L-HSL affected the fatality rate in both strains but not significantly ( $p = 0.6$ ) (Table 41). To determine whether this was the same across the different growth media, both E2348/69 and E2348/69 *hosA*<sup>-</sup> were grown in LB in the presence and absence of *N*-(3-oxohexanoyl)-L-HSL and injected into sets of 15 larvae.

E2348/69 grown in LB did not cause stress or death in the absence of AHL (Table 41). Addition of *N*-(3-oxohexanoyl)-L-HSL to the bacteria resulted in a fatality rate of 1 / 15 after 72 hours (Table 41). By comparison, E2348/69 *hosA*<sup>-</sup> was more pathogenic in LB than in DMEM, and was significantly more pathogenic than wild type E2348/69 ( $p = <0.0001$ ). In the absence of AHL infection with E2348/69 *hosA*<sup>-</sup> caused death in 10 / 15 larvae expiring as a result of infection (Table 41). In the presence of *N*-(3-oxohexanoyl)-L-HSL 12 /15 larvae died as a result of infection with E2348/69 *hosA*<sup>-</sup> (Table 41). These results suggest growth media does affect the

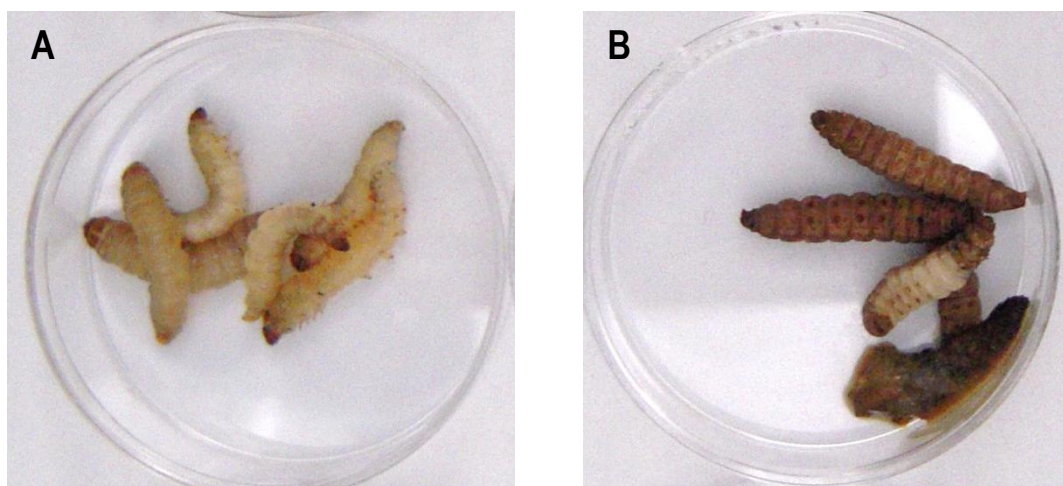


**Figure 84 – Effect of growth media on E2348/69 virulence and the impact on *Galleria mellonella* pigmentation**

Representative images of the melanin production by *G. mellonella* upon injection with E2348/69 when the bacteria were grown in different media. All larvae were incubated at 37°C for up to 72 hours. Images are representative of the pigmentation of the 6 larvae used for each treatment. Inoculum level for each treatment was measured at  $1 \times 10^7$  cfu/ml.

Inoculums used:

(A) Cells maintained in LB throughout growth prior to resuspension in PBS for inoculation

(B) Cells resuspended in DMEM for 3 hours in 5% CO<sub>2</sub> prior to resuspension in PBS for inoculation

**Table 41 – Effect of *N*-(3-oxohexanoyl)-L-HSL on the fatality rates of *Galleria mellonella* after inoculation with E2348/69 or E2348/69 *hosA*<sup>-</sup> grown in LB**

All infections involved 15 larvae, and the values in the table represent the total of dead larvae counted after each time point. The fatality rates are cumulative.

		24 Hours	48 Hours	72 Hours
E2348/69	No AHL	0	0	0
	<i>N</i> -(3-oxohexanoyl)-L-HSL (C6)	0	0	1
E2348/69 <i>hosA</i> <sup>-</sup>	No AHL	4	8	10
	<i>N</i> -(3-oxohexanoyl)-L-HSL (C6)	0	9	12

pathogenicity of EPEC, but further investigations would be required for any definitive conclusions to be drawn.

### **5.3 Discussion**

Enterohaemorrhagic *E. coli* O157:H7 is a zoonotic pathogen, moving from the bovine reservoir to a human host [14, 31, 44, 52, 54, 261]. The natural lifestyle of a gut bacterium regardless of host is to attach to the mucosal wall and successfully colonise or to disseminate to a new colonisation site within the same host or a new host [4, 6]. *E. coli* O157:H7 colonise the bovine hindgut in large numbers [4, 6]. A proportion of the population is excreted into the environment in faeces, with bacterial loads of between  $10^2$  and  $10^6$ cfu/g of faecal matter [6, 23, 27, 31]. Some cattle shed a higher proportion of the population to the environment than others. These individuals can be divided into super-spreaders and super-shedders, depending on the overall shedding pattern [23, 27, 39-41]. Super-spreaders excrete a high bacterial load and have increased opportunity to infect others, such as at markets or during transport and lairage [23, 27, 39-41]. In comparison, a super-shedder excretes a higher bacterial load than other members of the same herd for a defined period of time [23, 27, 39-41]. The bovine hindgut has the optimal conditions for successful *E. coli* O157:H7 colonisation. Of the 5 bovine isolates of *E. coli* O157:H7 analysed in this study, 3 were isolated from faeces and 2 from the hide. Using pulsed field gel electrophoresis analysis of the chromosomal DNA, it was observed that although similar, there were distinct genetic differences between this small subset of bovine isolates. It was not possible to compare the gel with a wider dataset of profiles due to the *Salmonella* *branderup* 4085 size ladder in this experiment not being compatible with the PulseNet profile.

Due to the high bacterial load, it is likely that within the bovine hindgut DNA exchange can occur, increasing genetic diversity. *E. coli* O157:H7 have a dual lifestyle, surviving both internal and external to the host. Outside the host, the bacteria exist in generally nutritionally poor conditions with lower temperatures that fluctuate. *E. coli* O157:H7 have been shown to exist for at least 49

days under these less than optimal conditions, shutting down all but the essential mechanisms required for survival [27, 39-41]. The bacteria can subsist either in or on the soils, plants and faecal matter on the ground. They can be picked up adhering to the hide of the animal and from there be ingested via grooming. Although nutrition may be poorer on the hide in comparison to the soil, the temperatures would be slightly raised from the body heat of the bovine host and therefore potentially less likely to fluctuate. By comparison, when within the host *E. coli* O157:H7 exist within an optimal environment with temperatures consistently above 37°C. These considerable differences in environment make efficient adaptation essential for the survival of this bacterium.

The concept of genetic drift describes a change in the frequency of a given variant within a population due to random sampling and spontaneous mutation [3]. Mutations occur randomly in *E. coli* and may be generated by replication errors. Within a given population multiple mutations will be simultaneously present, some of which may convey survival or growth advantages over the rest of the population. Individual bacteria possessing these advantageous mutations would proliferate, with the mutation becoming fixed within the population over the course of a number of cycles. Where selective pressures are important in the genetic fitness of a population, adaptive responses relate to the ability of a bacterium to change phenotype rapidly in response to a specific challenge such as temperature or acidity. Due to the instability of the external environment, those *E. coli* surviving outside the host may be better able to quickly adapt to changes in conditions when compared to those within the host.

Isolates N427 and N635 were isolated from different anatomical and geographical locations , however the restriction digest pattern shows that they were the most genetically similar of the 5 isolates tested. The genetic differences between these two isolates could potentially be the result of adaptive difference for survival in the two extreme environments. Further isolates will need to be analysed to determine the relevance of these differences.



*E. coli* O157:H7 are a common cause of food borne illness in humans, and have been associated with multiple large outbreaks around the world [2-4, 6, 14, 25, 27, 28, 31, 44, 47, 52, 54, 261]. A common route of transmission to a human host is via contaminated food or in water [2-4, 6, 14, 25, 27, 28, 31, 44, 47, 52, 54, 261]. Consumption of contaminated ground meat has been linked with some of the largest outbreaks of *E. coli* O157:H7 related illness [25, 31, 44]. Modern farming practices encourage the switch from small scale to intensive farming systems utilising feedlots or wintering barns. Both methods involve the herd standing on a hard surface, such as concrete, in close proximity for long periods of the day. Excrement and hide contaminants are easily transferred between individuals under these conditions.

During slaughter and processing of beef carcasses, the muscle becomes exposed and bacteria can be transferred from faecal matter or the hide onto the meat surface [39, 41, 45, 46]. Bacterial species isolated from the carcass surface include *E. coli* O157:H7 and other psychrotolerant Enterobacteriaceae, such as *Hafnia*, *Rahnella* and *Serratia* [42, 43, 45]. Multiple hurdle interventions comprising both chemical and physical methods are used by red meat industries around the world to reduce the bacterial load on meat but they do not eradicate the microflora completely [46]. Although the majority of cases of *E. coli* O157:H7 infection around the world have been associated with contaminated foodstuffs, in New Zealand reported cases tend to arise more from environmental sources [49-51]. There are few true outbreaks in New Zealand, with reported cases being more sporadic and arising from animal contact or rural associated activities, or from transfer within a family unit [49-51].

Diet is a major factor in the composition of the digestive material within the bovine gastrointestinal tract, with changes in diet likely to cause diarrhoea as the microbiota within the gut changes. This is important for bacterial nutrition and competition, but it is also important for quorum sensing-type signalling. *E. coli* utilise the AHL/SdiA system of quorum sensing, in addition to the AI-2 system. Although unable to produce AHL, *E. coli* are able to respond to those



produced by other bacteria within the same niche. Edrington *et al* confirmed that the pH of the bovine rumen changes in response to diet [35]. For example, barley-fed animals were shown to have a higher ruminal pH in comparison to corn-fed cattle (Section 1.1.3.1). Yates *et al* showed that pH is important for the functionality of the AHL, which undergo alkaline hydrolysis at pH above 6.5 at which the lactone ring opens, rendering the signal inactive [73, 93, 103, 175, 182]. In the case of *Yersinia pseudotuberculosis*, it was shown that the AHLs produced by the bacterium were susceptible to ring hydrolysis at alkaline pH, thereby initiating switches in phenotypic behaviour in response to changing environment cues [73, 93, 103, 175]. It is likely to be a similar regulatory system present in *E. coli*, where adaptation to changing environments is the key to survival. Ferrándiz *et al* showed that pathogenic strains of *E. coli* encode HosA, a transcriptional regulator associated with the adaptation to environmental stress [68]. While strongly associated with changes in temperature in chapter 3 of this study, it is likely HosA has a role in the adaptation to changes in pH as well. A SlyA homologue has been identified in *Yersinia* spp. regulating virulence factors further supporting this hypothesis [65-67].

The ability of cells within a population to swim was linked with the propensity to form aggregates. For enteropathogenic *E. coli* (EPEC) where cell aggregation increased, population expansion decreased. The cell aggregation was regulated not only by HosA, but also modulated by AHL-dependent quorum sensing. Wild type *E. coli* O157:H7 did not form aggregates, remaining instead as individual planktonic cells (Figure 74). HosA is present in EHEC and it would be interesting to determine whether HosA exerted a similar regulatory role on *E. coli* O157:H7 behaviour as in EPEC. This would require construction of a *hosA* deletion mutant in multiple isolates of *E. coli* O157:H7 from varying sources, such as faecal, environmental and clinical. An important point to note is that the observed change in population expansion in EPEC in response to temperature was not conserved in *E. coli* O157:H7, suggesting a difference in

environmental regulation between these two pathotypes. While probable that HosA has a role in this regulation, it is likely that the pathways are different.

Population expansion, or the ability of a population to swim, was shown to be important in dissemination [15, 63, 269]. Of the *E. coli* O157:H7 isolates used during this study those collected from faeces produced larger motility zones on swimming motility plates in comparison to those collected from the hide. Motility as a phenotype is metabolically expensive for a bacterium. While those adapted to survive within the host are potentially energy rich, those outside the host must conserve energy but also the opportunity to swim is reduced due to the lack of liquid. The need to swim would therefore be reduced when on the hide of an animal, most likely resulting in the regulon required for this phenotype being switched off. The bacterium must be able to initiate production of flagellin when ingested by a host. Although this would probably occur immediately upon a change in the environment, it is possible those bacteria adapted to survive outside the cow would not be able to adapt as quickly to the host environment, making them less likely to colonise and persist internally. Fitness to one environment would not necessarily convey fitness in another. In order to test this theory, evaluation of population expansion by more isolates from different anatomical locations is required.

Addition of specific AHL was shown to affect population expansion by *Yersinia* spp. and during this study in EPEC (Chapter 3) [182]. Sharma *et al* showed that expression from a single copy of *sdiA* from the chromosome repressed motility in *E. coli* O157:H7 [170]. The evidence presented in this study correlated well with this observation. Investigations into the effect of AHL on population expansion by *E. coli* O157:H7 showed that of those tested only *N*-(3-oxohexanoyl)-L-HSL significantly decreased the size of the motility zone (Tables 34 – 36). This observation was conserved across two temperatures and between all isolates tested.

The orphan LuxR homologue SdiA has been shown to optimally bind *N*-(3-oxohexanoyl)-L-HSL in *Salmonella* species [122, 136, 138, 155, 158, 159]. Studies have shown a 69%

homology at amino acid level between SdiA in *Salmonella* and *E. coli*, making it likely that they would bind similar cognate AHLs [136, 162]. In chapter 3 it was shown that addition of both short chain *N*-(3-oxohexanoyl)-L-HSL and long chain *N*-dodecanoyl-L-HSL significantly affected the population expansion of EPEC. Due to the nature of AHL binding in the hydrophobic pocket of the N-terminal in the LuxR proteins, it is likely that a single regulator would bind either short or long chain AHLs, but not both [73, 75, 93, 94, 98, 109, 110, 134-137]. In chapter 3 it was observed that both long and short chain AHLs had an effect on specific phenotypic behaviours of EPEC. Based on these observations the hypothesis was made that *E. coli* may encode a second AHL-binding protein responsible for binding the long chain AHLs. As addition of *N*-dodecanoyl-L-HSL had no significant effect on the population expansion of *E. coli* O157:H7, it may be possible that the hypothesised second regulator protein is not present *E. coli* O157:H7. Further investigations would be required to determine the presence and identity of this putative second regulator in both EPEC and EHEC. Although unsuccessful during this study (Chapter 3, Section 3.3), the production of an *sdiA* mutant in both EPEC and EHEC would allow further investigation of the presence of a putative second AHL-binding protein.

During this study AHLs were extracted from the rumen fluid of a grass fed cow. The pH of the rumen fluid when extracted was neutral measuring pH 6.96. Although acidification would have potentially closed the lactone rings and increased the concentration of the AHLs present and allowed their detection, one signal was successfully extracted from rumen fluid. Confirmation of identification was not possible due to the low concentration of AHL within the sample however, it was clear that the signal was a short chain AHL with a hydrocarbon tail in the range of 5 to 8 carbons in length (Figure 69). Methods such as mass spectrometry and liquid chromatography mass spectrometry, which are routinely used by research groups to identify quorum sensing cues within complex mixtures could be utilised to identify the AHL extracted from the rumen fluid used during this study. Other studies in the US and Canada have reported the presence of *N*-(3-

oxohexanoyl)-L-HSL in the rumen of cattle, confirming the hypothesis that *E. coli* could be exposed to this signal during passage through the bovine gut [35, 169, 173, 174].

During this study rumen fluid was sourced from two different cows; one animal was fed solely on grass, and the other on a mixture of grass and grain. AHL was only found in the extract of rumen fluid from the grass-fed animal, while no AHL was detected from the mixed diet rumen fluid. Diet has been shown to affect the pH within the rumen through changes in the concentration of volatile fatty acids [5]. In addition, rumen fluid is a highly complex biological matrix, which is constantly in flux due to digestion of food matter. The mixture of large particulates such as grass, coupled with digestive enzymes from the host, and exogenous substrates from the microflora alter the composition. Changes in diet and pH would alter the microflora and therefore available AHLs between individual animals, which may explain the inability to successfully extract signals from the second sample. While identified in the rumen, the presence of AHL in the hindgut of the cow remains undetermined. While pH may be a contributing factor to the unsuccessful attempts at extraction of AHL from faeces, it is likely the microbiota plays an important role. The hindgut is colonised by *E. coli* in high numbers, a bacterium incapable of producing AHL. The presence of short chain AHL was confirmed in conditioned media produced from particular psychrotolerant Enterobacteriaceae commonly found on meat surfaces. This suggests the *E. coli* O157:H7 may be exposed to AHL on meat surfaces under the optimal conditions for Enterobacteriaceae growth.

The quorum sensing regulon in *E. coli* O157:H7 controlled by AHL remains unknown, with no effect observed for any of the cell surface components tested during this study. Two putative protein targets were observed, but further analysis would be required to isolate and identify them.

*E. coli* O157:H7 form attaching/effacing (A/E) lesions on human gut epithelial cells, adhering to the surface and initiating host tissue damage. SdiA has been shown to be important

in the regulation of EspD, intimin and Ler, all of which are important in the formation of A/E lesions [58, 95, 201]. When compared to EPEC, *E. coli* O157:H7 did not produce many A/E lesions, those that were visible existing as single entities rather than large clusters. Interestingly of the isolates tested during this study, those sourced from the hide appeared to form a higher number of A/E lesions in comparison to those from the faeces, (Figures 76 - 80). Further analysis using more hide or faecal isolates is required to confirm this observation. While suggesting those adapted to survive in the environment are more suited to successfully adhere to the host, further testing of more isolates would be required before a hypothesis could be put forward. Addition of *N*-(3-oxohexanoyl)-L-HSL appeared to increase the number of A/E lesions formed by those isolates from faeces. This suggests that the low number of A/E lesions observed *in vitro* may be a consequence of the lack of signal molecule. Analysis with a more quantitative technique would be required to confirm any differences in fluorescence. An important point to note is that attachment within the bovine host is likely to be different to that observed on a human cell line. The conditions within the ruminant gut would be different to those within the human bowel, which is therefore likely to change the nature of adherence by *E. coli* O157:H7. Confirmation of this would require production of an immortalised cell line from the bovine hindgut.

In the bovine host *E. coli* O157:H7 do not cause disease, living in symbiosis with the host. In the human host disease can range from mild diarrhoea to more serious sequelae depending on the severity of the infection. *Galleria mellonella* larvae retain some immune responses in common with mammals, such as the production of enzymes and standard innate barrier mechanisms [222-225]. Injection with the bovine isolates of *E. coli* O157:H7 resulted in most of the larvae dying within 48 hours (Table 39). The evidence presented in this study suggests that the isolates from the hide of the cow initiate a greater response to AHL, however this would require further testing to confirm. A clinical isolate of *E. coli* O157:H7 from human faeces was analysed for population expansion during this study. PFGE analysis showed that the

clinical isolate NZRM3441 (E87) was genetically distinct from the other 5 *E. coli* O157:H7 isolates used in this study. Population expansion analysis suggested the clinical isolate may be phenotypically more similar to isolates from cattle faeces (Table 35; Figures 71 and 73). One hypothesis is that faecal isolates from humans and cattle share similar phenotypic traits while being genetically divergent, and the hide isolates are phenotypically more similar to environmental samples than those from the hide. Further phenotypic testing encompassing clinical, bovine and environmental isolates would be required to test this hypothesis fully.

By comparison, *G. mellonella* injected with EPEC had a significantly lower fatality rate than those infected with *E. coli* O157:H7. Interestingly, deletion of *hosA* increased the pathogenicity of EPEC resulting in a higher fatality rate of *G. mellonella* larvae. Addition of AHL appeared to have no obvious effect on the fatality rate, while growth of the HosA mutant in DMEM, which has been shown to increase expression of virulence factors, increased the number of larvae that died due to infection (Tables 40 and 41; Figure 83). It would be interesting to evaluate the effect of different growth conditions and quorum sensing modulation on the pathogenicity of *E. coli* O157:H7 using the *G. mellonella* model. Construction of a HosA mutant in multiple isolates would further increase the knowledge on regulatory pathways within this pathogen.

The evidence presented in this chapter supports the hypothesis of the existence of a complex network of regulation in *E. coli* aiding adaptation to different hosts, environmental conditions and changes in quorum sensing signal concentration.

## **6 General Discussion**

As part of a larger study, the overall goal of this research was to determine whether quorum sensing could be used as a mitigation strategy against *E. coli* O157:H7 contamination of cattle or carcasses, either on farm or during processing respectively. By combining biological data with computational mathematical modelling, the potential for a biocontrol strategy could be evaluated.

*E. coli* are gut organisms which can be either commensal or pathogenic [4, 6]. Whereas commensal strains of *E. coli* can be used for probiotic treatments, pathogenic strains of diarrheagenic *E. coli* can cause a range of sequelae from mild diarrhoea to potentially life threatening disease, including haemolytic uraemic syndrome (HUS), depending on the pathotype [4, 6]. Of the six pathotypes of diarrheagenic *E. coli*, enteropathogenic (EPEC) and enterohaemorrhagic (EHEC) strains are known to be closely related as they derive from a common progenitor, serotype O55 [15, 63, 269]. Enteropathogenic E2348/69 is the most studied strain of diarrheagenic *E. coli*, and shares specific virulence mechanisms with EHEC [4, 6, 13-15, 22, 52, 54, 57, 63, 269]. This study focused initially on EPEC to identify whether or not quorum sensing affected these shared traits, before moving into EHEC with a more targeted investigation.

EPEC is a human pathogen, transmitted predominantly through the faecal-oral route [4, 6]. Studies have shown that this pathogen may be carried on fomites such as dust, providing an airborne route of transmission [4, 6]. The main site of colonisation is the small intestine of the human host where it colonises and persists in high numbers, causing diarrhoea predominantly in children under the age of 2 years and the immunocompromised [4, 6]. Although EPEC are mainly transmitted directly from person to person, the potential for needing to survive in the environment does exist [6]. Fight or flight are two choices that pathogenic bacteria make to survive. When in fight mode, EPEC form communities which work in concert to overwhelm the host immune system and successfully colonise. Attachment to host tissue is important as it anchors the community to one place and allows the sharing of resources for more effective

replication and growth [4, 6, 14, 20, 57, 267, 268]. However, when conditions are not favourable, in order to survive EPEC must be able to disseminate (i.e. flight) to a new colonisation site either within the same host or to a new host where conditions are more favourable [15, 63, 269]. This stage could be described as selfish, being more focused on self-preservation than maintenance of a community. In order to disseminate, bacteria must be able to detach from the micro-colony and swim away [4, 6].

The first hypothesis of this study sought to identify whether exogenous AHL affected specific phenotypic behaviours in EPEC and EHEC. Over the course of this investigation it was observed that the ability of EPEC to disseminate or become motile was linked to the propensity of the population to form aggregates, which in turn, is tied to environmental cues including quorum sensing signals. When the EAF plasmid was present, EPEC did not form aggregates, suggesting this phenotype may be under regulation by a protein encoded on the plasmid, such as Per (Figures 52 and 53). In the absence of the EAF plasmid, the population was able to aggregate under quorum sensing modulation (Figures 29-31, and 55-57). This increase in aggregation would decrease the potential for successful dissemination within the host, but would increase the likelihood of successful colonisation (Table 10). Quantitative analysis of colonisation on immortalised epithelial cell lines and the link with aggregation could be determined using techniques such as flow cytometry, providing numerical data that could feed in to a computational model to understand the association between the two phenotypes. Quorum sensing was shown to be affected by the presence of the environmental regulator, HosA. This protein is part of the MarR family of transcriptional regulators that is responsible for the adaptation of the bacteria to environmental stress [68]. Deletion of HosA significantly increased the size of the aggregates formed in the absence of quorum sensing modulation (Figure 28).

The likelihood is that the switch from survival inside to outside the host and vice versa is associated with environmental cues. The ability to form communities or aggregates has been



linked to temperature, pH and the availability of quorum sensing molecules in other pathogens, such as *Yersinia* spp. [182, 242, 245]. Using quorum sensing the bacterial population is able to 'sense' the population density around it within a defined area [73, 92-95]. Using these cues the bacteria can initiate phenotypic switches allowing an individual bacterium within a population to exhibit multicellular behaviour [73, 93-95].

In other pathogens, such as *Ps. aeruginosa*, regulation by quorum sensing has been shown to occur through a complex hierarchy involving multiple regulators and different signals [73, 75, 96, 98, 109, 110, 185, 186]. Additional molecules can act as signals, such as cyclic-di-GMP. Initially described as cellulose synthase activator, it has since been shown to regulate the expression of virulence factors, such as those associated with the production of biofilms in pathogens including *Ps. aeruginosa* [65, 66, 204]. Quorum sensing and cyclic-di-GMP have been linked in regulatory pathways in *Vibrio cholerae* [270]. In this bacterium quorum sensing controls the expression of a small regulatory RNA which positively regulates the production of c-di-GMP. Research is currently underway to address the potential for using c-di-GMP as an antivirulent/antibiotic treatment [204, 271]. Orphan LuxR homologues and species-specific chemical cues, such as the *Pseudomonas* Quinolone Signal (PQS), add to this complexity [98, 110]. It is likely these types of hierarchical systems are found in other bacterial species, such as EPEC.

*E. coli* encode two quorum sensing systems, the AHL/SdiA and AI-2/LuxS systems [73, 75, 93, 94, 98, 109, 127, 137, 143, 144]. The production and regulation of AI-2 occurs in *E. coli* [73, 75, 94, 95, 192]. Raina *et al* identified 242 genes within the *E. coli* genome associated with virulence and cell division, the expression of which was affected by the presence of AI-2 [185]. Studies have also linked the presence of LuxS with expression of genes within the locus of enterocyte effacement (LEE), which is responsible for the intimate attachment of EPEC and EHEC to host cells [58, 95, 201]. Despite the evidence of quorum sensing modulation by AI-2 in

*Vibrio* spp., mounting evidence suggested a more metabolic role in *E. coli* as the signal is generated as a by-product of the activated methyl cycle (AMC) [194, 195]. During this cycle one AI-2 molecule is produced for each methionine molecule that is metabolised [195]. Concentrations of AI-2 have been shown to increase rapidly during the mid- to late-exponential phase of growth, thereby suggesting a link between the production of the signal to growth and metabolism rather than quorum sensing only [194, 195]. It is likely that LuxS and AI-2 have different roles in different bacterial species.

By comparison, *E. coli* do not encode a LuxI synthase and cannot produce AHLs, but they do contain an orphan LuxR-type AHL binding protein, SdiA [122, 136, 138, 155, 158, 159]. By binding exogenous AHL from the external milieu produced by other gram negative bacteria, *E. coli* can sense the total population density within a defined area [73, 92-94, 96, 111, 124, 127]. This voyeuristic approach allows *E. coli* to benefit from AHL-dependent quorum sensing without expending energy in signal production. Like the AI-2 system, SdiA has been associated with the regulation of expression of the LEE locus, specifically several secreted proteins required for the production of the attaching/effacing lesions [61, 134, 161, 168]. In addition, SdiA also functions as a transcriptional activator of the *ftsQAZ* operon required for cell division [61, 101, 122, 165, 166].

It was observed that addition of AHL to an EPEC isolate lacking HosA lead to decreased aggregation, thereby increasing the propensity of the population to disseminate (Table 12; Figures 32-34). The second hypothesis related to the identity of the regulatory network required to control these phenotypes (Introduction, section 1.7). Based on the evidence in this study, a hypothetical model for the regulation of aggregation was developed (Figure 85). In the presence of the EAF plasmid, the regulation of aggregation would be predominantly by Per via an unidentified regulatory pathway. However, in the absence of Per, the model combines hierarchical regulation by HosA and quorum sensing modulation.

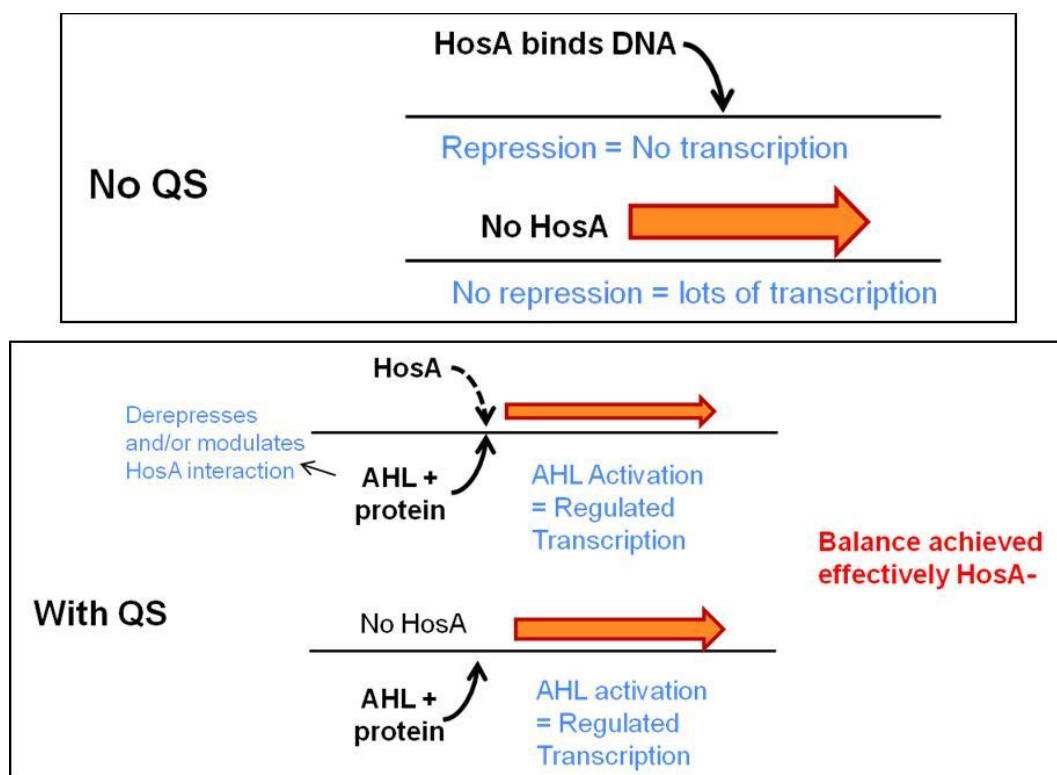


**Figure 85 – Hypothetical model of the regulation of aggregation in enteropathogenic *E. coli***  
 This model is based on the absence of the EAF plasmid, and could potentially be extrapolated to include *E. coli* O157:H7.

Wild type EPEC contains HosA [68]. In the model, HosA, acting as a repressor, would bind the promoter site of the gene encoding an unidentified protein required for cell aggregation. The resultant low level of transcription would therefore result in a non-aggregating population. In the presence of specific quorum sensing signals, such as *N*-(3-oxohexanoyl)-L-HSL, there would be competition for the DNA binding site between the AHL/SdiA complex and HosA. Successful binding by the AHL/SdiA complex would result in DNA transcription under quorum sensing modulation, leading to an increase in cell aggregation (Figures 29 and 30).

In the absence of HosA, the repression of DNA transcription would not occur, allowing the bacterial population to form large aggregates as observed for the HosA mutant (Figures 32 and 33). Addition of AHL to this strain would initiate the formation of AHL/SdiA complexes which would bind the DNA transcription site, modulating aggregation in a density-dependent manner. This would make the aggregation profile of the HosA mutant equivalent to the wild type, as observed during this study (Figure 35).

As part of the second hypothesis, the effects of a second signal, AI-2, was investigated. Addition of exogenous AI-2 via AI-2 positive CM was observed to affect the strength of the aggregates formed by EPEC. It is worth noting that although other exogenous factors may be added in addition to AI-2, the effect of these is mitigated by the use of appropriate control CMs. Although not confirmed by atomic force microscopy, differences in characteristics were observed during vortexing when the aggregates formed in the absence of CM were more difficult to disperse. Addition of AI-2 positive CM made disruption of the aggregates occur more readily. This suggests that although associated with metabolism, AI-2 may also have a regulatory role in cell aggregation in EPEC. Where this would fit in to the hypothetical model shown in Figure 85 is unclear at present. Further study is required to identify the regulatory bridge between the two quorum sensing systems.

*E. coli* O157:H7 is a common cause of foodborne related disease around the world (Section 1.1.3.2) [4, 6]. Although highly pathogenic to human hosts, this strain persists in high numbers in the hindgut of the bovine reservoir without causing disease [5, 23, 28, 31-33, 37, 39-41, 49, 50, 56, 85, 171, 250, 272]. It was hypothesised at the beginning of this study that not all *E. coli* O157:H7 isolates behaved the same. As observed for EPEC, *E. coli* O157:H7 exhibits a dual lifestyle requiring a switch from host to environment and vice versa.

*E. coli* O157:H7 colonises the bovine reservoir, increasing the bacterial population to between  $10^2$  and  $10^6$  cfu/g of faeces (Section 1.1.3.1) [6, 23, 27, 31]. This high population density results in regular dissemination of a proportion of the bacterial community to a new colonisation site or shed to the environment. *E. coli* O157:H7 is likely to undergo spontaneous mutation and acquisition of extracellular DNA, allowing adaptation to different environments and through natural selection those better adapted to a particular niche will survive. Excretion of *E. coli* O157:H7 in faeces ultimately requires adaptation to the new environment and a switch in the metabolic state of the bacterium. Those bacteria that can adapt are able to persist in that niche. This ability to adapt and survive within different environments may contribute to the evolution of novel pathogens, such as *E. coli* O103:H25 in Norway and *E. coli* O104:H4 in Germany (Section 1.1.3.2).

*E. coli* O157:H7 can survive in the environment for long periods of time, shutting down non-essential functions and diverting all energy to survival mechanisms [27, 39-41]. Attachment to the bovine hide can not only increase the temperature but also provide consistency, however this does not improve the nutrient availability. *E. coli* O157:H7 are transferred from the ground or hide into a new host by ingestion through licking or grooming by animals in the herd. Calves can acquire *E. coli* O157:H7 through feeding or grooming. The change from initially being external to the host to entering the host requires a behavioural switch [27, 39-41]. This ability to adapt to different environments was illustrated by the difference of the bacteria to disseminate (Tables 34-

36; Figures 71-73). Conversely to EPEC, *E. coli* O157:H7 did not form aggregates (Figure 74). The change in population expansion was therefore more likely to have occurred through changes in the regulation of other cell components, such as fimbriation and flagellation [170].

*E. coli* O157:H7 does not contain the EAF plasmid [4, 6]. If the hypothetical model in Figure 85 were true for EHEC, addition of *N*-(3-oxohexanoyl)-L-HSL would increase cell aggregation. As this was not observed, it is likely that aggregative behaviours by EHEC would be controlled by other regulatory pathways. During this study weak aggregates of *E. coli* O157:H7 were observed but were unstable and easily and quickly dispersed through movement of planktonic cells past the aggregates. Using different growth conditions, it may be possible to strengthen the interactions within aggregates of *E. coli* O157:H7 and thereby identify if AHL truly has an effect on these phenotype. *E. coli* O157:H7 contain the pO157 plasmid, which encodes a range of genes including those responsible for the production of several important adhesins (Section 1.1.4.5) [6]. Where *E. coli* O157:H7 lack regulation by Per, aggregation in *E. coli* O157:H7 could potentially be under the control of a regulator encoded on this EHEC specific plasmid. Production of a pO157 knock-out mutant would test this hypothesis.

HosA is encoded in all pathogenic strains of *E. coli* [68]. As in EPEC, aggregation may be part of a hierarchical regulatory system in *E. coli* O157:H7. Deletion of *hosA* from multiple strains of *E. coli* O157:H7 isolated from different environments would determine whether HosA has a similar role in EHEC as in EPEC with regard to cell aggregation and dissemination. When combined with the pO157 knock-out mutant, analysis of population expansion and the effect of quorum sensing would confirm whether the hypothetical model of regulation could be extrapolated to encompass *E. coli* O157:H7 (Figure 85).

The last hypothesis in this study pertained to the effect of exogenous AHL on the virulence of EPEC and EHEC strains. EPEC produce a large number of A/E lesions localised in clusters on human epithelial cells, but rarely cause death during infection as observed in the *G.*

*mellonella* infection studies (Tables 40 - 41; Figures 64 - 67 and 81 - 82). Conversely, *E. coli* O157:H7 form sporadic A/E lesions on human epithelial cells but infection of *G. mellonella* resulted in a significantly higher death rate, possibly due to the production of toxins (Table 39; Figures 76 - 80 and 82). Within a human host, the EHEC-released toxin binds to Gb<sub>3</sub> and Gb<sub>4</sub> receptors on the renal epithelia resulting in severe host damage and haemolytic diarrhoea in humans [4, 6]. *E. coli* O157:H7 cause asymptomatic infection in cows and the toxin has no effect on the host due to the lack of cognate receptors [4-6, 23, 28, 31-33, 37, 39-41, 49, 50, 56, 85, 171, 250, 272]. Although the pattern of attachment is unknown in the bovine host, it is likely to be more closely aligned to the EPEC model observed in humans due to the high *E. coli* density that builds in the hindgut.

*E. coli* O157:H7 are transferred from the bovine reservoir to the human host through direct contact with the animal, or consumption of contaminated foodstuffs such as undercooked meat, unpasteurised apple juice/ cider, raw milk or radish sprouts (Section 1.1.3.2) [4, 6]. The most common route of transmission in the USA and UK is the ingestion of contaminated red meat although incidences of *E. coli* O157:H7 infection via contact with animals at petting zoos in the UK has been recorded [25, 31, 44]. For example, In the USA approximately 20,000 cases of *E. coli* infection from ingestion of undercooked red meat are recorded every year, while over 700 cases were recorded in Scotland between 1990 and 1996 from the same vector of transmission [31, 39-41, 44]. In New Zealand contact with environmental sources is the main cause of *E. coli* O157:H7 related disease, particularly in areas of intensive dairy farming [23, 31, 49-51, 56]. Economically New Zealand relies on the export of raw red meat products to other countries. *E. coli* O157:H7 do not invade bovine tissue, but rather adheres to the epithelial layer in the intestinal tract [4, 6, 64]. During the slaughter process, muscle is exposed and the bacteria can be transferred from hide or faeces onto the exposed surfaces of the carcass [39, 41, 45, 46]. Treatment with multiple interventions, such as chemical washes, significantly decreases the

number of pathogenic bacteria on the meat surface, but does not eradicate them entirely [46].

Meat research does not look solely at processing, but has a wider aspect looking at the entire food chain. Often described as a 'farm to fork' approach, scientists are now considering the potential for *E. coli* O157:H7 mitigation on farm to decrease the load on the hide at slaughter, thereby decreasing the risk of transfer to the carcass.

Studies have shown AHL activity can be synergistic, agonistic or antagonistic, but can also be mimicked [110, 143]. The use of quorum quenching agents to inactivate the quorum sensing systems is one possible strategy being researched at present [144, 273-276]. The application and addition of antagonistic AHLs which would actively compete for binding of the N-terminal of the LuxR transcriptional regulator has been suggested as another mechanism for intervention [27, 39-41]. The use of biomimics, which are not AHLs but have a similar structure would potentially have the same effect as the antagonists [110]. In addition, acylases and lactonases are two families of enzyme produced by gram positive bacteria which inactivate the AHL signal [73, 100, 110]. Addition of any of these treatments may help decrease the *E. coli* O157:H7 population in the bovine reservoir.

However, *E. coli* are not the only bacteria present in the gastro-intestinal tract of the cow. The effect of any potential treatment would require the analysis of the effects on the entire microflora exposed to the mitigation. AHLs have not been successfully isolated from faeces [35, 173, 174]. Although this could suggest an absence of AHL-producing bacteria within the hindgut, it is more likely that extraction of these signals from the complex biological matrix is difficult. Identification of the microflora within bovine faeces would indicate whether AHL production was likely within this environment. By combining biological data with computational mathematical modelling, it may be possible to predict the effect of any treatment on the microflora within a host.

As part of this study the data collected on population expansion, cell aggregation and the effect of quorum sensing on these phenotypes is being used to develop a mathematical model.



The advantage in modelling specific behaviours is to assess the validity of multiple hypotheses *in silico* rather than *in vitro*, thereby saving on experimental costs.

Mathematical modelling of aggregation can be approached via a top-down or bottom-up perspective. In the top-down approach, differential equations are used to model the population behaviour, for example the proportion of a given population which are within aggregates. These are subject to assumptions of homogeneous distribution of the population in space and time, which is unlikely to occur during the aggregation of a bacterial population. The alternate bottom-up approach models individual bacteria as ‘particles’ which interact within their localised niche. This method uses interacting particle systems (IPS) to describe the behaviour of an individual bacterium at each time point using defined conditions within the milieu, for example a bacterium may aggregate if spatial and environmental conditions are suitable [277]. In terms of quorum sensing, this model would account for the effect of cell density and signal concentration. Using these defined characteristics of the behaviour of an individual bacterium, the population behaviour evolves with no assumptions of spatial homogeneity. For the modelling of the aggregation observed during this study, the model parameters would be inferred using a variety of methods, such as Approximate Bayesian Computing (ABC), where the behaviours arising from simulations are compared to the experimental results to identify parameters most closely resembling the biological data [211].

Using this type of model, it would be possible to determine the effect of a proposed intervention when given as a single treatment at a specific concentration, or as multiple treatments. It may also be possible to identify the optimal mitigation point along the farm-to-fork continuum. The model will therefore be a useful tool as it would predict behaviours allowing more targeted biological strategies to be adopted. The aim of any mitigation would be to increase shedding of *E. coli* O157:H7 for a short period of time prior to slaughter, particularly to provide an overall decrease in the bacterial load at the time of slaughter.

The key findings from this study are summarised in Figure 86. During this study it was observed that *N*-(3-oxohexanoyl)-L-HSL significantly decreased the potential for dissemination by *E. coli* O157:H7. By identifying an antagonistic treatment it may be possible to utilise quorum sensing as a mitigation strategy against contamination and persistence of *E. coli* O157:H7 in the future.



## **7 References**

1. Rajilić-Stojanović, M., H. Smidt, and W.M. De Vos, *Diversity of the human gastrointestinal tract microbiota revisited*. Environmental Microbiology, 2007. **9**(9): p. 2125-2136.
2. Mims, C., A. Nash, and J. Stephen, *Mims' Pathogenesis of Infectious Disease*. 5th ed. 2002, London: Elsevier Academic Press.
3. Madigan, M.T. and J.M. Martinko, *Brock Biology of Microorganisms*. 11 ed. 2000: Pearson Prentice Hall.
4. Kaper, J.B., J.P. Nataro, and H.L.T. Mobley, *Pathogenic Escherichia coli*. Nature Reviews Microbiology, 2004. **2**(2): p. 123-140.
5. Callaway, T.R., M.A. Carr, T.S. Edrington, R.C. Anderson, and D.J. Nisbet, *Diet, Escherichia coli O157:H7, and cattle: A review after 10 years*. Current Issues in Molecular Biology, 2009. **11**(2): p. 67-80.
6. Nataro, J.P. and J.B. Kaper, *Diarrheagenic Escherichia coli*. Clinical Microbiology Reviews, 1998. **11**(1): p. 142-201.
7. Auvray, F., F. Dilasser, D. Bibbal, M. Kérouédan, E. Oswald, and H. Brugère, *French cattle is not a reservoir of the highly virulent enteroaggregative Shiga toxin-producing Escherichia coli of serotype O104:H4*. Veterinary Microbiology, 2012.
8. Hao, W., V.G. Allen, F.B. Jamieson, D.E. Low, and D.C. Alexander, *Phylogenetic incongruence in E. coli O104: Understanding the evolutionary relationships of emerging pathogens in the face of homologous recombination*. PLoS ONE, 2012. **7**(4).
9. King, L.A., F. Nogareda, F.X. Weill, P. Mariani-Kurkdjian, E. Loukiadis, G. Gault, N. Jourdan-Dasilva, E. Bingen, M. MacÉ, D. Thevenot, N. Ong, C. Castor, H. Noël, D. Van Cauteren, M. Charron, V. Vaillant, B. Aldabe, V. Goulet, G. Delmas, E. Couturier, Y. Le Strat, C. Combe, Y. Delmas, F. Terrier, B. Vendrely, P. Rolland, and H. De Valk, *Outbreak of shiga toxin-producing escherichia coli O104:H4 Associated with organic fenugreek sprouts, France, June 2011*. Clinical Infectious Diseases, 2012. **54**(11): p. 1588-1594.
10. L'Abée-Lund, T.M., H.J. Jørgensen, K. O'Sullivan, J. Bohlin, G. Ligård, P.E. Granum, and T. Lindbäck, *The highly virulent 2006 Norwegian EHEC O103:H25 outbreak strain is related to the 2011 German O104:H4 outbreak strain*. PLoS ONE, 2012. **7**(3).

11. Laing, C.R., Y. Zhang, M.W. Gilmour, V. Allen, R. Johnson, J.E. Thomas, and V.P.J. Gannon, *A comparison of Shiga-Toxin 2 bacteriophage from classical enterohemorrhagic escherichia coli serotypes and the German E. coli O104:H4 outbreak strain*. PLoS ONE, 2012. **7**(5).
12. Wu, C.J., P.R. Hsueh, and W.C. Ko, *A new health threat in Europe: Shiga toxin-producing Escherichia coli O104:H4 infections*. Journal of Microbiology, Immunology and Infection, 2011. **44**(5): p. 390-393.
13. Bieber, D., S.W. Ramer, C.Y. Wu, W.J. Murray, T. Tobe, R. Fernandez, and G.K. Schoolnik, *Type IV pili, transient bacterial aggregates, and virulence of enteropathogenic escherichia coli*. Science, 1998. **280**(5372): p. 2114-2118.
14. Knutton, S., R.K. Shaw, R.P. Anantha, M.S. Donnenberg, and A.A. Zorgani, *The type IV bundle-forming pilus of enteropathogenic Escherichia coli undergoes dramatic alterations in structure associated with bacterial adherence, aggregation and dispersal*. Molecular Microbiology, 1999. **33**(3): p. 499-509.
15. Weiss-Muszkat, M., D. Shakh, Y. Zhou, R. Pinto, E. Belausov, M.R. Chapman, and S. Sela, *Biofilm formation by and multicellular behavior of Escherichia coli O55:H7, an atypical enteropathogenic strain*. Applied and Environmental Microbiology, 2010. **76**(5): p. 1545-1554.
16. Vieira, M.A.M., J.R.C. Andrade, L.R. Trabulsi, A.C.P. Rosa, A.M.G. Dias, S.R.T.S. Ramos, G. Frankel, and T.A.T. Gomes, *Phenotypic and genotypic characteristics of Escherichia coli strains of non-Enteropathogenic E. coli (EPEC) serogroups that carry eae and lack the EPEC adherence factor and shiga toxin DNA probe sequences*. Journal of Infectious Diseases, 2001. **183**(5): p. 762-772.
17. Cravioto, A., R.E. Reyes, R. Ortega, G. Fernandez, R. Hernandez, and D. Lopez, *Prospective study of diarrhoeal disease in a cohort of rural Mexican children: incidence and isolated pathogens during the first two years of life*. Epidemiol Infect, 1988. **101**(1): p. 123-34.
18. Gomes, T.A.T., V. Rassi, K.L. MacDonald, S.R.T.S. Ramos, L.R. Trabulsi, M.A.M. Vieira, B.E.C. Guth, J.A.N. Candeias, C. Ivey, M.R.F. Toledo, and P.A. Blake, *Enteropathogens associated with acute diarrheal disease in urban infants in Sao Paulo, Brazil*. Journal of Infectious Diseases, 1991. **164**(2): p. 331-337.
19. Robins-Browne, R.M., M.M. Levine, B. Rowe, and E.M. Gabriel, *Failure to detect conventional enterotoxins in classical enteropathogenic (serotyped) Escherichia coli strains of proven pathogenicity*. Infection and Immunity, 1982. **38**(2): p. 798-801.

20. Levine, M.M. and R. Edelman, *Enteropathogenic Escherichia coli of classic serotypes associated with infant diarrhea: epidemiology and pathogenesis*. Epidemiol Rev, 1984. **6**: p. 31-51.
21. Trabulsi, L.R., R. Keller, and T.A. Tardelli Gomes, *Typical and atypical enteropathogenic Escherichia coli*. Emerging Infectious Diseases, 2002. **8**(5): p. 508-513.
22. Krause, G., S. Zimmermann, and L. Beutin, *Investigation of domestic animals and pets as a reservoir for intimin- (eae) gene positive Escherichia coli types*. Veterinary Microbiology, 2005. **106**(1-2): p. 87-95.
23. Chase-Topping, M., D. Gally, C. Low, L. Matthews, and M. Woolhouse, *Super-shedding and the link between human infection and livestock carriage of Escherichia coli O157*. Nature Reviews Microbiology, 2008. **6**(12): p. 904-912.
24. Sperandio, V., A.G. Torres, B. Jarvis, J.P. Nataro, and J.B. Kaper, *Bacteria-host communication: The language of hormones*. Proceedings of the National Academy of Sciences of the United States of America, 2003. **100**(15): p. 8951-8956.
25. (WHO), W.H.O. *World Health Organisation*. 2010 23/02/2010]; Available from: <http://www.who.int>
26. Mellmann, A., M. Bielaszewska, L.B. Zimmerhackl, R. Prager, D. Harmsen, H. Tschäpe, and H. Karch, *Enterohemorrhagic Escherichia coli in human infection: In vivo evolution of a bacterial pathogen*. Clinical Infectious Diseases, 2005. **41**(6): p. 785-792.
27. Silagyi, K., S.H. Kim, Y. Martin Lo, and C.i. Wei, *Production of biofilm and quorum sensing by Escherichia coli O157:H7 and its transfer from contact surfaces to meat, poultry, ready-to-eat deli, and produce products*. Food Microbiology, 2009. **26**(5): p. 514-519.
28. Caprioli, A., S. Morabito, H. Brugère, and E. Oswald, *Enterohaemorrhagic Escherichia coli: Emerging issues on virulence and modes of transmission*. Veterinary Research, 2005. **36**(3): p. 289-311.
29. Bosilevac, J.M. and M. Koohmaraie, *Prevalence and characterization of non-O157 shiga toxin-producing Escherichia coli isolates from commercial ground beef in the United States*. Applied and Environmental Microbiology, 2011. **77**(6): p. 2103-2112.
30. (CDC), C.f.D.C.a.P. *Recommendations for diagnosis of shiga toxin-producing Escherichia coli infections by clinical laboratories*. 2009 29/03/2012].
31. Money, P., A.F. Kelly, S.W.J. Gould, J. Denholm-Price, E.J. Threlfall, and M.D. Fielder, *Cattle, weather and water: Mapping Escherichia coli O157:H7 infections in humans in England and Scotland*. Environmental Microbiology, 2010. **12**(10): p. 2633-2644.

32. Besser, T.E., B.L. Richards, D.H. Rice, and D.D. Hancock, *Escherichia coli* O157:H7 Infection of calves: Infectious dose and direct contact transmission. *Epidemiology and Infection*, 2001. **127**(3): p. 555-560.
33. Schurman, R.D., H. Hariharan, S.B. Heaney, and K. Rahn, *Prevalence and characteristics of Shiga toxin-producing Escherichia coli in beef cattle slaughtered on Prince Edward Island*. *Journal of Food Protection*, 2000. **63**(11): p. 1583-1586.
34. Naylor, S.W., J.C. Low, T.E. Besser, A. Mahajan, G.J. Gunn, M.C. Pearce, I.J. McKendrick, D.G.E. Smith, and D.L. Gally, *Lymphoid follicle-dense mucosa at the terminal rectum is the principal site of colonization of enterohemorrhagic Escherichia coli O157:H7 in the bovine host*. *Infection and Immunity*, 2003. **71**(3): p. 1505-1512.
35. Edrington, T.S., R.L. Farrow, V. Sperandio, D.T. Hughes, T.E. Lawrence, T.R. Callaway, R.C. Anderson, and D.J. Nisbet, *Acyl-homoserine-lactone autoinducer in the gastrointestinal tract of feedlot cattle and correlation to season, E. Coli O157:H7 prevalence, and diet*. *Current Microbiology*, 2009. **58**(3): p. 227-232.
36. Heinrichs, A.J. and C.M. Jones, *Feeding the newborn dairy calf*, P.S.U. College of Agricultural Sciences, Editor. 2003: USA.
37. Callaway, T.R., J.A. Carroll, J.D. Arthington, C. Pratt, T.S. Edrington, R.C. Anderson, M.L. Galyean, S.C. Ricke, P. Crandall, and D.J. Nisbet, *Citrus products decrease growth of E. coli O157:H7 and Salmonella typhimurium in pure culture and in fermentation with mixed ruminal microorganisms in vitro*. *Foodborne Pathogens and Disease*, 2008. **5**(5): p. 621-627.
38. Girenavar, B., M.L. Cepeda, K.A. Soni, A. Vikram, P. Jesudhasan, G.K. Jayaprakasha, S.D. Pillai, and B.S. Patil, *Grapefruit juice and its furocoumarins inhibits autoinducer signaling and biofilm formation in bacteria*. *International Journal of Food Microbiology*, 2008. **125**(2): p. 204-208.
39. Arthur, T.M., D.M. Brichta-Harhay, J.M. Bosilevac, N. Kalchayanand, S.D. Shackelford, T.L. Wheeler, and M. Koohmaraie, *Super shedding of Escherichia coli O157:H7 by cattle and the impact on beef carcass contamination*. *Meat Science*, 2010. **86**(1): p. 32-37.
40. Arthur, T.M., J.E. Keen, J.M. Bosilevac, D.M. Brichta-Harhay, N. Kalchayanand, S.D. Shackelford, T.L. Wheeler, X. Nou, and M. Koohmaraie, *Longitudinal study of Escherichia coli O157:H7 in a beef cattle feedlot and role of high-level shedders in hide contamination*. *Applied and Environmental Microbiology*, 2009. **75**(20): p. 6515-6523.

41. Arthur, T.M., X. Nou, N. Kalchayanand, J.M. Bosilevac, T. Wheeler, and M. Koohmaraie, *Survival of Escherichia coli O157:H7 on cattle hides*. Applied and Environmental Microbiology, 2011. **77**(9): p. 3002-3008.
42. Gill, C.O. and K.G. Newton, *The ecology of bacterial spoilage of fresh meat at chill temperatures*. Meat Science, 1978. **2**(3): p. 207-217.
43. Newton, K.G., J.C. Harrison, and A.M. Wauters, *Sources of psychrotrophic bacteria on meat at the abattoir*. Journal of Applied Bacteriology, 1978. **45**(1): p. 75-82.
44. Coia, J.E., *Clinical, microbiological and epidemiological aspects of Escherichia coli O157 infection*. FEMS Immunology and Medical Microbiology, 1998. **20**(1): p. 1-9.
45. Gill, C.O., *SPOILAGE, FACTORS AFFECTING | Microbiological*, in *Encyclopedia of Meat Sciences*, J. Werner Klinth, Editor. 2004, Elsevier: Oxford. p. 1324-1330.
46. Koutsoumanis, K. and J.N. Sofos, *MICROBIAL CONTAMINATION*, in *Encyclopedia of Meat Sciences*, J. Werner Klinth, Editor. 2004, Elsevier: Oxford. p. 727-737.
47. Rode, T.M., L. Axelsson, P.E. Granum, E. Heir, A. Holck, and T.M. L'Abée-Lund, *High stability of Stx2 phage in food and under food-processing conditions*. Applied and Environmental Microbiology, 2011. **77**(15): p. 5336-5341.
48. Cookson, A.L., M. Cao, J. Bennett, C. Nicol, F. Thomson-Carter, and G.T. Attwood, *Relationship between Virulence gene profiles of atypical enteropathogenic escherichia coli and shiga toxin producing E. coli isolates from cattle and sheep in New Zealand*. Applied and Environmental Microbiology, 2010. **76**(11): p. 3744-3747.
49. Irshad, H., A.L. Cookson, G. Hotter, T.E. Besser, S.L.W. On, and N.P. French, *Epidemiology of Shiga toxin-producing Escherichia coli O157 in very young calves in the North Island of New Zealand*. New Zealand Veterinary Journal, 2012. **60**(1): p. 21-26.
50. Baker, M., R. Eyles, J. Bennett, C. Nicol, W. Wong, and N. Garrett, *Emergence of verotoxigenic Escherichia coli (VTEC) in New Zealand*. New Zealand Public Health Report, 1999. **6**(2): p. 9-12.
51. ESR, E.S.a.R.L. *Public Health Surveillance*. 2012 [cited 2012 April 2012]; Public Health Surveillance, monthly and annual reports of notifiable and non-notifiable infections in New Zealand]. Available from: <http://www.surv.esr.cri.nz/>
52. Giron, J.A., H. Alice Suk Yue, and G.K. Schoolnik, *An inducible bundle-forming pilus of enteropathogenic Escherichia coli*. Science, 1991. **254**(5032): p. 710-713.
53. Kenny, B., *Enteropathogenic Escherichia coli (EPEC)-- a crafty subversive little bug*. Microbiology, 2002. **148**(Pt 7): p. 1967-78.



54. Saldaña, Z., A.L. Erdem, S. Schüller, I.N. Okeke, M. Lucas, A. Sivananthan, A.D. Phillips, J.B. Kaper, J.L. Puente, and J.A. Girón, *The Escherichia coli common pilus and the bundle-forming pilus act in concert during the formation of localized adherence by enteropathogenic E. coli*. Journal of Bacteriology, 2009. **191**(11): p. 3451-3461.
55. Castillo, A., L.E. Eguiarte, and V. Souza, *A genomic population genetics analysis of the pathogenic enterocyte effacement island in Escherichia coli: The search for the unit of selection*. Proceedings of the National Academy of Sciences of the United States of America, 2005. **102**(5): p. 1542-1547.
56. Garmendia, J., G. Frankel, and V.F. Crepin, *Enteropathogenic and enterohemorrhagic Escherichia coli infections: Translocation, translocation, translocation*. Infection and Immunity, 2005. **73**(5): p. 2573-2585.
57. Cleary, J., L.C. Lai, R.K. Shaw, A. Straatman-Iwanowska, M.S. Donneberg, G. Frankel, and S. Knutton, *Enteropathogenic Escherichia coli (EPEC) adhesion to intestinal epithelial cells: Role of bundle-forming pili (BFP), EspA filaments and intimin*. Microbiology, 2004. **150**(3): p. 527-538.
58. Sperandio, V., J.L. Mellies, W. Nguyen, S. Shin, and J.B. Kaper, *Quorum sensing controls expression of the type III secretion gene transcription and protein secretion in enterohemorrhagic and enteropathogenic Escherichia coli*. Proceedings of the National Academy of Sciences of the United States of America, 1999. **96**(26): p. 15196-15201.
59. Ritchie, J.M. and M.K. Waldor, *The locus of enterocyte effacement-encoded effector proteins all promote enterohemorrhagic Escherichia coli pathogenicity in infant rabbits*. Infection and Immunity, 2005. **73**(3): p. 1466-1474.
60. Hancock, D., T. Besser, J. Lejeune, M. Davis, and D. Rice, *The control of VTEC in the animal reservoir*. International Journal of Food Microbiology, 2001. **66**(1-2): p. 71-78.
61. Anand, S.K. and M.W. Griffiths, *Quorum sensing and expression of virulence in Escherichia coli O157:H7*. International Journal of Food Microbiology, 2003. **85**(1-2): p. 1-9.
62. Campellone, K.G., D. Robbins, and J.M. Leong, *EspFU is a translocated EHEC effector that interacts with Tir and N-WASP and promotes Nck-independent actin assembly*. Developmental Cell, 2004. **7**(2): p. 217-228.

63. Kyle, J.L., C.A. Cummings, C.T. Parker, B. Quiñones, P. Vatta, E. Newton, S. Huynh, M. Swimley, L. Degoricija, M. Barker, S. Fontanoz, K. Nguyen, R. Patel, R. Fang, R. Tebbs, O. Petrauskene, M. Furtado, and R.E. Mandrell, *Escherichia coli* Serotype O55:H7 Diversity Supports Parallel Acquisition of Bacteriophage at Shiga Toxin Phage Insertion Sites during evolution of the O157:H7 lineage. *Journal of Bacteriology*, 2012. **194**(8): p. 1885-1896.
64. Kaper, J.B., S. Elliott, V. Sperandio, N.T. Perna, G.F. Mayhew, and F.R. Blattner, *Attaching-and-Effacing Intestinal Histopathology and the Locus of Enterocyte Effacement*, in *Escherichia coli* O157:H7 and Other Shiga Toxin-Producing *E. coli* Strains, J.B. Kaper and A.D. O'Brien, Editors. 1998, ASM Press: Washington D.C. p. 163 - 182.
65. Ross, P., H. Weinhouse, Y. Aloni, D. Michaeli, P. Weinberger-Ohana, R. Mayer, S. Braun, E.d. Vroom, G.A.v.d. Marel, J.H.v. Boom, and M. Benziman, *Regulation of cellulose synthesis in Acetobacter xylinum by cyclic diguanylic acid*. *Nature*, 1987. **325**(6101): p. 279-281.
66. Kulesekara, H., V. Lee, A. Brencic, N. Liberati, J. Urbach, S. Miyata, D.G. Lee, A.N. Neely, M. Hyodo, Y. Hayakawa, F.M. Ausubel, and S. Lory, *Analysis of Pseudomonas aeruginosa diguanylate cyclases and phosphodiesterases reveals a role for bis-(3'-5')-cyclic-GMP in virulence*. *Proceedings of the National Academy of Sciences of the United States of America*, 2006. **103**(8): p. 2839-2844.
67. Lee, E.C., D. Yu, J. Martinez de Velasco, L. Tessarollo, D.A. Swing, D.L. Court, N.A. Jenkins, and N.G. Copeland, *A highly efficient Escherichia coli-based chromosome engineering system adapted for recombinogenic targeting and subcloning of BAC DNA*. *Genomics*, 2001. **73**(1): p. 56-65.
68. Ferrándiz, M.J., K. Bishop, P. Williams, and H. Withers, *HosA, a member of the SlyA family, regulates motility in enteropathogenic Escherichia coli*. *Infection and Immunity*, 2005. **73**(3): p. 1684-1694.
69. Atkinson, S., R.E. Sockett, M. Cámara, and P. Williams, *Quorum sensing and the lifestyle of Yersinia*. *Current Issues in Molecular Biology*, 2006. **8**(1): p. 1-10.
70. Schleheck, D., N. Barraud, J. Klebensberger, J.S. Webb, D. McDougald, S.A. Rice, and S. Kjelleberg, *Pseudomonas aeruginosa PAO1 preferentially grows as aggregates in liquid batch cultures and disperses upon starvation*. *PLoS ONE*, 2009. **4**(5).
71. Lawrence, E., ed. *Henderson's Dictionary of Biological Terms*. 12th Edition ed. 2000, Pearson Prentice Hall: Harlow, Essex, UK.

72. Costerton, J.W., P.S. Stewart, and E.P. Greenberg, *Bacterial biofilms: A common cause of persistent infections*. Science, 1999. **284**(5418): p. 1318-1322.
73. Frederix, M. and A.J. Downie, *Quorum Sensing. Regulating the Regulators*. 2011. p. 24-80.
74. Govan, J.R.W. and V. Deretic, *Microbial pathogenesis in cystic fibrosis: Muroid Pseudomonas aeruginosa and Burkholderia cepacia*. Microbiological Reviews, 1996. **60**(3): p. 539-574.
75. Miller, M.B. and B.L. Bassler, *Quorum sensing in bacteria*. 2001. p. 165-199.
76. Piletska, E.V., G. Stavroulakis, L.D. Larcombe, M.J. Whitcombe, A. Sharma, S. Primrose, G.K. Robinson, and S.A. Piletsky, *Passive control of quorum sensing: Prevention of pseudomonas aeruginosa biofilm formation by imprinted polymers*. Biomacromolecules, 2011. **12**(4): p. 1067-1071.
77. Popat, R., S.A. Crusz, and S.P. Diggle, *The social behaviours of bacterial pathogens*. British Medical Bulletin, 2008. **87**(1): p. 63-75.
78. Wagner, C., S. Zimmermann, G. Brenner-Weiss, F. Hug, B. Prior, U. Obst, and G.M. Hansch, *The quorum-sensing molecule N-3-oxododecanoyl homoserine lactone (3OC12-HSL) enhances the host defence by activating human polymorphonuclear neutrophils (PMN)*. Anal Bioanal Chem, 2007. **387**(2): p. 481-7.
79. Rowe, M.C., H.L. Withers, and S. Swift, *Uropathogenic Escherichia coli forms biofilm aggregates under iron restriction that disperse upon the supply of iron*. FEMS Microbiology Letters, 2010. **307**(1): p. 102-109.
80. Dunny, G.M., B.L. Brown, and D.B. Clewell, *Induced cell aggregation and mating in Streptococcus faecalis: evidence for a bacterial sex pheromone*. Proceedings of the National Academy of Sciences of the United States of America, 1978. **75**(7): p. 3479-3483.
81. Mellies, J.L., F. Navarro-Garcia, I. Okeke, J. Frederickson, J.P. Nataro, and J.B. Kaper, *espC pathogenicity island of enteropathogenic Escherichia coli encodes an enterotoxin*. Infection and Immunity, 2001. **69**(1): p. 315-324.
82. Stone, K.D., H.Z. Zhang, L.K. Carlson, and M.S. Donnenberg, *A cluster of fourteen genes from enteropathogenic Escherichia coli is sufficient for the biogenesis of a type IV pilus*. Mol Microbiol, 1996. **20**(2): p. 325-37.
83. Soheli, I., J.L. Puente, S.W. Ramer, D. Bieber, C.Y. Wu, and G.K. Schoolnik, *Enteropathogenic Escherichia coli: identification of a gene cluster coding for bundle-forming pilus morphogenesis*. J Bacteriol, 1996. **178**(9): p. 2613-28.

84. Pelayo, J.S., I.C. Scaletsky, M.Z. Pedroso, V. Sperandio, J.A. Giron, G. Frankel, and L.R. Trabulsi, *Virulence properties of atypical EPEC strains*. J Med Microbiol, 1999. **48**(1): p. 41-9.
85. Whitworth, J.H., N. Fegan, J. Keller, K.S. Gobius, J.L. Bono, D.R. Call, D.D. Hancock, and T.E. Besser, *International comparison of clinical, bovine, and environmental Escherichia coli O157 isolates on the basis of shiga toxin-encoding bacteriophage insertion site genotypes*. Applied and Environmental Microbiology, 2008. **74**(23): p. 7447-7450.
86. Tu, S.I., J. Uknalis, and Y. He. *Environmental effects on the production of Shiga-like toxins by Escherichia coli O157:H7 as revealed by sandwiched immunochemiluminescence detection*. 2009.
87. Rendón, M.A., Z. Saldaña, A.L. Erdem, V. Monteiro-Neto, A. Vázquez, J.B. Kaper, J.L. Puente, and J.A. Girón, *Commensal and pathogenic Escherichia coli use a common pilus adherence factor for epithelial cell colonization*. Proceedings of the National Academy of Sciences of the United States of America, 2007. **104**(25): p. 10637-10642.
88. Saldaña, Z., J. Xicohtencatl-Cortes, F. Avelino, A.D. Phillips, J.B. Kaper, J.L. Puente, and J.A. Girón, *Synergistic role of curli and cellulose in cell adherence and biofilm formation of attaching and effacing Escherichia coli and identification of Fis as a negative regulator of curli*. Environmental Microbiology, 2009. **11**(4): p. 992-1006.
89. Biscola, F.T., C.M. Abe, and B.E.C. Guth, *Determination of adhesin gene sequences in, and biofilm formation by, O157 and non-O157 Shiga toxin-producing Escherichia coli strains isolated from different sources*. Applied and Environmental Microbiology, 2011. **77**(7): p. 2201-2208.
90. Bai, A.J. and V.R. Rai, *Bacterial Quorum Sensing and Food Industry*. Comprehensive Reviews in Food Science and Food Safety, 2011. **10**(3): p. 183-193.
91. Gobetti, M., M. De Angelis, R. Di Cagno, F. Minervini, and A. Limitone, *Cell-cell communication in food related bacteria*. International Journal of Food Microbiology, 2007. **120**(1-2): p. 34-45.
92. Wei, J.R., P.C. Soo, Y.T. Horng, S.C. Hsieh, Y.H. Tsai, S. Swift, H. Withers, P. Williams, and H.C. Lai, *Regulatory roles of spnT, a novel gene located within transposon TnTIR*. Biochemical and Biophysical Research Communications, 2006. **348**(3): p. 1038-1046.
93. Williams, P., *Quorum sensing, communication and cross-kingdom signalling in the bacterial world*. Microbiology, 2007. **153**(12): p. 3923-3938.

94. Atkinson, S. and P. Williams, *Quorum sensing and social networking in the microbial world*. Journal of the Royal Society Interface, 2009. **6**(40): p. 959-978.
95. Withers, H., S. Swift, and P. Williams, *Quorum sensing as an integral component of gene regulatory networks in gram-negative bacteria*. Current Opinion in Microbiology, 2001. **4**(2): p. 186-193.
96. Diggle, S.P., A. Gardner, S.A. West, and A.S. Griffin, *Evolutionary theory of bacterial quorum sensing: When is a signal not a signal?* Philosophical Transactions of the Royal Society B: Biological Sciences, 2007. **362**(1483): p. 1241-1249.
97. Winzer, K., C. Falconer, N.C. Garber, S.P. Diggle, M. Camara, and P. Williams, *The Pseudomonas aeruginosa lectins PA-IL and PA-IIL are controlled by quorum sensing and by RpoS*. Journal of Bacteriology, 2000. **182**(22): p. 6401-6411.
98. Swift, S., Rowe, M.C., and Kamath, M, *Quorum Sensing*, in *Bacterial Physiology: A Molecular Approach*, W. El-Sharoud, Editor. 2008, Springer-Verlag Berlin Heidelberg p. 179-232.
99. Lerat, E. and N.A. Moran, *The Evolutionary History of Quorum-Sensing Systems in Bacteria*. Molecular Biology and Evolution, 2004. **21**(5): p. 903-913.
100. Defoirdt, T., N. Boon, and P. Bossier, *Can bacteria evolve resistance to quorum sensing disruption?* PLoS Pathogens, 2010. **6**(7): p. 1-6.
101. Withers, H.L. and K. Nordström, *Quorum-sensing acts at initiation of chromosomal replication in Escherichia coli*. Proceedings of the National Academy of Sciences of the United States of America, 1998. **95**(26): p. 15694-15699.
102. De Araujo, C., D. Balestrino, L. Roth, N. Charbonnel, and C. Forestier, *Quorum sensing affects biofilm formation through lipopolysaccharide synthesis in Klebsiella pneumoniae*. Research in Microbiology, 2010. **161**(7): p. 595-603.
103. Platt, T.G. and C. Fuqua, *What's in a name? The semantics of quorum sensing*. Trends in Microbiology, 2010. **18**(9): p. 383-387.
104. Choudhary, S. and C. Schmidt-Dannert, *Applications of quorum sensing in biotechnology*. Applied Microbiology and Biotechnology, 2010. **86**(5): p. 1267-1279.
105. Kolter, R., *Reflections on the history of microbial chemical ecology*. Microbe, 2010. **5**(5): p. 201-205.
106. Kempner, E.S. and F.E. Hanson, *Aspects of light production by Photobacterium fischeri*. Journal of Bacteriology, 1968. **95**(3): p. 975-979.
107. Nealson, K.H., T. Platt, and J.W. Hastings, *Cellular control of the synthesis and activity of the bacterial luminescent system*. Journal of Bacteriology, 1970. **104**(1): p. 313-322.

108. Eberhard, A., A.L. Burlingame, C. Eberhard, G.L. Kenyon, K.H. Nealson, and N.J. Oppenheimer, *Structural identification of autoinducer of Photobacterium fischeri luciferase*. Biochemistry, 1981. **20**(9): p. 2444-2449.
109. Swift, S., J. Allan Downie, N.A. Whitehead, A.M.L. Barnard, G.P.C. Salmond, and P. Williams, *Quorum sensing as a population-density-dependent determinant of bacterial physiology*. 2001. p. 199-270.
110. McDougald, D., S.A. Rice, and S. Kjelleberg, *Bacterial quorum sensing and interference by naturally occurring biomimics*. Analytical and Bioanalytical Chemistry, 2007. **387**(2): p. 445-453.
111. Fuqua, W.C., S.C. Winans, and E.P. Greenberg, *Quorum sensing in bacteria: The LuxR-LuxI family of cell density- responsive transcriptional regulators*. Journal of Bacteriology, 1994. **176**(2): p. 269-275.
112. Walters, M., M.P. Sircili, and V. Sperandio, *AI-3 synthesis is not dependent on luxS in Escherichia coli*. Journal of Bacteriology, 2006. **188**(16): p. 5668-5681.
113. Walters, M. and V. Sperandio, *Autoinducer 3 and epinephrine signaling in the kinetics of locus of enterocyte effacement gene expression in enterohemorrhagic Escherichia coli*. Infection and Immunity, 2006. **74**(10): p. 5445-5455.
114. Clarke, M.B., D.T. Hughes, C. Zhu, E.C. Boedeker, and V. Sperandio, *The QseC sensor kinase: A bacterial adrenergic receptor*. Proceedings of the National Academy of Sciences of the United States of America, 2006. **103**(27): p. 10420-10425.
115. Clarke, M.B. and V. Sperandio, *Transcriptional autoregulation by quorum sensing Escherichia coli regulators B and C (QseBC) in enterohaemorrhagic E. coli (EHEC)*. Mol Microbiol, 2005. **58**(2): p. 441-55.
116. Habdas, B.J., J. Smart, J.B. Kaper, and V. Sperandio, *The LysR-type transcriptional regulator QseD alters type three secretion in enterohemorrhagic Escherichia coli and motility in K-12 Escherichia coli*. Journal of Bacteriology, 2010. **192**(14): p. 3699-3712.
117. Kendall, M.M., D.A. Rasko, and V. Sperandio, *Global effects of the cell-to-cell signaling molecules autoinducer-2, autoinducer-3, and epinephrine in a luxS mutant of enterohemorrhagic Escherichia coli*. Infection and Immunity, 2007. **75**(10): p. 4875-4884.
118. Kendall, M.M., D.A. Rasko, and V. Sperandio, *The LysR-type regulator QseA regulates both characterized and putative virulence genes in enterohaemorrhagic Escherichia coli O157:H7*. Molecular Microbiology, 2010. **76**(5): p. 1306-1321.
119. Ahmer, B.M.M., *Cell-to-cell signalling in Escherichia coli and Salmonella enterica*. Molecular Microbiology, 2004. **52**(4): p. 933-945.

120. Hirakawa, H., M. Hayashi-Nishino, A. Yamaguchi, and K. Nishino, *Indole enhances acid resistance in Escherichia coli*. Microbial Pathogenesis, 2010. **49**(3): p. 90-94.
121. Lee, J., A. Jayaraman, and T.K. Wood, *Indole is an inter-species biofilm signal mediated by SdiA*. BMC Microbiology, 2007. **7**.
122. Lee, J., T. Maeda, S.H. Hong, and T.K. Wood, *Reconfiguring the quorum-sensing regulator sdiA of escherichia coli to control biofilm formation via indole and N-acylhomoserine lactones*. Applied and Environmental Microbiology, 2009. **75**(6): p. 1703-1716.
123. Lee, J., X.S. Zhang, M. Hegde, W.E. Bentley, A. Jayaraman, and T.K. Wood, *Indole cell signaling occurs primarily at low temperatures in Escherichia coli*. ISME Journal, 2008. **2**(10): p. 1007-1023.
124. Darch, S.E., S.A. West, K. Winzer, and S.P. Diggle, *Density-dependent fitness benefits in quorum-sensing bacterial populations*. Proceedings of the National Academy of Sciences of the United States of America, 2012. **109**(21): p. 8259-8263.
125. Schauder, S., K. Shokat, M.G. Surette, and B.L. Bassler, *The LuxS family of bacterial autoinducers: Biosynthesis of a novel quorum-sensing signal molecule*. Molecular Microbiology, 2001. **41**(2): p. 463-476.
126. Boedicker, J.Q., M.E. Vincent, and R.F. Ismagilov, *Microfluidic confinement of single cells of bacteria in small volumes initiates high-density behavior of quorum sensing and growth and reveals its variability*. Angewandte Chemie - International Edition, 2009. **48**(32): p. 5908-5911.
127. Williams, P., K. Winzer, W.C. Chan, and M. Cámara, *Look who's talking: Communication and quorum sensing in the bacterial world*. Philosophical Transactions of the Royal Society B: Biological Sciences, 2007. **362**(1483): p. 1119-1134.
128. Laue, B.E., Y. Jiang, S.R. Chhabra, S. Jacob, G.S.A.B. Stewart, A. Hardman, J.A. Downie, F. O'Gara, and P. Williams, *The biocontrol strain Pseudomonas fluorescens F113 produces the Rhizobium small bacteriocin, N-(3-hydroxy-7-cis-tetradecenoyl) homoserine lactone, via HdtS, a putative novel N-acylhomoserine lactone synthase*. Microbiology, 2000. **146**(10): p. 2469-2480.
129. Rivas, M., M. Seeger, E. Jedlicki, and D.S. Holmes, *Second acyl homoserine lactone production system in the extreme acidophile Acidithiobacillus ferrooxidans*. Applied and Environmental Microbiology, 2007. **73**(10): p. 3225-3231.

130. Nasser, W. and S. Reverchon, *New insights into the regulatory mechanisms of the LuxR family of quorum sensing regulators*. Analytical and Bioanalytical Chemistry, 2007. **387**(2): p. 381-390.
131. Gilson, L., A. Kuo, and P.V. Dunlap, *AinS and a new family of autoinducer synthesis proteins*. Journal of Bacteriology, 1995. **177**(23): p. 6946-6951.
132. Hanzelka, B.L., M.R. Parsek, D.L. Val, P.V. Dunlap, J.E. Cronan Jr, and E.P. Greenberg, *Acylhomoserine lactone synthase activity of the Vibrio fischeri AinS protein*. Journal of Bacteriology, 1999. **181**(18): p. 5766-5770.
133. Milton, D.L., V.J. Chalker, D. Kirke, A. Hardman, M. Cámara, and P. Williams, *The luxM homologue vanM from Vibrio anguillarum directs the synthesis of N-(3-hydroxyhexanoyl)homoserine lactone and N-hexanoylhomoserine lactone*. Journal of Bacteriology, 2001. **183**(12): p. 3537-3547.
134. Kanamaru, K., I. Tatsuno, T. Tobe, and C. Sasakawa, *SdiA, an Escherichia coli homologue of quorum-sensing regulators, controls the expression of virulence factors in enterohaemorrhagic Escherichia coli O157:H7*. Molecular Microbiology, 2000. **38**(4): p. 805-816.
135. Parsek, M.R. and E.P. Greenberg, *Acyl-homoserine lactone quorum sensing in Gram-negative bacteria: A signaling mechanism involved in associations with higher organisms*. Proceedings of the National Academy of Sciences of the United States of America, 2000. **97**(16): p. 8789-8793.
136. Patankar, A.V. and J.E. González, *Orphan LuxR regulators of quorum sensing: Review article*. FEMS Microbiology Reviews, 2009. **33**(4): p. 739-756.
137. Tsai, C.S. and S.C. Winans, *LuxR-type quorum-sensing regulators that are detached from common scents*. Molecular Microbiology, 2010. **77**(5): p. 1072-1082.
138. Smith, J.L., P.M. Fratamico, and X. Yan, *Eavesdropping by bacteria: The role of SdiA in escherichia coli and salmonella enterica serovar typhimurium quorum sensing*. Foodborne Pathogens and Disease, 2011. **8**(2): p. 169-178.
139. Soulère, L., M. Sabbah, F. Fontaine, Y. Queneau, and A. Doutheau, *LuxR-dependent quorum sensing: Computer aided discovery of new inhibitors structurally unrelated to N-acylhomoserine lactones*. Bioorganic and Medicinal Chemistry Letters, 2010. **20**(15): p. 4355-4358.



140. Yao, Y., M.A. Martinez-Yamout, T.J. Dickerson, A.P. Brogan, P.E. Wright, and H.J. Dyson, *Structure of the Escherichia coli quorum sensing protein SdiA: Activation of the folding switch by acyl homoserine lactones*. Journal of Molecular Biology, 2006. **355**(2): p. 262-273.
141. Borlee, B.R., G.D. Geske, H.E. Blackwell, and J. Handelsman, *Identification of synthetic inducers and inhibitors of the quorum-sensing regulator lasR in pseudomonas aeruginosa by high-throughput screening*. Applied and Environmental Microbiology, 2010. **76**(24): p. 8255-8258.
142. Khalilzadeh, P., B. Lajoie, S. El Hage, A.L. Furiga, G. Baziard, M. Berge, and C. Roques, *Growth inhibition of adherent Pseudomonas aeruginosa by an N-butanoyl-L-homoserine lactone analog*. Canadian Journal of Microbiology, 2010. **56**(4): p. 317-325.
143. Ni, N., M. Li, J. Wang, and B. Wang, *Inhibitors and antagonists of bacterial quorum sensing*. Medicinal Research Reviews, 2009. **29**(1): p. 65-124.
144. Waters, C.M. and B.L. Bassler, *Quorum sensing: Cell-to-cell communication in bacteria*. 2005. p. 319-346.
145. Choi, S.H. and E.P. Greenberg, *The C-terminal region of the Vibrio fischeri LuxR protein contains an inducer-independent lux gene activating domain*. Proceedings of the National Academy of Sciences of the United States of America, 1991. **88**(24): p. 11115-11119.
146. Parsek, M.R., D.L. Val, B.L. Hanzelka, J.E. Cronan Jr, and E.P. Greenberg, *Acyl homoserine-lactone quorum-sensing signal generation*. Proceedings of the National Academy of Sciences of the United States of America, 1999. **96**(8): p. 4360-4365.
147. Sitnikov, D.M., G.S. Shadel, and T.O. Baldwin, *Autoinducer-independent mutants of the LuxR transcriptional activator exhibit differential effects on the two lux promoters of Vibrio fischeri*. Molecular and General Genetics, 1996. **252**(5): p. 622-625.
148. Finney, A.H., R.J. Blick, K. Murakami, A. Ishihama, and A.M. Stevens, *Role of the C-terminal domain of the alpha subunit of RNA polymerase in LuxR-dependent transcriptional activation of the lux operon during quorum sensing*. Journal of Bacteriology, 2002. **184**(16): p. 4520-4528.
149. Stevens, A.M., K.M. Dolan, and E.P. Greenberg, *SYNERGISTIC BINDING OF THE VIBRIO-FISCHERI LUXR TRANSCRIPTIONAL ACTIVATOR DOMAIN AND RNA-POLYMERASE TO THE LUX PROMOTER REGION*. Proceedings of the National Academy of Sciences of the United States of America, 1994. **91**(26): p. 12619-12623.

150. Stevens, A.M., N. Fujita, A. Ishihama, and E.P. Greenberg, *Involvement of the RNA polymerase alpha-subunit C-terminal domain in LuxR-dependent activation of the Vibrio fischeri luminescence genes*. Journal of Bacteriology, 1999. **181**(15): p. 4704-4707.
151. Zhang, R.G., T. Pappas, J.L. Brace, P.C. Miller, T. Oulmassov, J.M. Molyneaux, J.C. Anderson, J.K. Bashkin, S.C. Wlnans, and A. Joachimiak, *Structure of a bacterial quorum-sensing transcription factor complexed with pheromone and DNA*. Nature, 2002. **417**(6892): p. 971-974.
152. Dobretsov, S., M. Teplitski, and V. Paul, *Mini-review: Quorum sensing in the marine environment and its relationship to biofouling*. Biofouling, 2009. **25**(5): p. 413-427.
153. Medina-Martínez, M.S., M. Uyttendaele, S. Meireman, and J. Debevere, *Relevance of N-acyl-L-homoserine lactone production by Yersinia enterocolitica in fresh foods*. Journal of Applied Microbiology, 2007. **102**(4): p. 1150-1158.
154. Bainton, N.J., P. Stead, S.R. Chhabra, B.W. Bycroft, G.P.C. Salmond, G.S.A.B. Stewart, and P. Williams, *N-(3-Oxohexanoyl)-L-homoserine lactone regulates carbapenem antibiotic production in Erwinia carotovora*. Biochemical Journal, 1992. **288**(3): p. 997-1004.
155. Michael, B., J.N. Smith, S. Swift, F. Heffron, and B.M.M. Ahmer, *SdiA of Salmonella enterica is a LuxR homolog that detects mixed microbial communities*. Journal of Bacteriology, 2001. **183**(19): p. 5733-5742.
156. Van Houdt, R., A. Aertsen, P. Moons, K. Vanoirbeek, and C.W. Michiels, *N-acyl-L-homoserine lactone signal interception by Escherichia coli*. FEMS Microbiology Letters, 2006. **256**(1): p. 83-89.
157. Oinuma, K.I. and E.P. Greenberg, *Acyl-homoserine lactone binding to and stability of the orphan pseudomonas aeruginosa quorum-sensing signal receptor qscr*. Journal of Bacteriology, 2011. **193**(2): p. 421-428.
158. Lindsay, A. and B.M.M. Ahmer, *Effect of sdiA on biosensors of N-acylhomoserine lactones*. Journal of Bacteriology, 2005. **187**(14): p. 5054-5058.
159. Yamamoto, K., K. Yata, N. Fujita, and A. Ishihama, *Novel mode of transcription regulation by SdiA, an Escherichia coli homologue of the quorum-sensing regulator*. Molecular Microbiology, 2001. **41**(5): p. 1187-1198.
160. Dyszel, J.L., J.A. Soares, M.C. Swearingen, A. Lindsay, J.N. Smith, and B.M.M. Ahmer, *E. coli K-12 and EHEC genes regulated by SdiA*. PLoS ONE, 2010. **5**(1).

161. Dyszel, J.L., J.N. Smith, D.E. Lucas, J.A. Soares, M.C. Swearingen, M.A. Vross, G.M. Young, and B.M.M. Ahmer, *Salmonella enterica* serovar typhimurium can detect acyl homoserine lactone production by *Yersinia enterocolitica* in mice. *Journal of Bacteriology*, 2010. **192**(1): p. 29-37.
162. Zhou, X., X. Meng, and B. Sun, *An EAL domain protein and cyclic AMP contribute to the interaction between the two quorum sensing systems in Escherichia coli*. *Cell Research*, 2008. **18**(9): p. 937-948.
163. Soares, J.A. and B.M.M. Ahmer, *Detection of acyl-homoserine lactones by Escherichia and Salmonella*. *Current Opinion in Microbiology*, 2011. **14**(2): p. 188-193.
164. KEGG - Kyoto Encyclopedia of Genes and Genomes, Kanehisa Laboratories.
165. Fuqua, C. and E.P. Greenberg, *Cell-to-cell communication in Escherichia coli and Salmonella typhimurium: They may be talking, but who's listening?* *Proceedings of the National Academy of Sciences of the United States of America*, 1998. **95**(12): p. 6571-6572.
166. Smith, J.N. and B.M.M. Ahmer, *Detection of other microbial species by Salmonella: Expression of the SdiA regulon*. *Journal of Bacteriology*, 2003. **185**(4): p. 1357-1366.
167. Gospodarek, E., T. Bogiel, and P. Zalas-Więcek, *Communication between microorganisms as a basis for production of virulence factors*. *Polish Journal of Microbiology*, 2009. **58**(3): p. 191-198.
168. Kanamaru, K., I. Tatsuno, T. Tobe, and C. Sasakawa, *Regulation of Virulence Factors of Enterohemorrhagic Escherichia coli O157:H7 by Self-Produced Extracellular Factors*. *Bioscience, Biotechnology and Biochemistry*, 2000. **64**(11): p. 2508-2511.
169. Sperandio, V., *SdiA sensing of acyl-homoserine lactones by enterohemorrhagic E. coli (EHEC) serotype o157:H7 in the bovine rumen*. *Gut Microbes*, 2010. **1**(6).
170. Sharma, V.K., S.M.D. Bearson, and B.L. Bearson, *Evaluation of the effects of sdiA, a luxR homologue, on adherence and motility of Escherichia coli O157:H7*. *Microbiology*, 2010. **156**(5): p. 1303-1312.
171. Dziva, F., P.M. van Diemen, M.P. Stevens, A.J. Smith, and T.S. Wallis, *Identification of Escherichia coli O157 : H7 genes influencing colonization of the bovine gastrointestinal tract using signature-tagged mutagenesis*. *Microbiology*, 2004. **150**(Pt 11): p. 3631-45.
172. Yakhnin, H., C.S. Baker, I. Berezin, M.A. Evangelista, A. Rassin, T. Romeo, and P. Babitzke, *CsrA Represses Translation of sdiA, Which Encodes the N-acylhomoserine-L-lactone receptor of Escherichia coli, by Binding exclusively within the coding region of sdiA mRNA*. *Journal of Bacteriology*, 2011. **193**(22): p. 6162-6170.

173. Erickson, D.L., V.L. Nsereko, D.P. Morgavi, L.B. Selinger, L.M. Rode, and K.A. Beauchemin, *Evidence of quorum sensing in the rumen ecosystem: Detection of N-acyl homoserine lactone autoinducers in ruminal contents*. Canadian Journal of Microbiology, 2002. **48**(4): p. 374-378.
174. Mitsumori, M., L. Xu, H. Kajikawa, M. Kurihara, K. Tajima, J. Hai, and A. Takenaka, *Possible quorum sensing in the rumen microbial community: Detection of quorum-sensing signal molecules from rumen bacteria*. FEMS Microbiology Letters, 2003. **219**(1): p. 47-52.
175. Decho, A.W., R.S. Norman, and P.T. Visscher, *Quorum sensing in natural environments: emerging views from microbial mats*. Trends in Microbiology, 2010. **18**(2): p. 73-80.
176. Kaplan, H.B. and E.P. Greenberg, *Diffusion of autoinducer is involved in regulation of the Vibrio fischeri luminescence system*. Journal of Bacteriology, 1985. **163**(3): p. 1210-1214.
177. Pearson, J.P., E.C. Pesci, and B.H. Iglewski, *Roles of Pseudomonas aeruginosa las and rhl quorum-sensing systems in control of elastase and rhamnolipid biosynthesis genes*. Journal of Bacteriology, 1997. **179**(18): p. 5756-5767.
178. Pearson, J.P., C. Van Delden, and B.H. Iglewski, *Active efflux and diffusion are involved in transport of Pseudomonas aeruginosa cell-to-cell signals*. Journal of Bacteriology, 1999. **181**(4): p. 1203-1210.
179. Hooshangi, S. and W.E. Bentley, *LsrR quorum sensing "switch" is revealed by a bottom-up approach*. PLoS Computational Biology, 2011. **7**(9).
180. Lee, J.H., Y. Lequette, and E.P. Greenberg, *Activity of purified QscR, a Pseudomonas aeruginosa orphan quorum-sensing transcription factor*. Molecular Microbiology, 2006. **59**(2): p. 602-609.
181. Li, L.L., J.E. Malone, and B.H. Iglewski, *Regulation of the Pseudomonas aeruginosa quorum-sensing regulator VqsR*. J Bacteriol, 2007. **189**(12): p. 4367-74.
182. Yates, E.A., B. Philipp, C. Buckley, S. Atkinson, S.R. Chhabra, R.E. Sockett, M. Goldner, Y. Dessaux, M. Cámara, H. Smith, and P. Williams, *N-acylhomoserine lactones undergo lactonolysis in a pH-, temperature-, and acyl chain length-dependent manner during growth of Yersinia pseudotuberculosis and Pseudomonas aeruginosa*. Infection and Immunity, 2002. **70**(10): p. 5635-5646.
183. Bassler, B.L., E.P. Greenberg, and A.M. Stevens, *Cross-species induction of luminescence in the quorum-sensing bacterium Vibrio harveyi*. Journal of Bacteriology, 1997. **179**(12): p. 4043-4045.

184. Bassler, B.L., M. Wright, R.E. Showalter, and M.R. Silverman, *Intercellular signalling in Vibrio harveyi: Sequence and function of genes regulating expression of luminescence*. Molecular Microbiology, 1993. **9**(4): p. 773-786.
185. Raina, S., D. De Vizio, M. Odell, M. Clements, S. Vanhulle, and T. Keshavarz, *Microbial quorum sensing: A tool or a target for antimicrobial therapy?* Biotechnology and Applied Biochemistry, 2009. **54**(2): p. 65-84.
186. Diggle, S.P., S. Matthijs, V.J. Wright, M.P. Fletcher, S.R. Chhabra, I.L. Lamont, X. Kong, R.C. Hider, P. Cornelis, M. Cámara, and P. Williams, *The Pseudomonas aeruginosa 4-Quinolone Signal Molecules HHQ and PQS Play Multifunctional Roles in Quorum Sensing and Iron Entrapment*. Chemistry and Biology, 2007. **14**(1): p. 87-96.
187. Winson, M.K., M. Camara, A. Latifi, M. Foglino, S.R. Chhabra, M. Daykin, M. Bally, V. Chapon, G.P.C. Salmond, B.W. Bycroft, A. Lazdunski, G.S.A.B. Stewart, and P. Williams, *Multiple N-acyl-L-homoserine lactone signal molecules regulate production of virulence determinants and secondary metabolites in Pseudomonas aeruginosa*. Proceedings of the National Academy of Sciences of the United States of America, 1995. **92**(20): p. 9427-9431.
188. Ling, E.A., M.L. Ellison, and E.C. Pesci, *A novel plasmid for detection of N-acyl homoserine lactones*. Plasmid, 2009. **62**(1): p. 16-21.
189. Singh, G., B. Wu, M.S. Baek, A. Camargo, A. Nguyen, N.A. Slusher, R. Srinivasan, J.P. Wiener-Kronish, and S.V. Lynch, *Secretion of Pseudomonas aeruginosa type III cytotoxins is dependent on pseudomonas quinolone signal concentration*. Microbial Pathogenesis, 2010. **49**(4): p. 196-203.
190. Fletcher, M.P., S.P. Diggle, S.A. Crusz, S.R. Chhabra, M. Cámara, and P. Williams, *A dual biosensor for 2-alkyl-4-quinolone quorum-sensing signal molecules*. Environmental Microbiology, 2007. **9**(11): p. 2683-2693.
191. Chugani, S.A., M. Whiteley, K.M. Lee, D. D'Argenio, C. Manoil, and E.P. Greenberg, *QscR, a modulator of quorum-sensing signal synthesis and virulence in Pseudomonas aeruginosa*. Proceedings of the National Academy of Sciences of the United States of America, 2001. **98**(5): p. 2752-2757.
192. Thiel, V., R. Vilchez, H. Sztajer, I. Wagner-Döbler, and S. Schulz, *Identification, quantification, and determination of the absolute configuration of the bacterial quorum-sensing signal autoinducer-2 by gas chromatography-mass spectrometry*. ChemBioChem, 2009. **10**(3): p. 479-485.

193. Byrd, C.M. and W.E. Bentley, *Quieting cross talk - The quorum sensing regulator LsrR as a possible target for fighting bacterial infections*. Cell Research, 2009. **19**(11): p. 1229-1230.
194. Winzer, K., K.R. Hardie, N. Burgess, N. Doherty, D. Kirke, M.T.G. Holden, R. Linforth, K.A. Cornell, A.J. Taylor, P.J. Hill, and P. Williams, *LuxS: Its role in central metabolism and the in vitro synthesis of 4-hydroxy-5-methyl-3(2H)-furanone*. Microbiology, 2002. **148**(4): p. 909-922.
195. De Keersmaecker, S.C.J., K. Sonck, and J. Vanderleyden, *Let LuxS speak up in AI-2 signaling*. Trends in Microbiology, 2006. **14**(3): p. 114-119.
196. Kadirvel, M., W.T. Stimpson, S. Moumene-Afifi, B. Arsic, N. Glynn, N. Halliday, P. Williams, P. Gilbert, A.J. McBain, S. Freeman, and J.M. Gardiner, *Synthesis and bioluminescence-inducing properties of autoinducer (S)-4,5-dihydroxypentane-2,3-dione and its enantiomer*. Bioorganic and Medicinal Chemistry Letters, 2010. **20**(8): p. 2625-2628.
197. Beeston, A.L. and M.G. Surette, *pfs-dependent regulation of autoinducer 2 production in Salmonella enterica serovar typhimurium*. Journal of Bacteriology, 2002. **184**(13): p. 3450-3456.
198. Miller, S.T., K.B. Xavier, S.R. Campagna, M.E. Taga, M.F. Semmelhack, B.L. Bassler, and F.M. Hughson, *Salmonella typhimurium recognizes a chemically distinct form of the bacterial quorum-sensing signal AI-2*. Molecular Cell, 2004. **15**(5): p. 677-687.
199. Smith, J.A.I., J.X. Wang, S.M. Nguyen-Mau, V. Lee, and H.O. Sintim, *Biological screening of a diverse set of AI-2 analogues in Vibrio harveyi suggests that receptors which are involved in synergistic agonism of AI-2 and analogues are promiscuous*. Chemical Communications, 2009(45): p. 7033-7035.
200. Xavier, K.B. and B.L. Bassler, *Regulation of uptake and processing of the quorum-sensing autoinducer AI-2 in Escherichia coli*. Journal of Bacteriology, 2005. **187**(1): p. 238-248.
201. Antunes, L.C.M., R.B.R. Ferreira, M.M.C. Buckner, and B.B. Finlay, *Quorum sensing in bacterial virulence*. Microbiology, 2010. **156**(8): p. 2271-2282.
202. Surette, M.G., M.B. Miller, and B.L. Bassler, *Quorum sensing in Escherichia coli, Salmonella typhimurium, and Vibrio harveyi: A new family of genes responsible for autoinducer production*. Proceedings of the National Academy of Sciences of the United States of America, 1999. **96**(4): p. 1639-1644.

203. Ling, H., A. Kang, M.H. Tan, X. Qi, and M.W. Chang, *The absence of the luxS gene increases swimming motility and flagella synthesis in Escherichia coli K12*. Biochemical and Biophysical Research Communications, 2010. **401**(4): p. 521-526.
204. Sintim, H.O., J.A. Smith, J. Wang, S. Nakayama, and L. Yan, *Paradigm shift in discovering next-generation anti-infective agents: Targeting quorum sensing, c-di-GMP signaling and biofilm formation in bacteria with small molecules*. Future Medicinal Chemistry, 2010. **2**(6): p. 1005-1035.
205. Pereira, C.S., A.K. De Regt, P.H. Brito, S.T. Miller, and K.B. Xavier, *Identification of functional LsrB-like autoinducer-2 receptors*. Journal of Bacteriology, 2009. **191**(22): p. 6975-6987.
206. Tsao, C.Y., S. Hooshangi, H.C. Wu, J.J. Valdes, and W.E. Bentley, *Autonomous induction of recombinant proteins by minimally rewiring native quorum sensing regulon of E. coli*. Metabolic Engineering, 2010. **12**(3): p. 291-297.
207. Wang, L., J. Li, J.C. March, J.J. Valdes, and W.E. Bentley, *luxS-dependent gene regulation in Escherichia coli K-12 revealed by genomic expression profiling*. Journal of Bacteriology, 2005. **187**(24): p. 8350-8360.
208. Zhu, C., S. Feng, V. Sperandio, Z. Yang, T.E. Thate, J.B. Kaper, and E.C. Boedeker, *The possible influence of LuxS in the in vivo virulence of rabbit enteropathogenic Escherichia coli*. Veterinary Microbiology, 2007. **125**(3-4): p. 313-322.
209. Nealson, K.H. and J.W. Hastings, *Bacterial bioluminescence: Its control and ecological significance*. Microbiological Reviews, 1979. **43**(4): p. 496-518.
210. Yang, Q., Y. Han, and X.H. Zhang, *Detection of quorum sensing signal molecules in the family Vibrionaceae*. Journal of Applied Microbiology.
211. Ulrich, S., *Identification of genes regulated by cold temperature - a study of mdtJI in E. coli O157:H7*, in *Biological Sciences*. 2009, University of Waikato: Hamilton.
212. Brackman, G., S. Celen, K. Baruah, P. Bossier, S. Van Calenberg, H.J. Nelis, and T. Coenye, *AI-2 quorum-sensing inhibitors affect the starvation response and reduce virulence in several Vibrio species, most likely by interfering with LuxPQ*. Microbiology, 2009. **155**(12): p. 4114-4122.
213. Natrah, F.M.I., H.A.D. Ruwandeepika, S. Pawar, I. Karunasagar, P. Sorgeloos, P. Bossier, and T. Defoirdt, *Regulation of virulence factors by quorum sensing in Vibrio harveyi*. Veterinary Microbiology, 2011. **154**(1-2): p. 124-129.

214. Bruhn, J.B., A.B. Christensen, L.R. Flodgaard, K.F. Nielsen, T.O. Larsen, M. Givskov, and L. Gram, *Presence of acylated homoserine lactones (AHLs) and AHL-producing bacteria in meat and potential role of AHL in spoilage of meat*. Applied and Environmental Microbiology, 2004. **70**(7): p. 4293-4302.
215. Gram, L., A.B. Christensen, L. Ravn, S. Molin, and M. Givskov, *Production of acylated homoserine lactones by psychrotrophic members of the Enterobacteriaceae isolated from foods*. Applied and Environmental Microbiology, 1999. **65**(8): p. 3458-3463.
216. Ferrocino, I., D. Ercolini, F. Villani, S.M. Moorhead, and M.W. Griffiths, *Pseudomonas fragi strains isolated from meat do not produce N-Acyl homoserine lactones as signal molecules*. Journal of Food Protection, 2009. **72**(12): p. 2597-2601.
217. Jay, J.M., J.P. Vilai, and M.E. Hughes, *Profile and activity of the bacterial biota of ground beef held from freshness to spoilage at 5-7°C*. International Journal of Food Microbiology, 2003. **81**(2): p. 105-111.
218. Viana, E.S., M.E.M. Campos, A.R. Ponce, H.C. Mantovani, and M.C.D. Vanetti, *Biofilm formation and acyl homoserine lactone production in Hafnia alvei isolated from raw milk*. Biological Research, 2009. **42**(4): p. 427-436.
219. Lu, L., M.E. Hume, and S.D. Pillai, *Autoinducer-2-like activity associated with foods and its interaction with food additives*. Journal of Food Protection, 2004. **67**(7): p. 1457-1462.
220. Blana, V.A., A.I. Doulgeraki, and G.J.E. Nychas, *Autoinducer-2-like activity in lactic acid bacteria isolated from minced beef packaged under modified atmospheres*. Journal of Food Protection, 2011. **74**(4): p. 631-635.
221. Soni, K.A., L. Lu, P.R. Jesudhasan, M.E. Hume, and S.D. Pillai, *Influence of autoinducer-2 (AI-2) and beef sample extracts on E. coli O157:H7 survival and gene expression of virulence genes yadK and hhA*. Journal of Food Science, 2008. **73**(3): p. M135-M139.
222. Andrejko, M., M. Mizerska-Dudka, and T. Jakubowicz, *Antibacterial activity in vivo and in vitro in the hemolymph of Galleria mellonella infected with Pseudomonas aeruginosa*. Comparative Biochemistry and Physiology - B Biochemistry and Molecular Biology, 2009. **152**(2): p. 118-123.
223. Bergin, D., M. Brennan, and K. Kavanagh, *Fluctuations in haemocyte density and microbial load may be used as indicators of fungal pathogenicity in larvae of Galleria mellonella*. Microbes and Infection, 2003. **5**(15): p. 1389-1395.
224. Brennan, M., D.Y. Thomas, M. Whiteway, and K. Kavanagh, *Correlation between virulence of Candida albicans mutants in mice and Galleria mellonella larvae*. FEMS Immunology and Medical Microbiology, 2002. **34**(2): p. 153-157.



225. Dunphy, G.B., D.B. Morton, A. Kropinski, and J.M. Chadwick, *Pathogenicity of lipopolysaccharide mutants of Pseudomonas aeruginosa for larvae of Galleria mellonella: Bacterial properties associated with virulence*. Journal of Invertebrate Pathology, 1986. **47**(1): p. 48-55.
226. Greenberg, E.P., J.W. Hastings, and S. Ulitzur, *Induction of luciferase synthesis in Beneckea harveyi by other marine bacteria*. Archives of Microbiology, 1979. **120**(2): p. 87-91.
227. Surette, M.G. and B.L. Bassler, *Quorum sensing in Escherichia coli and Salmonella typhimurium*. Proceedings of the National Academy of Sciences of the United States of America, 1998. **95**(12): p. 7046-7050.
228. Levine, M.M., J.P. Nataro, and H. Karch, *The diarrheal response of humans to some classic serotypes of enteropathogenic Escherichia coli is dependent on a plasmid encoding an enteroadhesiveness factor*. Journal of Infectious Diseases, 1985. **152**(3): p. 550-559.
229. Zhang, H.Z. and M.S. Donnenberg, *DsbA is required for stability of the type IV pilin of enteropathogenic Escherichia coli*. Molecular Microbiology, 1996. **21**(4): p. 787-797.
230. Baldini, M.M., J.B. Kaper, and M.M. Levine, *Plasmid-mediated adhesion in enteropathogenic Escherichia coli*. Journal of Pediatric Gastroenterology and Nutrition, 1983. **2**(3): p. 534-538.
231. Kenny, B., L.C. Lai, B.B. Finlay, and M.S. Donnenberg, *EspA, a protein secreted by enteropathogenic Escherichia coli, is required to induce signals in epithelial cells*. Molecular Microbiology, 1996. **20**(2): p. 313-323.
232. Snape, S., *The Role and Regulation of LuxS in enteropathogenic Escherichia coli*, in *Faculty of Medicine and Health Sciences*. 2004, University of Nottingham: Nottingham. p. 163.
233. McClean, K.H., M.K. Winson, L. Fish, A. Taylor, S.R. Chhabra, M. Camara, M. Daykin, J.H. Lamb, S. Swift, B.W. Bycroft, G.S.A.B. Stewart, and P. Williams, *Quorum sensing and Chromobacterium violaceum: Exploitation of violacein production and inhibition for the detection of N-acylhomoserine lactones*. Microbiology, 1997. **143**(12): p. 3703-3711.
234. Winson, M.K., S. Swift, P.J. Hill, C.M. Sims, G. Griesmayr, B.W. Bycroft, P. Williams, and G.S.A.B. Stewart, *Engineering the luxCDABE genes from Photobacterium luminescens to provide a bioluminescent reporter for constitutive and promoter probe plasmids and mini-Tn5 constructs*. FEMS Microbiology Letters, 1998. **163**(2): p. 193-202.

235. Bodet Iii, C.A., J.H. Jorgensen, and D.J. Drutz, *Simplified bioassay method for measurement of flucytosine or ketoconazole*. Journal of Clinical Microbiology, 1985. **22**(2): p. 157-160.
236. Siddique, I.H., K.I. Loken, and H.H. Hoyt, *Increase in sensitivity for the assay of neomycin in milk*. Applied microbiology, 1965. **13**(5): p. 635-637.
237. Ammor, M.S., C. Michaelidis, and G.J.E. Nychas, *Insights into the role of quorum sensing in food spoilage*. Journal of Food Protection, 2008. **71**(7): p. 1510-1525.
238. Blosser, R.S. and K.M. Gray, *Extraction of violacein from Chromobacterium violaceum provides a new quantitative bioassay for N-acyl homoserine lactone autoinducers*. Journal of Microbiological Methods, 2000. **40**(1): p. 47-55.
239. Fletcher, M.P., S.P. Diggle, M. Cámara, and P. Williams, *Biosensor-based assays for PQS, HHQ and related 2-alkyl-4-quinolone quorum sensing signal molecules*. Nature Protocols, 2007. **2**(5): p. 1254-1262.
240. Swift, S., A.V. Karlyshev, L. Fish, E.L. Durant, M.K. Winson, S.R. Chhabra, P. Williams, S. Macintyre, and G.S.A.B. Stewart, *Quorum sensing in Aeromonas hydrophila and Aeromonas salmonicida: Identification of the LuxR homologs AhyR<sub>i</sub> and AsaR<sub>i</sub> and their cognate N-acylhomoserine lactone signal molecules*. Journal of Bacteriology, 1997. **179**(17): p. 5271-5281.
241. Ortori, C.A., S. Atkinson, S.R. Chhabra, M. Cámara, P. Williams, and D.A. Barrett, *Comprehensive profiling of N-acylhomoserine lactones produced by Yersinia pseudotuberculosis using liquid chromatography coupled to hybrid quadrupole-linear ion trap mass spectrometry*. Analytical and Bioanalytical Chemistry, 2007. **387**(2): p. 497-511.
242. Atkinson, S., C.Y. Chang, R.E. Sockett, M. Cámara, and P. Williams, *Quorum sensing in Yersinia enterocolitica controls swimming and swarming motility*. Journal of Bacteriology, 2006. **188**(4): p. 1451-1461.
243. Khajanchi, B.K., J. Sha, E.V. Kozlova, T.E. Erova, G. Suarez, J.C. Sierra, V.L. Popov, A.J. Horneman, and A.K. Chopra, *N-acylhomoserine lactones involved in quorum sensing control the type VI secretion system, biofilm formation, protease production, and in vivo virulence in a clinical isolate of Aeromonas hydrophila*. Microbiology, 2009. **155**(11): p. 3518-3531.
244. Uhlich, G.A., N.W. Gunther Iv, D.O. Bayles, and D.A. Mosier, *The CsgA and Ipp proteins of an escherichia coli O157:H7 strain affect HEP-2 cell invasion, motility, and biofilm formation*. Infection and Immunity, 2009. **77**(4): p. 1543-1552.

245. Atkinson, S., J.P. Throup, G.S.A.B. Stewart, and P. Williams, *A hierarchical quorum-sensing system in Yersinia pseudotuberculosis is involved in the regulation of motility and clumping*. Molecular Microbiology, 1999. **33**(6): p. 1267-1277.
246. van den Hoogen, B.M., P.R. van Weeren, M. Lopes-Cardozo, L.M.G. van Golde, A. Barneveld, and C.H.A. van de Lest, *A Microtiter Plate Assay for the Determination of Uronic Acids*. Analytical Biochemistry, 1998. **257**(2): p. 107-111.
247. Bradford, M.M., *A rapid and sensitive method for the quantitation of microgram quantities of protein utilizing the principle of protein dye binding*. Analytical Biochemistry, 1976. **72**(1-2): p. 248-254.
248. Brett, M.S.Y., P. Short, and J. McLauchlin, *A small outbreak of listeriosis associated with smoked mussels*. International Journal of Food Microbiology, 1998. **43**(3): p. 223-229.
249. Cantor, C.R., C.L. Smith, and M.K. Mathew, *Pulsed-field gel electrophoresis of very large DNA molecules*. Annual review of biophysics and biophysical chemistry, 1988. **17**: p. 287-304.
250. Carlson, B.A., K.K. Nightingale, G.L. Mason, J.R. Ruby, W.T. Choat, G.H. Loneragan, G.C. Smith, J.N. Sofos, and K.E. Belk, *Escherichia coli O157:H7 strains that persist in feedlot cattle are genetically related and demonstrate an enhanced ability to adhere to intestinal epithelial cells*. Applied and Environmental Microbiology, 2009. **75**(18): p. 5927-5937.
251. Wild, C.J., *Chance encounters: A first course in data analysis and inference*. 2000.
252. Weisstein, E.W., *CRC concise encyclopedia of mathematics*. 2003: CRC press.
253. Morehouse, K.A., I.G. Goodfellow, and R.E. Sockett, *A chimeric N-terminal Escherichia coli-C-terminal Rhodobacter sphaeroides FliG rotor protein supports bidirectional E. coli flagellar rotation and chemotaxis*. Journal of Bacteriology, 2005. **187**(5): p. 1695-1701.
254. Shapiro, J.A., *Bacteria are small but not stupid: cognition, natural genetic engineering and socio-bacteriology*. Studies in History and Philosophy of Science Part C: Studies in History and Philosophy of Biological and Biomedical Sciences, 2007. **38**(4): p. 807-819.
255. Asahi, Y., Y. Noiri, J. Igarashi, H. Asai, H. Suga, and S. Ebisu, *Effects of N-acyl homoserine lactone analogues on Porphyromonas gingivalis biofilm formation*. Journal of Periodontal Research, 2010. **45**(2): p. 255-261.
256. Lee, D.J., L.E. Bingle, K. Heurlier, M.J. Pallen, C.W. Penn, S.J. Busby, and J.L. Hobman, *Gene doctoring: A method for recombineering in laboratory and pathogenic Escherichia coli strains*. BMC Microbiology, 2009. **9**.

257. Pearson, J.P., K.M. Gray, L. Passador, K.D. Tucker, A. Eberhard, B.H. Iglewski, and E.P. Greenberg, *STRUCTURE OF THE AUTOINDUCER REQUIRED FOR EXPRESSION OF PSEUDOMONAS-AERUGINOSA VIRULENCE GENES*. Proceedings of the National Academy of Sciences of the United States of America, 1994. **91**(1): p. 197-201.
258. Han, T.H., J.H. Lee, M.H. Cho, T.K. Wood, and J. Lee, *Environmental factors affecting indole production in Escherichia coli*. Research in Microbiology, 2011. **162**(2): p. 108-116.
259. Sezonov, G., D. Joseleau-Petit, and R. D'Ari, *Escherichia coli physiology in Luria-Bertani broth*. J Bacteriol, 2007. **189**(23): p. 8746-9.
260. Schembri, M.A., L. Hjerrild, M. Gjermansen, and P. Klemm, *Differential expression of the Escherichia coli autoaggregation factor antigen 43*. J Bacteriol, 2003. **185**(7): p. 2236-42.
261. Ramer, S.W., G.K. Schoolnik, C.Y. Wu, J. Hwang, S.A. Schmidt, and D. Bieber, *The type IV pilus assembly complex: biogenic interactions among the bundle-forming pilus proteins of enteropathogenic Escherichia coli*. J Bacteriol, 2002. **184**(13): p. 3457-65.
262. Delisa, M.P., J.J. Valdes, and W.E. Bentley, *Quorum signaling via AI-2 communicates the "metabolic burden" associated with heterologous protein production in Escherichia coli*. Biotechnology and Bioengineering, 2001. **75**(4): p. 439-450.
263. Sperandio, V., A.G. Torres, J.A. Girón, and J.B. Kaper, *Quorum sensing is a global regulatory mechanism in enterohemorrhagic Escherichia coli O157:H7*. Journal of Bacteriology, 2001. **183**(17): p. 5187-5197.
264. Stokes, R.W., R. Norris-Jones, D.E. Brooks, T.J. Beveridge, D. Doxsee, and L.M. Thorson, *The glycan-rich outer layer of the cell wall of Mycobacterium tuberculosis acts as an antiphagocytic capsule limiting the association of the bacterium with macrophages*. Infection and Immunity, 2004. **72**(10): p. 5676-5686.
265. Yoshida, K., T. Matsumoto, K. Tateda, K. Uchida, S. Tsujimoto, and K. Yamaguchi, *Role of bacterial capsule in local and systemic inflammatory responses of mice during pulmonary infection with Klebsiella pneumoniae*. J Med Microbiol, 2000. **49**(11): p. 1003-10.
266. Stevenson, G., K. Andrianopoulos, M. Hobbs, and P.R. Reeves, *Organization of the Escherichia coli K-12 gene cluster responsible for production of the extracellular polysaccharide colanic acid*. Journal of Bacteriology, 1996. **178**(16): p. 4885-4893.
267. Hartland, E.L., S.J. Daniell, R.M. Delahay, B.C. Neves, T. Wallis, R.K. Shaw, C. Hale, S. Knutton, and G. Frankel, *The type III protein translocation system of enteropathogenic Escherichia coli involves EspA-EspB protein interactions*. Molecular Microbiology, 2000. **35**(6): p. 1483-1492.

268. Brinkley, C., V. Burland, R. Keller, D.J. Rose, A.T. Boutin, S.A. Klink, F.R. Blattner, and J.B. Kaper, *Nucleotide sequence analysis of the enteropathogenic Escherichia coli adherence factor plasmid pMAR7*. Infect Immun, 2006. **74**(9): p. 5408-13.
269. Feng, P., K.A. Lampel, H. Karch, and T.S. Whittam, *Genotypic and phenotypic changes in the emergence of Escherichia coli O157:H7*. Journal of Infectious Diseases, 1998. **177**(6): p. 1750-1753.
270. Waters, C.M., W. Lu, J.D. Rabinowitz, and B.L. Bassler, *Quorum sensing controls biofilm formation in Vibrio cholerae through modulation of cyclic di-GMP levels and repression of vpsT*. J Bacteriol, 2008. **190**(7): p. 2527-36.
271. Kiburu, I., A. Shurer, L. Yan, and H.O. Sintim, *A simple solid-phase synthesis of the ubiquitous bacterial signaling molecule, c-di-GMP and analogues*. Mol Biosyst, 2008. **4**(6): p. 518-20.
272. Kobayashi, H., A. Miura, H. Hayashi, T. Ogawa, T. Endô, E. Hata, M. Eguchi, and K. Yamamoto, *Prevalence and characteristics of eae-positive Escherichia coli from healthy cattle in Japan*. Applied and Environmental Microbiology, 2003. **69**(9): p. 5690-5692.
273. Boyer, M. and F. Wisniewski-Dyé, *Cell-cell signalling in bacteria: Not simply a matter of quorum*. FEMS Microbiology Ecology, 2009. **70**(1): p. 1-19.
274. Di Cagno, R., M. De Angelis, M. Calasso, and M. Gobbetti, *Proteomics of the bacterial cross-talk by quorum sensing*. Journal of Proteomics, 2011. **74**(1): p. 19-34.
275. Huang, Y., Y. Zeng, Z. Yu, and J. Zhang, *Distribution and Diversity of Acyl Homoserine Lactone Producing Bacteria from Four Different Soils*. Current Microbiology, 2012: p. 1-6.
276. Romero, M., A.B. Martin-Cuadrado, A. Roca-Rivada, A.M. Cabello, and A. Otero, *Quorum quenching in cultivable bacteria from dense marine coastal microbial communities*. FEMS Microbiology Ecology, 2011. **75**(2): p. 205-217.
277. Wolfram, S., *Theory and Application of Cellular Automata*. Advanced Series on Complex Systems, ed. S. Wolfram. Vol. 1. 1986: World Scientific.